

# **Investigation of the role of bone marrow stromal cells in the microenvironment of acute myeloid leukaemia**

by

Amina Abdul-Aziz

M.Sc., University of Nottingham, 2011

A thesis submitted in partial fulfilment of the requirements for the  
degree of

Doctor of Philosophy

Faculty of Medicine and Health Sciences  
Norwich Medical School  
Department of Molecular Haematology

UNIVERSITY OF EAST ANGLIA

October 2017

This copy of my thesis has been supplied on condition that anyone who consults it is understood to recognise that its copyright rests with the author and that use of any information derived there from must be in accordance with current UK Copyright Law. In addition, any quotation must include full attribution.

Amina Abdul-Aziz, 2017

## Declaration

I declare that the content of this thesis entitled "Investigation of the role of bone marrow stromal cells in the microenvironment of acute myeloid leukaemia" was undertaken and completed by myself, unless otherwise acknowledged and has not been submitted in support of an application for another degree or qualification in this or any other university or institution.



-----

Amina Abdul-Aziz

## **Acknowledgement**

All praise and thanks are to Allah (the lord of all worlds), who is the most gracious and the most merciful. His continuous grace and mercy was with me throughout my life and ever more during the pursuit of my PhD.

It has been a long journey and I am in the debt of many...

My sincere thanks go to my enthusiastic supervisors. Prof. Kristian Bowles and Dr Stuart Rushworth. They have gone above and beyond to provide me with advice and support, both professionally and scientifically. Thank you for the constant faith in my work and for the many opportunities that helped make me the scientist I am today. Special mention goes to my colleagues Manar, Christopher, Rachel and Yu, who have been an amazing team to work with. Thank you for the laughs, happy surprises and words of encouragement when they are most needed.

I am greatly indebted to my friends around the globe. In particular, my friends in Norwich, who have been my family away from home and I cannot imagine this journey without them. Thank you for your kindness and never-ending support through good times and bad.

I am also hugely appreciative to my funder, The Ministry of Higher Education of The State of Libya, who have continued to support me despite the recent instability in the country. Without their generous grant this valuable research and my PhD could not have been achieved.

Finally, but by no means least, endless thanks go to my family. Especially, to my parents. None of this would have been possible without their unconditional love, support and constant reminders that I can, with the help of God, achieve more than I can imagine. Thank you for being understanding and for everything else that you have done for me, for which I am unable to express my gratitude in words.

## Abstract

Acute myeloid leukaemia (AML) is an aggressive malignancy of the haematopoietic system. With a median age of approximately 70 years at diagnosis, survival rates for AML patients lag behind other haematological malignancies. This is in part, due to existing comorbidities and patient inability to tolerate intensive chemotherapy. Moreover, chemotherapy mainly targets AML cells in the peripheral blood (PB) but not those harboured in the bone marrow (BM). While studies focusing on the malignant blasts helped achieve advances in understanding AML biology and chemoresistance, less is understood about the role of the bone marrow microenvironment (BMM) in the progression of AML. It is predicted that improved patient outcomes will come from novel treatment strategies resulting from an improved understanding of the biology of the microenvironment in AML.

Bone marrow stromal cells (BMSCs) are an instrumental component of the AML microenvironment and have been shown to play a role in its survival and evasion from apoptosis. The aims of my PhD research were to investigate novel interactions between AML cells and BMSCs which benefit AML survival *in vitro* and *in vivo*. Here, I identified an AML-BMSC feedback loop where AML-derived macrophage migration inhibitory factor (MIF) stimulated BMSCs, through the activation of stromal protein kinase C, to secrete the pro-survival cytokine interleukin-8 (IL-8). Moreover, I found that MIF expression in the AML compartment is regulated by hypoxia through stabilisation of HIF1 $\alpha$ . Inhibition of HIF1 $\alpha$  or MIF significantly enhanced survival and reduced tumour burden *in vivo*. Finally, I showed that AML cells induce senescence in BSMCs through upregulation of the cyclin-dependent kinase inhibitor, p16. Deletion of p16 in BMSCs reduced AML survival in co-culture models.

In summary, the data presented in this thesis provide important insights into the AML-BMSC interactions and could facilitate the development of future therapeutic approaches in the treatment of AML.

## List of publications and conference papers

These publications have been realised during the pursuit of this PhD thesis:

### Lead publications:

**A. Abdul-Aziz\***, M.S. Shafat\*, C.R. Marlein, R.E. Piddock, S.D. Robinson, D.R. Edwards, Z. Zhou, A. Collins, K.M. Bowles, S.A. Rushworth, Hypoxia drives chemokine factor pro-tumoral signaling pathways in acute myeloid leukaemia, under review in *Oncogene* (2017).

**A. Abdul-Aziz**, M. Shafat, T. Mehta, F. Di Palma, M. Lawes, S. Rushworth, K.M. Bowles, MIF-Induced Stromal PKC $\beta$ /IL8 Is Essential in Human Acute Myeloid Leukaemia, *Cancer Research* (2017). DOI: 10.1158/0008-5472.CAN-16-1095.

**A. Abdul-Aziz**, D.J. MacEwan, K.M. Bowles, S.A. Rushworth, Oxidative Stress Responses and NRF2 in Human Leukaemia, *Oxidative Medicine and Cellular Longevity* (2015). DOI: 10.1155/2015/454659.

### Co-authored publications:

Y. Sun, **A. Abdul-Aziz**, K.M. Bowles, S.A. Rushworth, NRF2 controls endoplasmic reticulum stress induced apoptosis via the negative regulation of CHOP in multiple myeloma, *Cancer letters* (2017). DOI: 10.1016/j.canlet.2017.10.005

S. Chandran, J. Watkins J, **A. Abdul-Aziz**, M. Shafat, PA. Calvert, KM. Bowles, MD. Flather, SA. Rushworth, AD. Ryding. Inflammatory Differences in Plaque Erosion and Rupture in Patients With ST-Segment Elevation Myocardial Infarction. *Journal of the American Heart Association* (2017). DOI: 10.1161/JAHA.117.005868.

M.S. Shafat, T. Oellerich, S. Mohr, S.D. Robinson, D.R. Edwards, C.R. Marlein, R.E. Piddock, M. Fenech, L. Zaitseva, **A. Abdul-Aziz**, J. Turner, J.A. Watkins, M. Lawes, K.M. Bowles, S.A. Rushworth, Leukaemic blasts program bone marrow adipocytes to generate a pro-tumoral microenvironment, *Blood* (2017). DOI: 10.1182/blood-2016-08-734798.

G. Pillinger, N.V. Loughran, R.E. Piddock, M.S. Shafat, L. Zaitseva, **A. Abdul-Aziz**, M.J. Lawes, K.M. Bowles, S.A. Rushworth, Targeting PI3Kdelta and PI3Kgamma signalling disrupts human AML survival and bone marrow stromal cell mediated protection, *Oncotarget* (2016). DOI: 10.18632/oncotarget.9289.

G. Pillinger, **A. Abdul-Aziz**, L. Zaitseva, M. Lawes, D.J. MacEwan, K.M. Bowles, S.A. Rushworth, Targeting BTK for the treatment of FLT3-ITD mutated acute myeloid leukaemia, *Scientific Reports* (2015). DOI: 10.1038/srep12949.

S.A. Rushworth, G. Pillinger, **A. Abdul-Aziz**, R. Piddock, M.S. Shafat, M.Y. Murray, L. Zaitseva, M.J. Lawes, D.J. MacEwan, K.M. Bowles, Activity of

Bruton's tyrosine-kinase inhibitor ibrutinib in patients with CD117-positive acute myeloid leukaemia: a mechanistic study using patient-derived blast cells, *The Lancet Haematology* (2015). DOI: 10.1016/S2352-3026(15)00046-0.

**Conference papers:**

A. Abdul-Aziz, MS. Shafat, R. Piddock, C. Marlein, J Campisi, K. Bowles, S. Rushworth. Acute Myeloid Leukaemia Induces p16 Driven Senescence in the Bone Marrow Microenvironment to Support Their Proliferation and Survival 59th ASH meeting, Atlanta. December 2017.

A. Abdul-Aziz, MS. Shafat, C. Marlein, R. Piddock, S. Robinson, D. Edwards, Z. Zhou, A. Collins, K. Bowles, S. Rushworth. Hypoxia drives AML proliferation in the tumor microenvironment through HIF1 $\alpha$ /MIF signalling. 22nd EHA Congress, Madrid. June 2017.

E. Forde\*, A. Abdul-Aziz\*, T. Mehta, F. Di Palma, C. Ingham, M. Lawes, K. Bowles, S. Rushworth. AML blasts induce a senescent phenotype in the BM-MSC through the upregulation of p21. 22nd EHA Congress, Madrid. June 2017.

A. Abdul-Aziz, MS. Shafat, L. Zaitseva, MJ. Lawes, SA. Rushworth, KM. Bowles. Hypoxia Drives AML Proliferation in the Bone Marrow Microenvironment Via Macrophage Inhibitory Factor. 58th ASH meeting, San Diego. December 2016.

A. Abdul-Aziz, MS. Shafat, M. Lawes, K. Bowles, S. Rushworth. Protein Kinase C- $\beta$  Dependent IL-8 Release Promotes Acute Myeloid Leukaemia Blast Cell Survival in Co-Cultures with Bone Marrow Stromal Cells. 57th ASH meeting, Orlando. December 2015.

A. Abdul-Aziz, MS. Shafat, S. Rushworth, K. Bowles. Acute Myeloid Leukaemia Derived Macrophage Migration Inhibitory Factor Drives Interleukin-8 Pro-Survival Signals In The Tumor Microenvironment. 20th EHA Congress, Vienna. June 2015.

## Table of contents

Declaration .....	2
Acknowledgement .....	3
Abstract .....	4
List of publications and conference papers .....	5
Table of contents .....	7
List of figures .....	12
List of tables .....	15
List of abbreviations.....	16
1. Chapter 1: Introduction .....	22
1.1. Haematopoiesis .....	22
1.2. Leukaemogenesis.....	23
1.3. Acute Myeloid Leukaemia .....	24
1.3.1. Genetic defects in AML.....	24
1.3.2. Classification of AML .....	26
1.3.3. Current treatment of AML .....	29
1.4. The bone marrow microenvironment (BMM) .....	29
1.4.1. Cellular components of the BMM.....	30
1.4.2. Bone marrow mesenchymal stem cells (BMSCs) .....	31
1.4.3. BMSCs and normal haematopoiesis.....	32
1.4.4. The role of BMSCs in the malignant BM .....	33
1.4.5. Leukaemic cell remodelling of the BMM.....	36
1.4.6. Niche-induced oncogenesis.....	37
1.4.7. Chemokine and cytokine profiles in the malignant BM .....	38
1.4.7.1. Interleukin-8 (IL-8).....	40
1.4.7.2. Interleukin-6 (IL-6).....	41
1.4.7.3. Macrophage migration inhibitory factor (MIF) .....	42
1.4.8. Cell signalling in the AML microenvironment .....	44
1.4.8.1. Phosphatidylinositol-3-kinase (PI3K)/AKT/mTOR signalling .....	44
1.4.8.2. Mitogen-activated protein kinase (MAPK) signalling .....	45
1.4.8.3. Protein kinase C (PKC) signalling .....	45
1.5. Hypoxia in Cancer.....	46
1.5.1. Hypoxia inducible factors (HIFs).....	47
1.5.2. Hypoxia as a component of the BMM .....	49
1.5.3. The role of hypoxia in HSC versus leukaemic cells.....	50
1.5.4. HIF1 $\alpha$ and HIF2 $\alpha$ in AML leukaemogenesis .....	52

1.6.	Senescence in health and disease.....	53
1.7.	Effector pathways of senescence and the senescent phenotype.....	54
1.8.	Role of senescence and SASP in tumourigenesis.....	56
1.9.	Therapy-induced senescence .....	57
1.10.	Research rationale, aims and objectives.....	59
1.10.1.	Rationale.....	59
1.10.2.	Aims.....	59
1.10.3.	Objectives .....	59
2.	Chapter 2: materials and methods .....	61
2.1.	Reagents and chemicals .....	61
2.2.	Blocking antibodies and recombinant cytokines .....	61
2.3.	Cell culture .....	63
2.3.1.	Cell lines.....	63
2.3.2.	Primary cell isolation and culture .....	64
2.3.3.	CD34+ magnetic purification.....	66
2.3.4.	Cryopreservation and defrosting of primary cells .....	67
2.3.5.	Cell viability assays:.....	67
2.3.5.1.	Trypan blue exclusion test using a haemocytometer .....	67
2.3.5.2.	CellTiter-Glo viability assay .....	68
2.3.5.3.	Annexin V – PI detection of apoptosis .....	68
2.3.6.	Hypoxic assays.....	69
2.3.7.	Methylcellulose Human Colony Forming Cell (CFC) Assay.....	69
2.4.	Molecular biology techniques .....	70
2.4.1.	RNA extraction .....	70
2.4.2.	Nucleic acid quantification using a Nanodrop .....	71
2.4.3.	Reverse transcription and cDNA synthesis .....	71
2.4.4.	Relative quantitative real-time PCR (qRT-PCR).....	71
2.4.5.	Analysis of qRT-PCR data .....	73
2.4.6.	Protein expression analysis .....	73
2.4.6.1.	Western immunoblotting.....	73
2.4.6.1.1.	Whole cell lysate preparation.....	73
2.4.6.1.2.	SDS-PAGE and immunoblotting .....	74
2.4.6.1.3.	Chemiluminescent detection.....	74
2.4.6.2.	ELISA.....	75
2.4.6.3.	Proteome Profiler Human XL Cytokine Array .....	76
2.4.6.4.	Flow cytometry.....	77
2.4.7.	shRNA-mediated gene silencing.....	78



2.4.7.1.	Amplification of bacterial cultures .....	80
2.4.7.2.	Plasmid DNA isolation and precipitation .....	81
2.4.7.3.	293T packaging cell transfection .....	82
2.4.7.4.	Viral RNA isolation .....	82
2.4.7.5.	Determination of viral titres.....	83
2.4.7.6.	Lentiviral infection of target cells .....	84
2.4.8.	Senescence associated $\beta$ - galactosidase staining .....	85
2.5.	<i>In vivo</i> animal models.....	85
2.5.1.	Non- diabetic (NOD) severe combined immunodeficiency (SCID) and gamma model (NSG) mice for human xenograft models.....	86
2.5.2.	Patient derived xenografts .....	86
2.5.3.	OCI-AML3 human xenograft model .....	87
2.5.4.	<i>In vivo</i> bioluminescent (BL) imaging .....	87
2.5.5.	Sacrificing animals and harvesting of the bone marrow and spleen cells.	88
2.6.	Bioinformatics analysis.....	89
2.7.	Statistical analyses.....	90
3.	Chapter 3: AML influences the secretory profile of BMSCs.....	91
3.1.	<i>In vitro</i> expansion of primary AML-derived BMSCs .....	91
3.2.	BMSCs support AML survival <i>in vitro</i> .....	93
3.3.	AML cells induce changes in the BMSC cytokine secretion profile .....	95
3.4.	AML but not BMSCs express high levels of MIF mRNA under normal basal conditions .....	101
3.5.	IL-8 specific ELISAs confirm IL-8 upregulation in AML/BMSC co-cultures.	102
3.6.	IL-6 is not upregulated in BMSCs in AML/BMSCs to co-cultures.....	103
3.7.	AML induced IL-8 expression in BMSCs is contact independent.....	104
3.8.	Recombinant human MIF (rhMIF) induces IL-8 expression in AML derived BMSCs but not normal cell line BMSCs .....	104
3.9.	Inhibition of AML-derived MIF downregulates IL-8 expression.....	106
3.10.	Inhibition of MIF significantly reduces AML survival on BMSCs .....	107
3.11.	Summary of the results presented in chapter 3.....	108
4.	Chapter 4: MIF induction of BMSC-derived IL-8 is mediated through CD74 and PKC $\beta$ signalling .....	109
4.1.	Identifying the receptor/s to which MIF binds and induces IL-8 in BMSCs.	109
4.2.	The primary MIF receptor involved in mediating IL-8 expression is CD74 .	110
4.3.	Pharmacological inhibition of MIF signalling pathways .....	113
4.4.	MAPK and AKT do not play a role in MIF-induced IL-8 in BMSCs.....	114
4.5.	PKC $\beta$ is activated in response to MIF in BMSCs.....	116
4.6.	MIF-induced IL-8 in BMSCs is signalled through PKC $\beta$ .....	116

4.7.	Knockdown of PKC $\beta$ inhibits MIF-induced IL-8 expression in BMSCs .....	117
4.8.	Targeting the MIF-PKC $\beta$ -IL-8 axis disrupts BMSC induced protection of primary human AML cells .....	119
4.9.	Summary of results chapter 4.....	120
5.	Chapter 5: Hypoxia regulates AML-derived MIF .....	122
5.1.	AML cells derived from the bone marrow express higher levels of MIF compared to cells in the systemic circulation and spleen .....	123
5.2.	MIF is part of a hypoxic gene signature in AML cells isolated from the BM, but not those isolated from the PB .....	126
5.3.	Hypoxia induces MIF in primary AML cells .....	127
5.4.	HIF1 $\alpha$ is a candidate regulator of MIF expression in Primary AML cells ....	128
5.5.	HIF1 $\alpha$ , but not HIF2 $\alpha$ is stabilised and induces MIF in primary AML cells in response to hypoxia.....	128
5.6.	MIF is not induced in normal non-leukaemic CD34+ cells .....	129
5.7.	Silencing of HIF1 $\alpha$ , but not of HIF2 $\alpha$ , significantly reduces MIF expression in primary AML cells .....	131
5.8.	MIF functions to promote AML tumour survival <i>in vitro</i> .....	133
5.9.	The leukaemic cell HIF1 $\alpha$ -MIF axis functions to promote tumour proliferation <i>in vivo</i>	135
5.10.	Pharmacological inhibition of MIF <i>in vivo</i> increases survival of AML xenograft models. ....	137
5.11.	Summary of results chapter 5.....	139
6.	Chapter 6: AML cells induce senescence in BMSCs through the upregulation of p16	141
6.1.	Proteome profile arrays from AML-BMSC co-cultures show an upregulation of SASP related factors.....	141
6.2.	BMSCs from late passages become senescent in culture .....	142
6.3.	AML cells increase senescence associated $\beta$ -Galactosidase staining in patient derived BMSCs .....	143
6.4.	AML cells induce p21 and p16 mRNA in BMSCs. ....	145
6.5.	Knockdown of p16 in BMSCs inhibits AML induced p16 expression in BMSCs. ....	146
6.6.	p16 deficient BMSCs have reduced ability to support AML survival <i>in vitro</i>	146
6.7.	<i>In vivo</i> modelling of the senescent BM phenotype using the p16-3MR mouse model	147
6.8.	Isolation and culturing of p16-3MR BMSCs.....	148
6.9.	MN1 AML cells induce p16 expression in p16-3MR derived BMSCs .....	149
6.10.	Summary of chapter 6 .....	150
7.	Chapter 7: discussion and conclusions .....	151

7.1. AML-derived MIF stimulates BMSC IL-8 expression through PKC $\beta$ and is essential for AML survival .....	151
7.1.1. Modelling the AML microenvironment using primary AML BMSCs.....	151
7.1.2. AML-induced alternations in BMSC secretory profiles .....	152
7.1.3. Characteristic primary AML cytokines, an emerging role for MIF .....	153
7.1.4. Clinical investigations of MIF inhibitors .....	155
7.1.5. PKC $\beta$ targeting in leukaemic cells .....	156
7.1.6. IL-8 as a key cytokine for AML survival.....	156
7.1.7. <i>In vivo</i> modelling of IL-8 may be challenging .....	157
7.2. Hypoxia regulates MIF expression through HIF1a.....	157
7.2.1. AML emerges as a hypoxia driven malignancy .....	158
7.2.2. The role of HIFs in AML remains to be delineated .....	159
7.2.3. <i>In vivo</i> modelling of the role of MIF in AML BMM .....	161
7.3. AML induces senescence in BMSC through upregulation of p16 .....	162
7.3.1. An ageing-induced malignant environment.....	162
7.3.2. Senescence in AML cells.....	163
7.3.3. <i>In vitro</i> markers and inducers of senescence.....	163
7.3.4. <i>In vivo</i> modelling of the senescent BMM in AML.....	164
7.4. Conclusions and future directions .....	165
References .....	167
Appendix .....	191
Table 1: Cytogenetic profiles of primary BMSCs.....	191
Table 2: AML, BMSC and AML/BMSC cytokine array data sets.....	196
Copies of publications arising from this thesis.....	200

## List of figures

### Chapter 1

Figure 1. 1 Normal haematopoiesis and Leukaemia stem cell model.....	23
Figure 1. 2 A model of the haematopoietic stem cell (HSC) niche.....	31
Figure 1. 3 Hypoxia gradient across the bone marrow. ....	48
Figure 1. 4 The Hypoxia gradient across the bone marrow. ....	50
Figure 1. 5 Effectors of the senescence pathway.....	56

### Chapter 2

Figure 2. 1 A schematic of the Histopaque density gradient centrifugation step in isolating AML cells from BM aspirates. ....	64
Figure 2. 2 A schematic of the additional centrifugation of large volumes of peripheral blood prior to Histopaque density gradient centrifugation and isolation of CD34+ cells. ....	66
Figure 2. 3 A schematic showing the work flow followed in the production of lentiviral particles from bacterial glycerol stocks.....	79
Figure 2. 4 Bones and spleens harvested from NSG mice.....	89

### Chapter 3

Figure 3. 1 In vitro expansion and characterization of bone marrow stromal cells (BMSCs).....	92
Figure 3. 2 Morphology of primary cultured BMSC over time. ....	93
Figure 3. 3 Primary AML survival in mono-cultures versus on primary BMSCs. ....	94
Figure 3. 4 A representative image of the developed cytokine array from AML, BMSC and AML/BMSC culture media.....	95
Figure 3. 5 Bar graphs comparing the fold increase in cytokines between BMSC/AML co-cultures and BMSC monocultures. ....	99
Figure 3. 6 Bar graph depicting the results of a cytokine array optical density quantification of AML only arrays. ....	100
Figure 3. 7 Bar graph comparing MIF mRNA expression levels in AML and BMSC cultures.....	102
Figure 3. 8 Bar graph representing IL-8 protein expression (pg/ml) in monocultures and AML/BMSC co-cultures over 24 hours. ....	102
Figure 3. 9 Bar graph representing MIF expression (pg/ml) in monocultures and AML/BMSC co-cultures over 24 hours. ....	103
Figure 3. 10 Bar graph depicting IL-6 expression (pg/ml) in monocultures and AML/BMSC co-cultures over a period of 24 hours. ....	103
Figure 3. 11 Bar graph comparing fold increase over control of IL-8 induction in AML/BMSC co-cultures in direct contact (DC) versus indirect contact (IC).....	104
Figure 3. 12 Bar graph comparing fold increase over control of IL-8 expression in BMSCs in response to MIF stimulation, over 24 hours.....	105
Figure 3. 13 Bar graph comparing fold change in IL-8 mRNA expression in HS-5 treated with rhMIF or co-cultured with AML.....	106
Figure 3. 14 Bar graph comparing IL-8 RNA expression levels in the absence (MIF) and presence (MIF+ISO-1) of the MIF inhibiting ISO-1. ....	107

Figure 3. 15 Scatter graph showing reduced AML survival in ISO-1 treated AML/BMSC co-cultures.....	108
--	-----

#### Chapter 4

Figure 4. 1 Representative flow cytometry analysis of cultured BMSCs stained with monoclonal antibodies against CD105, CD74, CXCR2 and CXCR4. ....	109
Figure 4. 2 Bar graph comparing MIF-induced IL-8 mRNA expression in BMSCs treated with the inhibitors of CD74, CXCR2 and CXCR4 receptors.....	110
Figure 4. 3 MIF-induced IL-8 upregulation is mediated through CD74, as seen in this bar graph which shows IL-8 mRNA expression levels for untreated, MIF-stimulated, PTX-treated, PTX-treated/MIF-stimulated BMSCs. ....	111
Figure 4. 4 CD74 protein levels in control versus knockdown BMSC samples, measured by qRT-PCR (A) and flow cytometry (B).....	112
Figure 4. 5 Bar graph depicting IL-8 mRNA expression levels after CD74 knockdown in BMSCs, which inhibited MIF induced IL-8 expression. ....	112
Figure 4. 6 Bar graphs showing that the pharmacological inhibition of PKC pathways, inhibit AML induced IL-8 expression levels in BMSCs.....	113
Figure 4. 7 Bar graph depicting IL-8 mRNA expression after pharmacological inhibition of MAPK and PKC signalling pathways, to examine its effects on MIF induced BMSC IL-8 mRNA expression. ....	114
Figure 4. 8 A western-blot image showing that pMAPK and pAKT are not activated in response to MIF in BMSCs. ....	115
Figure 4. 9 A western-blot image showing MIF activates PKC $\alpha$ / $\beta$ II and PKC $\beta$ in BMSCs. ....	116
Figure 4. 10 Bar graph comparing IL-8 mRNA expression levels in BMSCs treated with inhibitors to assess the effect of pPKC $\alpha$ / $\beta$ II and pPKC $\beta$ on MIF-induced IL-8 expression. ....	117
Figure 4. 11 Results depicting changes in PKC $\beta$ expression after knockdown in BMSCs. ....	118
Figure 4. 12 Bar graphs representing IL-8 mRNA expression levels in BMSCs, where PKC $\beta$ was knockdown. PKC $\beta$ knockdown inhibits MIF-induced IL-8 expression in BMSCs. ....	118
Figure 4. 13 Bar graphs showing IL-8 expression levels, following the knockdown of IL-8 in AML derived BMSCs.....	119
Figure 4. 14 Results depicting that the IL-8 inhibition in BMSCs reverses AML survival in co-cultures. ....	120

#### Chapter 5

Figure 5. 1 Scatter graph showing that BM AML cells express significantly higher MIF levels than circulating AML cells. ....	124
Figure 5. 2 Experimental plan of the patient-derived xenograft (PDX) model, and results that indicated successful engraftment.....	125
Figure 5. 3 Scatter graphs comparing MIF and GLUT1 RNA expression levels in the BM and spleen of the PDX animals.....	126
Figure 5. 4 Bar graphs depicting MIF mRNA and protein expression levels in AML cells following culture under hypoxic conditions <i>in vitro</i> .....	128

Figure 5. 5 Western blot demonstrating the stabilisation of HIF1 $\alpha$ but not HIF2 $\alpha$ in AML cells under hypoxic culture conditions.....	129
Figure 5. 6 Bar graphs depicting differences in the expression of MIF, mRNA and protein, in CD34+ cells versus AML cells. ....	130
Figure 5. 7 Bar graphs depicting the expression of MIF mRNA and protein in CD34+ cells under normoxic and hypoxic conditions. ....	130
Figure 5. 8 HIF1 $\alpha$ or HIF2 $\alpha$ lentiviral knockdown (KD) in primary AML cells .....	131
Figure 5. 9 Bar graphs showing the differences in basal MIF expression in HIF1 $\alpha$ or HIF2 $\alpha$ lentiviral knockdown (KD) primary AML cells. ....	133
Figure 5. 10 Figure 5.12 Bar graphs showing that lentiviral Knockdown of MIF in AML cells reduces cell survival and colony formation. ....	134
Figure 5. 11 Scatter plots depicting the apoptosis of AML cells, driven by MIF knockdown.....	135
Figure 5. 12 <i>In vivo</i> bioluminescence images depicting disease progression in HIF1 $\alpha$ and MIF KD AML xenograft model. ....	136
Figure 5. 13 Results summarizing that the inhibition of AML HIF1 $\alpha$ and MIF significantly increases survival of AML derived xenograft models. ....	137
Figure 5. 14 Summarised results of experiments showing that the pharmacological inhibition of MIF in an AML patient derived xenograft model (PDX) does not affect AML mobilisation, but significantly increases animal survival. ....	139

## Chapter 6

Figure 6. 1 Light micrographs of senescent patient-derived BMSCs. ....	143
Figure 6. 2 Light micrograph images showing that primary AML cells induce $\beta$ -Galactosidase staining in primary BMSCs. ....	144
Figure 6. 3 Bar graphs showing that primary AML cells increase p21 and p16 mRNA expression in primary BMSCs.....	145
Figure 6. 4 Results from experiments that reveal that the knockdown of p16 in BMSCs inhibits AML induced p16 expression. ....	146
Figure 6. 5 Dot plot depicting the survival of AML cells co-cultured with p16 deficient BMSCs. ....	147
Figure 6. 6 Schematic of the p16-3MR transgene. ....	148
Figure 6. 7 Light microscopy images from the In vitro cultures of p16-3MR derived BMSCs. ....	149
Figure 6. 8 Western-blots showing that MN1 AML cells induce p16 expression in p16-3MR derived BMSCs in vitro.....	150

## List of tables

### Chapter 1

Table 1. 1 WHO classification of AML and related neoplasms. ....	28
--	----

### Chapter 2

Table 2. 1 Antibodies used in flow cytometry analysis. ....	61
Table 2. 2 Primary and secondary antibodies used in western blotting. ....	62
Table 2. 3 KiCqStart® SYBR® Green Primers (Sigma). ....	72
Table 2. 4 QuantiTect Primers (Qiagen). ....	73
Table 2. 5 Sigma mission shRNAs used for stable knockdown of target genes.....	80

### Chapter 3

Table 3. 1 AML patient sample characteristics used in chapter 3 and 4. ....	94
Table 3. 2 Cytokine mean pixel densities data set for figure 3.4. ....	96

### Chapter 5

Table 5. 1 AML patient sample characteristics used in chapter 5. ....	123
---	-----

### Chapter 6

Table 6. 1 AML patient sample characteristics used in chapter 6. ....	141
---	-----

## List of abbreviations

aCD74 Ab	Anti-CD74 blocking antibody
ALL	Acute lymphoblastic leukaemia
AML	Acute myeloid leukaemia
aPKC	Atypical Protein Kinase C
AV	Annexin V
BCL-2	B-cell leukaemia/lymphoma 2
BLI	Bioluminescence intensity
BM	Bone marrow
BMM	Bone marrow microenvironment
BMSC	Bone marrow (mesenchymal) stromal cells
BSA	Bovine serum albumin
CAR cells	CXCL12-abundant reticular cells
CD	Cluster of differentiation
CDK	Cyclin dependent kinases
cDNA	Complementary DNA
CFC	Colony forming cell
CLL	Chronic lymphocytic leukaemia
CML	Chronic myeloid leukemia
CMP	Committed progenitor cells
CO <sub>2</sub>	Carbon dioxide
COCL <sub>2</sub>	Cobalt chloride
cPKC	Conventional protein kinase c
CSF-1	Colony stimulating factor-1
Ct	Cycle threshold
CXCL12	C-X-C motif chemokine 12
CXCR	C-X-C chemokine receptor
DC	Direct contact
dCT	Delta Ct
DDR	DNA-damage response



D-DT	D-dopachrome tautomerase
DFO	Desferrioxamine
DMEM	Dulbecco's Modified Eagle's medium
DMSO	Dimethyl sulfoxide
DMU	Disease modelling unit
DNA	Deoxyribonucleic acid
DNase	Deoxyribonuclease
DNMT3A	DNA (cytosine-5)-methyltransferase 3A
DNR	Daunorubicin
EC	Endothelial cells
ECM	Extracellular matrix
EDTA	Ethylenediamine tetra-acetic acid
ELISA	Enzyme-linked immunosorbent assay
ER	Endoplasmic reticulum
ERK	Extracellular signal-regulated kinase
FAB	French–american–british cooperative group
FcR	Fc receptor
FCS	Foetal calf serum
FL	Flt-3 ligand
FLT3	Fms-like tyrosine kinase 3
GAPDH	Glyceraldehyde 3-phosphate dehydrogenase
GEO	Gene expression omnibus
GLUT1	Glucose transporter 1
GM-CSF	Granulocyte macrophage colony- stimulating factor
GPCR	G-protein Coupled Receptors
GRO	Growth related oncogene
GVC	Gancyclovir
HGF	Hepatocyte growth factor
HIF $\alpha$	Hypoxia-Inducible Factor alpha
HPC	Haematopoietic progenitor cells
HRE	Hypoxia response element

HRP	Horseradish peroxidase
HSC	Haematopoietic stem cell
HSCT	Haematopoietic stem cell transplantation
HSV-TK	Herpes simplex virus thymidine kinase
ICAM-1	Intracellular adhesion molecule-1
IDH1/2	Isocitrate dehydrogenase 1/2
IDO	Indoleamine 2,3-dioxygenase
IFN- $\gamma$	Interferon- $\gamma$
IGF	Insulin-like Growth Factor
IGFBP2	Insulin growth factor binding protein 2
IgG	Immunoglobulin
IL	Interleukin
JNK	Jun NH <sub>2</sub> - terminal kinase
kb	kilobases
KD	Knockdown
LB	Lysogeny broth
LC	Leukaemic cell
LSC	Leukaemic stem cell
LDL	Low-density lipoprotein
LFA-1	Lymphocyte function-associated antigen-1
LIC	Leukaemia initiating cells
LIF	Leukaemia inhibitory factor
LNC	Lymph node cell
MACS	Magnetic-activated cell sorting
MAPK	Mitogen-activated protein kinase
MCL-1	Myeloid cell leukaemia 1
M-CSF	Macrophage colony-stimulating factor
MDS	Myelodysplastic syndromes
MDSC	Myeloid-derived suppressor cells
mg	Milligrams
MHC II	Major histocompatibility complex class ii

MIF	Macrophage migration inhibitory factor
MIF-AS1	MIF-antisense1
MIP-1a	Macrophage inflammatory protein 1 alfa
MM	Multiple myeloma
MMP	Matrix metalloproteinase
MPN	Myeloproliferative neoplasm
MPP	Multipotent progenitors
MRC	Medical research council
mRNA	Messenger RNA
mTOR	Mammalian Target Of Rapamycin
NF-κB	Nuclear factor kappa-light-chain enhancer of activated B cells
ng	Nanograms
NGS	Next generation sequencing
NHS	National health service
NK-cell	Natural Killer cell
NMP1	Nucleophosmin 1
NUUH	Norwich and Norfolk university hospital
NOD/SCID	Non-obese diabetes/severe combined immunodeficiency
nPKC	Novel protein kinase c
O <sub>2</sub>	Oxygen
OIS	Oncogene-induced senescence
oxMIF	Oxidised MIF
p16-3MR	P16- three modal reporter
PB	Peripheral blood
PBS	Phosphate buffered saline
PCR	Polymerase chain reaction
PDX	Patient-derived xenograft
Pen-srep	Penicillin-streptomycin
PGE <sub>2</sub>	Prostaglandin E 2
PHD	Prolyl-hydroxylase
PI	Propidium iodide

PI3K	Phosphatidylinositol-3 kinase
PKC	Protein kinase c
PS	Phosphatidylserine
PTX	Pertussis toxin
PVDF	Polyvinyladine fluoride
qRT-PCR	Quantitative real-time polymerase chain reaction
RB	Retinoblastoma protein
redMIF	Reducedmif
RenLuc	Renilla luciferase
RFP	Red fluorescent protein
RIPA	Radioimmunoprecipitation assay
RNA	Ribonucleic acid
ROS	Reactive oxygen species
RPGE2	Receptor of prostaglandin E2
RPMI	Roswell Park Memorial Institute medium
RS	Replicative senescence
RT	Room temperature
SASP	Senescence-Associated Secretory Phenotype (or profile)
SCF	Stem cell factor
SDF-1	Stromal derived factor-1
SNP	Single nucleotide polymorphism
SSC	Skeletal stem cells
STAT3	Signal Transducer and Activator of Transcription 3
TET2	Tet methylcytosine dioxygenase 2
TGF- $\beta$ 1	Transforming Growth Factor- $\beta$ 1
TIS	Therapy-induced senescence
TMB	3,3',5,5'-tetramethylbenzidine
TNF- $\alpha$	Tumour Necrosis Factor- $\alpha$
TPO	Thrombopoietin
TU/mL	Transducing units per ml
TW	Transwell

uPA/uPAR	Urokinase-plasminogen-activator/uPAR receptor
VCAM -1	Vascular cell adhesion molecule-1
VEGF	Vascular-endothelial growth factor
VHL	Von hippel-lindau
VLA-4/5	Very late antigen 4/5
WHO	World health organisation
$\beta$ -gal	B-galactosidase
$\mu$ g	Microgram
$\mu$ l	Microlitre

# **1. Chapter 1: Introduction**

## **1.1. Haematopoiesis**

Haematopoiesis is the process by which blood cells are generated in the bone marrow. Haematopoietic stem cells (HSCs) give rise to haematopoietic progenitor cells (HPCs) which in turn proliferate and differentiate to reconstitute all lineages of functional blood cells (1). Early findings that lead to the discovery of HSCs were made by Till, McCulloch, and colleagues in 1960. They showed that animals that received lethal doses of irradiation could be rescued from death via transplantation with unfractionated bone marrow cells from normal non-irradiated mice (2). Three years later, they demonstrated that the colonies they observed to have formed in the spleens of the irradiated animals were formed by single cells that were capable of multilineage differentiation (3). These cells are now referred to as HSCs and they are regulated by complex cellular and molecular signals, on both genetic and epigenetic levels. Modifications in these regulatory signalling networks can lead to the dysfunction and transformation of haematopoietic cells into leukaemic stem cells (LCS) and the induction of leukaemogenesis (Figure 1.1) (4, 5). Hence understanding the regulation of haematopoiesis is essential to understanding how leukaemia evolves.

Many models have been developed to describe the process of haematopoiesis and to elucidate its complexity (6, 7). At the root of haematopoiesis are HSCs, which are defined by their ability to self-renew to allow blood production over the lifetime of an organism, and to differentiate into functional blood cells. According to the classical hierarchical models of haematopoiesis, HSCs initially give rise to common myeloid and lymphoid progenitors. The myeloid lineage includes erythroid cells that form red blood cells, granulocytes and monocytes that play a role in pathogen immunity and megakaryocytes that are involved in the production of platelets. The lymphoid lineage gives rise to T-cells, NK cells, and dendritic and B-cells that are responsible for cell mediated immunity (8). Although this simplified model still holds true, as scientific

evidence accumulates, we now know that individual HSCs gradually acquire lineage biases along multiple directions and do not necessarily pass through discrete hierarchically organised progenitor populations (9). Genetic defects in the different progenitors give rise to the different types of haematological malignancies that we know of today.

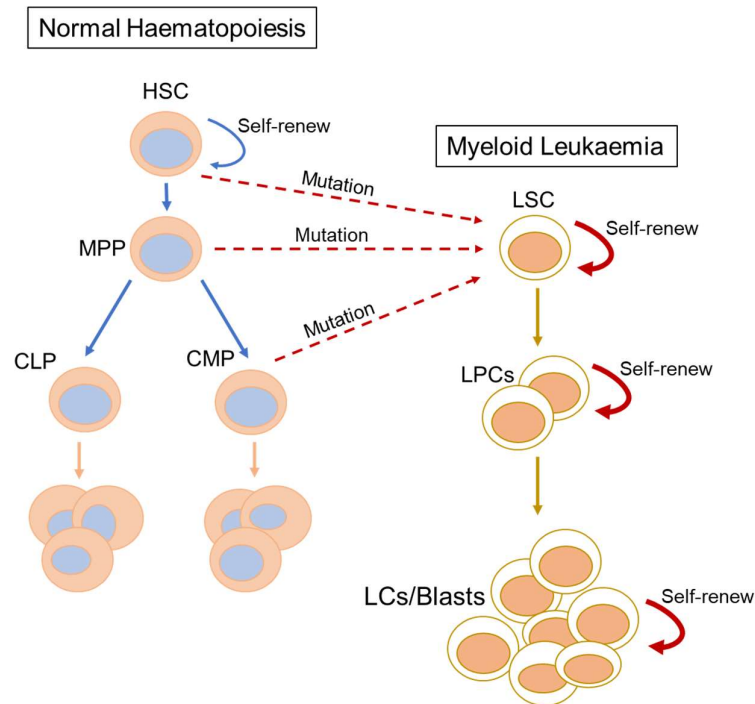


**Figure 1. 1 Normal haematopoiesis and Leukaemia stem cell model.**

Functional studies in acute and chronic leukaemias have led to the identification and characterisation of the leukaemic stem cell (LSC), which shares features with the normal haematopoietic stem cell (HSC). Leukaemic cells (LCs), also referred to as blasts, derive either from HSCs, multipotent progenitors (MPP) or committed progenitor cells (CMPs). They are characterised by increased self-renewal and reduced differentiation, compared to HSCs.

## 1.2. Leukaemogenesis

Leukaemogenesis is the process of developing leukaemia, during which many of the features of normal haematopoiesis are retained. Although genetic mutations in HSCs may pave the way for the malignant clonal expansion of leukaemic cells, these dominant clonal populations retain the hierarchical

organization found in normal haematopoiesis. Leukemic cells in acute leukaemias may acquire a primitive dysfunctional phenotype (10). Transcriptional regulators and signalling pathways that regulate the production of healthy blood cells may also be present in haematopoietic malignancies (11). Leukaemic cells replace normal bone marrow cells and, consequently, decrease and suppress haematopoiesis. Therefore, patients often present with anaemia, thrombocytopenia and granulocytopenia, that manifest in the form of frequent bruising or bleeding and a higher susceptibility to infections (12), resulting in fatigue and poor health.

Haematological malignancies originate from myeloid or lymphoid progenitors residing in the bone marrow or lymph tissues. Major myeloid malignancies include acute myeloid leukaemia (AML), which is characterised by immature and poorly differentiated cells, chronic myeloid leukaemia (CML), which is for most patients characterised by more mature cells, and myelodysplastic syndromes (MDS), which are generally disorders of bone marrow maturation where the blast count (< 20% myeloid blasts) is lower than a definite diagnosis of AML (>20% myeloid blasts). The molecular heterogeneity of these malignancies are increasingly recognised and revisions of their classification are constantly underway (13).

### **1.3. Acute Myeloid Leukaemia**

AML is the most common adult form of leukaemia and represents approximately 33% of all leukaemia cases in the UK. Over the last decade, AML incidence rates have increased by 8%, though this includes an incidence rate rise of 10% in male patients and stable rates in female patients (Cancer Research UK, 2014).

#### **1.3.1. Genetic defects in AML**

A large body of evidence indicates that AML arises through the accumulation of genomic alterations which affect the genes regulating cell proliferation, cell death and the tightly regulated pathways of haematopoietic differentiation. These key oncogenic events are often divided into two classes according to the two-hit model hypothesis of AML leukaemogenesis. In this model, class I



mutations impair normal haematopoietic differentiation, due to changes in the tyrosine kinase pathways, conferring a proliferation or survival advantage to blast cells (e.g. mutations in the fms-like tyrosine kinase-3 (FLT3), c-KIT/CD117 and RAS genes). Class II mutations are those that block myeloid differentiation and maintain self-renewability (e.g. via mutations in the AML1/ETO and CEBPA genes), or mutations that affect genes implicated in cell cycle regulation or apoptosis (e.g. p53 and nucleophosmin 1 (NPM1)) (14).

However approximately 50% of AML patients do not carry a class I mutation and recent research has shown the presence of numerous common mutations which cannot be identified as either class I or II (15). These mutations, generally termed class III, incorporate mutations in epigenetic modifiers such as DNA (cytosine-5)-methyltransferase 3A (DNMT3A), and mutations in the hydroxymethylation pathway, such as tet methylcytosine dioxygenase 2 (TET2) and isocitrate dehydrogenase 1/2 (IDH1/2) mutations (16). These findings demonstrate the limitations of the two-hit model. Furthermore, the identification of new groups of mutations would extend our understanding of the complex pathogenesis of AML.

In addition to genetic mutations, cytogenetic abnormalities can be detected in approximately 50% to 60% of newly diagnosed AML patients. These are mainly non-random chromosomal translocations that often result in gene rearrangements (17, 18). Cytogenetic and molecular genetic aberrations associated with AML are not mutually exclusive and often co-exist in the leukaemic cells (19). These co-existing aberrations can influence patient prognosis and/or predict response to therapy. Thus, their detection at the time of diagnosis represents an important clinical need.

An analysis of data collected from the Medical Research Council (MRC) AML 10 trial, which included 1612 children and adults up to 55 years of age, has shown that pre-treatment cytogenetics is an independent prognostic factor for AML. In this study, three prognostic groups (favourable, intermediate and poor prognosis) were defined by cytogenetic abnormalities detected at presentation in comparison with outcomes of patients with a normal karyotype (20).

Recently, McKerrell and colleagues developed and validated “*Karyogene*”, a comprehensive one-stop next generation sequencing (NGS)-based diagnostic platform for the genomic analysis of myeloid malignancies. It simultaneously detects substitutions, insertions, deletions, chromosomal translocations, copy number and zygosity changes in a single assay. The platform was validated on 62 AML and 50 MDS diagnostic samples previously characterised using conventional diagnostic approaches (21). The authors conclude that *Karyogene* represents an important advance that can accelerate the introduction of genomics to clinical diagnosis, this certainly holds true in the light of the complexity of AML.

### **1.3.2. Classification of AML**

A marrow or blood blast count of  $\geq 20\%$  with blasts expressing myeloid associated lineage and precursor cell markers is required for AML diagnosis. Additional specific lineage markers are helpful for identifying mixed-phenotype acute leukaemia, and so these may also be used (22).

The first descriptions of leukaemia as an alternation of “white blood” were made in 1844 by French physician, Alfred Donne, and a year later by John Hughes Bennett. In 1995, the Leukaemia Research Fund commemorated Bennett's work as the first description of leukaemia (23). What he imagined to be a single disease is now classified into multiple subgroups. The first internationally accepted classification of acute leukaemia was proposed in 1976 by the French–American–British (FAB) Cooperative Group (24). It relied primarily on morphologic and cytochemical characteristics of patient samples, and did not account for the diverse cytogenetic background of AML patients within a given group, which was, of course, unrecognised at the time of writing. Thus, this classification is presently thought to provide limited prognostic information for these groups (25) .

The more recent classification schemes proposed by the World Health Organization (WHO) require the additional evaluation of leukaemic blasts by molecular analysis and flow cytometry. This was last updated in 2008. Since then, there have been important advances in identifying unique biomarkers

associated with selected myeloid neoplasms and acute leukaemias, which were mainly obtained via gene expression analysis and NGS analysis (13).

Revisions to the categories of myeloid neoplasms and acute leukaemia were published in a monograph in 2016 and reflect a consensus of the opinions of haematopathologists, haematologists, oncologists, and geneticists (Table 1.1). The major changes in the classification and their rationale are presented in a review article by Arber et al (13) and summarised in Table 1.1 below.

Dr. Elli Papaemmanuil and colleagues (26) extended the WHO profile by combining clinical and cytogenetic information with targeted sequencing of 111 candidate driver genes in 1,540 AML patients. They concluded that 11 distinct subtypes of AML could be distinguished in their study. Most of patients in the study were younger, undergoing intensive therapy and enrolled in trials of the German-Austrian AML study groups. Interestingly, the existing WHO classification system could not sufficiently categorise 50% of the study patients. A key finding was the identification of three novel genetic subgroups that were not previously described in the WHO classification. These included mutations in genes encoding chromatin, RNA-splicing regulators, or both (18% of patients); *p53* mutations, chromosomal aneuploidies, or both (13% of patients); and an uncommon subgroup of *IDHR172* mutation (1% of patients) (26). In terms of prognosis, this study identifies that prognostic effects of some driver mutations were influenced by the presence or absence of mutations in other genes. For example, FLT3-ITD conferred a particularly poor prognosis when combined with NPM1 and DNMT3A mutations, supporting the notion that the clinical effect of some driver mutations may have depended on the existence of co-mutations in a broader genomic setting.

**Table 1. 1 WHO classification of AML and related neoplasms.**

Table extracted from Arber et al. 2016.

<b>Acute myeloid leukaemia (AML) and related neoplasms</b>
<b>AML with recurrent genetic abnormalities</b>
AML with t(8;21)(q22;q22.1); <i>RUNX1-RUNX1T1</i>
AML with inv(16)(p13.1q22) or t(16;16)(p13.1;q22); <i>CBFB-MYH11</i>
APL with <i>PML-RARA</i>
AML with t(9;11)(p21.3;q23.3); <i>MLLT3-KMT2A</i>
AML with t(6;9)(p23;q34.1); <i>DEK-NUP214</i>
AML with inv(3)(q21.3q26.2) or t(3;3)(q21.3;q26.2); <i>GATA2, MECOM</i>
AML (megakaryoblastic) with t(1;22)(p13.3;q13.3); <i>RBM15-MKL1</i>
<i>Provisional entity: AML with BCR-ABL1</i>
AML with mutated <i>NPM1</i>
AML with biallelic mutations of <i>CEBPA</i>
<i>Provisional entity: AML with mutated RUNX1</i>
<b>AML with myelodysplasia-related changes</b>
<b>Therapy-related myeloid neoplasms</b>
<b>AML, NOS</b>
AML with minimal differentiation
AML without maturation
AML with maturation
Acute myelomonocytic leukaemia
Acute monoblastic/monocytic leukaemia
Pure erythroid leukaemia
Acute megakaryoblastic leukaemia
Acute basophilic leukaemia
Acute panmyelosis with myelofibrosis
<b>Myeloid sarcoma</b>
<b>Myeloid proliferations related to Down syndrome</b>
Transient abnormal myelopoiesis (TAM)
Myeloid leukaemia associated with Down syndrome

### **1.3.3. Current treatment of AML**

AML is primarily a disease of the elderly with a median age at diagnosis of 72 years (quartile value, 60-79 years; range, 16-97 years; mean, 68 years) (27). Over the last 50 years there has been improved survival in the minority group of younger fitter patients mainly under the age of 65. However, older frail patients have seen no similar improvement, because the capacity to safely deliver the necessary intensive cytotoxic treatment to achieve a cure is compromised by the patients general physical health (28).

AML in younger fitter patients is mainly treated with chemotherapeutic drugs that inhibit cell proliferation. Induction therapy with cytarabine and an anthracycline remains the standard of care in AML Treatment happens in two phases – (i) intensive induction therapy to abolish the bulk of leukaemia cells, and (ii) a tailored consolidation therapy, aiming to maintain long term remission. The standard approach involves 7-10 days of cytarabine and 3 days of anthracycline administration (29).

Although advances in the treatment of AML have led to significant improvements in outcomes for younger patients, prognosis in the elderly who account for the majority of new cases remains poor (30). Even with current treatments, as much as 70% of patients aged  $\geq 65$  would die of their disease within 1 year of diagnosis (31). Current AML management still mostly depends on intensive chemotherapy and +/- allogeneic haematopoietic stem cell transplantation (HSCT), at least in younger patients who can tolerate such intensive treatments better, for older patients however, the existence of co-morbidities (non-AML related factors) complicates treatment decisions and calls for more personalised management plans and frequent palliative symptom based care (32).

### **1.4. The bone marrow microenvironment (BMM)**

The bone marrow (BM) is the major site of haematopoiesis and bone formation. Thus, in addition to containing haematopoietic cells, the BM contains cells that contribute to bone homeostasis. Recently, researchers have focused on the bone marrow microenvironment (BMM) and its role in

haematopoietic malignancies. Multiple studies have demonstrated that interactions with the different non-haematopoietic cell types in the BM contributes to the survival of leukaemic cells both *in vitro* and *in vivo*. Additional studies have shown that leukaemic cells compete for BMM resources, thereby creating a medium that co-participates in the development and progression of the disease. This section will give an overview of these studies and highlight the role of BM cells in regulating normal HSC function.

#### **1.4.1. Cellular components of the BMM**

The BM is made of a combination of cells that interact to regulate haematopoiesis, including arteriolar and sinusoidal type endothelial cells (ECs), osteolineage cells (osteoclasts and osteoclasts), fat cells (adipocytes), sympathetic neurons, non-myelinating Schwann cells, bone marrow (mesenchymal) stromal cells (BMSCs), CXCL12-abundant reticular cells (CAR cells), macrophages, megakaryocytes and the extracellular matrix (ECM) (33, 34). These cellular components work in harmony to regulate all the steps of the haematopoiesis cascade, and are thought to affect HSC and HPC number, location, proliferation, self-renewal, and differentiation. Therefore, they are also likely to affect the production parameters of leukaemic cells similarly (35).

Histological and functional assays indicated that HSCs and HPCs preferentially occupy the endosteal and subendosteal regions (endosteal niche) , closer to the bone surface (36). On the other hand, committed progenitors and differentiated cells are distributed in the central and peri-sinusoidal regions (vascular niche), respectively (Figure 1.2) (37-39). BM cells are organised into niches that support specific subsets of haematopoietic progenitors. A niche is defined as the anatomical location in which HSC reside (40). The existence of the niche was first proposed by Schofield in 1978 (41). Since then, considerable progress has been made in defining the structure and components of the niche (42, 43), which has helped to understand the contribution of each individual cell type within the BMM to the pathogenesis of AML.

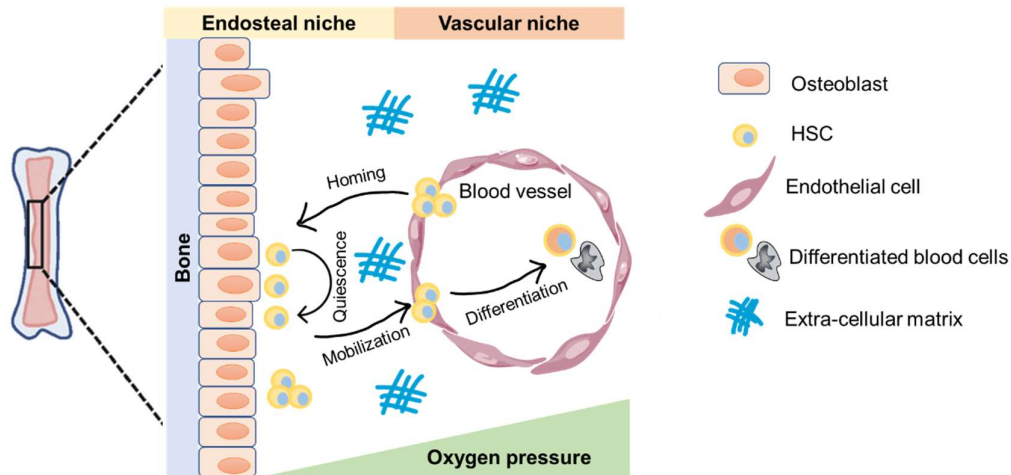


**Figure 1. 2 A model of the haematopoietic stem cell (HSC) niche.**

Regions within the BM are broadly divided into endosteal and vascular niches. HSCs transit between the endosteal and vascular niche, the endosteal niche facilitates HSC maintenance and quiescence (the state of cell dormancy) while the vascular niche facilitates HSC proliferation and differentiation.

Central to the establishment of the HSC niche are BMSCs, sometimes called multipotent or mesenchymal stem/stromal cells, which can differentiate into the different types of cells that make up the stromal components of the BM, including adipocytes, chondrocytes, myocytes, osteoblasts and osteoclasts (44, 45). The role of each of these cell types is extensively reviewed by Shafat et al. (46). The following sections will, however, focus on defining the BMSC population and explaining their role in haematopoiesis and in the leukaemogenesis of AML.

#### **1.4.2. Bone marrow mesenchymal stem cells (BMSCs)**

The identification of mesenchymal stem/stromal cells represents one of the most controversial and puzzling areas in stem cell biology. Recently, efforts have been made in this field to clearly define what BMSCs are and a common understanding is that they are ubiquitous in connective tissue and are phenotypically similar to skeletal progenitor cells and pericytes (46). Bianco et al., pioneers in the field of bone and marrow cell biology and development, have recently identified a progenitor for these BMSCs and have redefined them more stringently, based on *in vivo* differentiation capability, as skeletal

stem cells (SSC) (47). These cells are found on the surface of the blood vessels of the bone marrow (sinusoids) and are capable of organizing the haematopoietic microenvironment and stem cell niche (48). Sacchetti et. al. contributed further by demonstrating that BMSCs are not ubiquitous but have a different transcriptome and varying differentiation capacities for every tissue of a certain origin. They were identified as CD34 negative, CD45 positive, and CD146 positive cells and in the BM they are referred to as pericytes or perivascular cells (49).

Conventionally, BMSCs cultured *in vitro* are characterised by their adherence to plastic, their capacity for osteogenic, chondrogenic and adipogenic differentiation, their expression of a panel of fibroblast related surface markers, (namely CD105, CD106, CD90 and CD73) and their lack of expression of haematopoietic markers such as CD34 and CD45 (50). This characterization approach was applied to the cells used in the research presented in this thesis.

#### **1.4.3. BMSCs and normal haematopoiesis**

Nearly all factors that regulate HSC maintenance are expressed by multiple cell types in BM niches, including BMSCs. These factors interact with their counterparts that are expressed on HSCs. The crucial decision between self-renewal or differentiation and quiescence or proliferation is tightly regulated by the integration of intrinsic and extrinsic signals provided by the microenvironment in which HSCs reside (51).

BMSCs secrete a number of cytokines that are essential for HSC function and maintenance, including CXCL12 (also called stromal derived factor-1, SDF-1) and stem cell factor (SCF) which are involved in HSC maintenance (35). Depletion of SDF-1 expressing BMSCs leads to reduced retention of HSCs and to reduced homing of transplanted HSCs (52). HSC homing to and retention in the BM, or its mobilisation to the peripheral blood is to a large extent regulated through SDF-1 (53). SDF-1 is produced by more than one type of BM cell including osteoblasts (54), BMSCs and CAR cells (55, 56). SDF-1 binds and activates the CXCR4 receptor on HSCs (56). This is demonstrated by studies in which the administration of plerixafor (Mozobil,



AMD3100) – a bicyclam that inhibits SDF-1 binding to CXCR4 – resulted in the mobilisation of HSCs to the peripheral blood of healthy subjects (57, 58). Other studies have shown that SDF-1 and CXCR4 binding activated a number of integrins such as very late antigen 4/5 (VLA-4/5) and lymphocyte function-associated antigen-1 (LFA-1) on HSCs, which in turn induced cell adhesion to BMSCs and other BM cells that bore the vascular cell adhesion molecule-1 (VCAM-1) and the intracellular adhesion molecule-1 (ICAM-1) (59).

SCF functions by binding to c-Kit, a tyrosine kinase receptor expressed on all HSCs. It was found that even small changes in c-Kit signalling profoundly affected HSC function (60). Therefore, almost all cytokine combinations used for culturing HSCs, to date, include SCF. Deletion of SCF in perivascular BMSCs led to a decrease in HSC frequency in the BM of mice (61). The membrane-bound form of SCF is also an adhesive molecule for HSCs to the BMM (62).

In addition to SCF and SDF-1, BMSCs isolated from BM produce several other haematopoietic growth factors and chemokines, including Flt-3 ligand (FL), thrombopoietin (TPO), the interleukins (IL) IL-6, IL-7 and IL-11, macrophage colony-stimulating factor (M-CSF), tumour necrosis factor- $\alpha$  (TNF- $\alpha$ ), transforming growth factor- $\beta$ 1 (TGF- $\beta$ 1) and leukaemia inhibitory factor (LIF) (63, 64). Each of these factors, either individually or collectively, are known to contribute to haematopoietic homeostasis.

#### **1.4.4. The role of BMSCs in the malignant BM**

Genetic aberrations in self-renewing HSCs are well established as main intrinsic drivers of leukaemogenesis. These cells gain a competitive advantage over normal HSCs and give rise to the disease-propagating leukaemic cells, also referred to as leukaemic stem cells (LSCs) (65).

In the haematopoietic niche, leukaemic cells interact with BMSCs to create a microenvironment that is favourable for leukaemic cell survival. BMSCs play a fundamental role in the growth, proliferation and survival of leukaemic cells, by facilitating interactions between them both through paracrine and autocrine signalling molecules. Furthermore, cell–cell and cell–matrix adhesion

promotes leukaemia cell survival through activation of pro-survival and anti-apoptotic pathways, chemotherapy resistance, and consequently, the persistence of (minimal) residual disease (66-68).

For example, both direct stromal contact and stroma-derived soluble factors are involved in extracellular regulated kinase (ERK)-mediated resistance to FLT3 inhibitors in FLT3-mutated AML (69) and resistance to anti-CD44 therapy. CD44 is an adhesion molecule that is highly expressed by AML cells, where its inhibition induces differentiation and apoptosis of the leukaemic blasts (70-72). Likewise in CML, which overexpress CD44, anti-CD44 treatment reduces CML burden in CML xenografts (73). BMSCs can also activate survival pathways in leukaemic cells. Recently, AML-derived BMSCs have been shown to induce NOTCH signalling in AML cells, the inhibition of NOTCH in AML abrogated their chemo-resistance (74). Goh and colleagues found that the blockade of a stromal derived cytokine, named colony stimulating factor-1 (CSF-1), delayed AML progression *in vivo* (75). These studies, thus, highlight the role of BMSC-derived signals in the progression of myeloid malignancies and their resistance to chemotherapy.

The interaction between VCAM-1 and VLA-4 on BMSCs and AML cells, respectively, plays an integral role in the activation of nuclear factor kappa B (NF- $\kappa$ B) survival pathways in the stromal and tumour cell compartments (76). AML cells have been shown to express high levels of CXCR4 which responds to SDF-1 produced by BMSCs. Homing of leukaemic cells to the BM contributes to their protection from chemotherapy, which is why inhibitors have been developed to interrupt this interaction and mobilise AML cells to the peripheral blood where they can be killed by chemotherapy (77). In fact, the inhibition of the CXCR4–SDF-1 interaction overcomes AML cell line resistance to kinase inhibitors (78, 79).

AML cells have been found to remodel BMSCs and increase their expression of SDF-1 (80). However, in a recent study Agarwal and colleagues showed that in a mouse model of CML, the decreased expression of SDF-1 by ECs reduced the number of long term repopulating HSCs, whereas the decreased

expression of BMSC-derived SDF-1 lead to an increase in the number of the HSCs (81). These findings suggest that SDF-1 serves different functions depending on its cell of origin.

Since SDF-1 is expressed in both ECs and BMSCs (82) it could be assumed that a similar mechanism would hold plausible. A recent study has shown an interesting mechanism by which myeloproliferative neoplasm (MPN) cells caused the mobilisation of HSCs to the peripheral blood, due to increased neuropathy and BMSC apoptosis. These studies found that MPN-derived Interleukin-1 $\beta$  (IL-1 $\beta$ ) damaged Schwann cells that protect the endings of sympathetic nerves, leading to neuropathy, increased BMSC apoptosis, and the decreased expression of HSC retention factors and adhesion molecules by BMSCs (VCAM1, SDF-1 and SCF). This eventually lead to the mobilisation of normal HSCs to the peripheral blood (83). Taken together, these studies demonstrate that a deregulated expression of SDF-1 by BMSCs appears to be a common feature in myeloid malignancies.

Extracellular vesicles, such as exosomes, traffic protein and RNA between cells and are key players in cell-cell communications (84). In multiple myeloma (MM), which is a malignancy of plasma cells, exosomes isolated from BMSCs of patients with MM induced MM tumour growth and promote disease progression in an *in vivo* translational model (85). Similar findings have recently been demonstrated in MDS where MDS- patient derived macrovesicles were found to contain microRNAs that differed from those derived from healthy donors, which induced changes in CD34+ HSCs *in vitro* (86). Stromal exosome trafficking is also a candidate mechanism for extrinsic chemoresistance within the AML niche. Stromal exosomes have been shown to be enriched for a number of known pro-tumoural factors, including TGF- $\beta$ 1, MIR155 and MIR375 as well as cytokines essential for AML survival such as interleukin-8 (IL-8) (87). To summarise all the points above, BMSCs play a central role in AML pathogenesis via a multitude of cell-cell interactions.

#### 1.4.5. Leukaemic cell remodelling of the BMM

Leukaemic cells have been shown to modify niche signalling and to remodel the niche in their favour, allowing them to evade therapy and to disrupt normal HSC development (88-90). The mechanisms underlying this have been the focus of numerous studies. For instance, a number of AML mutations, including the FLT3-ITD mutation, can increase AML reactive oxygen species (ROS) levels (91). This in turn increases the proliferative ability of AML cells and, possibly, decreases the proliferation of the surrounding normal progenitor cells (92).

AML cells can also actively participate in boosting the BM vascular density, which is a recognised feature of the leukaemic BM (93). This happens partially due to the AML activating the endothelial cells (EC) and recruiting them to the site of vasculogenesis, and by inducing the ECs to produce vascular-endothelial growth factor (VEGF), which amplifies angiogenesis in the BM (94, 95).

Another common feature of myeloid malignancies is increased bone fibrosis. A landmark study by the Passegué laboratory demonstrated that through a combination of direct cell-cell contact and soluble factors (thrombopoietin, TPO and macrophage inflammatory protein 1a, MIP-1a), mouse CML cells were able to stimulate the overproduction of osteoblasts by BMSCs, thereby leading to fibrosis (96). In a human primary MDS co-culture model, MDS cells were sufficient to induce an MDS-like phenotype in BMSCs from healthy donors. MDS-like features included increased expression of proangiogenic factors (VEGF and IGFBP2 – insulin growth factor binding protein 2) and of fibrosis mediators such as LIF (97). Interestingly, MDS patients with fibrotic bone marrow are more likely to progress to AML than MDS patients with non-fibrotic BM features (98).

As mentioned earlier in Section 1.4.4, communication between BMSCs and MDS cells is partly mediated by extracellular vesicles. CML-derived exosomes stimulate BMSCs to produce IL-8, which in turn can modify the leukaemic malignant phenotype *in vitro* and *in vivo* (99). Similarly, primary AML cells and

AML cell lines release microvesicles containing RNAs that has been shown to alter the secretory profile of murine bone marrow stromal cells (100). More recently, Kumar et al elegantly demonstrated that AML-derived exosomes primed animals for accelerated AML growth, they found that treatment of BMSCs with AML-derived exosomes decreases the expression of genes supporting normal haematopoiesis and osteogenesis and increases expression of genes supporting AML growth (101). Therefore, exosomes appear to be part of the malignant phenotype across a spectrum of myeloid malignancies.

Jacamo and colleagues very recently performed gene expression profiling of BMSCs isolated from normal C57BL/6 mice versus BMSCs isolated from mice inoculated with syngeneic murine leukaemia cells carrying different human AML genotypes (that were developed in mice with p53 wild-type or nullgenetic backgrounds). They revealed that all the tested AML genotypes modified a unique set of genes in the BMSCs. Also, that there were sets of differentially-expressed genes in AML-exposed BMSCs that were unique to the particular AML genotype or p53 status (102). These findings support the hypothesis that AML cells alter the transcriptome of BMSCs, in both common and genotype-specific ways, and might, in part, explain the variation in response to therapy that is observed in AML patients of different genetic profiles.

Taken together these findings reinforce the notion that AML cells and BM niche cells are tightly interweaved dynamic structures that, together, drive the development and progression of disease in the BM microenvironment.

#### **1.4.6. Niche-induced oncogenesis**

Different niche cells can harbour genetic defects that may initiate and contribute to AML development. This is termed niche-induced oncogenesis. For instance, genetic modifications such as the deletion of *Dicer1* (coding for a protein involved in microRNA biogenesis) and *SBDS* (the gene mutated in Schwachman–Bodian–Diamond syndrome, related to bone marrow failure and with a high risk of developing leukaemia) in osteoprogenitor cells led to MDS and secondary AML in murine models (103-105). Reduced expression

of Dicer1 and the SBDS gene has also been observed in BMSC from patients with MDS (106, 107). Geyh and colleagues reported that AML and MDS derived BMSCs had limited osteogenic differentiation, partially due to an overexpression of Jagged1, a NOTCH signalling ligand (108, 109).

Cytogenetic abnormalities have been reported in 30-70% of BMSCs from MDS and AML patients, albeit in relatively small sample sizes (110, 111). Further studies have shown that BMSCs originating from MDS and AML patients have a distinct expression profile and harbour some genetic abnormalities that are believed to be pro-leukaemic (112-114), including transcriptional (97) and epigenetic modifications (115). Other studies, however, report that BMSCs from MDS, CML and AML patients exhibit normal differentiation, adhesion, expression, survivability and a capacity to normally support haematopoiesis *in vitro* (116, 117). Overall, these studies leave us with an open debate as to what the functional consequences of genetically deregulated BMSCs might mean for myeloid malignancies.

#### **1.4.7. Chemokine and cytokine profiles in the malignant BM**

Cytokines and chemokines are involved in the cross talk between AML cells and the microenvironment. Systemic (serum or plasma) chemokine levels are suggested to serve as biomarkers for disease development or activity, as well as treatment responses (118). The overexpression of cytokines in AML patients declines in complete remission, suggesting that these events are dependent on AML activity and, in part, due to autonomous blast cytokine secretion (119). High constitutive release is not necessarily associated with increased systemic chemokine levels however, this may, at least, partly be explained by the fact that the systemic levels are determined by a balance between release and binding/degradation. This observation also demonstrates that systemic cytokine levels do not necessarily reflect the local BM cytokine network (118).

Deregulated cytokine, chemokine and growth factor expression, and abnormal responsiveness to the aforementioned in leukaemia are well documented (120). For example, levels of interleukin-3 (IL-3), interleukin-6 (IL-6),

interleukin-8 (IL-8), thrombopoietin, tissue necrosis factor alfa (TNF- $\alpha$ ), macrophage colony-stimulating factor (M-CSF), interferon- $\gamma$  (IFN- $\gamma$ ), and SCF have been shown to be elevated in leukaemia patients compared to healthy controls (121). AML patients with a lower serum concentration of hepatocyte growth factor (HGF) had improved leukaemia-free survival rates compared to patients with higher HGF levels (122). In AML and MDS patients, higher levels of TNF- $\alpha$  negatively affected overall survival (123), whereas increased VEGF-A levels correlated with reduced survival in AML (124). These studies have mainly focused on cytokines, chemokines, and growth factors that are typically found in the serum of untreated or treated AML patients. Nevertheless, cytokine and chemokine profiles of BM samples from AML patients are relatively fewer, and are mainly derived from *in vitro* co-culture studies that aim to replicate the microenvironment.

A recent study by Reikvam and colleagues looked at the cytokine network in co-cultures of cells derived from 18 unselected AML patients, as well as with BMSCs derived from three healthy donors. They report that BMSCs cultured on their own showed relatively high levels (comparable or higher than the corresponding median level for AML cells alone) of IL-8, IL-6, and a few matrix metalloproteinases (MMP) (such as MMP-1, MMP-2 and TIMP-1). The levels of these mediators in AML–BMSC co-cultures were also relatively high, and included IL-8 and IL-6. Interestingly, normal HSCs did not induce as much change when co-cultured with BM-MSCs. AML cells increased the BMSC expression of genes involved in TLR initiated and NF $\kappa$ B mediated intracellular signalling, which is vital to cytokine/chemokine signalling in these cells (68).

A more recent study by Lope and colleagues employed a similar approach and methodology. However, this study used patient-derived BMSCs, and they reveal that de novo AML derived BMSCs expressed high levels of SDF-1, receptor of prostaglandin E2 (RPGE2), indoleamine 2,3-dioxygenase (IDO), interleukins IL-1 $\beta$ , IL-32, IL-6 and VEGF, which are secreted by the leukaemic cells to promote their survival and proliferation. Furthermore, the increased SDF-1, RPGE2 and IDO levels helped in remodelling the mesenchymal niche in the BM (125).

The cytokine/chemokine release profile of the bone marrow is modified by a number of factors including hypoxia, differentiation status, pharmacological interventions, and T-cell cytokine responses (126). So far, the best investigated single chemokine in AML is SDF-1, which binds to CXCR4, and which has been discussed in previous sections of this introduction (sections 1.4.3 and 1.4.4). Also of particular importance is IL-8, which is usually released at highest levels (126, 127). The research from this thesis will partially address the regulation of the AML pro-survival cytokine, IL-8, in the stromal compartment.

The following sub-sections will review cytokines and chemokines that are of relevance to the work presented in this thesis.

#### **1.4.7.1. Interleukin-8 (IL-8)**

IL-8, also called CXCL8, is a pro-inflammatory chemokine, which was first discovered to be associated with the promotion of neutrophil chemotaxis and degranulation (128). This chemokine activates multiple intracellular signalling pathways downstream of two cell-surface G protein-coupled receptors (GPCRs), namely CXCR1 and CXCR2 (129). Increased expression of IL-8 and/or its receptors has been observed and characterised in cancer cells, ECs, infiltrating neutrophils, and tumour-associated macrophages (130).

Bruserud and colleagues attempted to classify a cohort of AML patients based on constitutive chemokine release from AML cells. They investigated the release of a wide range of chemokines from 68 primary human AML blasts, and learned that chemokine levels varied widely, even for those patients with detectable release. They found that the highest level of constitutive expression was detected for IL-8, a mediator angiogenesis in the BM via its receptor, CXCR2 (127, 131). This data suggests that IL-8 may function as a significant regulatory factor within the tumour microenvironment. In fact, the importance of IL-8 and CXCR2 in the pathogenesis of cancer comes from studies in solid tumour, and in particular preclinical studies in breast cancer, in which IL-8 seemed to have an important microenvironmental role (132-134).



In AML, evidence of the importance of IL-8 to leukaemic cells dates back to 1993 (135). IL-8 was found to be overexpressed (136), and moreover serum IL-8 levels were found to be increased in haematological malignancies compared to healthy controls (137). Interestingly, in normal haematopoiesis, IL-8 seems to play an inhibitory role in proliferation and differentiation (138, 139), which suggests that IL-8 provides a survival advantage to leukaemic cells.

Jacamo et al. reported high IL-8 mRNA levels in BMSCs derived from AML and acute lymphoblastic leukaemia (ALL) patients, compared to BMSCs derived from healthy donors. In addition, co-cultures of normal BMSCs with AML and ALL cell lines and primary samples induced the expression of IL-8 in an NF- $\kappa$ B-dependent manner (76). Finally, in an another study, inhibition of the IL-8 receptor, CXCR2, selectively inhibited proliferation of MDS/AML cell lines and patient samples (140). Together, these studies suggest a complex role for IL-8 in regulating the survival and proliferation of multiple tumours, including AML.

#### **1.4.7.2. Interleukin-6 (IL-6)**

IL-6 is a multifunctional cytokine, with pleiotropic inflammatory effects, and is important for immune responses, cell survival, apoptosis, and proliferation (141). IL-6 has been reported to be important for the development of CML (142). A monoclonal antibody directed against human IL-6 has been evaluated in haematological malignancies such as MM, MDS and non-Hodgkin lymphomas (143). AML cells have been shown to secrete IL-6, however, IL-6 on its own is not known to be sufficient to stimulate *in-vitro* colony formation. Rather, it acts as a co-stimulator to enhance CSF-induced clonogenicity of AML blast cells (144).

Sanchez-Correa and colleagues reported that in AML, patients with higher serum IL-6 and lower serum IL-10 levels had worse survival rates than those with low IL-6 serum levels. Contrary to IL-8 which is consistently reported to be pro-leukaemic, IL-6 demonstrated different effects (stimulatory, inhibitory or neutral) on the growth of leukaemic cells derived from AML and MDS

patients (123, 145). These studies suggest that the role of IL-6 in AML remains undefined.

#### **1.4.7.3. Macrophage migration inhibitory factor (MIF)**

Macrophage migration inhibitory factor (MIF) is a pleiotropic cytokine that, under normal conditions, regulates cell mediated immunity and inflammation (146). MIF was originally discovered in 1966 by Bloom and Bennett as an activated T-cell and macrophage derived cytokine (147). In the early 1990s, MIF was rediscovered as a clinically relevant factor that potentiated lethal endotoxemia (defined as the presence of endotoxins in the blood) (148). In contrast to other pro-inflammatory cytokines that require *de novo* synthesis before being secreted MIF is pre-formed and stored within vesicles in the cell cytoplasm, allowing for rapid release upon cell stimulation (149).

Recently, a study investigating metastasis of pancreatic ductal adenocarcinomas showed that MIF can also be transported in exosomes that affect surrounding niche cells (150). The MIF gene does not encode for a N-terminal signal sequence and, therefore, the MIF protein cannot translocate to the endoplasmic reticulum (ER) for mediated secretion, following the classical ER pathway. MIF is released from cells via a non-classical pathway involving the ATP-binding cassette transporters (ABCA1), and exhibits autocrine as well as paracrine effects (151).

In terms of biological function, MIF has been shown to override the anti-inflammatory effects of glucocorticoids and its plasma levels have been shown to correlate to cortisol circadian levels. These observations led some to propose its principal role as that of an endogenous counter regulator of glucocorticoids (152, 153). In the context of human cancers, studies have shown that MIF can inhibit p53-mediated apoptosis of human lung adenocarcinoma cell lines and stimulate cell proliferation (154). Moreover, MIFs have also been shown to affect cell migration and chemotaxis in a pulmonary metastasis model, where it was identified as a key effector of human MSC tumour homing *in vitro* (155). These studies together suggest a wide spread activity of MIF in normal and malignant cells.

MIF has been shown to exert its effects by binding to CD74, CXCR2, CXCR4 and CXCR7 chemokine receptors (156). CD74 is MIFs widespread and most extensively studied receptor. It is a cell surface protein expressed as the invariant chain (Ii) of the major histocompatibility complex class II (MHC II) and forms a complex with CD44, initiating an intracellular signalling cascade (157, 158). Moreover, emerging evidence suggests the formation of heterodimers of CD74 with either CXCR2 or CXCR4 (159, 160) and MIF binding to CXCR7 (161).

In cancer, MIF has been shown to be overexpressed in various types of solid tumours including breast, prostate, and colon (162-164). In a model of lung cancer, a suicide substrate inhibition of MIF inhibited lung adenocarcinoma cell migration and anchorage-independent growth (165). In haematological malignancies, namely chronic lymphocytic leukaemia (CLL) and MM, MIF is believed to drive malignant development (166, 167). A number of mechanisms have been proposed as to how MIF may influence the development of cancer.

Recently, MIF has been shown to induce NF- $\kappa$ B activity and increase the expression of antiapoptotic molecules (168). Early evidence for MIF involvement in haematological malignancies came from a mouse model of myc-driven B-cell lymphoma where loss of MIF expression was shown to delay the onset of B-cell lymphoma development (169). In CLL, it has been shown that MIF is expressed by the malignant cells and induces protective IL-8 release in an autocrine dependent manner, and that blocking either MIF or IL-8 reduces the survival of CLL cells (170).

Taken together, these studies show that the heightened expression of MIF and the increased secretion of IL-8 has wider significance to the tumour microenvironment. This is of particular interest in AML, as evidenced by the role of IL-8 in its development. The role of MIF in AML remains to be addressed and the research in this thesis will in part define the role that MIF plays in the AML microenvironment.

#### **1.4.8. Cell signalling in the AML microenvironment**

Cytokines, chemokines, and adhesion molecules activate pro-survival signalling pathways in their target cells. A number of signalling pathways have been identified in AML. These include, but are not limited to the phosphatidylinositol-3 kinase PI3K/Akt/mTOR, mitogen-activated protein kinase (MAPK), signal transducer and activator of transcription 3 (STAT3), and NF- $\kappa$ B pathways, that regulate downstream components by promoting autonomous and microenvironment dependent survival and proliferation of AML cells (171).

Simultaneous activation of signalling pathways have been shown to confer adverse prognosis for AML patients (172). Several therapies have been developed to target these pathways in AML cells. However due to AML being a heterogeneous disease, and also due to the fact that these signalling pathways are important for stromal cells in the BM micro-environment, therapies undergoing developed will need to take these factors into consideration.

The following sections will briefly review the signalling kinase pathways that are relevant to the research presented in this thesis.

##### **1.4.8.1. Phosphatidylinositol-3-kinase (PI3K)/AKT/mTOR signalling**

The members of this pathway control the expression of proteins that regulate both apoptosis and cell cycle progression/proliferation (173, 174), and cell migration downstream of the SDF-1/CXCR4 axis (175). Studies have shown that 50%–80% of AML patients display Akt that is phosphorylated at T308, S473 or both. The causes for the activation of PI3K-Akt-mTOR signalling include activating mutations in FLT3, c-KIT/CD117 or RAS genes, as well as growth factor stimulation such as SDF-1. Taken together this has made inhibition of PI3K-Akt-mTOR a strong therapeutic strategy of interest in AML (176).

It is however, important to remember that this pathway is also important for signalling in other cellular components of the BM, including BMSCs, where it

is involved in BMSC differentiation into the three mesenchymal lineages and, furthermore, trans-differentiation into myoblasts and neurons (177). Moreover, the pathway is important for BMSC adaptation to the hypoxic BM microenvironment (178), and for regulation of BMSC metabolism and the induction of autophagy (179). Finally, the pathway contributes to the regulation of BMSC communication with other BMM cells (180). As a result, one would expect PI3K-Akt-mTOR inhibition to alter the BMSC functional characteristics and thus also affect the AML BM microenvironment crosstalk.

#### **1.4.8.2. Mitogen-activated protein kinase (MAPK) signalling**

Three major groups of MAP kinases exist: the p38 MAP kinase family, the extracellular signal-regulated kinase (ERK) family, and the c-Jun NH<sub>2</sub>-terminal kinase (JNK) family. All three are important signalling molecules in normal hematopoiesis as well as in leukaemogenesis (181). The relevance of these pathways in AML has been shown in several reports describing a constitutively activated MAPK in AML (182, 183). Therapeutic targeting of MAPK activation using a pharmacological blocker, PD98059 decreases both growth and survival of AML cell lines as well as primary cells (184).

The ERK pathway has been shown to cooperate with FLT-3 in regulation of cell survival (185). Moreover, BMSCs are known to activate PI3K/Akt and ERK/MAPK in FLT3 mutant AML cells, and to confer resistance to both chemotherapy and FLT3 inhibition (78). MAPK signalling in the stromal compartment is relatively less defined. Studies however, have exhibited the activation of this pathway in BMSCs. In a Chinese study, AML derived proteases have been shown to up-regulate VEGF production in AML BMSCs via the PAR-2, ERK1/2, and MAPK signalling pathways (186). Moreover, in a study on paediatric MDS, inhibition of MAPK disrupted proinflammatory factor production by MDS-derived BMSCs. Da Costa and colleagues observed MAPK to be constitutively expressed in MDS-AML derived BMSCs (187).

#### **1.4.8.3. Protein kinase C (PKC) signalling**

The PKC family comprises of 12 closely related serine/threonine kinase isoforms. Mammalian PKCs share common catalytic domains but differ in their

regulatory domains which dictate the co-factors required for required for the kinases' activation (188). PKC isoforms are subdivided into three subfamilies according to their activation profiles: conventional PKCs (cPKC:  $\alpha$ ,  $\beta$ I,  $\beta$ II,  $\gamma$ ), novel PKCs (nPKC:  $\delta$ ,  $\epsilon$ ,  $\eta$ ,  $\theta$ ), atypical PKCs (aPKC:  $\zeta$ ,  $\iota/\lambda$ ), and additionally, the more distantly related PKC $\mu$ /PKD and PKC $\nu$  (189). conventional PKCs require DAG, Ca<sup>2+</sup>, and phospholipid for activation. Novel PKCs do not require Ca<sup>2+</sup> for activation, but are still dependent on phospholipids and DAG. Atypical PKC isoforms are activated independently of Ca<sup>2+</sup> and DAG (190, 191).

PKCs are ubiquitously expressed and are essential for the regulation of cell proliferation, apoptosis, differentiation and migration (190, 192). PKCs have been linked to oncogenes, including RAS and MYC, which places them at the core of cancer signalling pathways (193). Interestingly not all PKCs act as oncoproteins, for example, PKC $\delta$  is anti-apoptotic in CLL (194), but pro-apoptotic in AML (195, 196). Also, PKC $\alpha$  shows proliferative functions in several malignancies but has antiproliferative functions in colon cancer cells (197). In AML, high levels of PKC $\alpha$  conferred an adverse prognosis for AML patients (198), while a PKC $\delta$  agonist, PEP005, induces apoptosis in AML cells (199). Interestingly, PEP005 can increase the release of several cytokines, both via AML cells and the neighbouring non-leukaemic immune cells (200).

Activation of PKC in the stromal environment has first been shown in CLL where the co-culturing of CLL cells with BMSCs led to an up-regulation in PKC $\beta$ II expression, and the consequent activation of NF- $\kappa$ B signalling in BMSCs, which was essential for CLL cell survival (201). Part of the research presented in this thesis investigates the role of PKCs in AML remodelling of BMSCs.

## **1.5. Hypoxia in Cancer**

Hypoxia is defined as a sub-physiological level of oxygen; the physiological range varies due to diverse vascular density in different organs (202). Hypoxic conditions develop during cancer progression due to rapidly proliferating tumour cells that reduce O<sub>2</sub> diffusion, as well as due to impaired perfusion of the abnormal blood vessels in the tumour. The oxygen level in hypoxic tumour

tissues is found to be less than 1.3% O<sub>2</sub>, far below the physiologic oxygenation level (5%–10% O<sub>2</sub>) (203).

The presence of hypoxia in cancerous tissue was first reported in solid tumours. In 1955, Thomlinson and Gray observed in samples of human lung cancer tissue that hypoxic, yet viable, lung carcinoma rods were surrounded by a necrotic core caused by a tissue oxygen gradient (204). All types of solid tumours, in particular malignant solid tumours, are subject to hypoxia. Often displaying oxygenation levels significantly lower than their tissue of origin, hypoxia in solid tumours is widely involved in angiogenesis, metastasis, and tumour resistance (205). The overexpression of hypoxia-inducible factor alpha (HIF $\alpha$ ) subunits in solid tumours is associated with aggressive cancer phenotype and is correlated with poor overall survival of patients (206). As haematological malignancies are not considered solid tumours, the role of hypoxia in these diseases was initially presumed to be insignificant (207). However, hypoxia is a hallmark of the haematopoietic niche (208, 209) and is now an actively researched topic in haematological malignancies.

Next, the current understanding of the role of both, hypoxia and hypoxia-inducible factors in the BMM, will be reviewed.

### **1.5.1. Hypoxia inducible factors (HIFs)**

The hypoxic state is principally maintained by members of the hypoxia-inducible factor (HIF) family. Both HIF1 $\alpha$  and HIF2 $\alpha$  respond to hypoxia; HIF1 $\alpha$  responds to acute hypoxia and HIF2 $\alpha$  to a chronic hypoxic state (210). HIF1 $\alpha$  is expressed ubiquitously in all cells, whereas HIF2 $\alpha$  is selectively expressed in specific tissues, including vascular ECs and cells of the myeloid lineage (211).

Upon hypoxia, the HIF $\alpha$  subunits are stabilised and accumulate in the nucleus, where they dimerise with HIF1 $\beta$ , allowing them to bind to DNA and stimulate the transcription of their target genes. There are over 70 known direct HIF target genes that function in normal physiology and disease processes. One of the largest functional categories of HIF target genes include those responsible for a shift in cellular energy metabolism from oxidative

phosphorylation towards glycolysis (212). Gene expression profiling confirms significant overlap between HIF1 $\alpha$  and HIF2 $\alpha$  regulated genes with a degree of non-redundancy of function, and differential basal and cell-specific expression of the HIF $\alpha$  isoforms (213). Notably, HIF1 $\alpha$  and HIF2 $\alpha$  exhibit different degradation kinetics, which have been shown to be cell-specific (214). To be tagged for degradation, the  $\alpha$  subunits are hydroxylated at conserved prolyl and asparaginyl residues by prolyl-hydroxylases (PHD), and are targeted for degradation by the von Hippel-Lindau (VHL) ubiquitin E3 ligase complex. Inhibition of hydroxylation results in the stabilisation of HIF1 $\alpha$  and HIF2 $\alpha$ , and leads to the transcriptional activation of target genes (215). The process of HIF stabilisation is depicted in Figure 1.3 (216). HIFs can also be stabilised independent of hypoxia, for instance in response to infections (217) and, chromosomal mutations. For example, aberrant c-Myc activation in MM (218) and growth factor signalling pathways such as PI3K and AKT, which upregulate protein translation of HIF genes (219). Non-hypoxic HIF1 $\alpha$  stabilisation can also be achieved through loss-of-function mutations in VHL, and lead to the full activation of HIF-mediated responses (220).

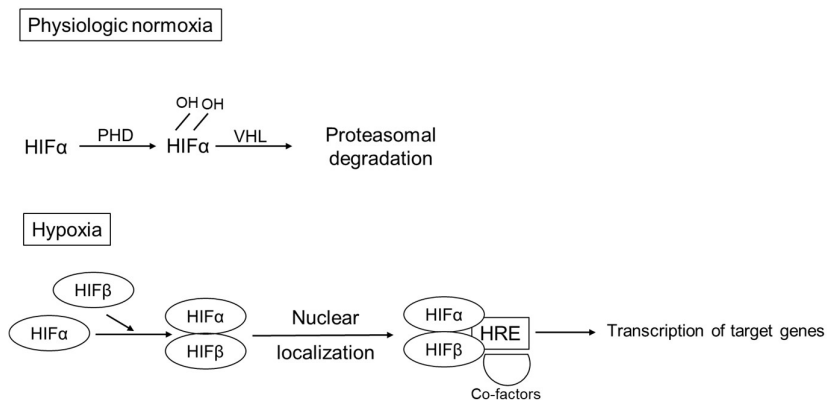


**Figure 1. 3 Hypoxia gradient across the bone marrow.**

The upper panel showing the oxygen-dependent degradation of HIF- $\alpha$  subunits, which when hydroxylated by prolyl hydroxylases (PHD) are ubiquitinated by the von Hippel-Lindau (VHL) complex and undergo proteasomal degradation. The lower panel shows the stabilisation of hypoxia-inducible factor  $\alpha$  (HIF- $\alpha$ ) subunits in low oxygen tension, and their heterodimerisation with the beta subunit, followed by translocation to the nucleus, and binding to the hypoxia response element along with other co-factors and transactivation of target genes.



### 1.5.2. Hypoxia as a component of the BMM

Several studies have analysed aspects of the composition and function of the complex bone marrow microenvironment. Spencer and colleagues measured oxygen pressure in live animals and found that cells residing in perisinusoidal areas, further away from the bone surfaces, encounter the lowest oxygen concentrations (pO<sub>2</sub> of ~5-20 mmHg or 2%) compared with those in the proximity of arterioles (pO<sub>2</sub> of ~35 mmHg or 4%–5%) (221). Jensen *et al.* observed an increase in BM hypoxia during disease progression, using a rat AML model. The BM became increasingly hypoxic, as detected by nitroimidazol, and hypoxic conditions were observed in 80% of AML cells in the bone marrow of rats and in 40% of circulating cells (222). Using pimonidazole staining for measuring hypoxia levels, Konopleva *et al.* elegantly demonstrated the high levels of hypoxia in human leukaemic BM (223).

In numerous other studies that aimed to define the haematopoietic niche, the BM has been shown to be hypoxic (224-227). Consequently, BM hypoxia is now a well-established key microenvironmental factor that influences the biology of the HSC as well as of leukaemic cells within the BM (209, 228, 229). A number of studies have shown that LSCs tend to localize in the more hypoxic regions of the BM (Figure 1.4) (208, 230, 231). However, *in situ* tissue analysis showed that HPCs exhibited a hypoxic profile regardless of cell-cycle status or localisation throughout the BM, suggesting that the distinctive hypoxic state of HPCs was a result of hypoxic niches as well as of cell-specific mechanisms (232).

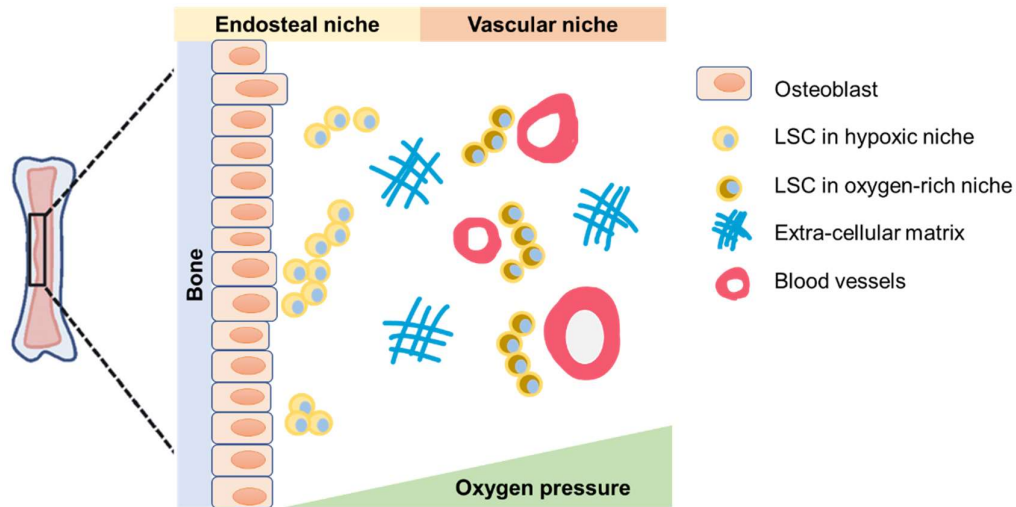


**Figure 1. 4 The Hypoxia gradient across the bone marrow.**

Diagram showing the distribution of leukaemic cells in the BM. More primitive, non-cycling leukaemic stem cells (LSC) localise to the hypoxic endosteal niche, while actively cycling leukaemic cells localise to the vascular niche.

### 1.5.3. The role of hypoxia in HSC versus leukaemic cells

The link between CXCR4 and hypoxia has been suggested: (i) after the recognition that the CXCR4 and SDF-1 genes are targets of HIF1 $\alpha$ , and (ii) after the observation that at 1% O<sub>2</sub> CXCR4 is up-regulated on monocytes, monocyte-derived macrophages, tumour-associated macrophages, ECs, and cancer cell lines (233). In relation to homing and migration, hypoxia has been shown to regulate SDF-1 (234) and CXCR4 expression on HSCs (235). These observations suggest that hypoxia enhances retention of HSC and arguably leukaemic cell retention in the BM as well.

Interestingly, HSCs seem to downregulate CXCR4 in response to pharmacological HIF1 $\alpha$  induction, whereas HIF1 $\alpha$  activation induces the opposite effect in leukaemic cells (236, 237). In fact, Azab and colleagues demonstrated that hypoxia regulates the trafficking of CML cells. Hypoxia was shown to decrease the CML expression of E-cadherin and increased CXCR4 expression *in vivo* and *in vitro*, resulting in decreased adhesion to BMSCs and enhanced chemotaxis (238). Moreover, blockade of HIF1 $\alpha$  impairs CLL cell homing into the BM and spleen in mouse models (239).

In AML, Fiegl and colleagues found that mild hypoxia (6% O<sub>2</sub>) increased CXCR4 surface expression on AML cells and its association to lipid rafts, conversely, re-oxygenation (20% O<sub>2</sub>) resulted in CXCR4 depletion (240). Hypoxia was shown to be important in maintaining leukaemia initiating cells (LIC) *in vitro*; Griessinger et. al. have shown that hypoxia is vital factor in creating an *in vitro* niche culture system, where AML LIC were cultured over a stromal cell feeder layer under hypoxia, incubated with recombinant IL-3, G-CSF and thrombopoietin and maintained in a stem-like state for over three weeks (241). Consequently, inhibition of hypoxia eliminated these cells.

Indeed, in a murine model, the HIF1 $\alpha$  inhibitor echinomycin seemed to selectively spare the self-renewal and differentiation capacity of normal HSCs while targeting AML leukaemic stem cells (242). Interestingly, in a more recent study on normal HSCs, data showed that HIF1 $\alpha$  was dispensable for self-renewal and long-term haematopoiesis in normal, unstressed HSCs (243). Finally HIF1 $\alpha$  was found to be highly expressed in the BM biopsy sections of normal karyotype AML patients and to be negatively correlated with survival (244). These observations suggest a fundamental difference in the role of hypoxia in HSCs versus leukaemic cells.

Understanding the altered hypoxic profile of the malignant BM has led to investigating the efficacy of a number of pro-drugs that are showing promising results in preclinical and clinical studies in solid tumours. Currently there are two hypoxa-activated prodrugs that are being investigated in AML:

- (i) TH-302, which effectively inhibited onset and progression of AML, extended the overall survival, both in systemic AML xenograft models and in mice with advanced AML disease. *In vitro*, TH-302 decreased HIF1 $\alpha$  protein expression and reduced ROS production, which resulted in decreased proliferation and increased cell-cycle arrest (245, 246).
- (ii) PR-104, which was evaluated in patients with refractory/relapsed AML in phase I/II study. Although PR-104 reduced hypoxia markers in this study, the treatment responses were transient and

higher doses resulted in prolonged myelosuppression (223). Nevertheless, these biomarker studies provided further evidence that hypoxia is a prevalent feature of the leukaemic microenvironment (247).

#### **1.5.4. HIF1 $\alpha$ and HIF2 $\alpha$ in AML leukaemogenesis**

Using a murine AML model, Velasco-Hernández et al investigated the contribution of HIF1 $\alpha$  to AML leukaemogenesis using models of oncogene-driven AML. Either Meis1 or Mml (both known to activate HIF1 $\alpha$ ) were retrovirally transduced into HSCs of HIF1 $\alpha$  conditional knockout mice, and subsequently transplanted into wild-type recipients. The authors found that HIF1 $\alpha$  loss-of-function did not affect AML initiation, progression or LSC self-renewal in the Meis1/Mml1- driven models, whereas it shortened LSC latency and accelerated disease in a third HIF1 $\alpha$ -independent Aml1-Eto9a-driven AML model (248, 249).

Altogether, these results suggest that the oncogene-enforced expression of HIF1 $\alpha$  does not play a role in leukaemia dormancy, and that HIF1 $\alpha$  does not act as a classical oncogene or tumour suppressor in this particular molecular context. However, one can conclude from the third Aml1-Eto9a-driven AML model, in which HIF1 $\alpha$  expression was independent of oncogene expression (and therefore was more subject to BM microenvironmental hypoxia) that hypoxic HIF1 $\alpha$  stabilisation limits AML progression, but not initiation, making it a tumour suppressor in this context (249).

In agreement with this study, pharmacological HIF1 $\alpha$  inhibition with echinomycin decreased CD34<sup>+</sup>CD38<sup>-</sup> LSC self-renewal and engraftment after serial transplantations in a mouse model of human AML. This effect was lost by HIF1 $\alpha$  silencing, suggesting that the inhibition of HIF1 $\alpha$ -dependent transactivation is a reasonable approach to eradicate LSCs in AML, thus, in theory, reducing the risk of relapse (250).

Fewer studies have investigated HIF2 $\alpha$  function in HSC and leukaemic cells. Recent work by Rouault-Pierre and colleagues showed that HIF2 $\alpha$  silencing

in patient-derived AML cells impaired engraftment in mouse transplantation experiments (251). In agreement with this, ectopic overexpression of HIF2 $\alpha$  accelerated disease progression in mouse AML models (252). In an elegant study, Vukovic et al. further addressed the role of both HIF1 $\alpha$  and HIF2 $\alpha$  in AML initiation and progression where they used a mouse model in which leukaemia was induced through co-expression of the AML proto-oncogenes Meis1 and Hoxa9. They showed that simultaneous deletion of HIF1 $\alpha$  and HIF2 $\alpha$  in pre-leukaemic HSCs resulted in a synergistic increase of AML proliferation and progression. Although HIF2 $\alpha$  silencing on its own did not impair LSC clonogenicity, it did increase the percentage of cycling cells (253). Taken together, these data suggest that HIF1 $\alpha$  and HIF -2 $\alpha$  can cooperate to maintain LSC quiescence, thus promoting self-renewal of the stem cell compartment.

HIFs have also been implicated in chemotherapy resistance of AML. AML chemoresistant LSCs were shown to favourably localize in the hypoxic endosteal regions of the mouse BM where they were protected from the proapoptotic effect of the chemotherapeutic agent Ara-Ca. Moreover, it has shown that hypoxic HIF1 $\alpha$  stabilisation decreased the *in vitro* sensitivity of AML cell lines to cytosine arabinoside (Ara-C) (254).

### **1.6. Senescence in health and disease**

Being a disease of the elderly, AML poses the question of whether age-related biological processes contribute to the pathology of the disease. One important process in aging is cell senescence. Cellular senescence was described over five decades ago by Hayflick (255) and it is defined as a state of irreversible arrest of cell proliferation in response to persistent DNA damage induced by a variety of potentially oncogenic signals. It is thought to function as a primary tumour-suppression mechanism (256).

In addition to arrested growth, senescent cells are thought to be “in disguise”, concealing a highly active metabolic cell state with diverse functionality. Furthermore, senescent cells show widespread changes in chromatin organization and gene expression (257). These changes include the secretion

of several inflammatory cytokines, chemokines, growth factors and matrix-remodelling factors, in a newly identified phenotype of cellular senescence, called senescence-associated secretory phenotype (or profile) (SASP). SASP incites not only tumour-suppressive, but also tumour-promoting responses, depending on the biological context (258, 259).

There is growing evidence that senescent cells contribute to age-related phenotypes and age-related pathologies (260). Furthermore, in the context of cancer, several cellular functions and organs can undergo distinct pathologic pro-tumoural changes (261). However, although SASP can contribute to a pro-carcinogenic microenvironment, recent findings show it can also promote tissue remodelling and wound healing (262). Therefore, depending on the context, it is now clear that cellular senescence and the SASP contribute to myriad physiological functions, both favourable and damaging.

This next section will review the pathways activated in senescent cells and the consequences, thereof, in the context of cancer.

### **1.7. Effector pathways of senescence and the senescent phenotype**

There are many inducers of the senescence phenotype: oncogene-induced senescence (OIS), telomere dysfunction (known as replicative senescence, (RS)), therapy-induced senescence (TIS), and chronic stress stimuli such as high levels of ROS, among others. All of these inducers converge upon the activation of a chronic DNA-damage response (DDR), the induction of the tumour suppressor p53, or the independent activation of the cell cycle inhibitor p16<sup>INK4A</sup> (shortly called p16) (263).

Activation of p16 drives cells to exit from the cell cycle through inhibition of cyclin dependent kinases (CDK) and the mediated phosphorylation of the retinoblastoma protein (RB) (264). The p21 protein, one of the cell cycle inhibitors, is the downstream target gene of the p53 pathway and its activation causes cell cycle arrest until repair takes place. In the case of the cells failing to repair, this pathway then activates p16 (265). Interestingly, p53 plays a key role in suppressing the SASP; indeed, loss of p53 in the face of a chronic DDR

leads to increased expression of various SASP factors (261). The processes activated in the senescent response are depicted in Figure 1.5.

It is important to note that cell cycle arrest in senescence is near permanent as compared to reversible cell cycle arrest that happens in quiescence. In a broader perspective, quiescence occurs due to a lack of nutrition and growth factors, while senescence takes place due to aging and serious DNA damages (266). Phenotypically, senescent cells have a large and flat cell morphology and acquire hyper-active cellular functions (267). Senescent cells often exhibit increased lysosomal b-galactosidase activity, which is responsible for the characteristic senescence-associated b-gal (SA-b-gal) staining at near neutral pH (268). While SASP cytokines may differ from one cell type to another, their production generally depends on stress-induced NF- $\kappa$ B and MAPK signalling, and their regulation is governed by the mTOR dependent protein translation (269).

SASP factors relevant for pro-tumoural activity can be divided into the following groups (270):

- (i) Inflammatory cytokines: ones such as TNF- $\alpha$  and IL-6, that affect neighbouring cells by activating the NF- $\kappa$ B pathway and by inducing epithelial-mesenchymal transition, which marks pre-malignant development
- (ii) Members of the CXCL and CCL families: ones like IL-8, growth related oncogene (GRO) - $\alpha$  and - $\beta$ , and SDF1 and its receptor CXCR4
- (iii) MMPs that alter the extracellular matrix
- (iv) The urokinase-plasminogen-activator/urokinase-plasminogen-activator receptor (uPA/uPAR) system
- (v) Almost all insulin-like growth factor (IGF)-binding proteins and their regulators

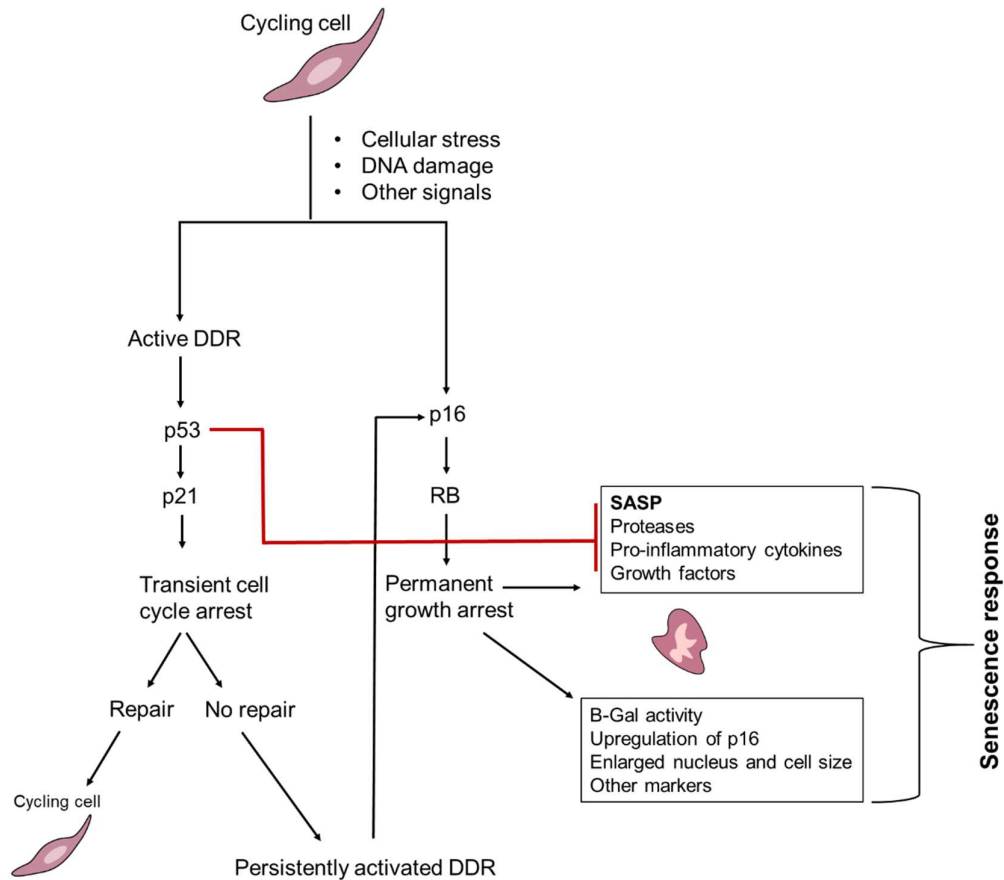


**Figure 1. 5 Effectors of the senescence pathway.**

DNA damage and various stress factors activate the DNA damage response (DDR) in the affected cells. This in turn activates either the p53/p21 pathway or the p16 pathway, or both. Activation of the former leads to a transient arrest of cell growth, which becomes irreversible in case the cell fails to repair. A persistent activation of the DDR then leads to prolonged arrest and, possibly, alterations in the SASP. P16 activation leads to a Cyclin-dependent kinase-mediated activation of retinoblastoma protein (RB). Early senescent cells are SA-β-GAL positive and may not have a SASP. However, senescent cells may evolve further into a truly irreversible full senescence with SA-β-GAL positivity and a SASP that can eventually promote tumourigenesis. SASP is negatively regulated by p53.

### 1.8. Role of senescence and SASP in tumourigenesis

Early evidence associating senescence with cancers comes from an observation in patients with Li-Fraumeni syndrome, where cells with mutated p53 suffered accelerated senescence, often preceding cancer development (271, 272). The presence of senescent cells in tissues with hyperplastic pathological or premalignant alterations might indicate that senescence is a



step in the process of cancer development, or, that cancer development is age-dependant, and a mechanism that is tumour-suppressive in young age is tumour-promoting in old age (273).

The SASP has been shown to create a pro-tumourigenic microenvironment in various ways. SASP factors promote cancer cell invasion and metastasis through tissue remodelling. Senescent cells secrete large amounts of proteases that degrade the ECM (extracellular matrix), making the tissue structure more relaxed and thus, facilitating the invasion of cancer cells (274). Recently, in a study on papillary thyroid carcinoma, Kim and colleagues showed that senescent tumour cells exhibited high invasion ability, compared to non-senescent tumour cells, through SASP expression. Interestingly, in this study senescent cells increased the survival of cancer cells via SDF-1/CXCR4 signalling, with the expression of SDF-1 being significantly increased in tumour areas where p16<sup>INK4A</sup>-immunopositive senescent cells were present (275).

Studies have also shown that the SASP promotes tumour growth by establishing an immunosuppressive microenvironment. Recently, in a study on metastatic bone lesions in breast cancer patients, Lou et al developed a model to induce reactive senescent osteoblasts and found that they increased breast cancer colonisation of the bone, which was also IL-6 mediated. Neutralisation of IL-6 was sufficient to limit senescence-induced osteoclast generation and tumour cell localisation to bone, thereby reducing tumour burden (276).

In a similar study, Ruhland et al developed a mouse model that mimicked the aged skin microenvironment and showed that senescent stromal cells secreted IL-6, a main interleukin in the SASP. As a result, this caused localised increases in suppressive myeloid cells, and inhibited anti-tumour T-cell responses, hence, contributing to tumour promotion (277).

### **1.9. Therapy-induced senescence**

Senescence can be induced in cancer cells upon treatment with a variety of drugs. In particular, chemotherapeutic agents that cause DNA damage. In this context, the induced senescence is expected to halt cancer progression (278).

However, a number of studies suggest that senescent cancer cells acquire resistance to cytotoxic chemotherapies (279) or give rise to stem-like cells accountable for post-therapy recurrence of cancer (280).

Young adult women who had breast cancer and were treated with cytotoxic chemotherapy showed increased expression of markers of cellular senescence for decades after chemotherapy. Astonishingly, a few months of adjuvant chemotherapy for breast cancer, on average, increases T cell p16 expression to an amount equivalent to 15 years of chronological aging (281).

Campisi and colleagues studied the role of senescent cells in the toxicities of cytotoxic chemotherapy by inducing senescence in murine tissues using a variety of DNA damaging chemotherapy agents. In the breast model used in this study, senescent non-tumour cells were important for cancer relapse and spread to distal tissues after chemotherapy. When these senescent cells were cleared, several side effects of chemotherapy were improved. In particular, senescence free animals were less fatigued compared to untreated mice. Moreover, in a cohort of 80 breast cancer patients that were included in the study, p16 expression in peripheral T-cells predicted chemotherapy-induced fatigue in these patients (282).

In another recent study, clearance of p16 positive senescent cell also delayed the onset of age related phenotypes and extended the murine lifespan (283). Thus, therapy-induced senescence may be relevant to AML as it is heavily treated with chemotherapeutic agents.

## **1.10. Research rationale, aims and objectives**

### **1.10.1. Rationale**

Acute myeloid leukaemia (AML) is a disease predominantly of older adults. However, the survival rate of AML patients has not been significantly favourably impacted, despite the development of currently available AML therapies and interventions targeting tumour cells. Extensive research has shown that leukaemic cells arise and thrive due to a leukaemia-permissive bone marrow microenvironment (BMM). Bone marrow stromal cells (BMSCs) are considered a major protective cell type that protect AML cells from spontaneous and chemotherapy-induced apoptosis.

So far, only few microenvironmental factors favouring leukaemogenesis have been identified, as opposed to the widely explored genetic landscape of AML. Characterising the AML-driven biologic changes that occur in the BMSCs of the marrow niche would help identify new therapeutic targets, that could disrupt the pro-tumoural relationship between AML and its microenvironment. Consequently, this may ultimately lead to much needed novel therapeutic approaches in AML.

### **1.10.2. Aims**

- To investigate the role of BMSCs in the microenvironment of AML.
- To identify AML-driven signals that alter the profile of BMSCs towards tumour-promotion.
- To identify possible new therapeutic targets that could disrupt the pro-tumoural relationship between AML and BMSCs.

### **1.10.3. Objectives**

The approach taken to achieve the above aims is as follows:

1. To establish an *in vitro* co-culture of patient derived AML cells and BMSCs, followed by determining the secretory profile thereof, and to identify potential AML-derived factors that regulate BMSC function (Chapter 3 and Chapter 6).

2. To develop investigations to determine the downstream effects of AML-derived factor(s) in the BMSCs, including signalling transduction pathways and their ultimate effect on AML survival (Chapter 4 and chapter 6).
3. To establish the regulatory mechanism of AML-derived factor(s), (identified in chapter 3) within the AML blast, and to identify the consequences of their inhibition in *in vivo* murine models of AML (Chapter 5 and chapter 6).

The materials and methods used in this research are presented in Chapter 2. A general discussion and concluding remarks are presented in Chapter 7.

## **2. Chapter 2: materials and methods**

### **2.1. Reagents and chemicals**

All reagents were obtained from Sigma-Aldrich (Dorset, UK), unless otherwise indicated in the text. All inhibitors were purchased from Tocris Bioscience (Bristol, UK).

### **2.2. Blocking antibodies and recombinant cytokines**

The CD74 blocking and IgG control blocking antibodies were purchased from BD Biosciences (Allschwil, Switzerland) and recombinant human MIF (rhMIF) was purchased from R&D Systems (Wiesbaden, Germany). Recombinant murine stem cell factor (SCF), murine Interleukin-6 (IL-6) and murine interleukin-3 (IL-3) were purchased from Peprotech (Neuilly-sur-Seine, France). Antibodies used in flow cytometry analysis are listed in table 2.1 and antibodies used in western blotting are listed in table 2.2 Assay kits were purchased from suppliers indicated in the text.

**Table 2. 1 Antibodies used in flow cytometry analysis.**

<b>Antibody</b>	<b>Clone</b>	<b>Supplier</b>
<b>Mouse IgG2a-FITC</b>	-	Miltenyi Biotec
<b>Mouse IgG2a-PE</b>	-	(Paris, France)
<b>Mouse IgG2a-APC</b>	-	
<b>Mouse IgG2a-VioBright FITC</b>	-	
<b>CD105-FITC</b>	43A4E1	
<b>CD73-PE</b>	AD2	
<b>CD74-FITC</b>	5-329	
<b>CD184 (CXCR4)-PE</b>	12G5	
<b>CD182 (CXCR2)-VioBright FITC</b>	REA208	
<b>CD33-APC</b>	AC104.3E3	
<b>CD34-PE</b>	AC136	
<b>CD45-FITC</b>	5B1	

**Table 2. 2 Primary and secondary antibodies used in western blotting.**

Antibody	Species and antibody clonality	MW (kDa)	Dilution	Supplier
<b>Primary antibodies</b>				
Anti-GAPDH	Rabbit mAb	37	1:2000	CST (Massachusetts, USA)
Anti- $\beta$ - actin	Mouse mAb	45	1:2000	Sigma (Dorset, UK)
Anti-Phospho-Akt (Ser473)	Rabbit mAb	60	1:1000	CST
Anti-Akt (pan) (C67E7)	Rabbit mAb	60	1:1000	CST
Anti-Phospho-p44/42 MAPK (Erk1/2) (Thr202/Tyr204)	Rabbit mAb	42, 44	1:1000	CST
p44/42 MAPK (Erk1/2)	Rabbit pAb	42, 44	1:1000	CST
Phospho-PKCa/b II (Thr638/641)	Rabbit pAb	80, 82	1:1000	CST
Phospho-PKC (pan) ( $\beta$ II Ser660)	Rabbit pAb	78, 80, 82, 85	1:1000	CST
Phospho-PKD/PKC $\mu$ (Ser916)	Rabbit pAb	115	1:1000	CST
Phospho-PKCd (Thr505)	Rabbit pAb	78	1:1000	CST
Phospho-PKC $\delta$ / $\theta$ (Ser643/676)	Rabbit pAb	78	1:1000	CST
PKCBII (pan) pAb	Mouse	78	1:500	R&D systems
HIF1 $\alpha$	Mouse mAb	116-120	1:500	BD Biosciences
HIF2 $\alpha$ /EPAS1	Rabbit pAb	118	1:500	Novus Bio
p16INK4a (CDKN2A)	Rabbit mAb	17	1:500	Abcam
<b>Secondary antibodies</b>				
Goat anti-Mouse IgG HRP	pAb		1:2000	Dako (Agilent)
Goat anti-Rabbit IgG HRP	pAb		1:2000	Dako (Agilent)

Abbreviations: mAb, monoclonal antibody, pAb, polyclonal antibody.

CST (Massachusetts, USA), Sigma (Dorset, UK), R&D Systems (Wiesbaden, Germany), BD Biosciences (Allschwil, Switzerland), Novus Bio (Colorado, USA), Abcam (Cambridge, UK), Dako – Agilent (Cheadle, UK).

## 2.3. Cell culture

### 2.3.1. Cell lines

**The human leukaemia OCI-AML3 cell line** was obtained the German Collection of Microorganisms and Cell Cultures (Braunschweig, Germany) and was maintained in RPMI-1640 medium, supplemented with 10% foetal calf serum (FCS), 2mM L-glutamine, 100U/ml penicillin and 10µg/ml streptomycin (pen-strep). Cells were kept at a density of 0.3-0.6 x10<sup>6</sup> cells/ml and sub-cultured accordingly.

**293T cells** were kindly provided by Dr Ariberto Fassati (University College London, London, UK) and maintained at 60-90% confluence in antibiotic-free Dulbecco's Modified Eagle's medium (DMEM) with 10% FCS and 6mM L-glutamine. 293T cells are a highly transfectable derivative of human embryonic kidney 293 cells. 293T cells were sub-cultured at a 1:4 ratio in fresh culture media; culture media was gently aspirated and the cells were washed once with phosphate buffered saline (PBS). Gentle pipetting was very critical as these cells easily detached. 0.25% Trypsin was diluted 1:1 with PBS and 5 ml of this mixture was added to each of the 10mm plates. The plates were then incubated at room temperature (RT) for 2 to 3 minutes and swirled from side to side to help detach the cells. Next, the cells were re-suspended in the appropriate volume to achieve the required sub-culturing ratio, and pipetted vigorously to obtain a single cell suspension. 10 ml of cell suspension was dispensed in 10 mm dishes and incubated overnight in a humidified culture incubator. Culture media was replaced with fresh media each following day, and returned to the incubator.

**The murine MN1 leukaemia cells** are lineage depleted murine mononuclear cells carrying the MN1 AML gene, these were kindly gifted by Professor Keith Humphries (Terry Fox Laboratory, Vancouver, Canada) (284), and cultured in DMEM supplemented with 20% FCS and murine recombinant cytokines – SCF at a final concentration of 100ng/ml final, and IL-6 and IL-3 at 10ng/ml. All cells were cultured in a humidified culture incubator at 5% CO<sub>2</sub> and 37 °C.

**HS-5 stromal cells** are a human stromal cell line derived from the bone marrow of a healthy volunteer and immortalized by transduction with human papilloma virus E6/E7 constructs (285) and were obtained from the American Type Culture Collection (ATCC, USA). Cells were maintained in DMEM with 10% FCS and subcultured when they were 80% confluent. Subculturing was performed in the same manner as BMSC subculturing described in section 2.3.2.

### 2.3.2. Primary cell isolation and culture

Primary AML cells were obtained from patient bone marrow, following informed consent and approval by the Health Research Authority of the National Health Service (NHS), United Kingdom (LRECref07/H0310/146). For primary cell isolation, 10 to 20 ml bone marrow aspirates were obtained in heparinised blood tubes., and mononuclear cells were isolated by Histopaque-1077 density gradient centrifugation. 10 ml of blood was carefully and slowly layered on 10 ml of Histopaque-1077 in a 50 ml falcon tube; the slow layering prevented mixing of the two layers. The tubes were then centrifuged at 400g for 20 minutes with slow acceleration and slow deceleration in order to aid the gentle separation of the different blood components. Figure 2.1 illustrates the different layers that formed at the end of this step.

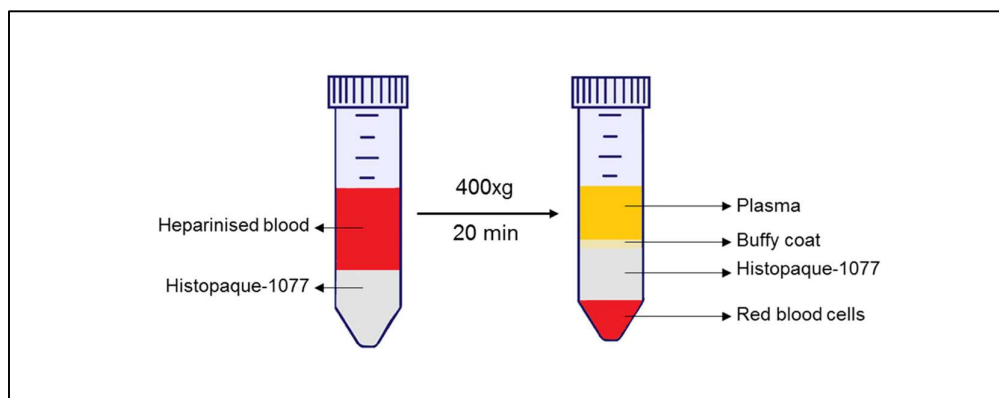


**Figure 2. 1 A schematic of the Histopaque density gradient centrifugation step in isolating AML cells from BM aspirates.**

Four layers resulted from the density gradient performed. The mononuclear cell layer was carefully aspirated and used for isolating AML cells.



The buffy coat layer containing mononuclear cells was diluted in 40 ml of FCS and centrifuged at 400g for 5 minutes at RT. Red cell lysis was performed by suspending the cell pellet in 1-3 ml Red Blood Cell Lysing Buffer Hybri-Max for 1 minute, and then diluting the buffer with 10-15 ml of sterile PBS. The suspension was centrifuged again at 400g for 5 minutes and the cell pellet was suspended in complete growth medium, containing DMEM supplemented with 20% FCS, 1% L-glutamine and pen-strep.

AML samples that contained less than 80% blasts were purified using the CD34 MicroBead Kit UltraPure (Miltenyi Biotec,), unless the sample was identified as CD34 negative by the pathology department at the Norwich and Norfolk University Hospital (NNUH). Next, the cells were cultured at a density of  $2 \times 10^6$  cells/ml, and incubated for the expansion of BMSCs. A fraction of the cells were cryopreserved in FCS with 10% Dimethyl sulphoxide (DMSO) for future use.

BMSCs were isolated by removing non-adherent cells after 2 days of AML culture. Fresh complete growth media containing 10% FCS was added and changed every 3 days. When the cells were 60%-80% confluent, adherent BMSCs were trypsinised by adding 2.5 ml of 0.25% trypsin, and incubated for no longer than 5 minutes at 5% CO<sub>2</sub> and 37 °C. Once the cells were detached, fresh complete growth medium was added and the cultures were expanded for 3-5 weeks. The cells were sub-cultured when they are about 80% confluent.

BMSCs were checked for positive expression of CD105, CD73, and CD90 and the lack of expression of the myeloid marker CD45 by flow cytometry. All cells were cultured in complete growth medium with 10% FCS at 5% CO<sub>2</sub> and 37 °C in a humidified tissue culture incubator.

Non-malignant normal CD34+ HSCs were obtained from the peripheral blood of patients with genetic haemochromatosis undergoing therapeutic venesection, but with non-raised ferritin levels. On average, 250 to 300 ml of heparinised peripheral blood were collected and aliquoted into 50 ml falcon tubes, followed by centrifugation at 400g for 30 minutes. This step separated

the blood into three layers as shown in Figure 2.2. The mononuclear cell layers were collected and pooled into a 50 ml falcon tube (an average of 25 ml would be recovered) and diluted 1:1 with PBS. 10 ml of diluted blood was carefully and slowly layered onto 10 ml of Histopaque-1077 in a 50 ml falcon tube, and centrifuged at 400g for 20 minutes. From this step onwards, the same isolation protocol that was used for AML cells was followed and the cells were purified using CD34+ magnetic cell purification.

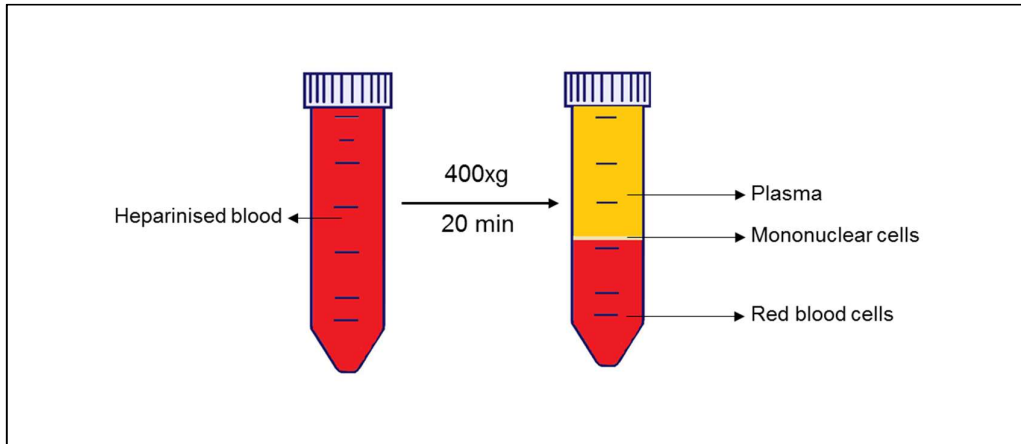


**Figure 2. 2 A schematic of the additional centrifugation of large volumes of peripheral blood prior to Histopaque density gradient centrifugation and isolation of CD34+ cells.**

Three layers were obtained after centrifugation at 400g for 30 minutes, the central layer of mononuclear cells was carefully aspirated and used for isolating normal CD34+ cells.

### **2.3.3. CD34+ magnetic purification**

CD34+ cells were isolated using positive selection of magnetically labelled CD34+ cells. The CD34 MicroBead Kit UltraPure, human (Miltenyi Biotec) was used to purify CD34+ AML and CD34+ HSCs. Cells were pelleted by centrifugation and re-suspended in 300 µl of MACS Buffer (a sterile solution of PBS containing 0.5% bovine serum albumin (BSA) and 2 mM EDTA, stored at 4°C). Next, 100 µl of human FcR Blocking Reagent (which helped eliminate non-specific binding) and 100 µl of the CD34 MicroBeads were added. The cell suspension was mixed well by pipetting, and incubated for 30 minutes at 4°C.

After incubation, the cells were washed in 5ml of MACS Buffer, and then pelleted and re-suspended in 500 µl of MACS buffer. The cell suspension was then applied to the MS MACS separation column fitted on the MiniMACS magnet. Only cells that were positively labelled with CD34 Microbeads were retained by the column. The column was then washed three times with 500 µl MACS Buffer and then removed from the separation magnet and placed in a 15 ml collection tube. 1ml of MACS Buffer was applied onto the column and, using the supplied plunger, labelled cells were forced out by firmly pushing the plunger through the column. Isolated CD34+ cells were then cultured in complete DMEM with 10% FCS.

#### **2.3.4. Cryopreservation and defrosting of primary cells**

Cells were collected by centrifugation at 350g for 5 minutes and re-suspended in freezing medium (10% DMSO in FCS). 1 ml cell aliquots were transferred into labelled cryovials and stored overnight at -80°C in a CoolCell cell freezing container, before being transferred to the appropriate storage facilities. When needed, cells were defrosted quickly by briefly immersing the bottom part of the cryovial in a water bath at 37 °C. This was done to ensure maximum cell recovery. Next, the cell suspension was transferred to a 15 ml falcon tube containing 9 ml of complete growth medium, and centrifuged at 350g for 5 minutes. The cell pellet was then suspended in complete growth medium with 20% FCS, and incubated at 5% CO<sub>2</sub> and 37 °C in a humidified tissue culture incubator.

#### **2.3.5. Cell viability assays:**

##### **2.3.5.1. Trypan blue exclusion test using a haemocytometer**

The Trypan blue exclusion assay is an inexpensive and widely used cell viability assay. Trypan blue is taken up by dead cells and excluded by viable cells due to their intact cell membranes. In this assay, A 10 µl aliquot of cell suspension was mixed in a 1:1 ratio with trypan blue solution (0.4% w/v). Cells were then pipetted onto a Neubauer Haemocytometer Counting Chamber, and those that had excluded the dye were counted as viable cells. All four quadrants were counted and averaged. The total number of cells in the original

suspension was calculated by multiplying this value by 10,000 x dilution factor of two. Only cell cultures that were  $\geq 85\%$  viable were used in experiments.

#### **2.3.5.2. CellTiter-Glo viability assay**

AML cells were seeded into 96-well plates in quadruples and their viability was determined at the time points indicated in the results section. Cell viability was determined indirectly by measuring the intracellular levels of ATP using the Cell Titer-Glo Luminescent Cell Viability Assay kit (Promega, Wisconsin, USA), where a luminescent signal was produced due to a firefly luciferase reaction and was directly proportional to cell number and viability. The test was performed according to the manufacturer's instructions: 50  $\mu\text{l}$  of the cell suspension was transferred to a white 96 well plate. Cells were lysed by the addition of 50  $\mu\text{l}$  of the CellTiter-Glo reagent and incubated for 10 minutes at RT with gentle shaking. Luminescence was measured at a peak emission wavelength of 560nm on a lumiStar Microplate Reader (BMG Labtech GmbH, Ortenberg, Germany).

#### **2.3.5.3. Annexin V – PI detection of apoptosis**

This assay is based on the fact that dead cells are able to take up the membrane impermeable fluorescent propidium iodide (PI) dye, which then binds to DNA and enhances its fluorescence properties, while Annexin V binds to the exposed phosphatidylserine (PS) molecules on the outer side of the plasma membrane, this being one of the early events of apoptosis (286)

The percentage of early apoptotic, apoptotic or dead (necrotic) cells is calculated according to the cell PIV Annexin V staining parameters. The eBioscience Annexin V-FITC Apoptosis detection kit (Thermo Fisher Scientific, UK) was used to determine the percentage of apoptotic cells. Cells were harvested by centrifugation and washed twice in cold PBS (350g for 5 min) and resuspended to  $0.2 \times 10^6$  cells/ml. 5  $\mu\text{l}$  of Annexin V-FITC was then added to 195  $\mu\text{l}$  cell suspension, mixed and incubated for 10 minutes at RT. Next, the cells were washed with 200  $\mu\text{l}$  binding buffer and resuspended in 190  $\mu\text{l}$  bidding buffer. Finally, 10  $\mu\text{l}$  PI (20  $\mu\text{g}/\text{ml}$ ) was added to the sample and

incubated for 1-2 minutes at RT in the dark. Cells were immediately analysed by flow cytometry.

### **2.3.6. Hypoxic assays**

To establish hypoxic cultures, cells were either incubated in a hypoxia chamber (Billups-Rothenberg Inc, Del Mar, USA) at 1% O<sub>2</sub>/ 5% CO<sub>2</sub>/ N<sub>2</sub> 200 bar at 37 °C for the periods of time indicated in the text, or treated with cobalt chloride (CoCl<sub>2</sub>) and desferrioxamine (DFO) at 100uM or 150uM respectively at the time points indicated in the text. Control cell cultures, not deprived of oxygen, were incubated under normal culture conditions.

### **2.3.7. Methylcellulose Human Colony Forming Cell (CFC) Assay**

The colony forming cell (CFC) assay, also called the methylcellulose assay, is one that aims to determine the progenitor capacity of the haematopoietic cells of interest. The assay is based on the ability of haematopoietic progenitors to proliferate and differentiate into colonies in a semi-solid media, in response to cytokine stimulation. The colonies formed can then be counted and characterised according to their unique morphologies (287).

4x10<sup>4</sup> cells were washed in sterile PBS and re-suspended in 400 ul cell resuspension solution (R&D systems). The cells were added to 4 ml of human methylcellulose complete media HSC003 (R&D systems) in a 15 ml falcon tube, mixed by a brief vortex. A quick centrifuge on a short spin setting for 20 seconds allowed any bubbles in the solution to rise to the surface and any media that was stuck on the inside walls of the tube to be recovered. It was vital that the spin was short, to prevent cells from pelleting or becoming concentrated towards the bottom of the semi-solid media.

Next, 1.1 ml of the solution was aspirated using a 16 gauge 1½ inch blunt end needle, and dispensed into a 35mm culture dish. This step was repeated a total of three times to obtain triplicate samples. The three dishes, as well as an uncovered dish containing 3-4 ml sterile water, were placed in a Corning square bioassay dish and were loosely covered to allow for gas exchange. The sterile water dish served to maintain the humidity necessary for colony

development. Finally, the plates were incubated for 10-14 days at 37 °C and 5% CO<sub>2</sub>. It was essential to avoid disturbing the cultures during the incubation period to prevent shifting of the colonies. Light microscopy was used to visualise and score colonies at days 10-14 using a scoring grid.

## **2.4. Molecular biology techniques**

### **2.4.1. RNA extraction**

Total RNA was extracted from cells using the ReliaPrep RNA extraction kit from Promega, according to the manufacturer's instructions. Suspension cells (OCI-AML3 cell line or primary AML cells) were collected by centrifugation at 400g for 5 minutes. The supernatant was either discarded or stored at -20 for cytokine analysis. Culture media was collected from adherent BMSCs and either discarded or stored at -20 for cytokine analysis.

Adherent or suspension cells were washed once with PBS. 250µl BL+TG lysis buffer was then added and the solution was pipetted up and down 7 times to lyse the cells. The lysate was transferred to a ReliaPrep™ minicolumn and centrifuged at 14000g for 30 seconds at RT. Next, 500µl of RNA Wash solution were added to the minicolumn and centrifuged at 14000g for 30 seconds. 24µl of Yellow Core Buffer, 3µl 0.09M MgCl<sub>2</sub> and 3µl of DNase I enzyme were mixed in order and added to each minicolumn membrane, followed by incubation for 15 minutes at RT. 200µl of column wash solution was added and centrifuged at 14000g for 15 seconds. 500µl of RNA wash solution were added and the minicolumn was centrifuged at 14000g for 30 seconds. The minicolumn was placed into a new collection tube, 300 µl of RNA wash solution added, and they were centrifuged at 14000g for 2 minutes. Finally, the minicolumn was transferred to an elution tube, and 20 µl nuclease-free water was added directly onto the membrane and incubated at RT for 1min. The minicolumn was centrifuged at 14000g for 1min to elute RNA, which was stored at -20°C until further use.

#### **2.4.2. Nucleic acid quantification using a Nanodrop**

RNA yield was quantified and its purity determined using a NanoDrop 2000 Spectrophotometer (ThermoScientific, UK). Briefly, 1  $\mu$ l sample was measured and referenced to a blank sample of nuclease-free water, in which the RNA was eluted. An RNA sample with an A260/A280 ratio of 1.9-2.1 was considered pure and of accepted quality. For plasmid DNA, an A260/A280 ratio of 1.7–2.0 was accepted as sufficiently pure.

#### **2.4.3. Reverse transcription and cDNA synthesis**

Reverse transcription was performed using the qPCRBIO cDNA synthesis kit (PCR Biosystems, London, UK). For a 10  $\mu$ L reaction, 2  $\mu$ L of 5x cDNA Synthesis Mix and 0.5  $\mu$ L of 20x RTase were added to 7.5  $\mu$ L nuclease free water, carrying up to 100ng RNA. The PCR tubes are incubated in the Thermocycler (Bio-Rad, Watford, UK) at 42°C for 30 minutes and at 85°C for 10 minutes to denature RTase, and then kept at 4°C for up to three hours or stored at -20°C. The samples were diluted 1:5 or 1:10 before performing gene expression using qRT-PCR.

#### **2.4.4. Relative quantitative real-time PCR (qRT-PCR)**

qRT-PCR was performed using the qPCRBIO SyGreen Mix (PCR Biosystems, London, UK) on cDNA generated from the reverse transcription of purified RNA. For a 10  $\mu$ L reaction, 5  $\mu$ L of SyGreen Mix and 1  $\mu$ l of forward and reverse primer mix were added to 4  $\mu$ L of diluted cDNA. Samples were run in triplicates on a 96-well white PCR plate. Larger qRT-PCR sample runs were performed in 384-well plates and a 5  $\mu$ l reaction volume was used instead of 10  $\mu$ l.

After a pre-amplification incubation step (95°C for 2 minutes), the cDNAs were amplified over 45 cycles (95°C for 15 seconds, 60°C for 10 seconds and 72°C for 10 seconds), followed by a melting curve analysis (95°C for 5 seconds, 65°C for 1 minute and 97°C continuous). The melting curve analysis was performed to confirm product specificity and to detect the formation of primer

dimers which could give false positives if unidentified. Finally, the reactions were cooled at 40°C for 30 seconds.

The qRT-PCR reactions were run on a LightCycler 480 (Roche Life Science, Burgess Hill, UK). Predesigned qRT-PCR primers were purchased from Sigma (KiCqStart® SYBR® Green Primers, Cat. No. KSPQ12012) and are listed in table 2.3. qRT-PCR primers to detect PKCB, IL-8 and CD74 mRNA expression were purchased from Qiagen (Hilden, Germany) (QIAGEN QuantiTect Primer Assay) and are listed in table 2.4. The lyophilised primers were dissolved in the volumes of nuclease free water specified by the manufacturers, briefly vortexed and then stored at -20°C until further use.

**Table 2. 3 KiCqStart® SYBR® Green Primers (Sigma).**

Gene name, forward and reverse primer sequences are shown in the table.

Gene	Forward primer sequence 5' → 3'	Reverse primer sequence 5' → 3'
GAPDH	CTTTTGCCTCGCCAG	TTGATGGCAACAATATCCAC
β -actin	GATCAAGATCATTGCTCCTC	TTGTCAAGAAAGGGTGTAAC
MIF	AACTATTACGACATGAACGC	AAACCGTTTATTTCTCCCC
IL-6	GCAGAAAAAGGCAAAGAATC	CTACATTTGCCGAAGAGC
HIF1α	GAAACTACTAGTGCCACATC	GGAAGTGTAGTTCTTTGACTC
GLUT1 (SLC2A1)	AGTTCCTACAACCAGACATGG	CAGGTTTCATCATCAGCATTG
HIF2α (EPAS1)	CAGAATCACAGAACTGATTGG	TGACTCTTGGTCATGTTCTC
p16 (CDKN2A)	AGGTCCCTCAGACATCC	AATGAAAACCTACGAAAGCGG
p21 (CDKN1A)	CAGCATGACAGATTTCTACC	CAGGGTATGTACATGAGGAG

Because MIF gene contains an antisense coding sequence on the minus strand (MIF-AS1, Entrez ID: 284889), it is possible that the MIF gene is expressed in both directions, generating (i) MIF mRNA from the sense strand and possibly a (ii) MIF antisense 1 from the minus strand. The RT-PCR reactions used in this study, utilised sense-directed primers and hence should only amplify transcripts from the sense strand. Moreover, using the BLAST tool to test primer specificity helped determine that the primers would only amplify MIF transcripts and not non-specific or antisense transcripts.



## Table 2. 4 QuantiTect Primers (Qiagen).

Primer sequences were not disclosed by the manufacturer.

Gene	Assay name	Catalogue number
IL-8 (CXCL8)	Hs_CXCL8_1_SG	QT00000322
PKCB (PRKBC)	Hs_PRKCB_1_SG	QT00073920
CD74	Hs_CD74_1_SG	QT00059402

### 2.4.5. Analysis of qRT-PCR data

A cycle threshold (Ct) value was measured and generated at the end of the reaction described in 2.5.1.4. GAPDH or  $\beta$ -actin were used as housekeeping genes to calculate a fold change correction for each sample (Delta Ct = Ct target gene – Ct housekeeping gene), the house keeping genes were selected based on the fact that their expression does not change with treatment or genetic manipulation of the cells. Next, the Delta-Delta Ct method was used for analysis. The change in expression was expressed as a fold change relative to control samples (equivalent to  $2^{-(\text{Delta Ct treated} - \text{Delta Ct control})}$ ).

### 2.4.6. Protein expression analysis

#### 2.4.6.1. Western immunoblotting

##### 2.4.6.1.1. Whole cell lysate preparation

Whole cell lysate was extracted using radioimmunoprecipitation assay (RIPA) buffer supplemented with protease and phosphatase inhibitors (Roche Life Sciences) to inhibit protein dephosphorylation and degradation. For adherent cells, media was removed and cells were washed with cold PBS. For suspension cells, the cells were pelleted at 400 g for 5 min and the supernatant was discarded.

Next, 100  $\mu$ L of RIPA buffer was added to the cells and a cell scraper was used to aid the lysis of the adherent cells, while pipetting was used to aid the lysis of the suspension cells. Cells were collected in a 1.5 ml eppendorf tube and incubated on ice for 20 minutes, followed by a spin at 15000 g and 4°C for 20 minutes. The supernatant was collected and the pellet was discarded.

Finally, 4x sample loading buffer, containing  $\beta$ -mercaptaethanol, glycine and bromophenol blue were added to the samples, mixed and then denatured at 100 °C for 5 minutes. Thereafter, the samples were ready to be loaded onto the gels.

#### **2.4.6.1.2. SDS-PAGE and immunoblotting**

10% acrylamide gels (30% Acrylamide/Bis Solution, BioRad) were casted for resolving proteins of large molecular weight and 12-14% acrylamide gels, for proteins of lower molecular weight. The gel mix contained 10% SDS (to linearise and mask protein charge), 7.5 M of Tris-EDTA at pH 8, 10% Ammonium persulphate and TEMED, to aid polymerisation. Samples were loaded into the designated wells of the gels alongside Precision Plus Protein™ All Blue Prestained Protein Standards (Bio-rad). Gels were run at 200V for 55 minutes in running buffer containing 10% SDS, 20 $\mu$ M Glycine and 157 $\mu$ M Tris-Base. For lower molecular weight proteins, gels were run at 180V, to start off with, and then at 200V under careful observation, so that the proteins did not run off the gel.

At the end of the run, proteins were transferred from the gel onto a polyvinyladine fluoride (PVDF) membrane pre-treated with methanol and pre-wetted in transfer buffer containing 20  $\mu$ M Glycine and 157  $\mu$ M Tris-Base. The transfer took place at 100V for 50 minutes. An ice pack was placed in the transfer tank to lower the temperature from the heat generated due to the electric current. The membranes were then blocked for 1 to 2 hours at RT in 5% BSA for total proteins and in 5% non-skimmed milk for phosphorylated proteins. Membranes were then incubated overnight at 4°C in primary antibodies at the dilutions indicated in table 2.1. Horseradish peroxidase (HRP) conjugated secondary antibodies were used for detection. The blots were incubated with respective secondary antibodies for an hour at RT, followed by five 5 minute washes in PBS + 0.01% Tween 20.

#### **2.4.6.1.3. Chemiluminescent detection**

Membranes were imaged using enhanced chemiluminescence (ECL) reagent (GE healthcare, Little Chalfont, UK). Solution A and solution B were mixed in

a 1:1 ratio. The membranes were then covered in the resulting solution and incubated for 1 minute, before excess solution was drained off. The membranes were imaged on a Chemdoc-It2 Imager (UVP, LLC, Upland, CA, USA), with the UVP set to filter 3.

#### **2.4.6.2. ELISA**

To examine MIF and IL-8 secretion into culture media, the Human MIF Douset ELISA Kit (R&D systems) and Human IL-8 ELISA Ready-SET-Go ELISA kit (eBioscience) were used.

For the Human MIF Douset ELISA Kit, capture antibody was diluted in coating buffer and 100 µL of the solution was pipetted into each micro-well of a 96 micro-well plate, using a multi-channel pipette. The plate was incubated overnight at RT. The next day, the micro-wells were washed four times with 300 µl wash buffer. For blocking, 300 µl reagent diluent was added to each well and the plate was incubated for one hour at RT. The micro-wells were then washed three times with wash buffer. Thereafter, 100 µL aliquots of standard solutions, blanks and samples were added in duplicates to the micro-wells, and were then diluted 1:2 in reagent diluent. The plate was incubated for 3 hours at RT. Next, the micro-wells were washed four times with wash buffer. 100 µL of the detection antibody diluted in reagent diluent was subsequently added, and the plate was incubated for 2 hours at RT. At the end of the incubation time, the micro-wells were washed to remove excess detection antibody and to minimize unspecific binding. 100 µl streptavidin-HRP was added to each well and incubated for 20 minutes in the dark. The micro-wells were washed to remove excess streptavidin-HRP. Substrate A and substrate B were mixed in a 1:1 ratio, 100 µl of which was subsequently added to all wells. The plate was incubated in the dark for 20 min, at which point a blue colour started to develop. Following this colour change, 50 µL of stop solution was added to quench the reaction and the absorbance was immediately recorded at 450 nm and 570nm on a FLUQstar Omega plate reader (BMG Labtech, Offenburg, Germany). The colour remains stable for up to four hours after the stop solution is added.

For the IL-8 ELISA Ready-SET-Go ELISA kit, a 96 micro-well plate was incubated overnight at 4°C, with 100 µL of well coating-antibody solution. The micro-wells were then washed three times with 300 µL wash buffer (PBS containing 0.05% Tween20) and were then blocked by adding 200 µL of 1X ELISA/ELISPOT diluent for 1-2 hours at RT. The micro-wells were washed three times with wash buffer, then 100 µL of standards, blanks and samples were added in duplicates to the micro-wells, each of which were diluted 1:2 in reagent diluent. The plate was incubated overnight at 4°C. Next, the micro-wells were washed 5 times with wash buffer and 100 µL of diluted detection antibody was added to the wells and incubated for 2 hours. Excess detection antibody was later washed off, as previously described, and 100 µL streptavidin-HRP was added to each well and incubated for 30 minutes in the dark. The micro-wells were then washed 7 times to remove excess streptavidin-HRP, after which 100 µL of 1X TMB solution was added to all the wells and incubated for 15 minutes in the dark. Next, 50 µL stop solution (2N H<sub>2</sub>SO<sub>4</sub>, sulphuric acid) was added, and the absorbance was immediately read at 450 nm and 570nm on a FLUQstar Omega plate reader.

To analyse the readouts, the readings at 570nm were subtracted from the readings at 450nm, to reduce disturbance from dust and air particulates that absorb light equally at both wavelengths. A four-parameter logistic regression fitting method was employed to analyse standard curves, using the ELISAanalysis online software (ELISAKIT, Australia). Standard curves with R values of 0.9-0.99 were used to calculate unknown cytokine concentrations.

#### **2.4.6.3. Proteome Profiler Human XL Cytokine Array**

The Proteome Profiler Human XL Cytokine Array (R & D systems, # ARY022) was used to determine the levels of 102 secreted cytokines in AML only, BMSC only or AML/BMSC co-cultures. It employs capture and control human antibodies that have been pre-spotted in duplicates on a nitrocellulose membrane. Then, via a series of incubation steps gives a measure of cytokine protein expression in a sample of culture media, cell lysate, serum or plasma.

Each well contained a final volume of 1 ml culture supernatant. The supernatant culture media was collected, and particulate matter was disregarded after centrifugation at 400 g for 5 minutes, and the supernatant stored at -20°C. When the array was due to be performed, the samples were defrosted on ice. The array membranes were blocked by adding 2 ml of the provided block buffer and incubated for 1 hour at RT. Next, 0.5 ml block buffer was added to 1 ml of the cell culture supernatant, which was then applied onto each of the respective membranes and left overnight at 4°C with gentle rocking. The membranes were then washed three times for 10 minutes (while on a rocking platform for efficient washing), with the provided wash buffer. Thereafter, the supplied detection antibody cocktail was added and the membranes were incubated for 1 hour on a rocking platform. The detection cocktail was aspirated and the array washed three times for 10 minutes. Streptavidin-HRP was then added at 1:2000 (diluted with array buffer) and incubated for 30 minutes with gentle rocking. After the membranes were washed thrice for 10 minutes, the array ECL detection reagent was made by mixing Chemi reagent 1 and Chemi reagent 2 in a 1:1 ratio. Each of the membranes were then covered with 1 ml of the mixed chemi solution, after which the array membranes were wrapped in plastic wrap and imaged as described in section 2.5.2.1.3.

The optical density of the resulting images were quantified and analysed using the HImage++ software (Western Vision Software, Salt Lake City, UT, USA) which had pre-designed templates for all R and D protein arrays. The output files, contained average pixel densities of each of the duplicates representing each cytokine. They also contained reference spots that were used to confirm that the assay had worked, and to compare assay to assay variability.

#### **2.4.6.4. Flow cytometry**

Flow cytometry was used to measure surface and internal protein expression on target cells. For surface marker staining, cells were washed with cold MACS buffer (PBS + 0.5% BSA + 2 mM EDTA) and centrifuged at 300 g for 5 min. Next, the cells were re-suspended in 90 µl MACS buffer and 10 µl FCR

blocking reagent. Thereafter, 2  $\mu$ l of the respective control, or marker of interest fluorochrome-conjugated antibodies were added. Cells were incubated for 10-15 minutes at 4°C in the dark. At the end of incubation, cells were washed with MACS buffer, pelleted at 300 g for 5 minutes, and then re-suspended in 1 ml cold filtered PBS. The cells were immediately analysed on the BD Accuri C6 (BD Biosciences, Allschwil, Switzerland) or on the CyFlow® Cube 6 (Sysmex-Partec, Görlitz, Germany) flow cytometers. A minimum of 3000 events were collected and data was analysed on the respective software.

Newly synthesised CD74 is expressed on the cell surface, followed by rapid internalisation to the endosomal pathway. The surface half-life of CD74 is very short (less than 10min) (288). Therefore, experiments that study cell surface CD74 expression are complicated by the fact that CD74 remains on the cell surface for a very short time. Accordingly, various flow cytometry protocols recommend cells to be fixed and permeabilised when staining for CD74. The fix and perm kit (Invitrogen, Thermo Fisher Scientific, UK) was used to detect CD74 expression in BMSCs. First, BMSCs were trypsinised, pelleted and washed once in PBS with 5% FCS (wash buffer). Next, the cells were re-suspended in 100  $\mu$ l Reagent A (fixation medium) and incubated for 15 minutes at RT. The cells were then washed with 1.5 ml wash buffer, re-suspended in 100  $\mu$ l of Medium B, followed by the addition of 2  $\mu$ l CD74-FITC antibody – this suspension was then vortexed and incubated for 20 minutes at RT in the dark. 3 ml wash buffer was then added to wash off excess antibody. Finally, the cells were re-suspended in 1 ml of filtered PBS for analysis on the CyFlow® Cube 6 flow cytometer. A minimum of 3000 events were collected. Data was subsequently analysed using the FCS express 5 software (FCS express version 5 software (De Novo Software, Thornhill, ON, Canada).

#### **2.4.7. shRNA-mediated gene silencing**

In this study, MISSION shRNA lentiviral knockdown was used to achieve long term silencing of gene expression in target cells. MISSION shRNA lentiviral clones are sequence-verified shRNA lentiviral plasmids for gene silencing in mammalian cells (Sigma). The MISSION® TRC shRNA plasmid was

transformed into *E.coli* strain DH5 $\alpha$ T1R, expressing shRNA, which targeted either MIF, HIF1 $\alpha$  or HIF2 $\alpha$  genes (in pLKO.1-puro plasmid vectors).

The plasmids expressing the shRNAs can either be directly transfected into target cells to attain transient gene knockdown, or they can be co-transfected with packaging plasmids into the 293T cell line, for long-term knockdown by integration into the host cell genome. The latter method was used in the research presented in this thesis.

Bacterial cultures were amplified from glycerol stocks in order to extract sufficient amounts of shRNA plasmid DNA. Lentiviral stocks were prepared by co-transfecting 293T cells with the shRNA plasmid and two other plasmids: a packing plasmid, pCMV $\Delta$ R8.91 (expressing gag-pol) and an envelope plasmid, pMD.G (expressing VSV-G). These were kindly provided by Dr Ariberto Fassati (University College London, London, UK).

Lentiviral titres were determined using the Lenti-X™ qRT-PCR titration kit (ClonTech Laboratories, California, USA) and viral stocks were concentrated using Amicon® Ultra centrifugal filters (EMD Millipore, Massachusetts, USA). Figure 2.3 shows a schematic summarising the work-flow that was followed to obtain successful knockdown of target genes.

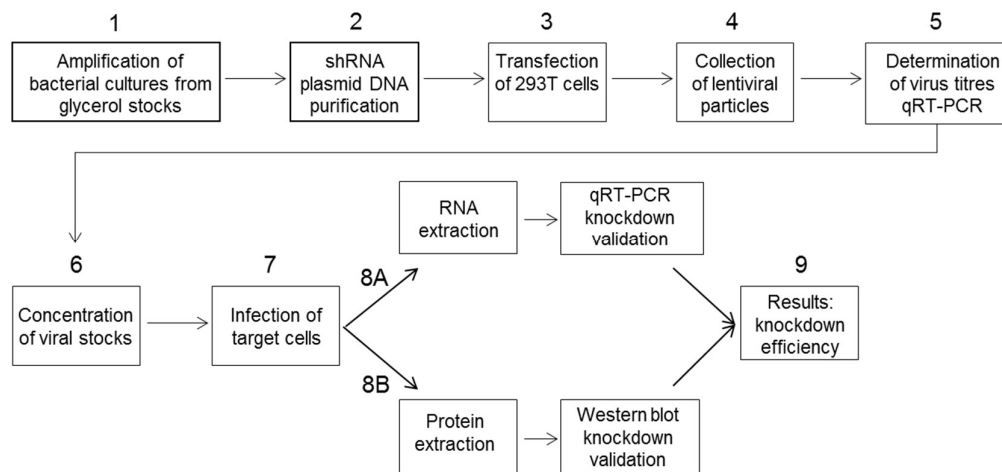


**Figure 2. 3 A schematic showing the work flow followed in the production of lentiviral particles from bacterial glycerol stocks.**

For silencing of IL-8, CD74 and PKC $\beta$  PKC $\beta$  genes, pre-packaged MISSION<sup>®</sup> TRC shRNA Lentiviral Transduction Particles were used. In this case, step 1 to 6 of the workflow shown in Figure 2.3 was performed. The MISSION pLKO.1-puro Control Vector (SHC001, Sigma-Aldrich) was used as a control, which is an empty vector confirmed to not activate the RNAi pathway, as it does not contain an shRNA insert. All bacterial glycerol stocks were stored at -80°C. ShRNA sequences of mission shRNA lentiviral particles are provided in table 2.3. The following sections will cover the process of lentiviral knockdown in detail.

**Table 2. 5 Sigma mission shRNAs used for stable knockdown of target genes.**

Gene	Clone ID	TRC number	Sequence 5' → 3'
IL-8	NM_000584.2-178s1c1	0000058030	CCGGCAAGGAGTGCTAAAGAACTTACTCG AGTAAGTTCTTTAGCACTCCTTGTTTTTG
PKC $\beta$	NM_002738.6-292s21c1	0000435447	CCGGATGAGGTCAAGAACCACAAATCTCG AGATTTGTGGTTCTTGACCTCATTTTTTTG
CD74	NM_004355.1-742s1c1	0000008635	CCGGCCACACAGCTACAGCTTTTCTTCTCG AGAAGAAAGCTGTAGCTGTGTGGTTTTT
MIF	NM_002415.1-374s1c1	0000056818	CCGGGACAGGGTCTACATCAACTATCTCG AGATAGTTGATGTAGACCCTGTCTTTTTG
HIF1 $\alpha$	NM_001530.x-1492s1c1	0000010819	CCGGCCGCTGGAGACACAATCATATCTCG AGATATGATTGTGTCTCCAGCGGTTTTT
p16	NM_058197.3-971s21c1	0000255849	CCGGGCTCTGAGAAACCTCGGGAAACTC GAGTTTCCGAGGTTTCTCAGAGCTTTTTG
HIF2 $\alpha$	NM_001430.x-2419s1c1	0000003805	CCGGGCGCAAATGTACCCAATGATACTCG AGTATCATTGGGTACATTTGCGCTTTTT

#### 2.4.7.1. Amplification of bacterial cultures

For bacterial cultures, agar plates were made by combining Lysogeny Broth (LB) (containing 10 g/L Tryptone, 10 g/L NaCl and 5 g/L yeast) with agar at 10 g/L. The LB-Agar media was sterilised and cooled to 50°C before supplementing with ampicillin at 100  $\mu$ g/ml. 10 ml aliquots were pipetted into 10 cm dishes and stored for usage at 4°C for up to a month. Frozen bacterial glycerol stocks were rapidly thawed at RT and streaked onto the agar plates using a sterile streaking loop, followed by incubation at 37°C overnight. Thereafter, single bacterial colonies were picked with a sterile pipette tip and inoculated in 5 ml of LB broth with shaking at 37°C for 16 hours.



The selection of Individual, isolated colonies ensured colony homogeneity and helped to avoid picking satellite colonies that tend to grow in antibiotic depleted areas of the plate. 4 to 5 colonies were cultured per plasmid to ensure high yield of plasmid DNA.

#### **2.4.7.2. Plasmid DNA isolation and precipitation**

kit (Macherey-Nagel, Germany). Firstly, the bacterial cultures were pelleted by centrifugation and re-suspended in 500 µl re-suspension buffer A1, followed by the addition of 500 µl of SDS/alkaline lysis buffer A2, and incubation at RT for 4 min. Next, 300 µl A3 buffer was added to neutralise the suspension and aid the binding of plasmid DNA onto the silica membrane of the spin columns. The contents were mixed by gentle inversion. Precipitated proteins, genomic DNA and cell debris were pelleted by centrifuging the tubes at 11000 g for 7 minutes. The supernatant was then loaded onto the spin column. The column was washed twice at 11000 g for 1 minute using ethanolic wash buffer A4, followed by a final drying spin for 3 min. Finally, the DNA was eluted in 50ul nuclease-free water at 70°C.

The optimal concentration of plasmid DNA required for transfection of packaging cells is <180ng/µl. To achieve this, plasmid DNA of the highest purity from different colonies was pooled together and ethanol-precipitated. Ethanol precipitation is a well-established method for the concentration and desalting of nucleic acids. In this method, 3M solution of sodium acetate (pH 5.2) was added at 1/10<sup>th</sup> of the volume of pooled plasmid DNA. Next the volume was completed to 1 ml with ice-cold ethanol, which forced the plasmid DNA to precipitate out of solution. The resulting solution was then stored overnight at -20°C, or for 4-5 hours at -80°C to precipitate. After precipitation, the DNA was pelleted by centrifugation at maximum speed (14000 g) for 15 minutes. The pellet was washed in cold 70% ethanol and centrifuged again. Ethanol was aspirated without disturbing the pellet, which was then left to dry in a culture hood. As it dried, the translucent pellet became whiter and more opaque. Finally, the pellet was rehydrated in nuclease free water and stored at -20°C.

#### **2.4.7.3. 293T packaging cell transfection**

24-48 h prior to transfection, 293T cells were cultured in 10 cm culture dishes and passaged so that the cells were ~ 80% confluent. On the day of transfection, packaging cell media was replaced with 7.5-8 ml of fresh, antibiotic free, complete culture media. DNA mix was prepared so that it contained 1 µg of each of the packaging plasmids, 1.5 µg of the specific shRNA plasmid and TE buffer up to 15 µL. In a separate tube, a transfection vehicle was prepared by adding 18 µL FuGENE® (Promega, Fitchburg, WI, USA), and 6 to 200 µl of Opti-MEM (Life Technologies, Gaithersburg, MD, USA.) reduced serum media. The DNA mix was then added onto the transfection vehicle mix, and the two were gently mixed by pipetting, before being incubated at RT for 15 minutes. The resulting solution was added drop wise onto the plate of packaging cells. The plates were incubated in normal culture conditions and the media was changed every 24 hours, with 7.5 ml of fresh culture media. Culture media was collected in 15 ml falcon tubes at 48, 72 and 96 hours. 150 µl was also taken from each plate at specific time points to be used for extraction of viral RNA. All media was stored at -80 °C.

#### **2.4.7.4. Viral RNA isolation**

Viral RNA was isolated using the NucleoSpin® RNA Virus isolation kit (Macherey-Nagel). Aliquots of media that were frozen in the previous step were defrosted on ice. 70 µl from the media collected at each time point was pooled into one Eppendorf. From this, a 150 µl aliquot was taken out into a new Eppendorf tube. 600 µl of RAV1 was added to the tube, vortexed, and incubated at RT for 5 minutes. 600 µl of absolute ethanol was next added and the tube was vortexed for 30 seconds. 675 µl of this solution was transferred into a spin column and centrifuged at 8,000g for 1 minute. The spin step was repeated with the remaining 675 µl. Next, the column was washed once with 500 µl of (full form) RAW buffer and then with 600ul of RAV3, followed by centrifugation at 8,000g for 1 minute. Waste was discarded after every wash step. To dry the columns, a final wash step was required, where 200 µl of

RAV3 was added to the tube and centrifuged at 11,000g for 5 minutes. Finally, viral RNA was eluted by adding 50 µl of nuclease-free water (at 70 °C, as hot water aids in RNA elution), and incubating at RT for 1 – 2 minutes followed by a spin at 11,000 g for 1 minute. Viral RNA was then stored at -80 °C for long term use.

#### **2.4.7.5. Determination of viral titres**

(Thermo Fisher Scientific) to remove any contaminating plasmid DNA prior to qRT-PCR. DNase treatment is key, as contaminating plasmid DNA could lead to false high copy numbers. 25 µl reactions were incubated at 30°C for 30 minutes and at 70°C for 5 minutes with a 4°C hold.

Serial dilutions of the stock DNase-treated viral RNA and of an RNA control (known copy number of  $10^9$ – $10^2$ , provided with the kit) were prepared, and 2 µl each were aliquoted per well, in a 96 multi-well PCR plate. Next, a master mix was made following the manufacture's recommendation, using the Quant-X™ One-Step qRT-PCR SYBR® kit (Clontech). 18 µl of the master mix was added to the samples to make a final reaction volume of 20 µl and the plate was sealed. The following program was used for the qRT-PCR run: RT Reaction (42°C for 5 minutes and 95°C for 10 seconds), qPCR x 40 cycles (95°C for 5 seconds and 60°C for 30 seconds) and melt Curve analysis (95°C for 15 seconds, 60°C for 30 seconds).

The lentiviral copy number in the initial viral stocks was determined by comparing their Ct values to Ct values on a standard curve generated from serial dilutions of the calibrated Lenti-X RNA Control Template, and by accounting for the dilution factors. A copy number of at least  $X10^8$  is required to achieve reasonable knockdown. The formula below was used for back-calculating copy number/ml:

$$\text{Copies/mL} = \frac{\text{Concentration from PCR (X10}^7\text{) (1000uL/mL)(2xDNase)(50 } \mu\text{L elution)}}{(150 \mu\text{L sample})(2 \mu\text{L added to PCR well)}}$$

Next, copies per ml were converted into transducing units per ml (TU/mL):

$$\text{TU/mL} = \frac{\text{Copies/mL}}{100000}$$

The division factor (100,000) was estimated from an experiment where the qRT-PCR titration method was normalised to a conventional fluorescent microscopy method for titrating lentiviral vectors expressing GFP. GFP positive cells/colonies were counted and a normalising factor was generated (performed by Dr Lyuba Z, Norwich Medical School, UEA, Norwich, UK).

Next, using the determined values for TU/ml, the volume needed to achieve the desired number of viral particles was calculated for multiplicities of infections (MOI) ranging from 1-30 as follows:

$$\text{Volume required} = \frac{\text{Number of cells to be infected}}{\text{TU/mL}} \times \text{desired MOI}$$

Viral stocks were concentrated using Amicon® Ultra centrifugal filters. During the concentration procedure, all plastic ware and samples were kept on ice to prevent degradation of viral particles at RT. The above calculated volume was divided by the concentration factor to obtain the right volume of concentrated stock required to achieve the desired infectious particles/cell. A range of MOIs were tried out to determine an MOI that achieves gene knockdown with minimal off target effect and without compromising cell viability.

#### **2.4.7.6. Lentiviral infection of target cells**

Viral stocks were stored in -80°C and when needed, thawed at 4°C on ice. The required number of cells to be infected was cultured in 0.5 ml of antibiotic free complete culture media, in 12 well culture plates. Polybrene was added at a final concentration of 1 µg/ml to the cell cultures, to increase the efficiency of infection. Polybrene works by countering electrostatic charges between the virus and the cell membrane, which both have a negative charge on their surfaces. Next, the required volume of virus for the desired MOI was added and the plate was gently swirled to ensure even distribution. At 24 hours, the

cultures are topped up with an additional 500 µl of antibiotic-free culture media and incubated for an additional 48 hours at RT. At 72 hours, RNA was extracted as described before (section 2.4.1) and the gene knockdown efficiency was determined by qRT-PCR. At 96 hours, protein was extracted as described before (2.4.6.1.1) and western blotting was performed (2.4.6.1) to determine protein knockdown.

#### **2.4.8. Senescence associated $\beta$ -galactosidase staining**

The senescence  $\beta$ -galactosidase staining kit (Cell Signaling Technology (CST), Massachusetts, USA) was used to detect Senescence associated  $\beta$ -galactosidase in BSMCs. Cells of interest were cultured and treated in 35 mm culture dishes. The culture media was removed and cells were washed once with PBS and fixed with 1 ml 1x fixative solution for 15 minutes at RT. Cells were next washed twice with PBS and incubated at 37°C overnight, in 1 ml of  $\beta$ -galactosidase staining solution. The pH of the staining solution was measured and, if needed, adjusted to a pH of 6. A low pH can result in false positives while a high pH can result in false negatives. The plates were sealed with parafilm to prevent changes in pH due to atmospheric carbon dioxide.

The cells were checked for the development of a blue colour, which usually happens within 48 hours, and is indicative of SA- $\beta$  galactosidase positive cells. The staining solution was removed and replaced with 1 ml of 70% glycerol. Stained plates were viewed under a light microscope and pictures were acquired using a camera and the 10x lens. The plates were resealed and stored at 4°C. The fixed plates are stable for over 12 months if stored properly.

#### **2.5. *In vivo* animal models**

All animal work was carried out in accordance with regulations set by the UK Home Office and the guidelines outlined in the Animal Scientific Procedures Act, 1986. Animals were housed in the Disease Modelling Unit (DMU) facility at the University at East Anglia, in individually ventilated cages, and maintained under specific pathogen-free conditions. The animals were regularly screened for common mouse pathogens. 8 – 10 week old mice were used for all the experiments. Non-obese diabetic/severe combined

immunodeficiency (NOD/SCID) mice were purchased from Jackson Laboratories (Bar Harbor, ME, USA). The p16-3MR senescence mouse model was kindly gifted to our lab by Dr Campisi (The Buck Institute for Research on Aging, Novato, USA). A full description of the procedure employed to generate the p16-3MR Mouse model is described by Demaria et. al., 2014 (262).

### **2.5.1. Non- diabetic (NOD) severe combined immunodeficiency (SCID) and gamma model (NSG) mice for human xenograft models**

Cell line and primary patient derived xenografts require the recipient animal to be immunodeficient to avoid rejection of transplanted human cells. The most commonly used immunodeficient mouse strain is the NSG or NOD *scid* gamma mouse, also called the NOD.Cg-Prkdcscid IL2rgtm1Wjl/SzJ mouse, developed by Dr. Leonard Shultz at The Jackson Laboratory. Genetically, this mouse model harbours a functionally null allele for the IL-2 receptor gamma chain (IL2Rg<sup>null</sup>) and the severe combined immune deficiency mutation (*Prkdc<sup>scid</sup>*) on the nonobese diabetic NOD/ShiLtJ background (289). Phenotypically, these mutations translate into the lack of mature B and T, natural killer cells, and defective dendritic cells. Together, this makes it possible for cancer cell lines and human cells to be engrafted easily in this model (290).

### **2.5.2. Patient derived xenografts**

Primary AML cells were infected with a pCDHluciferase-T2A-mCherry lentiviral construct, kindly gifted by Prof. Dr. Med. Irmela Jeremias, (Helmholtz Zentrum München, Munich, Germany) (291), and sorted by flow cytometry using the red channel on a BD FACSAria III cell sorter (BD Biosciences), with the help of Zhigang Zhou (School of Biological Sciences, UEA, Norwich, UK). The luciferase moiety allowed monitoring of disease development via *in vivo* bioluminescent (BL) imaging.  $2 \times 10^6$  viable AML cells were washed and re-suspended in PBS.

Injections of the AML cells into non-irradiated, 6-8 week-old, NSG was performed by Chris Marlein, R Piddock and S Rushworth (Norwich Medical School, UEA, Norwich, UK). Prior to being injected, the mice were warmed in

individual warming boxes at 37°C for 10 minutes (which helped to dilate the tail veins for easy and visible introduction of needles). 200 µl of AML cell suspension was injected into their tail veins using a sterile, 27-gauge needle, attached to a 1 ml syringe. Immediately following injections, mice were closely monitored for signs of bleeding from the injection site and returned to the cages.

### **2.5.3. OCI-AML3 human xenograft model**

OCI-AML3 cells were infected with the pCDH-luciferase-T2A-mCherry lentiviral construct, followed by infection with control-ShE, MIF KD or HIF KD lentiviral particles. Next, the cells were sorted on a BD FACSAria III (BD Biosciences, Allschwil, Switzerland) cell sorter.  $1 \times 10^6$  cells were washed and re-suspended in PBS. The cells were then injected into the tail vein of NSG mice, as described in section 5.2.5. The MIF-KD and the HIF1 $\alpha$ -KD *in vivo* experiments were carried out simultaneously, therefore, the same control-KD (ShE-KD) mice were used for both, MIF-KD and HIF1 $\alpha$ -KD mice.

### **2.5.4. *In vivo* bioluminescent (BL) imaging**

Animals were imaged on the Bruker In-Vivo Xtreme Imaging Systems (Bruker Corp., Massachusetts, USA) imager. *In vivo* imaging was performed with the help of Chris Marlein, R Piddock and S Rushworth (Norwich Medical School, UEA, Norwich, UK). Each animal was imaged at the days specified in the text (section 5.9). D-luciferin (Thermo Fisher Scientific) was dissolved in sterile PBS (15 mg/ml) and aliquots were stored at -20°C. Each animal was injected with 200 µl of D-luciferin at RT by intraperitoneal injection (IP), and allowed to settle for 10 minutes before they were anaesthetised with 2-3% isoflurane/oxygen in an induction chamber, and then carefully transferred to the Bruker specimen chamber.

Anaesthesia was maintained during imaging using a nose cone isoflurane-oxygen delivery device fitted in the chamber. Bioluminescent images were acquired within 20 minutes after IP of D-Luciferin. The camera took a light, an X-ray and a luminescent image of the animals. Finally, the animals were allowed to recover under close observation and returned to their cages. Luminescent signal intensity was quantified and final images were analysed

using the Bruker MI SE software. The output images represented matched-scale luminescent images overlaid on light images showing the animal skeleton, thus allowing to determine where the tumour cells are (as seen in Figure 5.14A).

#### **2.5.5. Sacrificing animals and harvesting of the bone marrow and spleen cells**

Animals were monitored daily for the development of clinical signs of illness, and when these became apparent (such as weight loss, reduced motility, bilateral hind leg paraplegia due to tumour burden, over grooming and rough, patchy fur), mice were sacrificed by exposure to CO<sub>2</sub> and dislocation of the neck. BM and spleen cells were harvested and analysed for human CD33 and CD45 expression. The tibia and femurs (Figure 2.4A) were isolated whole and de-fleshed (Figure 2.4B). Next the bones were cut from the thinner end and placed in a 0.5 ml Eppendorf tube in which a hole was made using an 18 gauge syringe. This tube was placed in an intact 1.5 ml Eppendorf tube and centrifuged at high speed for 10 seconds to collect total BM cells. The open end allowed BM cells to escape into the 1.5 ml collection tube.

The spleen was immersed in PBS, minced in a 35 mm culture dish using a 1 ml sterile tip and filtered through a 4 micron mesh to obtain a single cell suspension. Red cell lysis was performed with the Hybri-Max buffer. BM and spleen cells were then double stained for CD33/CD45 and assayed by flow cytometry. If more than 1% of human CD33/CD45 cells were detected in the BM or spleen, the AML sample was considered to have been successfully engrafted. 5 x10<sup>6</sup> cells were re-suspended in RNA BL+TG lysis buffer for mRNA expression. Excess cells were discarded.



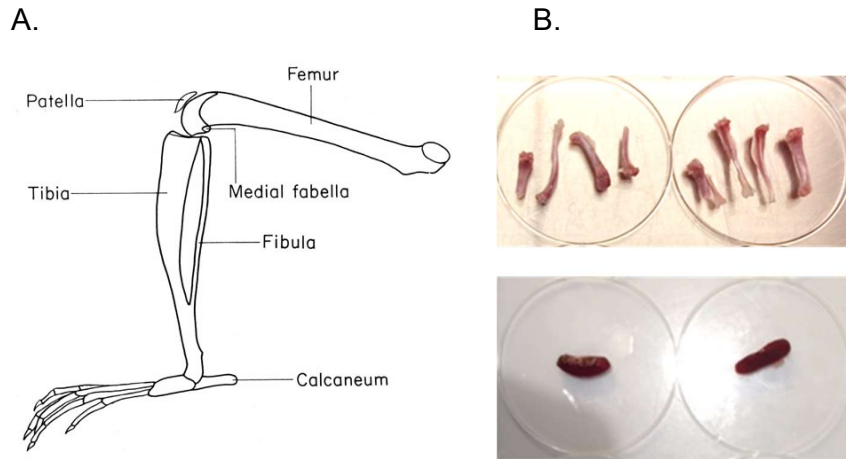


**Figure 2. 4 Bones and spleens harvested from NSG mice.**

(A) A schematic depicting the different parts of the hind limbs of a mouse (adapted from *The Anatomy of the Laboratory Mouse*, Margaret J. Cook (292)). (B) The top panel shows excised and de-fleshed tibias and femurs from 2 NSG mice; the bottom panel shows excised spleens from 2 NSG mice.

## 2.6. Bioinformatics analysis

Bioinformatics analysis was performed with the help and guidance of Manar Shafat (Norwich Medical School, UEA, Norwich, UK). Publicly available RNA sequencing data were downloaded for a panel of 43 AML patients, comprised of 22 AML samples obtained from peripheral blood and 21 AML samples obtained from BM aspirates (Gene Expression Omnibus Accession ID: GSE49642).

Reads per kilobase per million (RPKM) data for MIF were extracted and processed further by first replacing zero-valued entries, with one followed by logarithmic transformation to the base 2. MIF RPKM values for blood and bone marrow samples were compared with a Wilcoxon rank-sum test. Data were extracted for genes that have been shown to be upregulated as a result of HIF1 $\alpha$  overexpression, HIF2 $\alpha$  overexpression and hypoxia (293). These data were processed further by first replacing zero-valued entries with one, followed by logarithmic transformation to the base 2.

## **2.7. Statistical analyses**

All data were analysed using Prism software (Version 5.0, GraphPad Software, San Diego, CA, USA). The Mann-Whitney U test was used to compare test groups unless stated otherwise in the figure legend. Survival data were analysed by Kaplan-Meier log-rank test. Results where  $P < 0.05$  were considered statistically significant and are denoted by \*. Results represent the mean  $\pm$  standard deviation of 3 or more independent experiments. Standard error of the mean was used to present cytokine array data deviation (Figure 3.5 and Figure 3.6).

### **3. Chapter 3: AML influences the secretory profile of BMSCs**

In this chapter, I first aimed to *in vitro* characterise BMSCs and subsequently establish an AML/BMSC co-culture. From the co-cultures, using a cytokine array assay, I determined potential AML pro-survival cytokines.

#### **3.1. *In vitro* expansion of primary AML-derived BMSCs**

Whole BM aspirates from AML patients, who consented at the NNUH haematology clinic, were processed in the tissue culture laboratory according to the protocol described in materials and methods (section 2.3.2). I used isolated mononuclear cells to expand BMSCs *in vitro*. Human BMSCs are initially isolated based on their selective adherence to plastic culture surfaces, followed by phenotypic characterisation to confirm the expression of a panel of cell surface molecules, including CD90, CD105 and CD73, and excluding of CD45 (294).

I cultured the isolated bone marrow mononuclear cells at 1 million cells per mL in T-75 culture flasks overnight and observed the cells the next day for adherence. Contrarily to BMSCs, AML cells are non-adherent to plastic, and thus, can be selectively removed from culture after the initial medium change, 24 - 48 hours post isolation. The chosen time point depended on when I was able to identify adherent BMSCs that were 80% confluent. Any contaminating AML cells were eliminated as the BMSC cultures were passaged and this process was usually complete at passage 2 or 3 (Figure 3.1A). Before using the BMSC cells for experiments, I would check for expression of BMSC markers (CD90, CD105 and CD73) and negative expression of the myeloid marker CD45 (Figure 3.1B) to further confirm the purity of the BMSC population. Purities of > 99.99% were routinely achieved with this method.

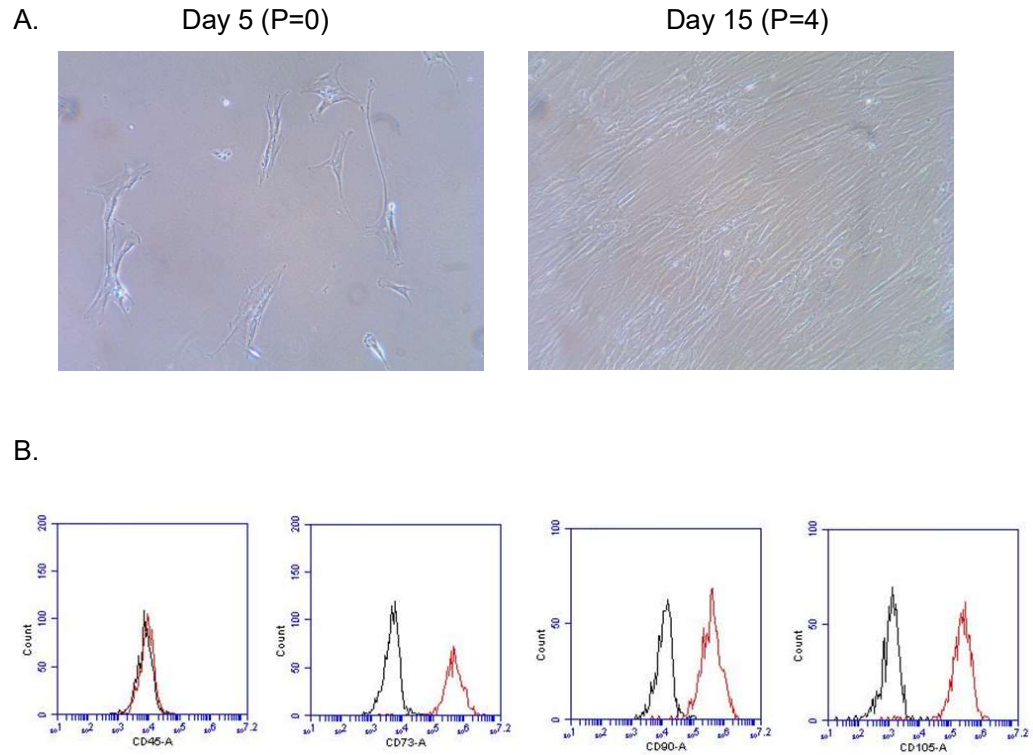


**Figure 3. 1 *In vitro* expansion and characterization of bone marrow stromal cells (BMSCs).**

(A) Growth of BMSCs over 15 days. P, passage number. (B) Surface marker expression on BMSCs at day 15 of culture, cultured cells were CD45 negative and CD73, CD90 and CD105 positive – which is characteristic of BMSCs. The red peak represents the marker of interest and the black peak represents the isotype control.

Over time, I noticed that after 6-8 weeks of passaging (the average number of passages depended on the individual BMSC sample), cell proliferation began to slow down and their morphology changed from a fibroblastic spindly shape, to a flatter rounder shape with cell-free gaps (Figure 3.2). When the cells started displaying this phenotype, I would deem them unsuitable for further use and the culture would be terminated. No primary BMSCs were cultured past passage 6. BMSCs could also be derived from cryopreserved AML cell samples with a similar prolifere.

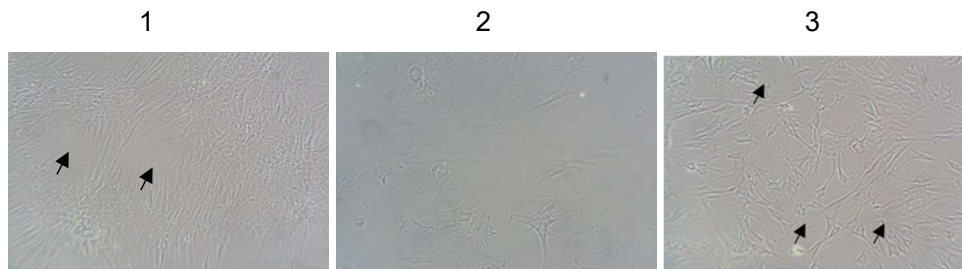


**Figure 3. 2 Morphology of primary cultured BMSC over time.**

(1) BMSCs after 7 passages; the arrows indicate cell-free gaps (2) BMSCs after 9 passages (3) BMSCs after 10 passages; the arrows indicate cells with a different morphology.

Cytogenetics of the six primary BMSCs used for the experiments described below were initially examined, following Huang et. al.'s previous observations of cytogenetic abnormalities in 75% of the BMSCs of patients with AML (295). My results found three of six to be normal, whereas genotyping failed for the other three (table 1 of the appendix).

### **3.2. BMSCs support AML survival *in vitro***

AML cells exhibit a high level of spontaneous apoptosis when cultured *in vitro* but have a prolonged survival time *in vivo*, indicating that the BMM plays a critical role in promoting AML cell survival and proliferation (296-298). For my research, I aimed to investigate how well BMSCs support the *in vitro* survival of primary human AML cells, and to do so I established a co-culture system with primary AML cells and BMSCs from AML patients who never had chemotherapy to treat the AML.

For the co-culture I used two cell populations in transwell plates, with BMSCs cultured on the bottom of the plate and AML cells placed above. As a monoculture control, AML cells were placed in the transwell with no BMSCs. The survival of AML cells with BMSCs versus monoculture was assessed by viable cell counting, utilising trypan blue exclusion and a hemocytometer on day 6 (n=20) and day 14 (n=6). I found that AML survival was significantly improved when co-cultured with BMSCs, compared to the controls at both,

days 6 and 14 (Figure 3.3). The cytogenetics and WHO diagnosis of the AML patient samples used in chapter 3 and 4 are shown in table 3.1.

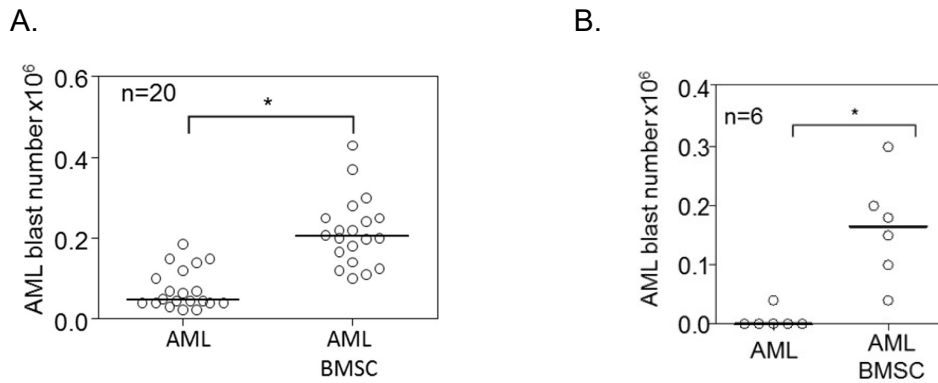


**Figure 3. 3 Primary AML survival in mono-cultures versus on primary BMSCs.**

Scatter graph depicting the survival of AML cells cultured on BMSCs versus AML cells alone (A) for 6 days and (B) for 14 days. AML blasts ( $0.25 \times 10^6$ ) were co-cultured with primary BMSCs on a 12 well plate for 6 days ( $n=20$ ) or 14 days ( $n=6$ ), AML blast number was assessed using a trypan blue exclusion hemocytometer-based counts. \* denotes  $p < 0.05$ .

**Table 3. 1 AML patient sample characteristics used in chapter 3 and 4.**

This table defines the nature of the AML patient samples used in the studies conducted in chapter 3 and 4.

AML	Age	sex	Who Classification	cytogenetics
AML#1	59	F	AML with t(8;21)(q22;q22) RUNX1-RUNX1T1	t(8;21)
AML#2	51	M	AML with Monocytic differentiation	pending
AML#3	44	F	AML with (t(8;21)(q21;q22); RUNX1/RUNX1T1	45,X,-X,t(8;21)(q22;q22),del(9)(q13q22)
AML#4	74	F	Acute monoblastic and monocytic leukaemia	46,XX,t(1;17)(q21;q11.2)
AML#5	65	M	AML with maturation	Trisomy 13
AML#6	74	F	AML without maturation	Normal
AML#7	48	M	AML with myelodysplasia related changes	Not aviable
AML#8	65	M	Acute myelomonocytic leukaemia	normal
AML#9	64	F	AML with myelodysplasia related changes	Normal
AML#10	23	F	AML without maturation	46,XX,t(5;12)(q13;q24)
AML#11	83	M	AML with maturation	Normal
AML#12	42	M	AML without maturation	Normal
AML#13	61	F	AML without maturation	Normal
AML#14	37	M	AML without maturation	Normal
AML#15	59	M	AML with (t(8;21)(q21;q22); RUNX1/RUNX1T1	46,XY,t(8;21)(q22;q22)
AML#16	65	M	AML with maturation	pending
AML#17	76	M	AML without maturation	46,XY,add(5)(q35),add(6)(q22)
AML#18	88	M	AML with maturation	47,XY,+8
AML#19	35	M	AML without maturation	46 XY
AML#20	72	M	AML with myelodysplasia - related changes	46,XY, isochrome(17)(q10)

### 3.3. AML cells induce changes in the BMSC cytokine secretion profile

Both BMSCs and primary AML cells demonstrate constitutive release of several soluble mediators (295). Previous studies have shown that BMSCs can inhibit AML apoptosis, be it cell line or murine stromal cell derived BMSCs (66, 299). To study cell-cell communication between BMSCs and AML cells, and to understand the role of soluble factors in mediating the cross-talk between them, I analysed cytokines and chemokines from the supernatants of cultures of AML only, BMSC only and AML cells with BMSCs (AML/BMSC). I performed this assay on six different primary AML samples cultured on four different BMSCs. Figure 3.4 shows a representative cytokine array of one data-set. Table 3.2 contains the corresponding data set for figure 3.4. Full data sets of the co-cultures are provided in Table 2 of the appendix.

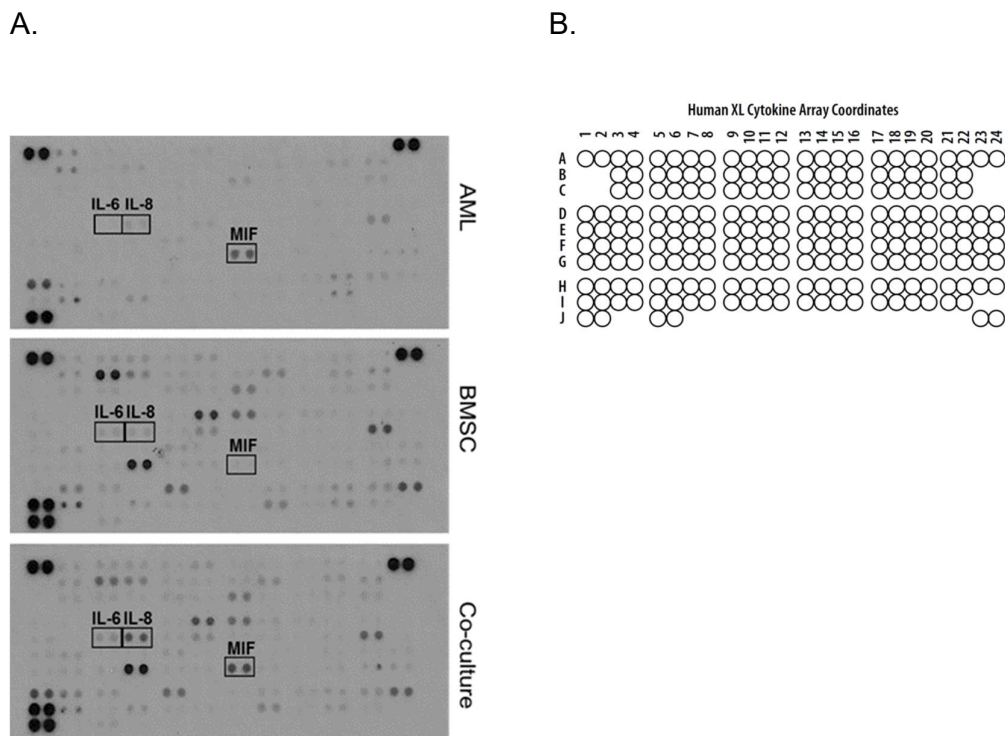


**Figure 3. 4 A representative image of the developed cytokine array from AML, BMSC and AML/BMSC culture media.**

(A) Representative cytokine antibody arrays of cell culture conditioned media, using the Human cytokine proteome profiler array is shown; from top to bottom: AML cells ( $0.25 \times 10^6$ ) only, BMSCs only, and BMSC/AML co-culture, after 24 h ( $n=6$ ). (B) Corresponding cytokine array coordinates, cross-reference with table 3.2.

**Table 3. 2 Cytokine mean pixel densities data set for figure 3.4.**

Coordinates correspond to the location of the cytokine duplicate on the nitrocellulose membrane.

(coordinate)(Cytokine)	Culture condition		
	AML only	BMSC Only	Co-culture
	AML#6	BMSC#4	+ AML#6
<b>(A1-A2)(Reference Spots)</b>	<b>63192.82</b>	<b>48901.689</b>	<b>62755.2</b>
(A3-A4)(Adiponectin)	884.41	547.75556	1088.22
(A5-A6)(Aggrecan)	1047.96	2305.5867	3694.74
(A7-A8)(Angiogenin)	605.73	2309.6489	3505.02
(A9-A10)(Angiopoietin-1)	1425.77	873.39556	1256.51
(A11-A12)(Angiopoietin-2)	2070.05	1115.5422	1615.3
(A13-A14)(BAFF)	936.83	592.82667	936.61
(A15-A16)(BDNF)	1009.02	1187.7467	1790.19
(A17-A18)(CC C5/C5a)	433.14	492.33333	357.21
(A19-A20)(CD14)	800.94	752.84444	909.27
(A21-A22)(CD30)	3027.78	1376.2489	1248.02
<b>(A23-A24)(Reference Spots)</b>	<b>63176.06</b>	<b>49905.689</b>	<b>62734.33</b>
(B3-B4)(CD40 ligand)	1574.01	621.29778	1278.62
(B5-B6)(Chitinase 3-like 1)	1062.98	12551.991	30837.3
(B7-B8)(Complement Factor D)	1823.75	2890.0756	4093.83
(B9-B10)(C-Reactive Protein)	1592.78	992.85778	1288.39
(B11-B12)(Cripto-1)	970.45	552.02667	910.9
(B13-B14)(Cystatin C)	1321.68	1550.1822	2361.83
(B15-B16)(Dkk-1)	1722.99	25905.956	41937.41
(B17-B18)(DPPIV)	273.54	277.12889	148.29
(B19-B20)(EGF)	2454.38	1698.12	1796.85
(B21-B22)(EMMPRIN)	4671.4	2785.5289	5266.98
(C3-C4)(ENA-78)	1428.45	868.36889	3777.9
(C5-C6)(Endoglin)	2662.32	2087.3022	5554.34
(C7-C8)(Fas Ligand)	1135.54	718.50667	989.58
(C9-C10)(FGF basic)	2283.03	1350.8933	1880.08
(C11-C12)(FGF-7)	880.67	930.12889	1619.2
(C13-C14)(FGF-19)	3639.62	2693.4311	6549.95
(C15-C16)(Flt-3 Ligand)	470.05	550.09778	792.47
(C17-C18)(G-CSF)	458.74	421.57778	445.61
(C19-C20)(GDF-15)	1231.6	2432.0089	7845.77
(C21-C22)(GM-CSF)	3148.77	2467.7022	4411.59
(D1-D2)(GRO-a)	895.58	498.23556	861.27
(D3-D4)(Growth Hormone)	716.54	319.39556	521.8
(D5-D6)(HGF)	5712.68	1626.0711	4255.5
(D7-D8)(ICAM-1)	1019.02	837.54667	1267.75
(D9-D10)(IFN-?)	1727.49	847.39556	983.44
(D11-D12)(IGFBP-2)	425.47	10678.218	21641.79
(D13-D14)(IGFBP-3)	1107.73	9329.8622	14991.33
(D15-D16)(IL-1a)	2176.53	950.63556	1667.69
(D17-D18)(IL-1β)	893.32	747.32444	1466.6
(D19-D20)(IL-1ra)	245.31	292.50667	612.91
(D21-D22)(IL-2)	922.69	983.55556	1052.91
(D23-D24)(IL-3)	483.34	572.78667	500.68
(E1-E2)(IL-4)	729.22	506.43556	879.42
(E3-E4)(IL-5)	394.21	129.09778	81.62
<b>(E5-E6)(IL-6)</b>	<b>3088.62</b>	<b>25541.88</b>	<b>45003.57</b>
<b>(E7-E8)(IL-8)</b>	<b>3785.28</b>	<b>27160.342</b>	<b>56680.79</b>
(E9-E10)(IL-10)	740.96	681.05333	729.94
(E11-E12)(IL-11)	2816.3	9500.0933	12850.61
(E13-E14)(IL-12 p70)	1367.28	770.91111	1253.46
(E15-E16)(IL-13)	616.07	484.37333	616.05
(E17-E18)(IL-15)	517.27	451.75111	878.56



Table 3. 2 continued

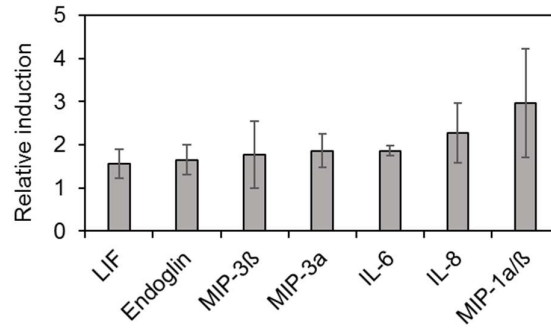
(coordinate)(Cytokine)	Culture condition		
	AML only	BMSC Only	Co-culture
	AML#6	BMSC#4	+ AML#6
(E19-E20)(IL-16)	1496.52	252.32444	1250.05
(E21-E22)(IL-17A)	3719.76	4590.3511	7113.14
(E23-E24)(IL-18 BPa)	451.64	526.77778	492.61
(F1-F2)(IL-19)	1430.78	574.78667	1058.75
(F3-F4)(IL-22)	1869.53	986.90667	1694.07
(F5-F6)(IL-23)	568.16	619.91556	1372.52
(F7-F8)(IL-24)	1246.49	1063.1467	2039.13
(F9-F10)(IL-27)	1967	874.72	1232.97
(F11-F12)(IL-31)	1024.71	511.66667	533.34
(F13-F14)(IL-32a/β/?)	1141.81	570.42222	912.98
(F15-F16)(IL-33)	887.65	381.99556	656.82
(F17-F18)(IL-34)	336.94	284.54222	535.43
(F19-F20)(IP-10)	278.34	315.70667	719.82
(F21-F22)(I-TAC)	532.48	780.64	652.21
(F23-F24)(Kallikrein 3)	1180.96	1353.6178	1556.86
(G1-G2)(Leptin)	862.54	311.87111	660.63
(G3-G4)(LIF)	698.36	5493.4889	8668.34
(G5-G6)(Lipocalin-2)	4285.76	873.42222	2245.12
(G7-G8)(MCP-1)	3099.85	17755.151	37175.71
(G9-G10)(MCP-3)	1057.68	714.72	1173.28
(G11-G12)(M-CSF)	1781.94	856.75556	998.53
<b>(G13-G14)(MIF)</b>	<b>32650.14</b>	<b>2950.8044</b>	<b>16923.52</b>
(G15-G16)(MIG)	1169.51	677.63111	1142.44
(G17-G18)(MIP-1a/MIP-1β)	207.31	98.462222	603.61
(G19-G20)(MIP-3a)	246.06	750.36444	1959.89
(G21-G22)(MIP-3β)	449.45	466.06222	567.42
(G23-G24)(MMP-9)	937.32	727.62667	1432.96
(H1-H2)(Myeloperoxidase)	1280.86	297.56444	1340.23
(H3-H4)(Osteopontin)	2653.11	1742.9378	3287.79
(H5-H6)(PDGF-AA)	7407.75	7417.8133	11701.57
(H7-H8)(PDGF-AB/BB)	686.42	356.8	536.45
(H9-H10)(Pentraxin-3)	3262.26	9850.3822	19073.93
(H11-H12)(PF4)	498.75	278.16	819.94
(H13-H14)(RAGE)	815.25	491.02667	769.31
(H15-H16)(RANTES)	1765.24	636.97778	1237.22
(H17-H18)(RBP4)	1744.64	1141.5956	1610.47
(H19-H20)(Relaxin-2)	1174.76	768.87556	933.84
(H21-H22)(Resistin)	2871.19	1802.7644	3246.27
(H23-H24)(SDF-1a)	712.46	7946.1289	10744.88
(I1-I2)(Serp1 E1)	3989.99	27899.329	62439.02
(I3-I4)(SHBG)	1379.65	945.24	1716.52
(I5-I6)(ST2)	1231.26	1340.3289	1870.67
(I7-I8)(TARC)	1487.42	833.50667	1314.85
(I9-I10)(TFF3)	312.72	537.66222	1358.82
(I11-I12)(TfR)	1168.7	468.81778	1259.33
(I13-I14)(TGF-a)	556.73	483.05333	541.6
(I15-I16)(Thrombospondin-1)	2817.13	4882.6489	7540.79
(I17-I18)(TNF-alpha)	779.46	636.26222	801.67
(I19-I20)(uPAR)	1261.01	3206.6756	5474.14
(I21-I22)(VEGF)	213.56	10987.147	19452.53
<b>(J1-J2)(Reference Spots)</b>	<b>63192.82</b>	<b>48901.689</b>	<b>62753.72</b>
(J5-J6)(Vitamin D BP)	3962.03	1639.5867	2455.87
<b>(J23-J24) negative control</b>	<b>0</b>	<b>0</b>	<b>0</b>

I next analysed the cytokine array blots using HLIImage++ software to quantify the duplicate dots for each cytokine. Ultimately the aim of this experiment was to determine what cytokines and chemokines were differentially expressed by BMSCs in response to co-culture with AML cells. Therefore, I performed the analysis of the array data in two ways:

1. I subtracted the AML mono- culture profile from the AML/BMSC co-culture profile, and then used the latter for comparison with the BMSC mono-culture profile (Figure 3.5A). This enabled me to correct for any background readings from the AML only mono-culture data. There are associated caveats in this method of analysis which are mentioned in the discussion (section 7.1.2).
2. Comparison of the AML/BMSC co-culture profile directly with that of the BMSC mono-culture (Figure 3.5B).

The two methods showed a consistent number of cytokines and chemokines that were differentially expressed in the media of the AML/BMSC co-culture, versus the BMSC monoculture (Figure 3.5). Cytokines that were consistently upregulated in all co-cultures from both analyses were IL-6 and IL-8.

A.



B.

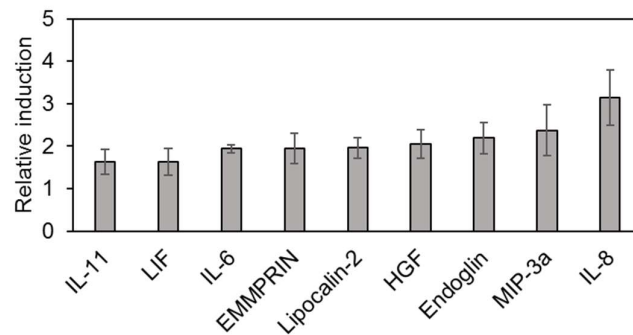


**Figure 3. 5 Bar graphs comparing the fold increase in cytokines between BMSC/AML co-cultures and BMSC monocultures.**

(A) Cytokines that were upregulated in co-cultures after subtraction of the AML monoculture profile. (B) Cytokines that are upregulated in the co-cultures, without subtraction of AML monocultures. Results from 7 different primary AML samples on four different BMSCs are shown, together with the mean and standard error of the mean (SEM).

I also wanted to determine the cytokines and chemokines that were high in AML samples only. I did this because I wanted to verify if there was an AML derived factor that was responsible for activating BMSCs. For this analysis, I compared the optical density values obtained by the HImage++ software in all three culture conditions (AML only, BMSC only, AML/BMSC). The results showed that a number of cytokines and chemokines were high in AML and AML/BMSC cultures, but low in BMSC media (Figure 3.6). Particularly, it was apparent that levels of macrophage migration inhibitory factor (MIF), were consistently high in all AML and AML/BMSC supernatants, but low in the BMSC supernatants.

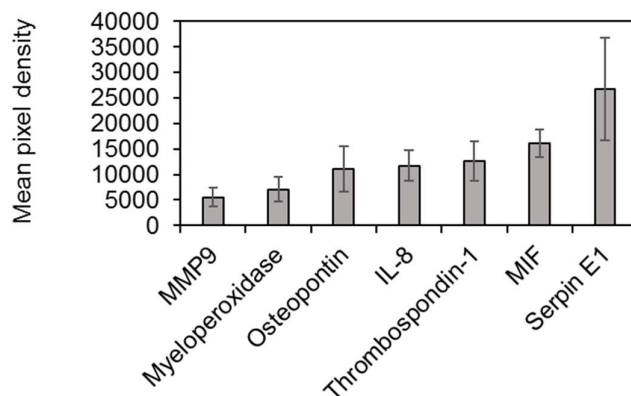


**Figure 3. 6 Bar graph depicting the results of a cytokine array optical density quantification of AML only arrays.**

The graph reports the expression levels of the top 7 cytokines found in the media of AML monocultures, in the form of mean pixel density. 8 individual AML samples were included in the analysis, 6 of which were used in the co-cultures. Bars, mean and SEM.

In summary, from the cytokine and chemokine array experiments I identified MIF as being highly expressed in AML cells compared to BMSCs. On the other hand, I found IL-6 and IL-8 to be increasingly upregulated in the AML/BMSC co-cultures, compared to BMSC monocultures.

Serum IL-8 is known to be higher in patients with AML, myelodysplasia (MDS) and non-Hodgkin Lymphoma than in normal controls. Also, levels of IL-8 in these patients are comparable to those found in patients with multiple organ failure of non-septic origin (118, 137). Furthermore, leukaemic cells from patients with AML have been shown to constitutively express IL-8 (136) and, inhibition of the IL-8 receptor, CXCR2 selectively inhibits proliferation of MDS/AML cell lines and patient samples (140).

MIF overexpression has been observed in a cohort of AML patients and was found to be related to poor outcomes for these patients (300). Moreover, in CLL, MIF was observed to induce IL-8 production by primary CLL, and targeted deletion of the MIF gene delayed the development of CLL *in vivo*, thereby resulting in prolonged survival of the CLL mice models (166). Together these studies suggest a link between MIF and IL-8, which lead me to

hypothesise that MIF and IL-8 have a unique function in establishing AML/BMSC crosstalk which could drive AML survival.

AML cells have been shown to spontaneously secrete IL-6 (301) and survival of patients with AML have been shown to be inversely correlated with IL-6 expression (302). In 1988, Hoang and colleagues reported that IL-6 had little effect by itself. However, it synergised with granulocyte macrophage colony-stimulating factor (GM-CSF) and IL-3, thus stimulating AML blast colony formation (303). Nevertheless, it seems that IL-6 may have a direct effect on the growth of leukaemic blasts: Saily et. al. demonstrated that only three of the 16 AML samples in their study were influenced by IL-6, two of them being stimulated and, one inhibited by it (145).

IL-6 has been shown to be regulated by MIF in lymph node cells (LNC) in MIF knockout mice (*mif*<sup>-/-</sup>), where they had severely impaired production of IL-6 (304). Furthermore, MIF was shown to regulate *Vibrio vulnificus*-induced IL-6 production in human peripheral blood cells (305). MIF was also shown to cause dose-dependent increase in IL-6, IL-8, and prostaglandin E2 (PGE2) release from chondrocytes (306) and to induce IL-6 and IL-12 production from macrophages (307). These data lead me to hypothesise that MIF may regulate IL-6 secretion in AML cells as well.

Next, I examined the effect of AML on IL-8 and IL-6 expression in BMSCs.

#### **3.4. AML but not BMSCs express high levels of MIF mRNA under normal basal conditions**

To confirm which cell type (BMSCs or AML cells) are the main producers of MIF in the co-cultures, I examined mRNA expression levels of MIF monocultures of primary AML cells (n=5) and BMSCs (n=5). This showed that AML but not BMSCs, express high levels of MIF mRNA under normal basal conditions (Figure 3.7).

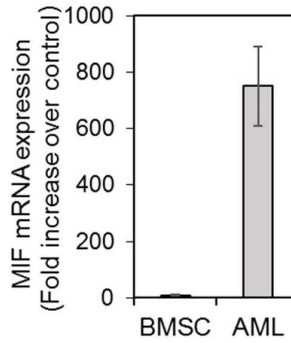


**Figure 3. 7 Bar graph comparing MIF mRNA expression levels in AML and BMSC cultures.**

BMSCs and primary AML cells were cultured alone for 48 hours and measured for MIF mRNA levels using qRT-PCR, mRNA expression was normalised to GAPDH mRNA levels, (n=5).

### 3.5. IL-8 specific ELISAs confirm IL-8 upregulation in AML/BMSC co-cultures

To verify that MIF was highly expressed in AML and that IL-8 was up-regulated in AML/BMSC cultures, I used MIF and IL-8 specific ELISA. I found that IL-8 concentrations peak at 8 and 24 hours in the AML/BMSCs co-culture supernatants (Figure 3.8), whereas MIF concentrations were high at similar levels in both AML only and in AML/BMSCs co-culture supernatants (Figure 3.9). This data shows that MIF is constitutively secreted by the AML cells, and that IL-8 levels are maintained high in co-cultures over a 24-hour period.

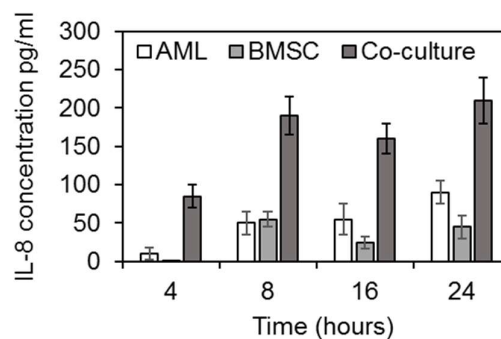


**Figure 3. 8 Bar graph representing IL-8 protein expression (pg/ml) in monocultures and AML/BMSC co-cultures over 24 hours.**

AML cells or BMSCs were cultured alone or together for the indicated times. IL-8 ELISA was used to determine IL-8 concentration in culture supernatants (n=3).

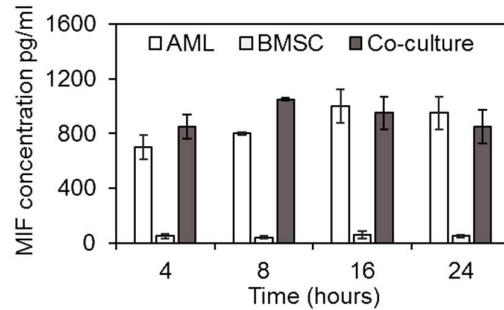


**Figure 3. 9** Bar graph representing MIF expression (pg/ml) in monocultures and AML/BMSC co-cultures over 24 hours.

MIF ELISA of each of the cell culture conditioned media from various time points are plotted, similar to Figure 3.8 above (n=3).

### 3.6. IL-6 is not upregulated in BMSCs in AML/BMSCs to co-cultures

To determine if IL-6 is up regulated in AML/BMSC co-cultures, I used target specific ELISA and found that IL-6 concentrations are high in BMSC monocultures but not upregulated in co-culture (Figure 3.10A). Moreover, I extracted total RNA from BMSC mono- and co-cultures and performed real-time PCR for IL-6 mRNA expression. Figure 3.10B shows that IL-6 mRNA expression is not upregulated in BMSCs co-cultures with AML cells at any of the chosen time points. This result led me to focus my further experiments towards the role of BMSC-derived IL-8 in regulating AML survival.

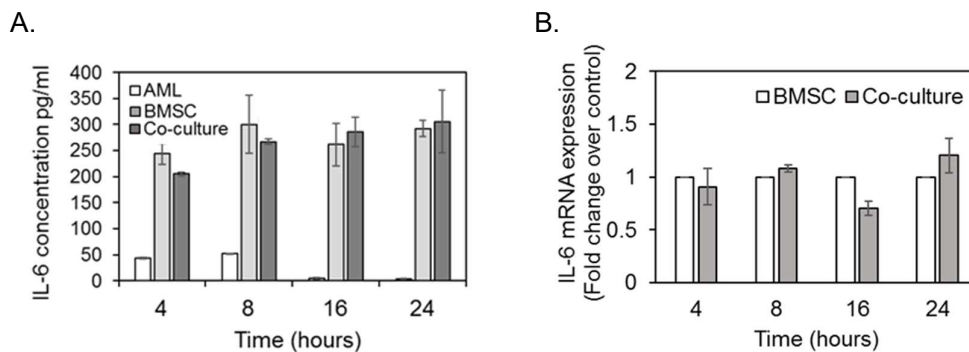


**Figure 3. 10** Bar graph depicting IL-6 expression (pg/ml) in monocultures and AML/BMSC co-cultures over a period of 24 hours.

(A) IL-6 ELISA of each of the cell culture conditioned media from various time points. (B) IL-6 mRNA expression was determined using qRT-PCR, expression was normalised to GAPDH mRNA levels (n=3).

### 3.7. AML induced IL-8 expression in BMSCs is contact independent

Interactions between AML cells and BMSCs can take many forms. Some interactions require cell-to-cell contact while others do not (78, 308). I wanted to determine if BMSCs needed direct contact with AML cells to increase IL-8 in the co-cultures. I therefore, co-cultured BMSCs in direct contact with AML or with the AML held within transwell inserts. The transwell inserts prevent cell to cell contact but allow the transfer of soluble factors between the two compartments. Figure 3.11 shows that IL-8 mRNA from BMSCs incubated with AML increased 57-fold when in direct contact (DC), and 50-fold when in indirect contact (IC) using transwell inserts. This confirms that direct tumour cell to stromal cell contact is not necessary for AML to induce increased IL-8 expression by human BMSCs.

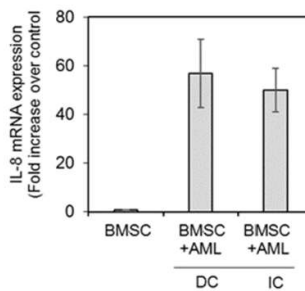


**Figure 3. 11 Bar graph comparing fold increase over control of IL-8 induction in AML/BMSC co-cultures in direct contact (DC) versus indirect contact (IC).**

AML cells ( $0.25 \times 10^6$ ) were co-cultured with primary BMSC either in DC or with indirect contact (transwell insert) for 24 h (n=5). RNA was extracted and IL-8 mRNA in the BMSC was assessed by real-time PCR. mRNA expression was normalised to GAPDH mRNA levels (n=5).

### 3.8. Recombinant human MIF (rhMIF) induces IL-8 expression in AML derived BMSCs but not normal cell line BMSCs

Since MIF has been shown to be over expressed in AML patients and is associated with poor outcome (300), and that MIF can induce IL-8 production by primary CLL (170), I hypothesised that the MIF from AML cells could be



increasing IL-8 in the BMSCs. To test this hypothesis, I stimulated BMSCs with 100ng/mL of recombinant human MIF (rhMIF) (309, 310) and assayed for IL-8 mRNA and protein expression over a period of 24 hours. I found that IL-8 mRNA and protein increased (Figure 3.12) in response to rhMIF, demonstrating that MIF causes an increase in IL-8 expression by BMSCs.

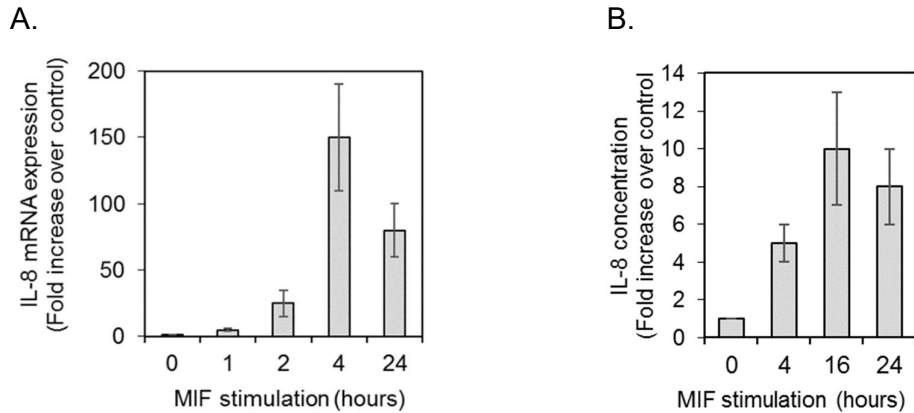


**Figure 3. 12 Bar graph comparing fold increase over control of IL-8 expression in BMSCs in response to MIF stimulation, over 24 hours.**

(A) BMSCs from 5 patients were treated with rhMIF (100 ng/mL) for indicated times, and then extracted RNA was assessed for IL8 mRNA by qRT-PCR. mRNA expression was normalised to GAPDH mRNA levels. (B) BMSCs from 5 patients were treated with rhMIF (100 ng/mL) for indicated times, and then, media were assessed for IL8 protein expression by ELISA.

Due to the number of experiments I needed to perform with patient BMSCs and AML together, with only limited availability of primary tissue, I attempted to mimic the effect of AML on BMSC by using a cell line known to be derived from BMSCs. The HS-5 cell line has been shown to support AML survival, proliferation and to protect AML cells from drug-induced apoptosis (66, 311), I therefore treated HS-5 with rhMIF. Figure 3.13A shows that MIF does not stimulate IL-8 mRNA expression in HS-5 cells. Moreover, when I cultured AML cells with HS-5, I observed no increase of IL-8 mRNA in BMSCs. (Figure 3.13B). This suggests that the HS-5 cell line is not an ideal model for studying AML/BMSC interactions and this therefore, confirmed my understanding that

using primary AML with primary BMSCs is the only way to study the true nature of the AML microenvironment.

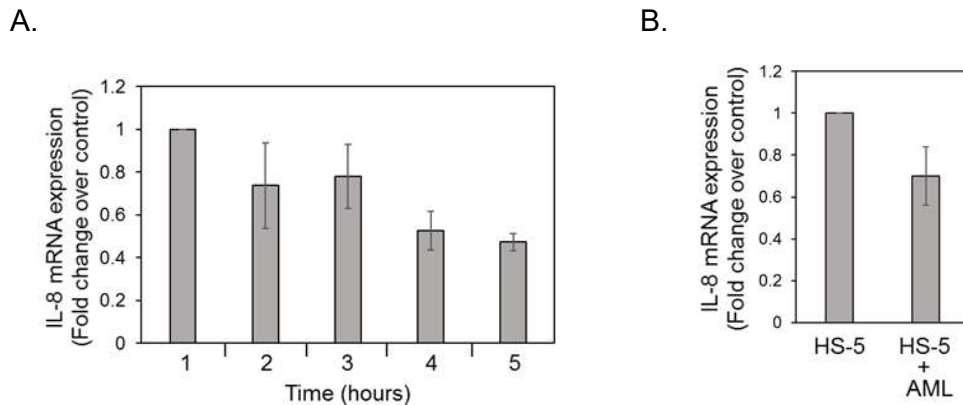


**Figure 3.13** Bar graph comparing fold change in IL-8 mRNA expression in HS-5 treated with rhMIF or co-cultured with AML.

(A) HS-5 were treated with rhMIF (100 ng/ml) for the indicated times and then RNA extracted and assessed for IL-8 mRNA by qRT-PCR or (B) HS-5 were cultured alone or co-cultured with three different primary AML cells for 4 h. HS-5 RNA was extracted and IL-8 mRNA expression was analysed by qRT-PCR. IL-8 mRNA was normalised to GAPDH mRNA levels (n=3).

### 3.9. Inhibition of AML-derived MIF downregulates IL-8 expression

To confirm that MIF secreted from AML cells regulates IL-8 expression in BMSCs, I used ISO-1, a nontoxic inhibitor of MIF which functions by binding to bioactive MIF at its N-terminal tautomerase site (312). To perform these experiments, I cultured AML with BMSCs in the presence and absence of ISO-1. I then extracted RNA from the BMSCs and analysed for IL-8 mRNA levels using qRT-PCR. Figure 3.14 shows that ISO-1 inhibited AML induced BMSC IL-8 mRNA expression. Taken together, this indicates that MIF secreted by AML cells induces IL-8 expression in BMSCs.

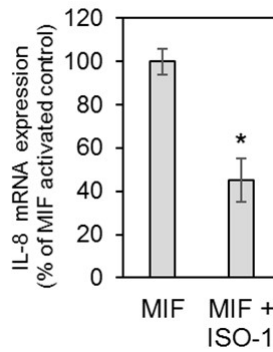


**Figure 3. 14 Bar graph comparing IL-8 RNA expression levels in the absence (MIF) and presence (MIF+ISO-1) of the MIF inhibiting ISO-1.**

BMSCs were treated with rhMIF (100 ng/ml) and the MIF inhibitor ISO-1 (10  $\mu$ M) for 4 h then assessed for IL-8 mRNA expression (n=4). \* denotes  $p < 0.05$ .

### **3.10. Inhibition of MIF significantly reduces AML survival on BMSCs**

To determine the effect of MIF inhibition by ISO-1 on AML survival when cultured on BMSCs, I co-cultured AML cells on BMSC cells in the presence and absence of ISO-1 for 48h. AML survival was significantly reduced when cultured with BMSC in the presence of ISO-1 compared to control AML-BMSC co-cultures (Figure 3.15). I also included an AML mono-culture as a control.

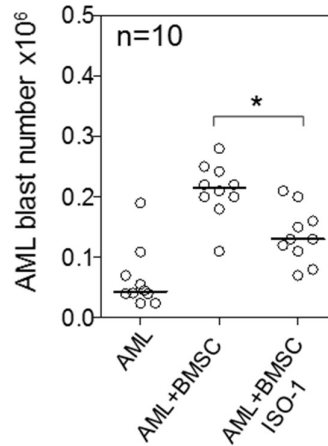


**Figure 3. 15 Scatter graph showing reduced AML survival in ISO-1 treated AML/BMSC co-cultures.**

BMSCs were pretreated with ISO-1 (10  $\mu$ M) for 5 mins before the addition of primary AML cells from 10 patient samples for 48 h. AML blast number was assessed using a trypan blue exclusion hemocytometer-based counts (n=10). \* denotes  $p < 0.05$ .

### 3.11. Summary of the results presented in chapter 3

MIF-induced stromal IL-8 (but not IL-6) is essential to human AML survival *in vitro*. This process is cell-cell contact independent. Demonstrating this, required experiments to be performed using primary BMSCs and not the HS5 cell line. This was deduced as MIF stimulated IL-8 expression in primary BMSC but not HS-5 cell line.

## **4. Chapter 4: MIF induction of BMSC-derived IL-8 is mediated through CD74 and PKC $\beta$ signalling**

In this chapter I describe the signalling which occurs in BMSCs in response to MIF. Here I aim to identify the receptor located on the BMSC surface to which MIF binds and then investigate the downstream signalling molecules.

### **4.1. Identifying the receptor/s to which MIF binds and induces IL-8 in BMSCs**

Depending on the cellular context and the disease involved, MIF signalling is mediated by its receptors CXCR2 (IL-8 receptor, ILR8) (313), CXCR4 (SDF-1 receptor) (314), and/or CD74 (158). BMSCs have been reported to express all three receptors (315-317). I used flow cytometry to measure the expression of CXCR2, CXCR4 and CD74 and of CD105 (as a positive BMSC marker to confirm stromal cell phenotype). Figure 4.1 shows that BMSCs are positive for CD105, CD74 and CXCR4 but that CXCR2 is not expressed at a level detectable by flow cytometry.

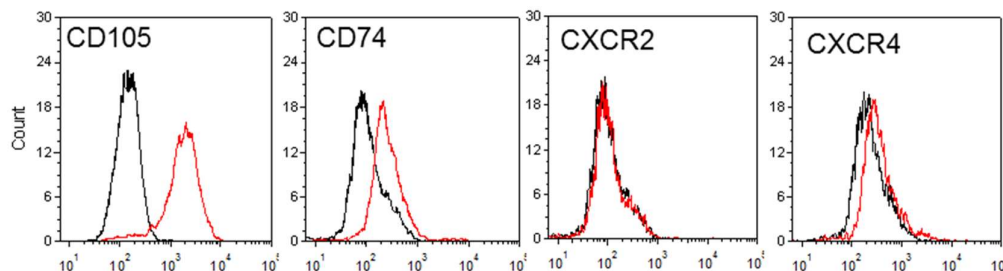


**Figure 4. 1 Representative flow cytometry analysis of cultured BMSCs stained with monoclonal antibodies against CD105, CD74, CXCR2 and CXCR4.**

The black line indicates isotype control and the red line indicates cells stained with anti-CD105-FITC, anti-CD74-FITC, anti-CXCR2-viobright-FITC and anti-CXCR4-PE.

To determine the role of each receptor in mediating MIF response in BMSCs, I used specific inhibitors of CXCR2, CXCR4 and CD74 and measured IL-8 mRNA expression. Figure 4.2 shows that the inhibition of CXCR2 using SB225002, CXCR4 using AMD3100 and of CD74 using an anti-CD74 blocking

antibody (αCD74 Ab) were all able to decrease MIF-induced IL-8 mRNA expression in BMSCs. These results suggest that all three receptors (CXCR2, CXCR4 and CD74) are involved to some degree in regulating MIF-induced IL-8 expression in BMSCs.

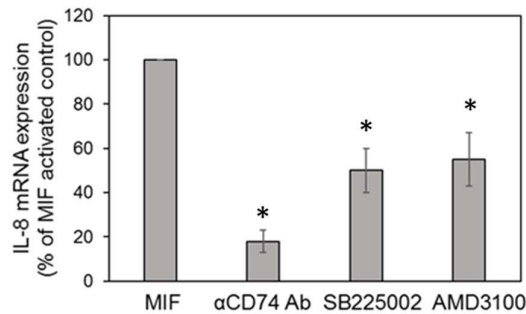


**Figure 4. 2 Bar graph comparing MIF-induced IL-8 mRNA expression in BMSCs treated with the inhibitors of CD74, CXCR2 and CXCR4 receptors.**

BMSCs were pretreated with vehicle control (DMSO) or inhibitors for CD74 (αCD74 Ab at 10 µg/ml), CXCR2 (SB225002 at 100 nM) and CXCR4 (AMD3100 at 100 nM) for 30 minutes before being stimulated with 100 ng/ml MIF for 4 h. RNA was extracted and assessed for IL-8 mRNA by qRT-PCR. mRNA expression was normalised to GAPDH mRNA levels (n=4). \* denotes  $p < 0.05$ .

#### **4.2. The primary MIF receptor involved in mediating IL-8 expression is CD74**

To determine the key receptor that mediates MIF-induced IL-8 in BMSCs, I attempted to inhibit CXCR2 and CXCR4, which are G-protein coupled receptors (GPCRs), using pertussis toxin (PTX), an inhibitor of GPCR signalling produced by the *bacterium Bordetella pertussis* (318). PTX would not inhibit CD74, as it is not a GPCR, but rather the cell surface form of the Class II invariant chain (158). MIF binding to CD74 results in the serine phosphorylation of its short intracytoplasmic domain, and in modulation of the phosphorylation of its signalling co-receptor, CD44 (159). I found that PTX mediated inhibition of CXCR2 and CXCR4 did not reduce MIF-induced IL-8 in

BMSCs (Figure 4.3). These data suggest that the primary receptor involved in MIF signalling in human AML is CD74.

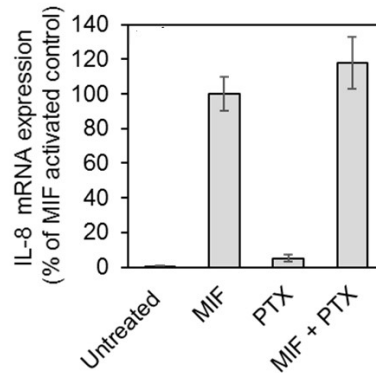


**Figure 4. 3 MIF-induced IL-8 upregulation is mediated through CD74, as seen in this bar graph which shows IL-8 mRNA expression levels for untreated, MIF-stimulated, PTX-treated, PTX-treated/MIF-stimulated BMSCs.**

BMSCs were pre-treated for 45 min with pertussis toxin (PTX) (50 ng/mL) then stimulated with MIF (100 ng/mL) for 4 h. RNA was then extracted and assessed for IL-8 mRNA by qRT-PCR. mRNA expression was normalised to GAPDH mRNA levels (n=4).

To determine if CD74 is the main receptor to which MIF binds on BMSCs to induce IL-8, I used lentiviral mediated knockdown (KD) of CD74 in AML patient BMSCs. BMSCs were infected with lentivirus containing an shRNA that targeted the 3'UTR of CD74. After 72 hours of incubation, BMSCs were analysed for CD74 knockdown. Figure 4.4 shows that both, mRNA and protein expression of CD74, after infection with control KD or CD74 KD lentivirus, are significantly reduced, thus confirming the successful knockdown of CD74.

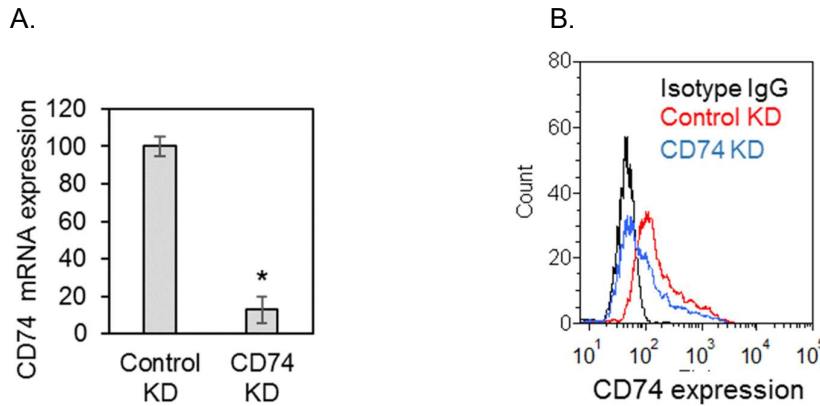


**Figure 4. 4 CD74 protein levels in control versus knockdown BMSC samples, measured by qRT-PCR (A) and flow cytometry (B).**

BMSCs from 4 patient samples were incubated with control shRNA or CD74 shRNA for 72 h and analysed for CD74 mRNA expression by qRT-PCR, as shown by the bar graph (A), and for protein expression, as measured by flow cytometry in (B). \* denotes  $p < 0.05$ .

Next, I wanted to examine if CD74 knockdown inhibited MIF induced IL-8 expression. Indeed, the data in Figure 4.5 confirms that the aforementioned inhibits MIF induced IL-8 mRNA expression in AML patient BMSCs. Together, these results demonstrate that MIF induces IL-8 in BMSCs via CD74.

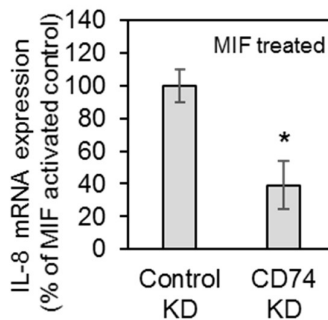


**Figure 4. 5 Bar graph depicting IL-8 mRNA expression levels after CD74 knockdown in BMSCs, which inhibited MIF induced IL-8 expression.**

BMSCs from 4 patient samples were infected with control shRNA or CD74 shRNA for 72 h then treated with recombinant MIF and analyzed for IL-8 mRNA expression by qRT-PCR. \* denotes  $p < 0.05$ .



### 4.3. Pharmacological inhibition of MIF signalling pathways

I next investigated the signalling cascade in BMSCs downstream of AML and MIF induced activation. It has been shown that MIF binding to CD74 activates downstream signalling through PI3K/AKT and MAPK signalling pathways and promotes cell proliferation and survival (170, 319). Both AKT and MAPK pathways have also been described to be downstream of CXCR2 and CXCR4 in AML and bladder cancer cells, respectively (79, 320). Additionally, Lutzny et. al. recently described activation of a PKC pathway in murine stromal cells co-cultured with CLL cells (201).

In my experiments, I pre-treated BMSCs with LY294002 – a PI3K/AKT inhibitor, with PD098059 – a MAPK kinase (MEK) 1 inhibitor, or with Ro-31-8220 – a pan PKC inhibitor. This was done to determine which pathway(s) regulate AML induced BMSC IL-8 mRNA induction. I found that Ro-31-8220, the PKC inhibitor could significantly inhibit IL-8 expression (Figure 4.6A). Contrarily, LY294002 and PD098059 had little or no effect. As a control, I examined AML cells that had been incubated with the BMSCs, which also demonstrated that IL-8 in AML cells is not inhibited by Ro-31-8220, LY294002 or PD098059 when cultured with BMSC (Figure 4.6B).

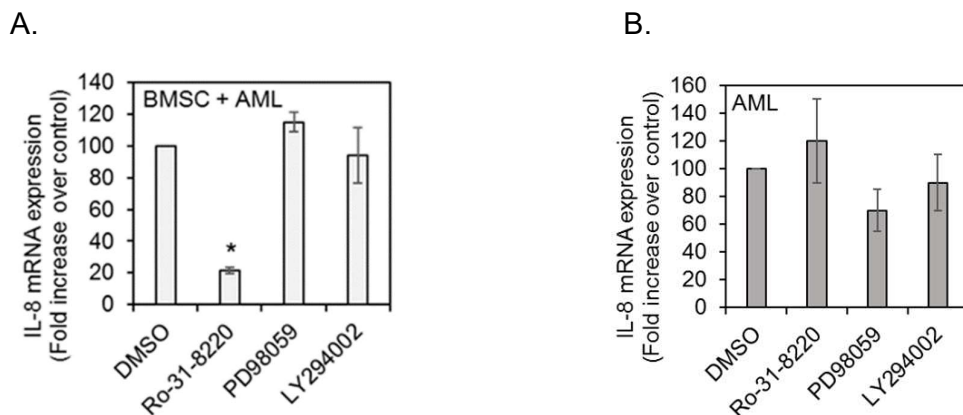


**Figure 4. 6 Bar graphs showing that the pharmacological inhibition of PKC pathways, inhibit AML induced IL-8 expression levels in BMSCs.**

BMSCs were pre-treated with vehicle control (DMSO), Ro-31-8220 (1 $\mu$ M), PD98059 (10  $\mu$ M) and LY294002 (10  $\mu$ M) and then incubated with primary AML cell for 4 h. AML cells were removed and RNA extracted from both BMSC (A) and AML cells (B) and assessed for IL-8 mRNA by qRT-PCR. mRNA expression was normalised to GAPDH mRNA levels (n=4). \* denotes p < 0.05.

Next, I wanted to determine the effect of Ro-31-8220, LY294002 or PD098059 on MIF induced IL-8 in BMSCs. To do this I pre-treated BMSCs with the respective drugs for 30 minutes and stimulated them with 100ng/mL of rhMIF for 4 hours. I found that Ro-31-8220 and PD098059 both inhibited MIF induced IL-8, whilst LY294002 had no effect (Figure 4.7). These results suggested that both MAPK and PKC signalling may be integral to the process of MIF induction of IL-8 in BMSCs.

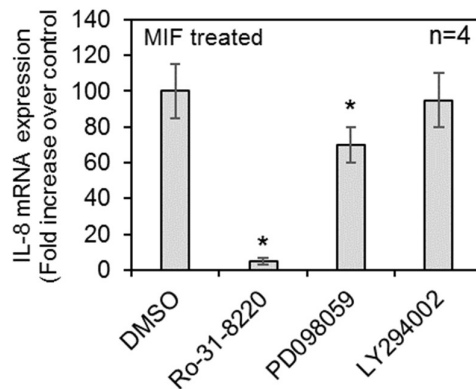


**Figure 4. 7 Bar graph depicting IL-8 mRNA expression after pharmacological inhibition of MAPK and PKC signalling pathways, to examine its effects on MIF induced BMSC IL-8 mRNA expression.**

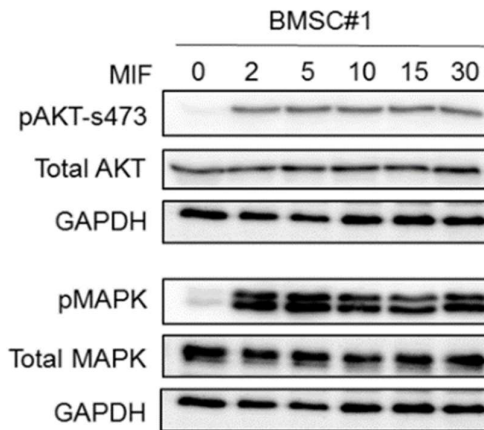
BMSCs were pre-treated with vehicle control (DMSO), Ro-31-8220 (250 nM), PD98059 (10  $\mu$ M) and LY294002 (10  $\mu$ M) and then incubated with 100ng/mL MIF for 4 h. RNA was extracted from BMSCs and assessed for IL-8 mRNA by qRT-PCR. mRNA expression was normalised to GAPDH mRNA levels (n=4). \* denotes  $p < 0.05$ .

#### **4.4. MAPK and AKT do not play a role in MIF-induced IL-8 in BMSCs**

To clarify whether PKC or MAPK or both are activated in response to MIF, I performed Western blot analysis on one BMSC sample for specific phosphorylation of AKT (at s473) and MAPK in response to stimulation with MIF for specified time points. I found that, MAPK and AKT were phosphorylated in the MIF treated samples compared to the control sample (Figure 4.8A). I next wanted to confirm this in the same sample as well as another three BMSC samples. Contrary to what I initially observed, there was no activation of MAPK or AKT in any of the BMSC cells I used (Figure 4.8B). It was unclear as to why the above results were obtained. Therefore, since the

AKT and MAPK inhibitors had limited effect on MIF induced IL-8 mRNA expression, I concluded that MAPK or AKT may not play a key role in BMSC response to MIF.

A.



B.

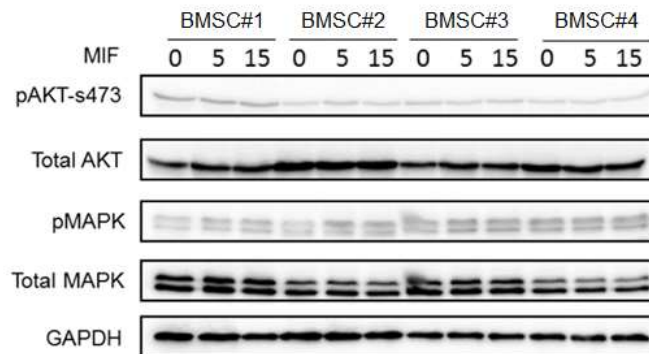


**Figure 4. 8 A western-blot image showing that pMAPK and pAKT are not activated in response to MIF in BMSCs.**

(A) BMSC#1 was activated with rhMIF (100ng/ml) for 0, 2, 5, 10, 15 and 30 minutes. Protein was extracted and Western blotting was performed for pAKT, total AKT, pMAPK and total MAPK. Western blots were re-probed for B-actin to confirm equal sample loading, (B) Four different BMSCs were activated with rhMIF (100 ng/ml) for various times. Protein was extracted and Western blotting performed. Blots were probed for pAKT and pMAPK as well as total AKT and total MAPK. Blots were then re-probed for GAPDH to show equal sample loading.

#### 4.5. PKC $\beta$ is activated in response to MIF in BMSCs

Since Ro-31-8220 could inhibit MIF induced IL-8 mRNA expression in BMSCs, and PKC exists in multiple isoforms, I next wanted to determine which PKC isoform is activated in response to MIF in BMSCs. To do this I performed Western blot analysis on BMSCs for specific phosphorylation of PKC isoforms in response to MIF activation. I activated BMSCs with pre-conditioned AML cells for 15 minutes or MIF (100ng/ml) over various time points (0, 5 and 15 minutes). Figure 4.9 shows that MIF and AML both induce phosphorylation of PKC $\alpha/\beta$ II and PKC $\beta$  in BMSCs.

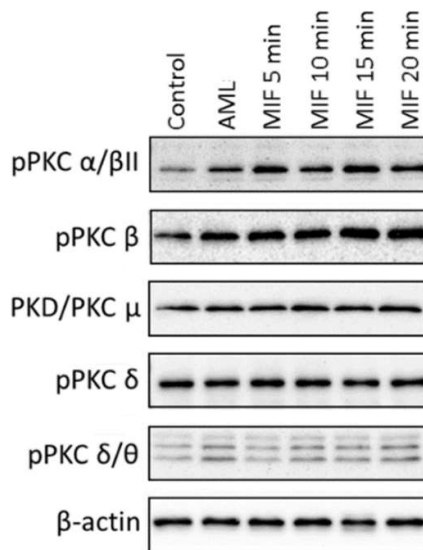


**Figure 4. 9 A western-blot image showing MIF activates PKC $\alpha/\beta$ II and PKC $\beta$  in BMSCs.**

BMSCs were cultured with preconditioned AML for 15 minutes or rhMIF (100 ng/mL) for various times. Protein was extracted and Western blotting performed. Blots were probed for pPKC $\alpha/\beta$ II, pPKC $\beta$ , PKD/PKC $\mu$ , PKC $\delta$  and PKC $\delta/\theta$ . Blots were then re-probed for  $\beta$ actin to show equal sample loading.

#### 4.6. MIF-induced IL-8 in BMSCs is signalled through PKC $\beta$

As both pPKC $\alpha/\beta$ II and pPKC $\beta$  protein in BMSCs showed an increase in signal when treated with either AML or MIF, I wished to determine which isoform was responsible for MIF induced IL-8 expression. To do this I used isoform specific

inhibitors: Go6976 to inhibit PKC $\alpha/\beta$  and Enzastaurin to inhibit PKC $\beta$ , to block MIF-induced IL-8 expression in BMSCs. Both inhibitors showed similar levels of inhibition of MIF-induced IL-8 up-regulation (Figure 4.10). Together these results support the view that MIF-induced IL-8 expression in AML patient BMSCs requires PKC $\beta$ .

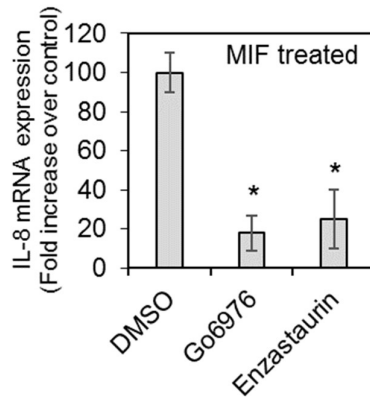


**Figure 4. 10 Bar graph comparing IL-8 mRNA expression levels in BMSCs treated with inhibitors to assess the effect of pPKC $\alpha/\beta$ II and pPKC $\beta$  on MIF-induced IL-8 expression.**

BMSCs were treated with vehicle control (DMSO), Go6976 (1  $\mu$ M) or enzastaurin (1  $\mu$ M) for 30 minutes before treatment with rhMIF (100 ng/ml) for 4 h. RNA was extracted and analysed for IL-8 mRNA expression by RT-PCR. \* denotes  $p < 0.05$ .

#### **4.7. Knockdown of PKC $\beta$ inhibits MIF-induced IL-8 expression in BMSCs**

To confirm that PKC $\beta$  is required for MIF-induced IL-8 expression in BMSCs, I employed shRNA knockdown of the PKC $\beta$  mRNA and protein. To do this I infected BMSCs with control shRNA, or shRNA with a lentivirus targeting PKC $\beta$  RNA coding sequence. Figure 4.11 shows that shRNA inhibits PKC $\beta$  mRNA and protein expression.

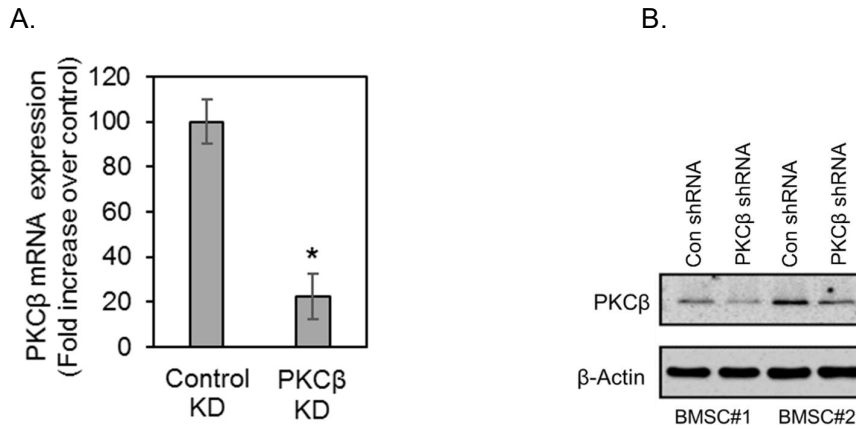


**Figure 4. 11 Results depicting changes in PKCβ expression after knockdown in BMSCs.**

BMSCs were infected with lentivirus containing control or PKCβ shRNA for 72 h and then analysed for (A) PKCβ mRNA using qRT-PCR and (B) protein expression, where the western blots were re-probed with β-actin to show equal sample loading, (n=2). \* denotes  $p < 0.05$ .

Next, I wanted to determine if the knockdown of PKCβ would inhibit MIF induced IL-8 expression. Figure 4.12 shows that PKCβ shRNA, indeed inhibits MIF-induced IL-8 mRNA and protein expression into culture supernatants of BMSCs, thus confirming that PKCβ influences MIF-induced IL-8 up-regulation in BMSCs of AML patients.

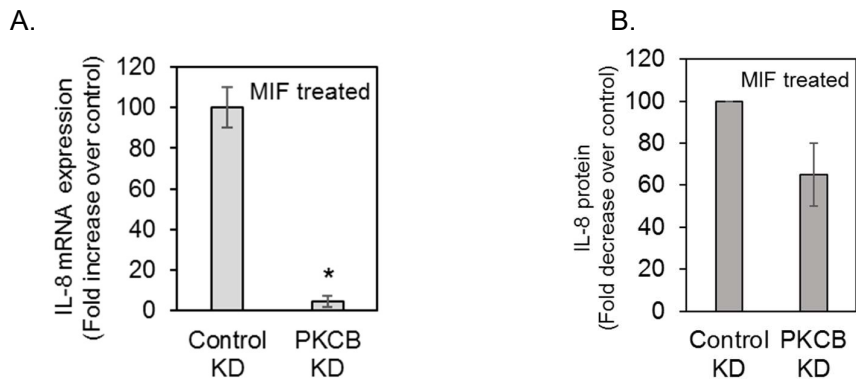


**Figure 4. 12 Bar graphs representing IL-8 mRNA expression levels in BMSCs, where PKCβ was knockdown. PKCβ knockdown inhibits MIF-induced IL-8 expression in BMSCs.**

BMSCs were infected with lentivirus containing control shRNA, or PKCβ shRNA for 72 h, followed by treatment with recombinant MIF. They were then analysed for IL-8

mRNA using qRT-PCR (A), and for IL-8 protein by ELISA (B) (n=3). \* denotes  $p < 0.05$ .

#### 4.8. Targeting the MIF-PKC $\beta$ -IL-8 axis disrupts BMSC induced protection of primary human AML cells

To examine the effect of blocking IL-8 on BMSC-induced protection and survival of primary AML cells, I co-cultured primary AML cells with BMSCs (either control-KD or IL-8-KD). Firstly, I used lentivirus to deliver shRNA, targeted to knockdown IL-8. Figure 4.13A and 4.13B show that IL-8 mRNA and protein expression was inhibited in BMSCs after transduction of with the IL-8 knockdown virus. Next, I stimulated control-KD and IL-8-KD BMSCs with 100 ng/ml rhMIF for four hours and found that the knockdown of IL-8 inhibits MIF induced IL-8 mRNA and protein expression in BMSC (Figure 4.13C).

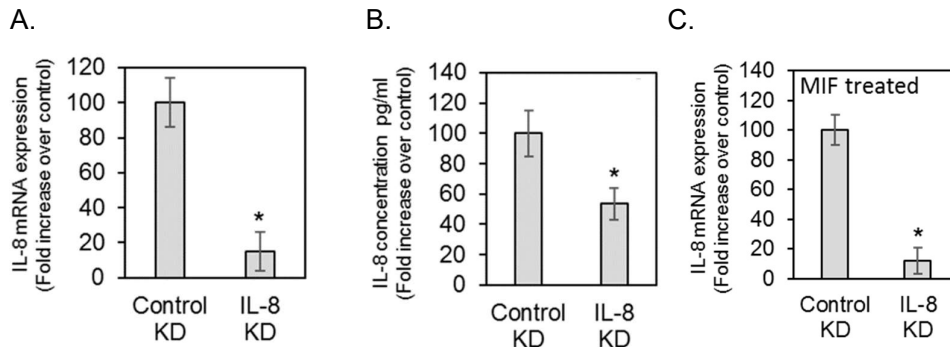


**Figure 4. 13 Bar graphs showing IL-8 expression levels, following the knockdown of IL-8 in AML derived BMSCs.**

BMSCs were infected with lentivirus containing control shRNA or IL-8 shRNA for 72 h. (A) RNA was extracted and analyzed for IL-8 mRNA expression by qRT-PCR. (B) Media was also taken and analysed for IL-8 protein expression by ELISA. (C) BMSCs were then treated with rhMIF (100ng/ml) for 4 hours. RNA was extracted and analysed for IL-8 mRNA expression by qRT-PCR, (n=6). \* denotes  $p < 0.05$ .

Next, I sought to determine the effect of IL-8 knockdown in BMSCs, on AML survival in co-cultures. To do this, I infected BMSCs with control KD and IL-8 KD lentivirus and then cultured AML on these for 48 hours. Figure 4.14A shows that the knockdown of IL-8 in BMSCs significantly inhibits AML survival when in co-culture, compared to control KD BMSCs. I also used SB225002 to

inhibit IL-8 in culture. Figure 4.14B shows that AML survival is reduced in the cultures treated with SB225002.

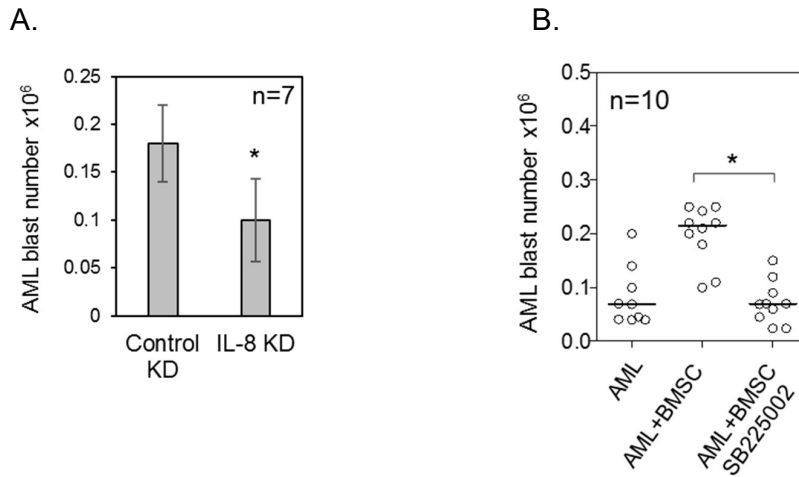


**Figure 4. 14 Results depicting that the IL-8 inhibition in BMSCs reverses AML survival in co-cultures.**

A) Bar graph showing AML blast numbers in co-cultures with control versus IL-8 KD BMSCs. BMSCs were infected with lentivirus containing control shRNA or IL-8 shRNA for 72 h. BMSCs were then co-cultured with AML cells from seven samples for 48 h. AML blast number was assessed using a trypan blue exclusion hemocytometer-based counts (n=7). (B) Scatter graph depicting AML blast numbers. BMSCs were pre-treated with SB225002 (100 nM) for 30 minutes before the addition of primary AML cells from 10 samples for 48 hours. AML blast number was assessed using a trypan blue exclusion hemocytometer-based counts. \* denotes  $p < 0.05$ .

#### 4.9. Summary of results chapter 4

Altogether, these results identify a novel pro-tumoural regulatory pathway in the AML microenvironment, whereby AML derived MIF binds to receptors on BMSCs, and primarily through surface CD74 induced stromal cell production of IL-8 via a PKC $\beta$  dependent pathway. The schematic in Figure 4.15 illustrates my proposed mechanism for the AML derived MIF stimulation of stromal IL-8.



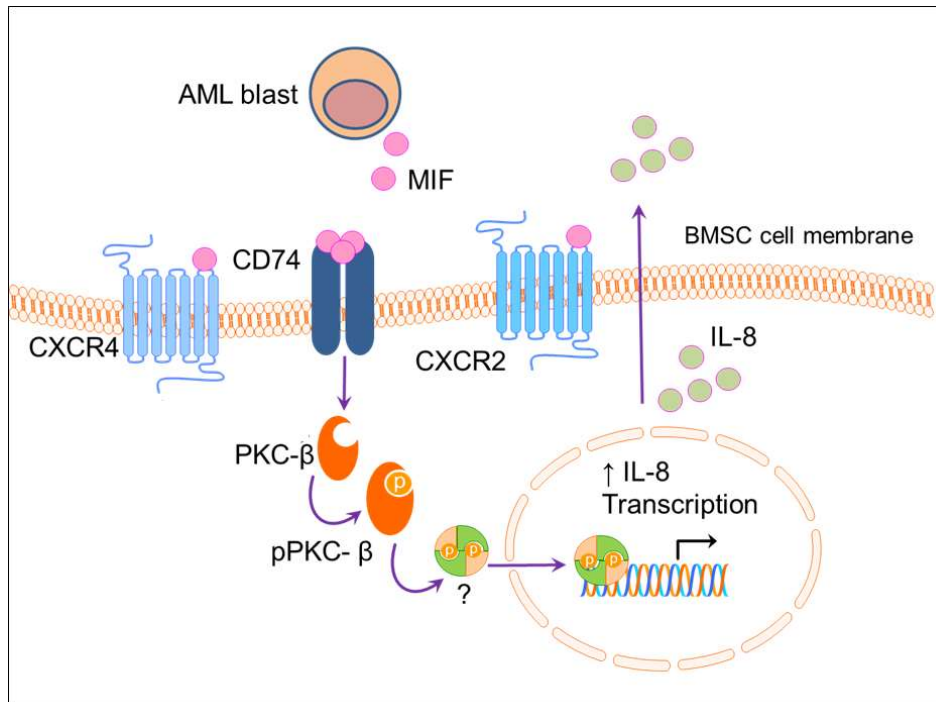


**Figure 4.15. Schematic of the proposed MIF/PKCB/IL-8 survival pathway in AML.**

In the AML BMM, AML-derived MIF stimulated BMSC expression of IL-8, through binding of cell surface CD74 and subsequent activation of PKC $\beta$  in the BMSC compartment.

## **5. Chapter 5: Hypoxia regulates AML-derived MIF**

In the previous chapter I showed that AML cells constitutively express high levels of macrophage migration inhibitory factor (MIF) which drives IL-8 expression in BMSCs, which in turn supports AML cell survival and proliferation.

The BMM is hypoxic and targeting hypoxia inducible genes has been shown to eliminate cancer stem cells in haematological malignancies (250). HIF1- $\alpha$  expression in AML patient samples has been found to be associated with poor prognosis (244). Moreover, targeting HIF1 $\alpha$  in AML cancer stem cells abrogated their colony forming activity (250). Recent data showed that HIF2 $\alpha$  silencing impairs long term engraftment of HSC and inhibits proliferation of primary AML *in vitro* (251). Another study has shown that HIF2 $\alpha$  is high in subsets of both human and mouse AML cells, and that overexpression of HIF2 $\alpha$  accelerated disease progression in AML mouse models. However, it also highlights that patients with high HIF2 $\alpha$  expression levels trend toward disease free survival (252). Together these data describe a complex interplay between hypoxia regulated transcription factors HIF1 $\alpha$  and HIF2 $\alpha$  and their regulatory role in normal HSCs and AML cells.

Hypoxia has been identified as a potent inducer of the pro-inflammatory cytokine MIF in inflammatory diseases (321, 322). Hypoxia-induced MIF expression is dependent upon a hypoxia response element (HRE) in the 5'UTR of the MIF gene (323). Specifically, a single nucleotide polymorphism (SNP) mapping to a functional HRE in the MIF locus, prevents induction of MIF by hypoxia (324). Consequently, these studies lead me to hypothesise a role for hypoxia in regulating MIF survival signals in AML.

In the work presented in this chapter, I aim to determine if there is a connection between the hypoxic BMM and MIF in regulating AML survival. Then, I further examine the role of HIF1 $\alpha$  and HIF2 $\alpha$  in this response, and evaluate the functional consequences and potential therapeutic effect of inhibiting such a

pathway *in vivo*, in AML patient-derived xenograft models. AML patient samples used in this study are shown in table 5.1 below.

**Table 5. 1 AML patient sample characteristics used in chapter 5.**

AML#	Age	Sex	WHO classification	Cytogenetics
AML#21	65	male	AML with maturation	Trisomy 13
AML#22	37	male	AML without maturation	Normal
AML#23	59	male	AML with maturation	46,XY,t(8;21)(q22;q22)
AML#24	88	male	AML with maturation	Trisomy 8
AML#25	45	male	AML with maturation	Normal
AML#26	74	male	AML with minimal differentiation	47 XY +13
AML#27	69	female	AML with minimal differentiation	failed
AML#28	59	male	Acute monoblastic and monocytic leukaemia	46,XY, +21
AML#29	66	male	AML with minimal differentiation	inv(16)(p13q22) and +8

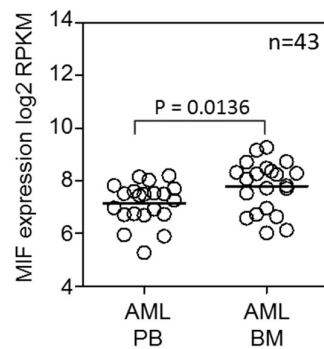
### **5.1. AML cells derived from the bone marrow express higher levels of MIF compared to cells in the systemic circulation and spleen**

To determine whether high and constitutive expression of MIF in AML cells is a function of the BMM, I examined if the expression levels of MIF in AML cells from an AML BM sample would be lower compared to one from the peripheral blood (PB). This stage was threefold:

- (i) *In silico*: As a proof of concept, using a publicly available RNA sequencing data set (GEO accession number GSE49642) (325) for a panel of 43 AML patients (comprising of 22 unmatched AML samples from the PB and 21 AML samples obtained from BM aspirate), and with the help of my colleague Manar Shafat, a differential expression analysis of MIF in this data set was performed (described in section 2.6). The analysis showed that MIF gene expression was significantly higher in AML samples from the BM compared to those from the PB (Figure 5.1A).
- (ii) *In vitro*: I obtained five patient matched primary AML samples (both BM and PB) from the haematology department at the NNUH and freshly extracted RNA from these samples. It was crucial that this step was performed as soon as the samples were obtained from the hospital, to avoid any changes in gene expression of these cells once they were

extracted from the BM/PB, and risk re-oxygenation. Samples were, therefore, transported to the research lab immediately after they were taken. I next performed cDNA synthesis and carried out qRT-PCR for MIF and GLUT1 expression. GLUT1 is a common target gene of HIF1 $\alpha$  and HIF2 $\alpha$  (326, 327) and serves as a positive control for hypoxia in this model. I found that AML cells from the BM expressed significantly higher levels of MIF and GLUT1 than those taken from the PB (Figure 5.1B).

A.



B.

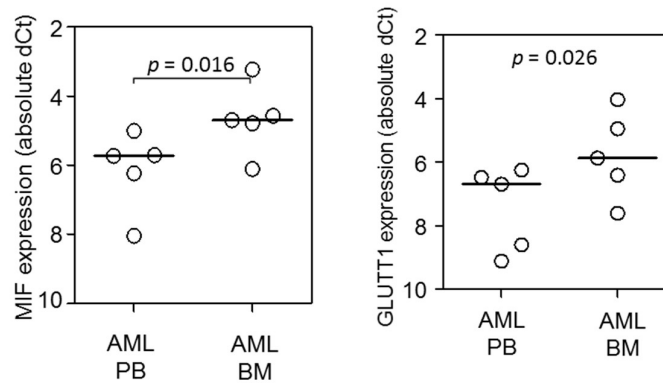
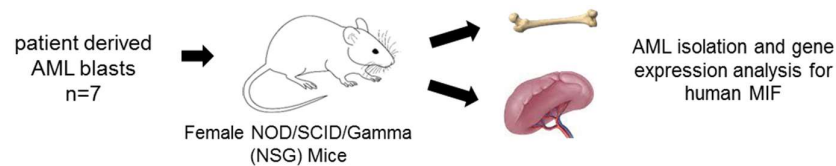


**Figure 5. 1 Scatter graph showing that BM AML cells express significantly higher MIF levels than circulating AML cells.**

(A) MIF gene expression (expressed in log<sub>2</sub> RPKM values) was obtained from GSE49642 for 22 peripheral blood (PB) and 21 bone marrow (BM) AML patient samples. *p*-value was obtained by Wilcoxon rank-sum test. Line denotes the median value. (B) RNA was extracted from AML originating from the BM and PB of matched patients. MIF and GLUT1 mRNA expression was determined by qRT-PCR and normalised to B-actin. *p*-value was obtained by Wilcoxon rank-sum test. Line denotes the median value.

(iii) *In vivo*: To replicate the *in silico* and *in vitro* results *in vivo*, I used a patient-derived xenograft (PDX) model that has been set up by members of our research group. In this model, 9 primary AML patient BM samples were injected into female NSG mice and allowed to engraft in their BM and to infiltrate the spleen. Animals were then sacrificed once they met pre-defined severity end points. The experimental design of this *in vivo* model is depicted in Figure 5.2A. To determine if AML cells were engrafted in the BM and spleen of these animals, I isolated total cells from both organs and used a fraction of these cells to determine engraftment, by measuring human CD33 and CD45 levels in these samples. The second fraction was kept for RNA analysis. Figure 5.2B confirms that the primary AML successfully engrafted the BM and spleen of NSG mice (engraftment presented as % of CD33-positive CD45-positive cells/total number of cells. Samples with values above 1% were considered to have been successfully engrafted).

A.



B.

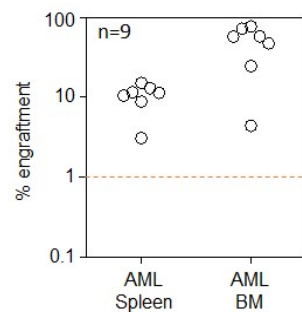


**Figure 5. 2 Experimental plan of the patient-derived xenograft (PDX) model, and results that indicated successful engraftment.**

(A)  $2 \times 10^6$  primary AML cells (from the BM of 7 AML patients) were injected into the tail-vein of NSG mice. At the end of the experiment, AML cells were isolated from the BM and spleen for RNA analysis (B) Engraftment was measured using flow cytometry after double staining with human CD33 and CD45, the dot plot presents each AML engraftment into NSG mice and is shown for BM and spleen.

I next extracted RNA from the second fraction of cells and used specific qRT-PCR primers to analyse human MIF and GLUT1 gene expression levels in AML cells engrafted in the BM, and in AML cells engrafted in the spleen. Figure 5.3A shows that MIF had a lower deltaCT (dCt) value in AML cells from the BM, compared to those from the spleen (the lower the dCt value, the higher the gene expression level). Furthermore, GLUT1 expression was significantly higher in samples from the BM compared to those from the spleen (Figure 5.3B).

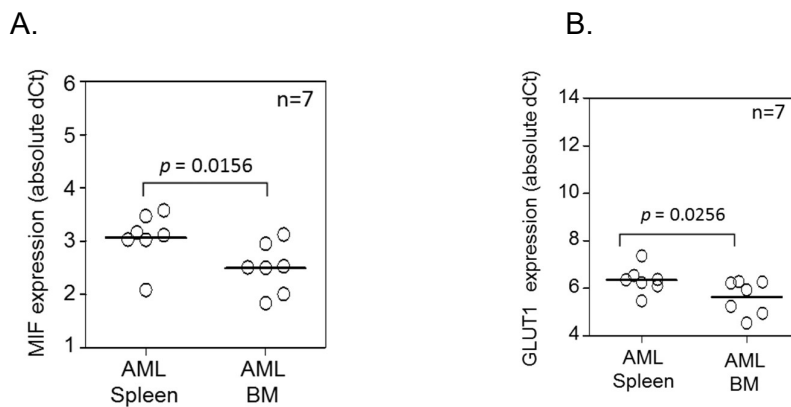


**Figure 5. 3 Scatter graphs comparing MIF and GLUT1 RNA expression levels in the BM and spleen of the PDX animals.**

RNA was extracted from AML cells isolated from the BM and spleen as explained in Figure 5.2. RNA was analysed for (A) MIF mRNA and (B) GLUT1 mRNA using human specific primers. mRNA differences are presented as delta cycle threshold (dCt), normalised to human B-actin.

### **5.2. MIF is part of a hypoxic gene signature in AML cells isolated from the BM, but not those isolated from the PB**

As the BM has been shown to be hypoxic (224-227) and as hypoxia has been shown to regulate the expression of MIF in various cells (321, 326, 328), I hypothesised that hypoxia was responsible for the higher expression of MIF in AML cells located in the BM. In 2014, Wierenga and colleagues set up a study to identify the downstream molecular mechanisms of hypoxia in regulating HSC function. They were able to identify common and unique hypoxia, HIF1 $\alpha$

and HIF2 $\alpha$  gene signatures through exposure of CD34+ cord blood cells to hypoxic conditions, and through the overexpression of HIF1 $\alpha$  and HIF2 $\alpha$  in CD34+ cord blood cells (293). Using the hypoxia specific gene list that they generated and with the help of my colleague Manar Shafat, I determined the differential expression of these genes in the data set used in Figure 5.1A. The aim here was to (i) confirm if AML cells from the BM would be enriched for hypoxia related genes compared to AML cells from the PB, and (ii) whether MIF is part of this hypoxic signature.

The analysis generated three lists of genes that are differentially expressed in the BM compared to the data set used in Figure 5.1A. The analysis revealed that a set of hypoxia-related genes were preferentially expressed in AML cells in the BM, compared to the PB, with MIF being amongst a significantly enriched group of genes.

### **5.3. Hypoxia induces MIF in primary AML cells**

Next, I wanted to determine whether hypoxic conditions could induce expression of MIF in AML cells, *in vitro*. I established hypoxic culture conditions in the OCI-AML3 cell line and AML cells, either via treatment with hypoxia-mimicking agents, cobalt chloride (CoCl<sub>2</sub>) and desferrioxamine (DFO) for 4 hours, or by culturing the cells in a hypoxic chamber (1% O<sub>2</sub>) for 24h. I then assayed for MIF mRNA using qRT-PCR, and for protein secretion using an MIF specific ELISA. Figure 5.4 shows that CoCl<sub>2</sub> treatment and 1% O<sub>2</sub> significantly induced MIF mRNA expression, while only DFO and 1% O<sub>2</sub> significantly induced MIF protein secretion in the OCI-AML3 cell line and primary AML samples.

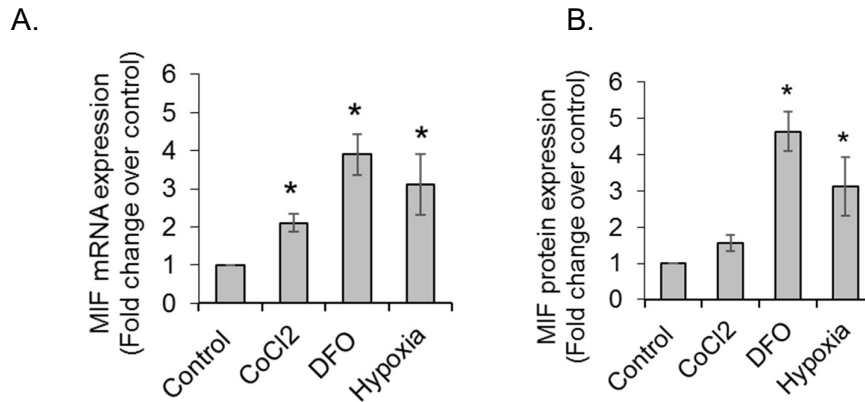


**Figure 5.4 Bar graphs depicting MIF mRNA and protein expression levels in AML cells following culture under hypoxic conditions *in vitro*.**

OCI-AML3 and primary AML cells (n=3) were either treated with CoCl<sub>2</sub> (100uM) or DFO (150uM) for 4 hours, or cultured under hypoxic conditions for 24 hours, (A) RNA was extracted and MIF mRNA expression was determined with qRT-PCR. (B) Media was collected from the respective conditions described in (A) and MIF protein secretion was determined by target-specific ELISA, (n=4). \* denotes p < 0.05.

#### **5.4. HIF1 $\alpha$ is a candidate regulator of MIF expression in Primary AML cells**

Next, I wanted to determine the contribution of HIF1 $\alpha$  or HIF2 $\alpha$  in regulating the expression of MIF in the BM. The differential expression analysis described in section 5.2 for hypoxia, was also performed with HIF1 $\alpha$  or HIF2 $\alpha$  gene lists to determine the significantly upregulated HIF1 $\alpha$  and HIF2 $\alpha$  genes in AML BM samples compared to AML PB samples (GEO accession number GSE49642). The analysis showed that MIF expression is part of the HIF1 $\alpha$  signature, but not of HIF2 $\alpha$ . Based on these findings, I hypothesise that HIF1 $\alpha$  plays a significant role in upregulating MIF in primary AML.

#### **5.5. HIF1 $\alpha$ , but not HIF2 $\alpha$ is stabilised and induces MIF in primary AML cells in response to hypoxia**

To further characterise the role of HIF1 $\alpha$  and HIF2 $\alpha$  in primary AML cells, I used western blotting to assay for HIF1 $\alpha$  and HIF2 $\alpha$  protein expression in AML cells cultured under normoxic and hypoxic conditions (1% O<sub>2</sub>), using a hypoxic chamber. It has been previously reported that under prolonged hypoxia, HIF1 $\alpha$



protein degrades, while HIF2 $\alpha$  exhibits minimal change (329), Hence, I began with a short incubation time of 4 h, to detect changes in HIF1 $\alpha$  and HIF2 $\alpha$  levels. I found that HIF1 $\alpha$  was stabilised after 4h under hypoxic conditions in the OCI-AML3 cell line and in three primary AML blast samples, but HIF2 $\alpha$  was undetectable at 4 hours, and detectable but not stabilised upon 12 h of hypoxia (figure 5.5). Moreover, the Western blots showed that HIF2 $\alpha$  was expressed under normoxia in all the samples tested, as revealed by the occurrence of multiple bands at 90 – 120 kD in the western blot showed. Other studies have observed detection of multiple bands of HIF2 $\alpha$  protein (330, 331).

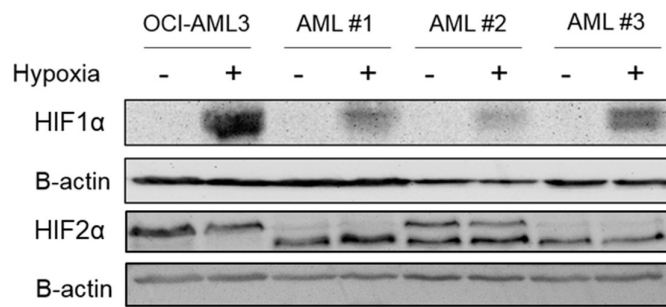


**Figure 5. 5 Western blot demonstrating the stabilisation of HIF1 $\alpha$  but not HIF2 $\alpha$  in AML cells under hypoxic culture conditions.**

OCI-AML3 and primary AML cells were cultured under hypoxic conditions for 4 hours to detect HIF1 $\alpha$ , and for 12 hours to detect HIF2 $\alpha$ . Protein was then extracted from the cells and Western blotting was performed.

### 5.6. MIF is not induced in normal non-leukaemic CD34+ cells

Leukaemic cells and normal HSCs have been shown to co-exist within one compartment in the BM of AML patients (332). Hence, it is important to determine the effect of hypoxia on MIF expression in normal CD34+ cells. I obtained normal CD34+ cells from peripheral blood venesections, from patients without AML (from patients with genetic haemochromatosis, undergoing therapeutic venesection, but with non-raised ferritin levels). Firstly, I determined the expression of MIF in CD34+ cells compared to AMLs. Figure 5.6 shows that at the mRNA level CD34+ cells express significantly higher

levels of MIF mRNA compared to AML cells, however, on the protein level, CD34+ cells secrete less MIF protein than AML cells as confirmed by ELISA.

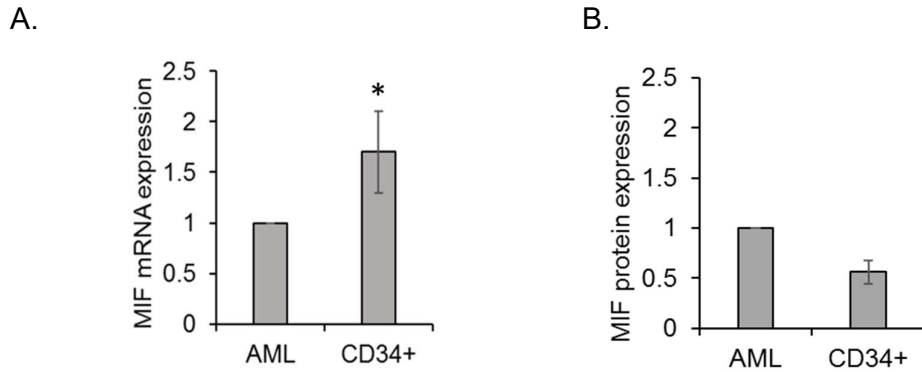


**Figure 5.6** Bar graphs depicting differences in the expression of MIF, mRNA and protein, in CD34+ cells versus AML cells.

0.25x10<sup>6</sup> AML or non-malignant CD34+ cells were cultured under normal culture conditions for 24h. (A) RNA was extracted and MIF mRNA expression was determined with qRT-PCR. (B) Culture media was assayed for MIF cytokine secretion, (AML, n=4, CD34+, n=5). \* denotes p < 0.05.

Next, I cultured CD34+ cells under normoxic or hypoxic conditions using a hypoxia chamber for 24h. Figure 5.7 shows that MIF mRNA expression and protein secretion was not induced in non-malignant CD34+ cells under hypoxia. This finding demonstrates that hypoxic regulation of MIF is a tumour specific event.

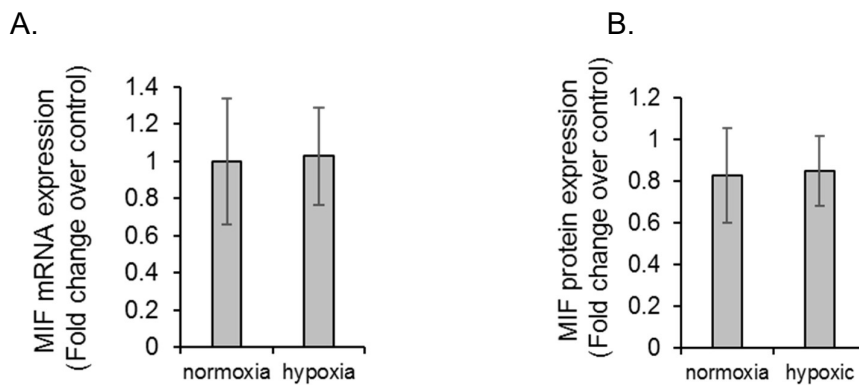


**Figure 5.7** Bar graphs depicting the expression of MIF mRNA and protein in CD34+ cells under normoxic and hypoxic conditions.

Non-malignant CD34+ cells were cultured under normoxic and hypoxic conditions for 24 hours. (A) RNA was extracted and MIF mRNA expression was determined with qRT-PCR (B) culture media was assayed for MIF cytokine secretion, (n= 5). Minor differences in the MIF expression levels denote that hypoxia does not induce MIF expression in normal CD34+ cells.

### 5.7. Silencing of HIF1 $\alpha$ , but not of HIF2 $\alpha$ , significantly reduces MIF expression in primary AML cells

To further characterise the role of HIF1 $\alpha$  in regulating MIF, and to confirm the specificity of its response to HIF1 $\alpha$  versus HIF2 $\alpha$ , I used lentiviral-mediated knockdown (KD) of HIF1 $\alpha$  or HIF2 $\alpha$  in AML patient cells. Lentiviral vectors provide a tool to express short hairpin RNA (shRNA) to induce stable and long-term gene silencing in both dividing and non-dividing cells (333). Figure 5.8A confirms the reduced mRNA expression of HIF1 $\alpha$  and HIF2 $\alpha$  after infection with HIF1 $\alpha$ -KD and HIF2 $\alpha$ -KD lentivirus. Furthermore, Figure 5.8B shows a representative western blot of reduced HIF1 $\alpha$  or HIF2 $\alpha$  stabilisation under hypoxic conditions in KD cells when compared to control-KD cells. These results confirm successful knockdown of HIF1 $\alpha$  or HIF2 $\alpha$  in AML cells.

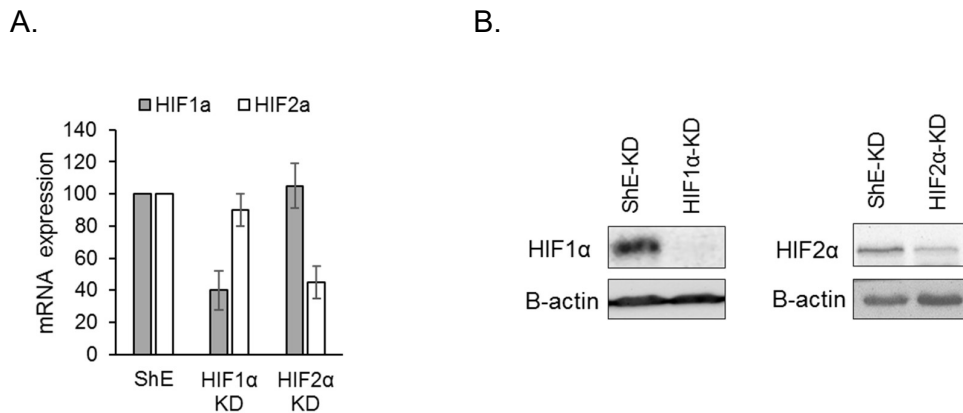


**Figure 5. 8 HIF1 $\alpha$  or HIF2 $\alpha$  lentiviral knockdown (KD) in primary AML cells**

AML cells were infected with lentivirus against HIF1 $\alpha$  or HIF2 $\alpha$  for 72h, (A) lentiviral knockdown (KD) in AML cells was determined by qRT-PCR for mRNA expression (B) HIF1 $\alpha$  KD, HIF2 $\alpha$  KD or control-KD AML cells were cultured under hypoxic conditions for 4 and 12 hours to detect HIF1 $\alpha$  KD and HIF2 $\alpha$  KD respectively, then western blotting performed for protein expression (n=4).

Next, I wanted to determine the effect of silencing HIF1 $\alpha$  or HIF2 $\alpha$  on MIF expression in AML cells. I cultured HIF1 $\alpha$  KD, HIF2 $\alpha$  KD or control ShE-KD cells under normoxic conditions and assayed for basal expression of MIF mRNA and protein. I found that basal MIF mRNA expression was reduced in both HIF1 $\alpha$  KD and HIF2 $\alpha$  KD AML cells (Figure 5.9A). However, MIF protein secretion was only significantly reduced in HIF1 $\alpha$  KD AML cells, but not in HIF2 $\alpha$  KD AML cells (Figure 5.9B). Moreover, when HIF1 $\alpha$  KD cells were cultured under hypoxic conditions for 24h, the MIF induction under hypoxia was significantly inhibited (figure 5.9C). I could also visually observe this in culture, as control (ShE) and HIF2 $\alpha$  KD cells continued to grow and survive, while HIF1 $\alpha$  KD cell counts remained low over culture periods. Specifically, at 5 days of culture, the HIF1 $\alpha$  KD AML blast cells reduced leukaemic survival by 65% compared to control cells while HIF2 $\alpha$  KD had no impact on cell survival (Figure 5.9D). Together, these results demonstrate that HIF1 $\alpha$  regulates MIF secretion in AML cells under hypoxic conditions.

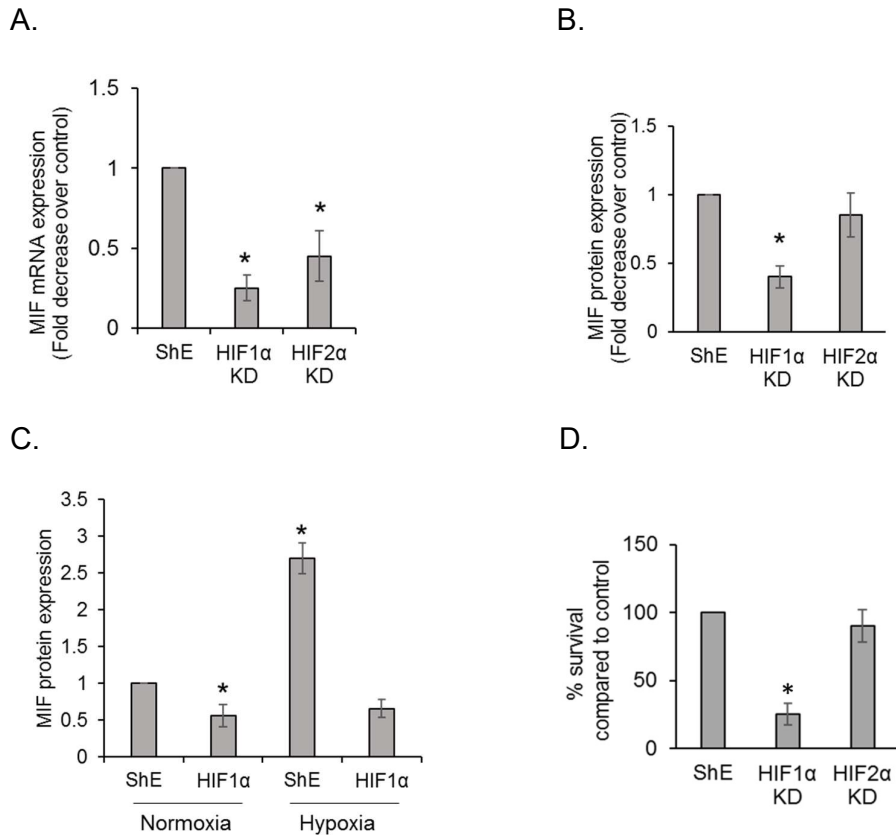


**Figure 5.9** Bar graphs showing the differences in basal MIF expression in HIF1 $\alpha$  or HIF2 $\alpha$  lentiviral knockdown (KD) primary AML cells.

(A) RNA was extracted from cultured AML HIF1 $\alpha$  or HIF2 $\alpha$ -KD, or control-KD cells, and MIF mRNA expression was determined with qRT-PCR. (B) Protein expression in culture media from the cells in A was determined by ELISA (C) HIF1 $\alpha$  KD and control-KD cells were cultured under normoxic or hypoxic conditions for 24 h, MIF protein secretion was then evaluated using ELISA (D) Control-KD, HIF1 $\alpha$  or HIF2 $\alpha$  KD AML cells were cultured for 5 days post-infection, and cell survival was measured with the CellTiter-Glo Luminescent Cell Viability Assay, (n=4). \* denotes  $p < 0.05$ .

### 5.8. MIF functions to promote AML tumour survival *in vitro*

To understand the importance of MIF for the survival of AML cells *in vitro*, I carried out lentiviral-mediated knockdown of MIF in AML cells. I first confirmed the reduced mRNA and protein expression of MIF, prior to functional analysis of the cells (Figures 5.10A and 5.10B). Next, to determine the effect of MIF KD on cell survival, I cultured the cells under normal conditions for 5 days post infection and found that MIF-KD significantly reduced survival of OCI-AML3 cells and of primary AML cells *in vitro* (figure 5.10C); it also compromised the

leukaemic colony-forming ability of primary AML cells in methylcellulose media assays (Figure 5.10D).

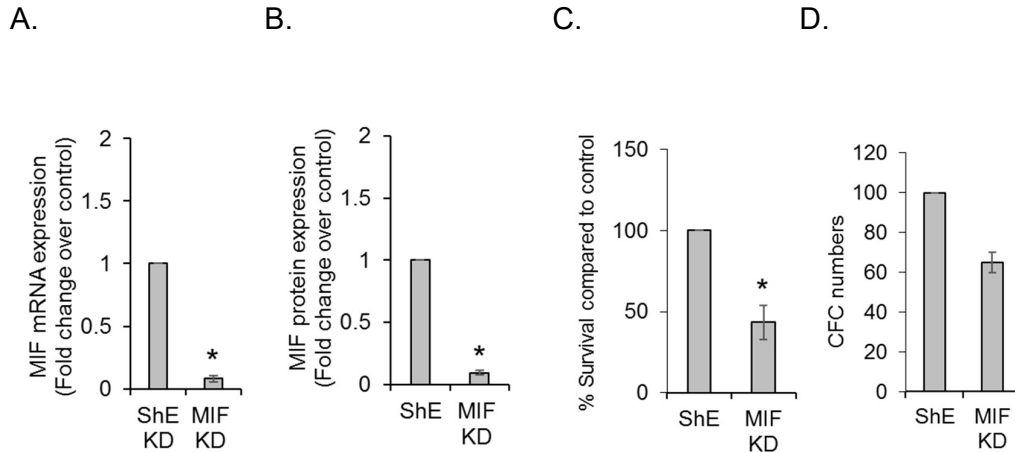


**Figure 5.10 Figure 5.12 Bar graphs showing that lentiviral Knockdown of MIF in AML cells reduces cell survival and colony formation.**

OCI-AML3 cells and primary AML cells (n=3) were infected with Lentivirus against the MIF gene; the successful knockdown of MIF was confirmed by (A) mRNA expression analysis with qRT-PCR, and (B) secreted MIF protein analysis using ELISA. (C) ShE-KD and MIF-KD cells were cultured in basal media for 5 days post-infection; cell survival was measured using the CellTiter-Glo Luminescent Cell Viability Assay. (D) Colony-forming assays of ShE-KD and MIF-KD cells were performed in methylcellulose media. \* denotes  $p < 0.05$ .

To determine if the reduced cell survival was due to an increase in apoptosis, I stained MIF KD AML cells with Annexin V and performed flow cytometry. Figure 5.11 shows that knocking down MIF in AML cells induced apoptosis, as evidenced by an increase in the positive expression of Annexin V, which can be seen in Figure 5.11 below (percentage of cells in the bottom right quadrant increased from circa 10% to 30% AV positive cells).

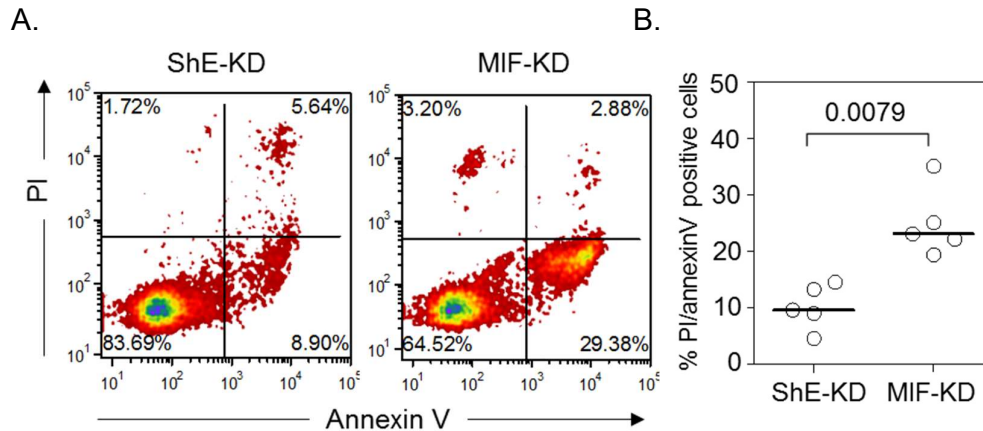


**Figure 5.11 Scatter plots depicting the apoptosis of AML cells, driven by MIF knockdown.**

Apoptosis assays of ShE-KD and MIF-KD cells were performed using annexin V (AV) and propidium iodide (PI) (A) representative scatter plot of AV PI staining of control ShE-KD and MIF-KD AML cells (n=5) after 5 days post lentiviral infection. Bottom right quadrant represents apoptotic cells (B) Column scatter graph showing % PI/AV positive cells of control ShE-KD and MIF-KD AML cells. P value indicated on the figure.

### **5.9. The leukaemic cell HIF1 $\alpha$ -MIF axis functions to promote tumour proliferation *in vivo***

Next, I wanted to determine the role of HIF1 $\alpha$ -regulated MIF in AML progression *in vivo*. To track AML disease progression *in vivo*, I transduced OCI-AML3 cells with a luciferase construct that is detectible by bioluminescence (BLI), upon injecting the animals with luciferin. Successful infection of OCI-AML3 with the luciferase construct was determined by qRT-PCR and flow cytometry. These cells will be referred to as OCI-AML3-luc. Next, I infected OCI-AML3-luc cells with control lentivirus (ShE-KD) or HIF1 $\alpha$ -KD or MIF-KD lentivirus. NSG mice (6-8 weeks) were injected with 0.5x10<sup>6</sup> OCI-AML3-luc cells from ShE-KD, HIF1 $\alpha$ -KD or MIF-KD cultures. Animals were imaged at day 21 and 28 post-injection. The time points were chosen based on experience gained from experimentation with previous AML models in our research group. I found that at both time points mice transplanted with HIF1 $\alpha$ -KD and MIF-KD cells had lower BLI detection, and thus, lower tumour

burden compared to control ShE-KD transplant animals (Figures 5.12A and 5.12B).

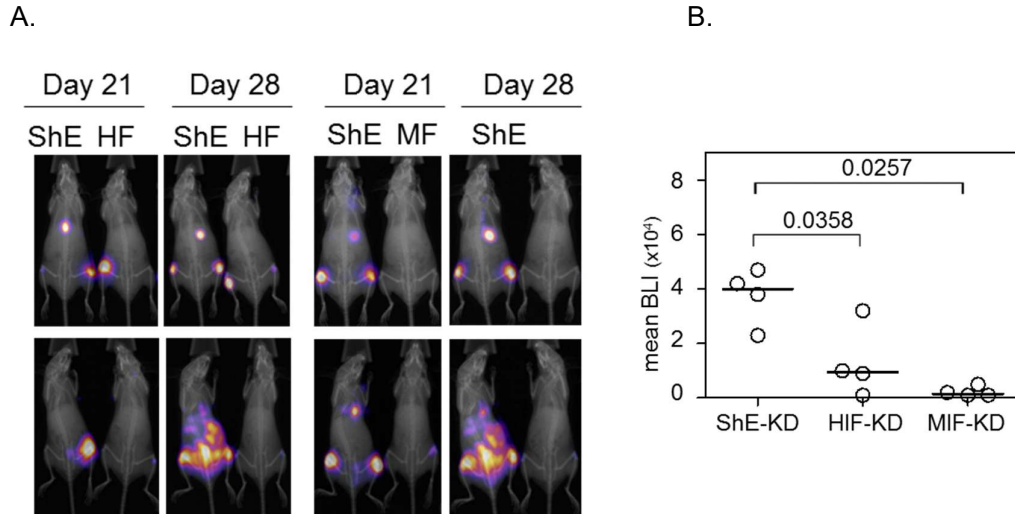


**Figure 5. 12 *In vivo* bioluminescence images depicting disease progression in HIF1 $\alpha$  and MIF KD AML xenograft model.**

0.5x10<sup>6</sup> control-KD (ShE) OCI-AML3-luc and HIF1 $\alpha$ -KD or MIF-KD OCI-AML3-luc cells were injected into NSG mice (n=4 in each group). NSG mice were monitored for disease progression using bioluminescence and sacrificed upon signs of disease. (A) Bioluminescence images of recipient mice, with control-KD (ShE) and HIF1 $\alpha$ -KD (HF) OCI-AML3-luc cells on day 21 and day 28 respectively. (B) The mean bioluminescence intensity (BLI) at day 28 of each image was determined with Image J software. P value indicated on the figure.

Animals were sacrificed at pre-defined severity end points. I then determined AML cell engraftment in the BM by using flow cytometry, by determining human CD33 and CD45 expression (Figure 5.13A). Finally, I found that NSG mice that were engrafted with HIF1 $\alpha$ -KD or MIF-KD OCI-AML3-luc cells had significantly increased survival compared to control animals as evident from the Kaplan-Meier survival curves shown in Figure 5.13B.



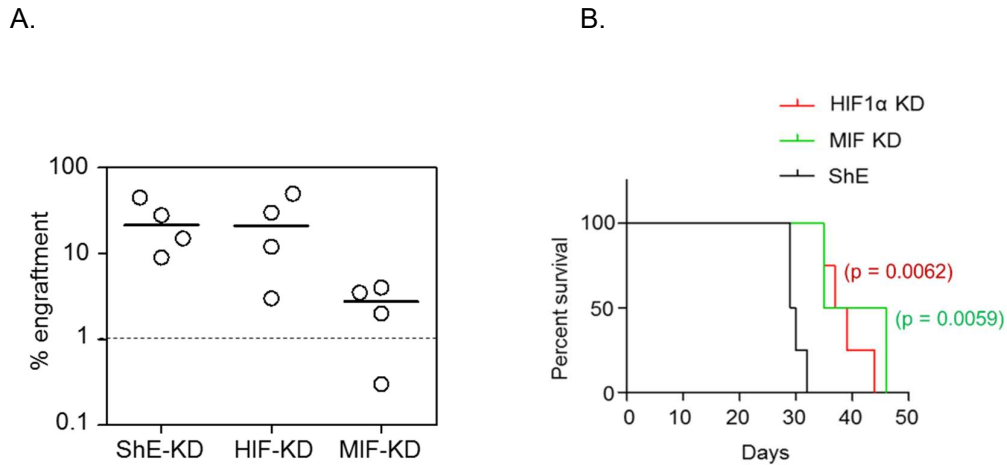


**Figure 5.13 Results summarizing that the inhibition of AML HIF1 $\alpha$  and MIF significantly increases survival of AML derived xenograft models.**

(A) Column scatter graph showing engraftment of OCI-AML3-Luc cells, engraftment was measured using human CD33 and CD45 expression. In the dot plot each AML engraftment into NSG mice is shown for control-KD (ShE), HIF1 $\alpha$ -KD and MIF-KD cells (B) Kaplan-Meier survival curves for NSG mice injected with OCI-AML3-luc HIF1 $\alpha$ -KD cells or OCI-AML3-luc control-KD cells.

### 5.10. Pharmacological inhibition of MIF *in vivo* increases survival of AML xenograft models.

To evaluate the consequences of pharmacological inhibition of MIF in human AML cells on disease progression, I used an AML PDX model, hereby mice were injected with cells from one primary AML sample. The experiment mainly aimed to evaluate the effect of ISO-1 (a specific MIF inhibitor, utilised in experiments presented in chapter 3 and chapter 5) on animal survival. However, since MIF has been reported to be a ligand of CXCR4 (334), and its inhibition hinders the migration of lung and prostate cancer cells (165, 335), I hypothesised that the inhibition of MIF with ISO-1 might affect the retention and mobilisation of AML cells to the PB in a similar manner to the inhibition of the SDF-1/CXCR4 axis by AMD3100 (336).

At day 17 post injection of AML cells, mice were imaged to confirm the establishment of AML tumour in the BM. Animals with established tumour were randomly assigned to be treated with ISO-1 for 7 days (10mg/kg/day, IP) or vehicle control (Figure 5.14A). On the first day of treatment, 50uL of PB were

collected from the tail-veins of the animals at 4, 8 and 24 hours. Total cells were isolated by centrifugation and double stained for human CD33 and CD45. I found that there was no significant difference in the percentage of PB cells positive for human CD33 and CD45, between treated and untreated animals at all three time points. This suggested that the ISO-1, at least at the chosen dose, did not affect AML mobilisation from the BM to the PB. Moreover, the percentage of human CD33 and CD45 positive cells declined in both, treated and untreated animals (figure 5.14B). However, the decline was not statistically significant, and could be attributed to more cells infiltrating the spleen, and less cells circulating in the PB, as evident from the spleen engraftment data in figure 5.14C. Figure 5.16C shows that AML cells were successfully engrafted, as confirmed by positive human CD33 and CD45 expression. Finally, I found that treatment with ISO-1 for 7 days significantly improved the survival rate of the AML PDX animals, compared to the treatment control (Figure 5.14D).

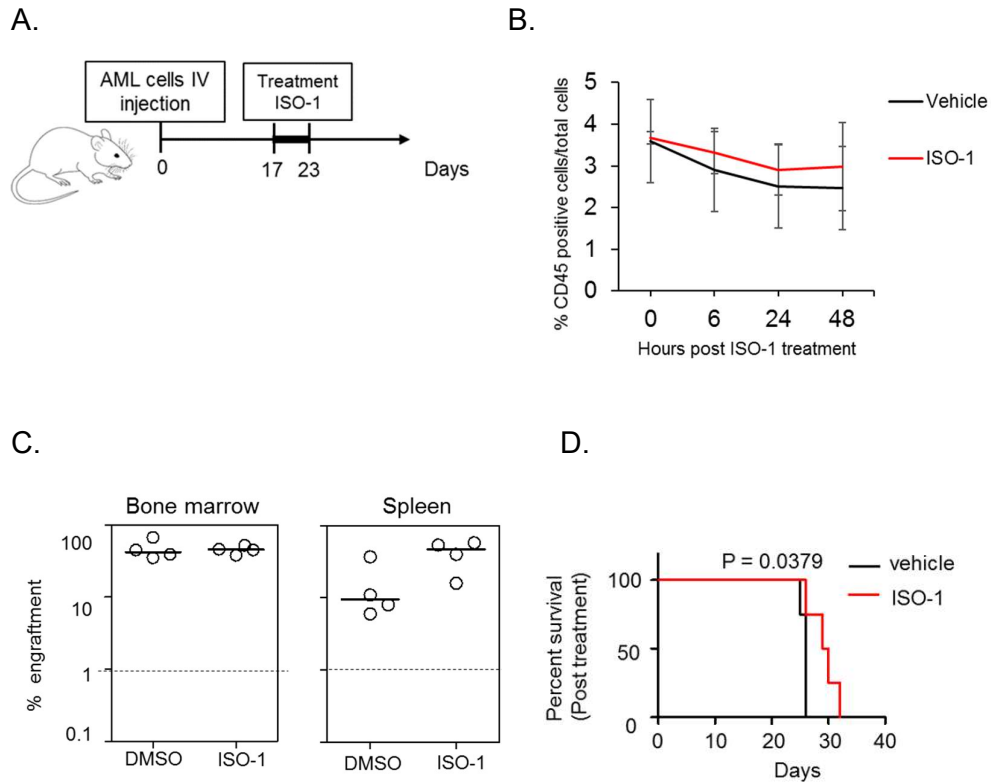


**Figure 5. 14 Summarised results of experiments showing that the pharmacological inhibition of MIF in an AML patient derived xenograft model (PDX) does not affect AML mobilisation, but significantly increases animal survival.**

(A) Representative diagram of the PDX model showing ISO-1 treatment timeline. (B) Percent human CD33 and CD45 positive cells in the PB of control and in ISO-1 treated animals at 4, 8 and 24 hours post ISO-1 or vehicle treatment. (C) Column scatter graph showing engraftment of primary AML cells. Engraftment was measured using flow cytometry to detect human CD33 and CD45 expression. In the dot plot each AML engraftment into NSG mice is shown for the BM and spleen for either control or treated animals. (D) Kaplan-Meier survival curves for NSG mice treated with either vehicle control or ISO-1.

### 5.11. Summary of results chapter 5

In this chapter, I demonstrated that hypoxia, acting through HIF1 $\alpha$ , is responsible for the up-regulation of MIF in primary AML cells, and their proliferation and survival in the tumour microenvironment. I found that AML cells from the BM have increased levels of MIF compared to AML cells from the PB or spleen. I found that MIF is up-regulated under hypoxic conditions at both, the transcriptional and protein levels in AML, but not in normal CD34+

cells. Functionally, it can be deduced that the hypoxia/HIF1 $\alpha$ /MIF axis plays an important role in tumour survival and in proliferation of AML within the BM microenvironment *in vivo*, as inhibition of this axis improved animal survival in AML-derived xenograft models.

## **6. Chapter 6: AML cells induce senescence in BMSCs through the upregulation of p16**

As reviewed in section 1.6, recent investigations into the role of senescence in tumorigenesis have shown that acute senescence contributes to the prevention of cancer. However, more chronic forms of senescence promote tumour development and progression through the senescence associated secretory profile (SASP). AML is primarily a disease of old age and is mainly managed through chemotherapy. Moreover, chemotherapy has been shown to induce senescence that persists after therapy is discontinued (282), and recently, BMSCs from MDS and AML patients have been shown to be senescent (337). These findings make a strong argument to hypothesise that a senescent BM microenvironment may be essential for the development of AML and its relapse after chemotherapy.

In this chapter I present data investigating a novel aspect of AML remodelling of BMSCs, namely AML-induced senescence in BMSCs. Table 6.1 shows the characteristics of the AML samples used in this study.

**Table 6. 1 AML patient sample characteristics used in chapter 6.**

<b>AML#</b>	<b>Age</b>	<b>Sex</b>	<b>WHO calssification</b>	<b>Cytogenetics</b>
AML#25	45	male	AML with maturation	Normal
AML#26	74	male	AML with minimal differentiation	47 XY +13
AML#27	69	female	AML with minimal differentiation	failed
AML#28	59	male	Acute monoblastic and monocytic leukaemia	46,XY, +21
AML#29	66	male	AML with minimal differentiation	inv(16)(p13q22) and +8

### **6.1. Proteome profile arrays from AML-BMSC co-cultures show an upregulation of SASP related factors**

From the cytokine array data of primary AML, primary BMSCs and AML/BMSC co-cultures that were described in chapter 3 (section 3.3), I found that six cytokines were significantly up-regulated in the AML/BMSC co-cultures (Figure 3.5). Further analysis showed that four of these (IL-6, IL-8, MIP-1a and MIP-3a) were shown to be associated with SASP in studies conducted on age-

related diseases, including cancer (274, 338). In the analysis in Figure 3.5, I aimed to account for AML derived cytokines by subtracting the data from the AML cultures from the AML/BMSC co-cultures. Moreover, and as I have previously shown, BMSCs express high levels of IL-8 and IL-6 (Figure 3.8 and Figure 3.10). This led me to hypothesise that AML cells may be inducing BMSCs to become senescent, and to secrete SASP related factors that promote AML survival in the tumour microenvironment.

## **6.2. BMSCs from late passages become senescent in culture**

In section 3.1, I reported that after 6-8 weeks of passaging BMSCs, cell proliferation started to slow down, and that their morphology changed from a fibroblastic, spindly shape to a flatter, rounder shape with cell-free gaps. This morphological phenotype has been reported to be an attribute of senescent cells (339, 340). Since the aim of the work reported in this chapter is to determine if primary AML cells induce senescence in BMSCs *in vitro*, I had to ensure that the BMSCs used were not senescent. Thus, before performing any co-cultures, in addition to observing morphology and taking note of growth rate, I checked for  $\beta$ -Galactosidase staining in the BMSCs. Figure 6.1 presents images of BMSCs that have undergone senescence in culture and are positive for  $\beta$ -Galactosidase staining. Therefore, I deemed them unsuitable for use in my co-culture studies. The BMSCs that I used in the following experiment were passaged 2-4 times, and only BMSCs that did not stain for  $\beta$ -Galactosidase were employed.

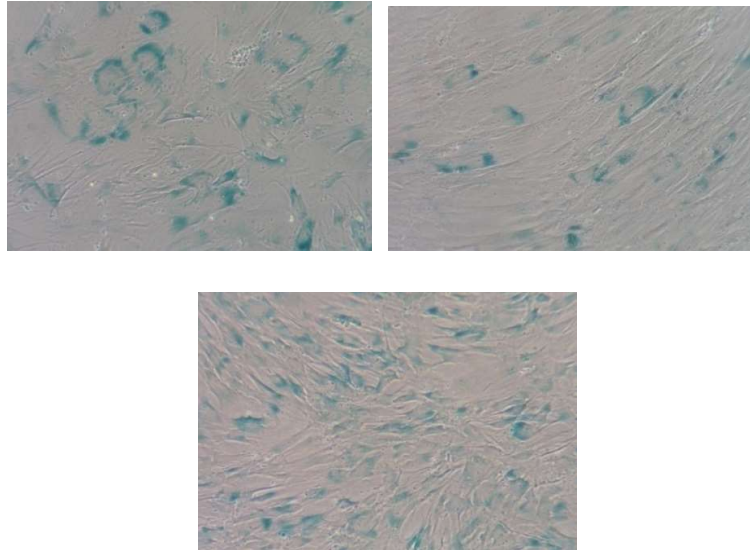


**Figure 6. 1 Light micrographs of senescent patient-derived BMSCs.**

Late passage BMSCs were plated in 35mm dishes close to confluence and  $\beta$ -Galactosidase staining was performed. A blue stain indicated senescent BMSCs (n=3).

### **6.3. AML cells increase senescence associated $\beta$ -Galactosidase staining in patient derived BMSCs**

To determine if primary AML cells induce senescence in patient derived BMSCs *in vitro*, I cultured non-senescent BMSCs alone or in co-culture with primary AML cells for 6 days, and assayed for  $\beta$ -Galactosidase staining. As a positive control for senescence, I included a culture of BMSCs treated with 0.05uM daunorubicin (DNR). I performed this experiment on 3 different BMSCs, using 3 different primary AML samples. Before staining, I aimed to remove the AML cells off the BMSCs, however, some AML samples were highly adhesive to the BMSCs and were not completely removed. I found that DNR and AML cells, both, induce a change in the general morphology of BMSCs, and increase  $\beta$ -Galactosidase staining; in particular, the blue stain is darker in the BMSCs in close proximity to the AML cells (Figure 6.2). These observations suggest that AML cells could be inducing senescence in BMSCs *in vitro*.

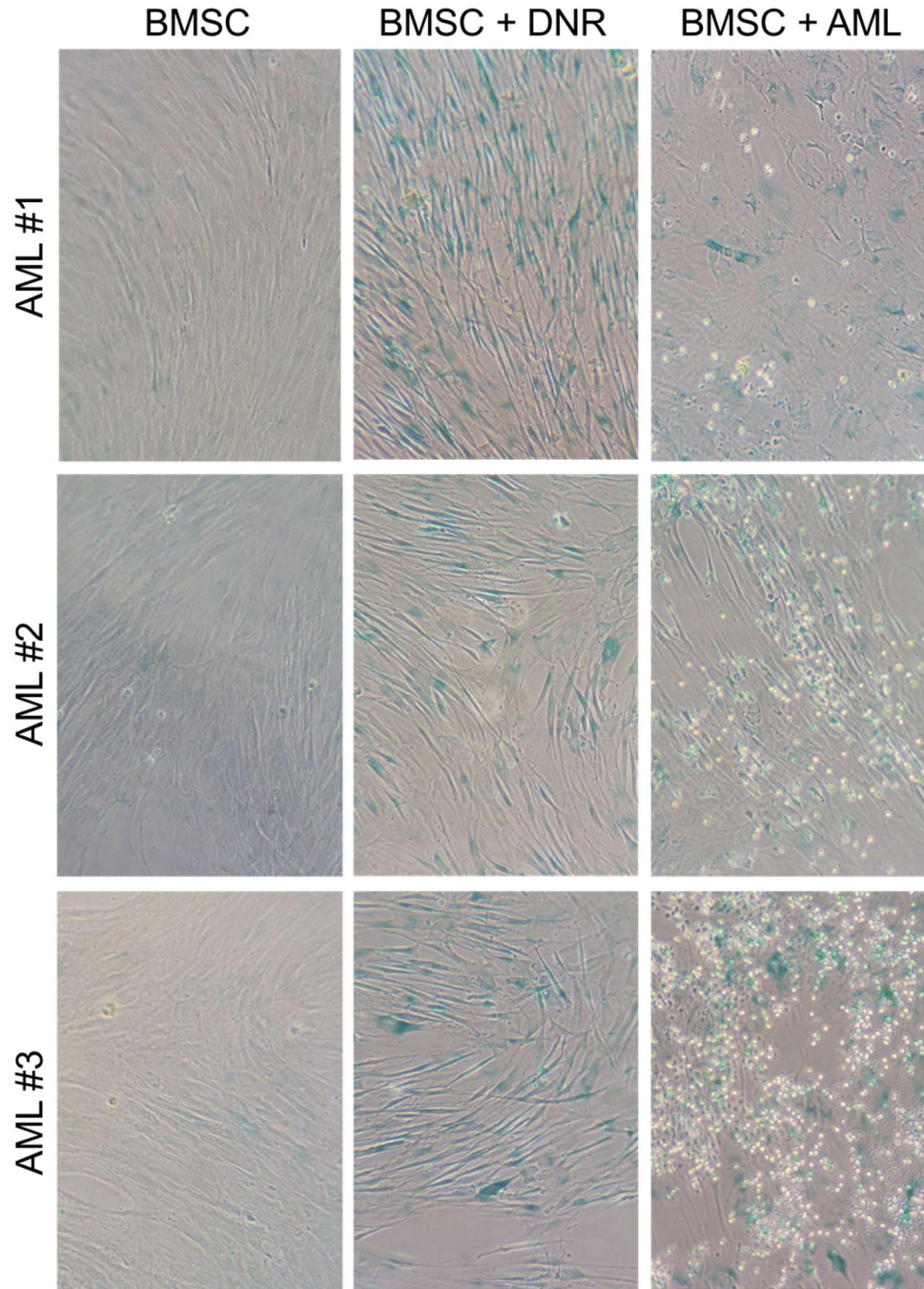


**Figure 6. 2 Light micrograph images showing that primary AML cells induce  $\beta$ -Galactosidase staining in primary BMSCs.**

BMSCs were treated with 0.05uM daunorubicin (DNR) or co-cultured with  $0.5 \times 10^6$  primary AML cells for 6 days, AML cells were removed and  $\beta$ -Galactosidase staining performed. The blue staining indicates senescent BMSCs (n=3).



#### 6.4. AML cells induce p21 and p16 mRNA in BMSCs.

Studies have shown that the contributions of the p53–p21 and the p16Ink4a–RB effector pathways, to the initial growth arrest in cells can vary depending on the type of stress (338). However, it is thought that the p53/p21 pathway establishes growth arrest. On the other hand, the pRB/p16 pathway reinforces the irreversibility of senescent cells by inhibiting cell cycle progression, and is important for the full senescence of stromal cells (341). To determine the contribution of each of the effector pathways to AML-induced senescence in BMSCs, I co-cultured primary BMSCs with primary AML cells in transwell inserts for 6 days. This allowed me to prevent AML adhesion to BMSCs, and AML contamination to the BMSC compartment. I found that primary AML cells induced p21 and p16 mRNA expression in BMSCs (Figure 6.3). At this point, I decided to focus on investigating the role of p16 in AML-induced senescence, as the p16 axis is permanently activated under persistent stress stimuli.

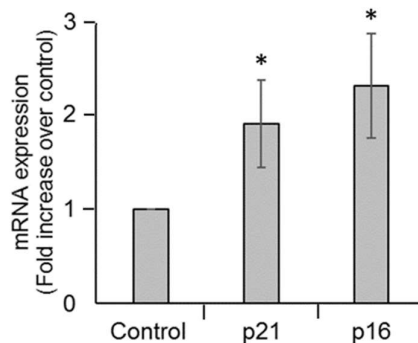


**Figure 6. 3 Bar graphs showing that primary AML cells increase p21 and p16 mRNA expression in primary BMSCs.**

BMSCs were co-cultured with  $0.5 \times 10^6$  primary AML cells for 6 days using a transwell insert. mRNA was extracted and qRT-PCR was performed using p21 and p16 primers. mRNA expression is normalised to  $\beta$ -actin (n=3). \* denotes  $p < 0.05$ .

### 6.5. Knockdown of p16 in BMSCs inhibits AML induced p16 expression in BMSCs.

To decipher the contribution of BMSC p16 towards AML cell survival in co-culture, I used lentiviral-mediated knockdown of p16 in primary BMSCs. Figure 6.4A confirms reduced p16 mRNA in BMSCs 72-hours post infection. To confirm knockdown at a protein level, and to determine if this knockdown is consistent with the well-defined AML-induced p16 activation in BMSCs, I carried out a western blot on BMSCs with p16 knockdown (p16 KD) and control (ShE), that were co-cultured with AMLs. I found that p16 knockdown in BMSCs inhibited AML induced p16 expression in BMSCs (Figure 6.4B). This also confirmed successful knockdown of p16 in primary BMSCs.

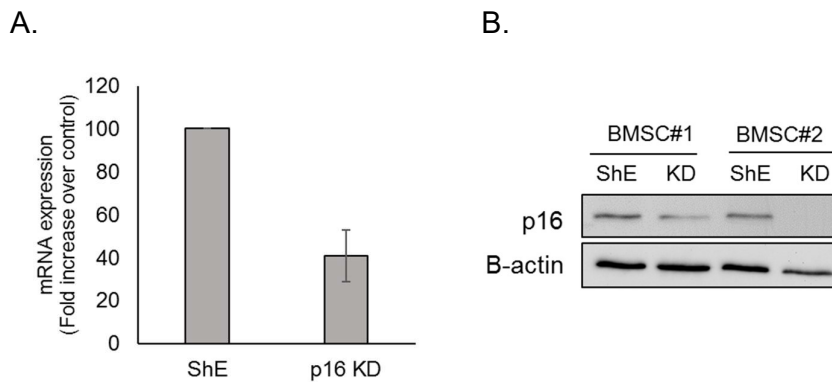


**Figure 6. 4 Results from experiments that reveal that the knockdown of p16 in BMSCs inhibits AML induced p16 expression.**

Control (ShE) or p16 KD BMSCs were co-cultured with  $0.5 \times 10^6$  primary AML cells for 6 days using a traswell insert. (A) mRNA was extracted and qRT-PCR performed using p16 primers, mRNA expression is normalised to  $\beta$ -actin ( $n=3$ ) and (B) protein was extracted from BMSCs and western blotting was performed for p16 expression ( $n=2$ ).

### 6.6. p16 deficient BMSCs have reduced ability to support AML survival *in vitro*

I co-cultured AML cells from 5 primary AML patients on five different BMSCs that had either been infected with ShE control lentivirus or with p16-KD lentivirus. I found that AML cells co-cultured with p16-KD BMSCs had

significantly reduced survival compared to AML cells co-cultured with ShE-control BMSCs (Figure 6.5).

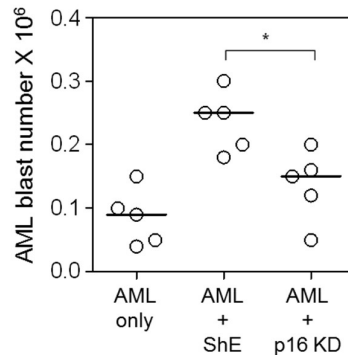


**Figure 6. 5** Dot plot depicting the survival of AML cells co-cultured with p16 deficient BMSCs.

AML cells ( $0.25 \times 10^6$ ) were co-cultured with control (ShE) or p16 KD primary BMSCs in 12 well plate for 6 days (n=5). AML blast number was assessed using trypan blue exclusion hemocytometer-based counts. \* denotes  $p < 0.05$ .

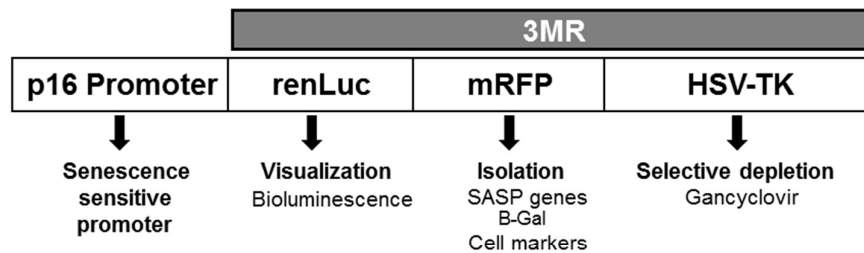
### 6.7. *In vivo* modelling of the senescent BM phenotype using the p16-3MR mouse model

A number of murine models have been developed to study p16 driven senescence *in vivo* (265). Of importance to this work is the p16-3MR senescence reporter mouse, developed by our collaborator Dr J Campisi (262). Dr Campisi's research team developed a transgenic mouse model to label and eliminate cells undergoing p16 driven senescence. In this model, the p16 senescence-sensitive promoter drives expression of 3MR, a fusion protein that is composed of renilla luciferase (renLuc) and monomeric red fluorescent protein (RFP) reporters, and of herpes simplex virus-1 thymidine kinase (HSV-TK), which converts ganciclovir (GCV) into an apoptosis inducer in cells where the p16 promoter is activated.

The luciferase reporter allows the visualisation of senescent cells from live p16-3MR, using bioluminescence; RFP permits the identification and isolation of senescent cells by flow cytometry; HSV-TK facilitates the depletion of senescent cells *in vivo* (Figure 6.6). Eventually, our group would use the p16-

3MR mouse model, and engraft MN1 transduced lineage depleted murine mononuclear cells to generate AML *in vivo*. The initial step to realise this would be to determine if MN1 cells would induce p16 expression in murine BMSCs derived from young, 6 to 8 weeks old p16-3MR mice, *in vitro*.

A



B

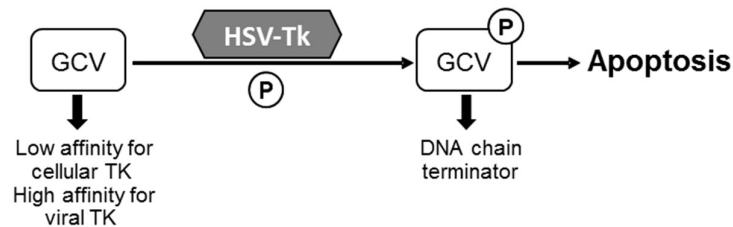


**Figure 6. 6 Schematic of the p16-3MR transgene.**

(A) The tri-modal reporter is under the control of the p16 promoter, which allows the visualisation/tracking, isolation and selective depletion of senescent cells *in vivo*, due to the renilla luciferase (renLuc), monomeric red fluorescent protein (mRFP), and Herpes simplex virus thymidine kinase (HSV-TK) proteins, respectively. (B) A diagram explaining the mechanism by which Gancyclovir (GCV) is phosphorylated by HSV-TK. This forms a purine analogue that inhibits DNA polymerase and causes chain termination and apoptosis of the affected senescent cells.

### 6.8. Isolation and culturing of p16-3MR BMSCs

Once total BM cells from the femurs and tibias of animals were isolated, as described in the methods section 2.5.5, I suspended the cells in DMEM supplemented with 10% FCS and pen-strep, and cultured them in a T-75 flask. The cells were allowed to adhere for 48 hours in normal culture conditions. At 72-hours, I discarded cells that did not adhere, as this was indicative of dead or dying cells, and added 12-15mL fresh growth media. I found that adherent BMSCs could be observed at week 1, and gradually become confluent over 2

weeks (Figure 6.7). I found that replacing media with fresh media every third day is essential to preserve the replicative capacity of cells, and to prevent culture-stress or contact inhibition growth arrest. When needed, I trypsinised the cells and plated them into 12 well plates for further experimentation.

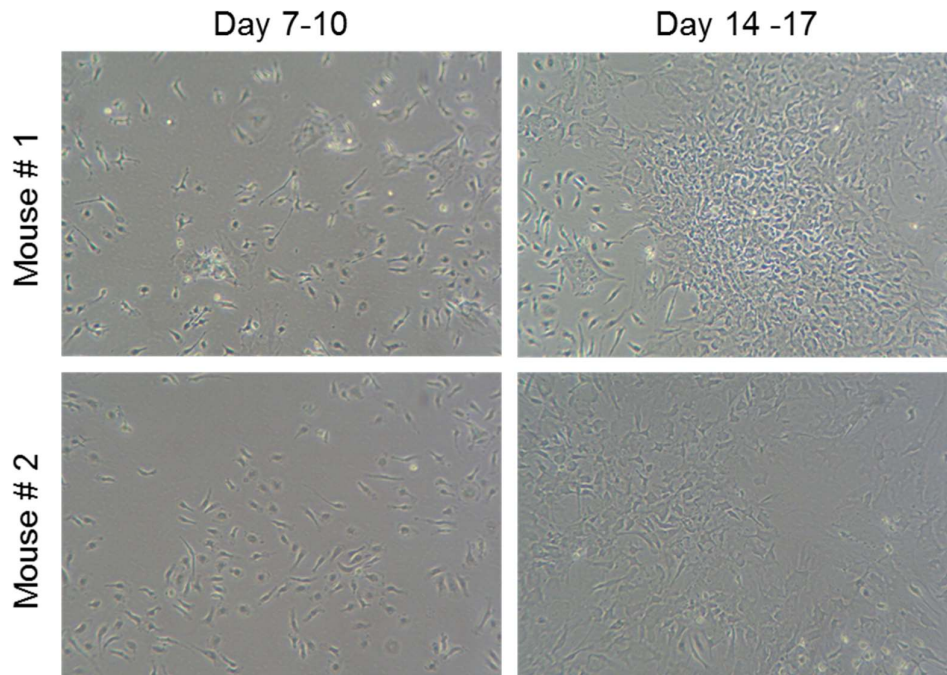


**Figure 6. 7 Light microscopy images from the *In vitro* cultures of p16-3MR derived BMSCs.**

Representative images of two samples of p16-3MR BMSCs in culture at specified days, post isolation.

### **6.9. MN1 AML cells induce p16 expression in p16-3MR derived BMSCs**

After successful expansion of the p16-3MR BMSCs, I wished to determine if murine AML MN1 cells, could induce p16 expression in p16-3MR BMSCs. Thus, I co-cultured MN1 cells with p16-3MR BMSCs in either direct contact (DC) or in transwell inserts (TW) for 7 days. Media was replaced on day 3. Using western blotting, I determined p16 protein expression in p16-3MR BMSCs. Figure 6.8 shows that MN1 cells induced p16 protein expression in

p16-3MR BMSCs. These preliminary results provide the scientific rationale for an initial *in vivo* syngeneic MN1 – p16-3MR senescence model.

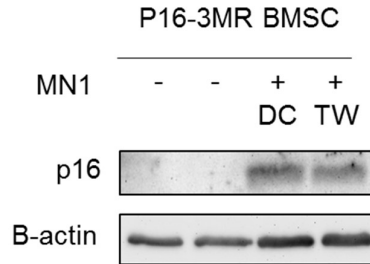


**Figure 6. 8 Western-blot showing that MN1 AML cells induce p16 expression in p16-3MR derived BMSCs *in vitro*.**

$1 \times 10^5$  P16-3MR derived BMSCs were cultured with  $0.5 \times 10^6$  murine MN1 AML cells for 7 days, and p16 expression determined by western blotting. Blots were then re-probed for  $\beta$ -actin as a control (n=1).

#### **6.10. Summary of chapter 6**

In summary, the results presented in this chapter show that AML cells induce a senescent phenotype in BMSCs, accompanied by an upregulation of p16. Knockdown of p16 in BMSCs leads to reduced AML survival in co-culture. Further replication of these results, as well as *in vivo* validation of the MN1 AML – p16-3MR senescence model are required. These are planned by the team in Norwich and potentially as part of my first post-doc. The new project will potentially use this model, amongst others, to further investigate the role of senescence and ageing in the initiation and progression of AML.

## **7. Chapter 7: discussion and conclusions**

### **7.1. AML-derived MIF stimulates BMSC IL-8 expression through PKC $\beta$ and is essential for AML survival**

In chapter 3, I have identified MIF as an AML-derived cytokine that alters the cytokine expression profile of primary BMSCs *in vitro*, specifically through the upregulation of the pro-survival chemokine, IL-8. I have shown that MIF is not just highly expressed by AML cells, but that it also stimulates IL-8 expression in primary AML-derived BMSCs. This upregulation of IL-8 in the BMSCs, induced by MIF, is not seen in normal BMSCs, suggesting a malignancy exclusive phenomenon. Inhibition of either MIF or IL-8 in the leukaemic setting significantly reduces AML survival *in vitro*.

#### **7.1.1. Modelling the AML microenvironment using primary AML BMSCs**

Previous studies have also reported both, human and murine BMSC's ability to support AMLs in co-cultures (70, 131, 299, 342). A caveat in these findings, however, is that the BMSCs used in the reported studies were primarily healthy, non-malignancy-derived BMSCs; thus, they may not ideally represent a malignancy-associated secretory profile. All cytokine arrays and analyses presented in this work were derived from six primary AML BM samples, thereby representing more closely the malignancy-associated secretory profile.

Additionally, upon karyotyping, three of the six primary samples revealed a normal karyotype. The karyotypes for the other three BMSCs could not be determined, as the samples failed to yield analysable metaphases. This issue has been reported by other studies as well (343). My findings contrast those of Huang et. al., who found that three out of four BMSCs from AML patients were cytogenetically abnormal (295). Nevertheless, the sample numbers in both our series are too small to be statistically sufficient, and so the real incidence of cytogenetic abnormalities in the BMSCs of AML patients remains uncertain.

### **7.1.2. AML-induced alternations in BMSC secretory profiles**

The cytokine array data were produced from 24-hour co-culture systems. A limitation to this end-point assay, is that it does not account for real-time events, such as autocrine and paracrine responses in all three culture conditions (AML only, BMSC only and AML/BMSC co-cultures). Hence, it is possible that the contribution of some cytokines might have been overlooked due to these effects.

The cytokine profile of the six BMSC and AML co-cultures showed an upregulation of LIF, endoglin, MIP-3 $\alpha$ , MIP-3 $\beta$ , MIP-1 $\alpha/\beta$ , IL-6 and IL-8 in their culture media. IL-8 mRNA was upregulated 50 to 57-fold. These changes in AML-induced mRNA and protein expression in BMSCs have been reported by other studies, including Civini et. al., where TF-1 and K562 AML cell lines were co-cultured with healthy BMSCs, thus showing a varied increase in BMSC mRNA expression of IL-8 in the co-cultures (344). In my research, I show a consistent increase in all BMSC IL-8 mRNA expression from co-cultures. This strongly suggests that cell lines may not be an accurate representative of the responses seen with primary tissue.

In a recent study, Reikvam and colleagues investigated the secretory profile of AML co-cultured with healthy BMSCs and observed a constitutive secretion of IL-8, IL-6 and VEGF amongst other cytokines from BMSCs (68). Their findings are partially consistent with my findings. However, when I co-cultured AML cells with HS-5, a normal BMSC cell line, I did not observe an upregulation of IL-8 mRNA. Moreover, the HS-5 cell line has been reported to support AML survival and to protect AML cells from spontaneous drug induced-apoptosis through direct contact (66, 311). Taken together, this indicates that the change in secretory profile is unique to AML-derived BMSCs, and also, that the HS-5-induced protection may be independent of the MIF-IL8 axis.

Ryningen et al. co-cultured fibroblast cell lines and one healthy primary BMSCs with AML cells and observed an upregulation of IL-8 secretion in the co-cultures. They hypothesised that the overall increase in IL-8 is due to



fibroblast and BMSC-induced changes in AML cells, causing an increase in their constitutive release of IL-8 (131). Moreover, Huang et. al. reported that the canonical IL-8 pathway was upregulated in AML cells compared to BMSCs (295). These studies neither reported BMSCs as the main source of IL-8 in the co-cultures, nor did they use primary AML-derived BMSCs; however, they indicated that IL-8 played an important role in the AML microenvironment. Furthermore, Huang et. al. also reported that BMSCs derived from AML patients differ from those of healthy donors, mainly in terms of monocyte chemoattractant protein-1 (MCP-1) levels. Hence, it is not unreasonable to suggest that healthy BMSCs and AML-derived BMSCs differ in their secretory profiles when cultured with AMLs. However, due to lack of healthy primary BMSCs in my study, I was unable to make any definitive conclusions as to how normal BMSCs differ from AML-derived BMSCs in my co-culture model.

### **7.1.3. Characteristic primary AML cytokines, an emerging role for MIF**

In monoculture, I found that AMLs secrete high levels of myeloperoxidase, MMP9, osteopontin, IL-8, thrombospondin, MIF and serpine1. Interestingly, myeloperoxidase is a widely accepted gold standard marker for AML diagnosis. It is indicative of a myeloid lineage commitment and is associated with favourable prognosis (345). Furthermore, MMPs and osteopontin have been shown to be expressed by AML cells and to be associated with poor patient prognosis (346, 347). The MMP network is thought to cross-talk with other chemokine networks in AML to promote disease progression (348). Finally, serpine1 is also known to be secreted by AML cells and plays a role in pro-tumoural angiogenesis (349).

In a recent study investigating the expression of a panel of hypoxia-regulated genes in AML and MDS patients, Falantes et. al. showed that MIF was highly expressed by a cohort of AML patients compared to those of the MDS cohort. Further analysis showed that MIF gene expression correlated with poor patient outcomes (300). MIF has also been shown to be overexpressed in other haematological malignancies, such as CLL. Binsky et. al. demonstrated that CLL cells overexpress the MIF receptor, CD74, and are responsive to

recombinant human MIF. Moreover, treatment with ISO-1 inhibited IL-8 mRNA and protein expression in CLL cells (170). Nonetheless, MIF protein secretion was not determined in this study. They concluded that MIF was secreted by CLL cells based on reduced IL-8 levels (which is in line with my findings), and furthermore, based on lower antiapoptotic BCL-2 mRNA expression when the cells were treated with ISO-1, thereby resulting in reduced cell survival and increased cell apoptosis.

While Binsky and colleagues identified MIF to activate a CLL autocrine loop, my findings suggest that MIF activates a paracrine pathway in BMSCs, subsequently altering the microenvironment in a pro-tumoural manner. Unlike Binsky et. al.'s work, I have not investigated the effect of exogenous MIF or IL-8 on AML expression of MIF, IL8 or CD74. However, CD74 has been shown to be expressed on the cell surface and in the cytoplasm of primary AML cells and AML cell lines (350), and to be associated with a poor outcome in younger AML patients (351). These studies make it reasonable to hypothesise that MIF might have an autocrine effect on the malignant cells as well as BMSCs and warrants further investigation of MIF receptor expression and function in the AML cells.

I found that the inhibition of MIF using ISO-1 significantly reduced AML survival in co-culture. These results support previous findings that indicated reduced CLL survival following functional MIF inhibition, when cultured on a macrophage feeder layer (166). Interestingly, in *an vivo* model of breast cancer, MIF have been shown to promote tumour growth and pulmonary metastasis by inducing a highly immune suppressive subpopulation of myeloid-derived suppressor cells (MDSCs) (352).

Recently, in a similar breast cancer mouse model, MIF was found to decrease the number of intra-tumoural CD8+ T cells, and to inhibit their ability to produce the cytokine IFN-gamma, resulting in inhibition of the immune function of these cells (353). From these studies and my findings, it is possible to deduce that MIF may have a broader effect on cellular components of the BMM, including immune cells and BMSCs

MIF protein is roughly 30% homologous with the related protein, D-dopachrome tautomerase (D-DT), also referred to as MIF-2 (354). MIF and D-DT genes are located on the same chromosome in both human and mouse and are ~ 80 kb apart (355, 356). D-DT expression has been detected in a number of human organs, however, a comparison of enzymatic activity of the two proteins showed that human MIF is about 10-times more active than the human D-DT protein (356). Both MIF and D-DT have been shown to have overlapping functions in solid tumours, for instance, in a study on renal clear-cell carcinoma, D-DT and MIF showed additive protumourigenic effects (357), similar findings were shown in a model of non-small cell lung carcinoma (358). However, there is no data on the expression or role of D-DT in haematological malignancies. Taken together, it is plausible that D-DT, if expressed in leukemic cells, might play an independent or cooperative role with MIF in AML cells.

My findings only identified MIF-driven survival signals in AML microenvironment. The homology in protein structure and similar activity of MIF and D-DT, could present an issue of specificity of the assays used to detect MIF and MIF-derived responses. In my study, MIF RT-PCR primers and MIF ELISA kits were not tested for cross-reactivity with D-DT. Although the ELISA assay used to detect MIF protein was validated by the suppliers to be MIF specific, ideally, recombinant human D-DT could have been used to determine any detection of D-DT. To rule out detection of D-DT using MIF RT-PCR primers, the PCR transcript can be sequenced to determine the specificity of the product and primers used. Most importantly, these measures are valid if mRNA and protein expression of D-DT were detected in AML cells used in the study.

#### **7.1.4. Clinical investigations of MIF inhibitors**

Recently MIF has been shown to exist in two immunologically distinct redox-dependent isoforms, known as oxidised MIF (oxMIF) and reduced MIF (redMIF), total MIF was defined as the sum of oxMIF and redMIF, oxMIF is believed to be disease-associated (359). In solid tumours, oxMIF inhibition

sensitised human cancer cell lines to cytotoxic drugs (360). In my experiments, I assayed for total MIF cytokine secretion. In early phase trials of colorectal cancer and selected solid tumours, a novel oxMIF inhibitor (imalumab) was found to be effective and well tolerated (361, 362). Therefore, it would be interesting to identify the relative abundance of the two MIF isoforms in AML patient samples and to evaluate the efficacy of imalumab in *in vitro* and *in vivo* models of AML. This could help evaluate the plausibility of an MIF inhibitor trial in patients with AML.

#### **7.1.5. PKC $\beta$ targeting in leukaemic cells**

In chapter 4, I demonstrated that MIF binding of CD74 on the surface of BMSCs activated PKC $\beta$  signalling, and that the knockdown of PKC $\beta$  in BMSCs significantly reduced AML survival in co-culture. PKC signalling has been shown to be altered in cancer cells (363). Members of the PKC family have been implicated in haematological malignancies. In line with what I have shown in AML cells, inhibition of PKC $\beta$  with enzastaurin has been shown to abrogate the protective effect of BMSCs on MM cell lines (364). PKC $\beta$ II is over expressed in CLL cells and is downstream of the B cell receptor (365).

El Gamal et al demonstrated that PKC inhibition in CLL promotes apoptosis, inhibits proliferation, and abrogates microenvironment mediated protection of CLL cells (366). In their study, microenvironmental protection was simulated using a cytokine cocktail which mimicked the cytokines shown to be essential for CLL survival, whereas in my model, I aimed to mimic the microenvironment by co-culturing AML cells with BMSCs. Additionally, activation of PKC $\beta$ II in a murine stromal cell line EL08-1D2 was shown to be essential for the survival of leukaemic cells from CLL, ALL and MCL patients (28). Taken together, it is postulated that PKC $\beta$  is commonly activated in haematological malignancies, which supports my hypothesis of its importance in the leukaemic microenvironment.

#### **7.1.6. IL-8 as a key cytokine for AML survival**

In 1993, Tobler et. al. described the constitutive expression of IL-8 and its receptor in AML (136). More recently, Schinke et. al. reported that IL-8 is

overexpressed in primary AML samples compared to normal HSCs. Inhibition of the IL-8 receptor CXCR2 selectively decreased proliferation and cell cycle arrest of AML cells (140). In line with these studies, I found that the inhibition of CXCR2, or the knockdown of IL-8 in BMSCs reduced AML survival in co-culture. Elaborating on the role of IL-8 in the AML microenvironment, AML cells have been shown to have a higher low-density lipoprotein (LDL) uptake compared to normal mononuclear blood cells, which in turn resulted in higher cellular cholesterol levels. Cellular cholesterol is essential for membrane protein structure and function, and so the inhibition of this uptake sensitised AML cells to chemotherapy in clinical trials (367, 368). Very recently, Bhuiyan et. al. reported that autocrine and paracrine IL-8 (and IL-6) stimulated LDL uptake in AML cells, thereby increasing AML cellular levels of cholesterol (369). Taken together, these studies further support the broader role of IL-8 in the survival of AML cells.

#### **7.1.7. *In vivo* modelling of IL-8 may be challenging**

Because mice lack a direct homologue of IL-8, MIF stimulation of human IL-8 could not be demonstrated *in vivo*. An accepted homologue of IL-8 is murine MIP-2 (370). HSCs have been shown to respond to murine MIP-2 (371), however, to this date, leukaemic cell response to murine MIP-2 has not been reported. An alternative model could be a syngeneic murine model in which murine AML cells overexpress MIF. However, since IL-8 upregulation is the ultimate effect of AML-derived MIF, it is also imperative to evaluate the effect of MIF-deletion in AML cells on animal survival. I have presented these results in chapter 5, where AML-derived MIF inhibition resulted in reduced tumour burden and significantly increased animal survival.

In summary, I have described how AML stimulates the production of IL-8 from BMSCs and using pharmacological and lentiviral intervention, inhibiting this process significantly reduces AML survival *in vitro*.

#### **7.2. Hypoxia regulates MIF expression through HIF1 $\alpha$**

In the previous section I discussed the importance of MIF as a mediator of AML survival. In chapter 5, I reported that hypoxia, acting through HIF1 $\alpha$ , is

responsible for the up-regulation of MIF, and the subsequent proliferation and survival of AML in the tumour microenvironment.

Hypoxia has as broader malignant phenotype in the proliferation of solid tumour cells in studies of breast, prostate, ovarian and pancreatic cancers (372-374). Under normal physiological conditions, the BM is a known hypoxic environment. Fiegl et. al. have established that the AML BM is also hypoxic (240). Furthermore, tumour-specific transcriptional programs in AML patient samples included an up-regulation of the hypoxic response genetic signature (375).

### **7.2.1. AML emerges as a hypoxia driven malignancy**

In a study evaluating the effectiveness of hypoxia-activated pro-drug TH-302, Benito et al report that BM and PB AML samples exhibited a greater hypoxic signature than those of healthy controls. This suggests that AML cells retain a hypoxia-induced gene signature even after they exit the hypoxic BM (246). However, the study does not report a direct comparison of hypoxic signatures between AML PB samples and normal PB samples. Moreover, it has been reported that AML PB CD34+ cells are functionally different from those in the BM. Cheung et. al. identified 9 genes whose expression was significantly higher in BM CD34+ cells compared to PB CD34+ cells (376). Among these genes, MCL-1 and DUSP1 have been shown to be HIF1 $\alpha$  target genes (377, 378).

In line with these studies and, using bioinformatic analysis, I reported that AML samples from the BM are enriched in hypoxia regulated genes compared to samples from the PB (section 5.2). I further confirmed this *in vitro*, using five primary AML samples, in which hypoxia regulated GLUT1 and MIF were higher in BM AML cells than in the PB. I found that hypoxia did not induce MIF expression in normal peripheral CD34+ cells. However, normal CD34+ in this experiment were derived from healthy donors and may be intrinsically different from AML PB CD34+ cells. Whether PB AML cells are different from healthy PB CD34+ cells warrants further investigation. In summary, these findings

suggest that hypoxia is key to AML pathogenesis and, most importantly, it is a tumour-specific feature.

I report above in chapter 5 that the upregulation of MIF is a functional consequence of the hypoxic microenvironment. Interestingly, others have shown in their studies that it was hypoxia that regulated MIF expression in endothelial cells and vascular smooth muscle cells (321, 328). MIF was shown to be up-regulated by hypoxia in several tumour cell types *in vitro* including in breast carcinoma cells (323). Interestingly, CLL cells are highly dependent on MIF for their survival (166) and have been shown to constitutively express HIF1 $\alpha$  under normoxic conditions (379). Hence, the inhibition of HIF1 $\alpha$  or MIF interactions have been suggested as a plausible therapeutic approach for CLL (380). Following these, I demonstrated that by silencing HIF1 $\alpha$ , using a lentivirus-mediated knockdown in both primary AML and in the OCI-AML3 cell line, the expression of MIF is regulated by hypoxia driven HIF1 $\alpha$ .

### **7.2.2. The role of HIFs in AML remains to be delineated**

In my studies, the knockdown of HIF1 $\alpha$  in primary AML cells significantly reduced their proliferation in culture, and significantly increased the survival of NSG mice injected with HIF1 $\alpha$ -KD OCI-AML3luc cells. Previously published results using a syngeneic murine AML model showed that genetic deletion of HIF1 $\alpha$  had no effect on mouse AML maintenance, and may accelerate disease development (248). In another study by the same group, it was shown that the loss of HIF1 $\alpha$  accelerated murine FLT3-ITD induced myeloproliferation (381). This observation appears contrary to my own data, where I found that the loss of HIF1 $\alpha$  reduced the number of AML cells, compared to controls (section 5.7, Figure 5.11D).

However, other studies have shown that deleting HIF1 $\alpha$  in a subset of primary AML LSCs led to a decrease in their sensitivity to HIF1 $\alpha$  inhibition. Wang et. al. demonstrated an important role for HIF1 $\alpha$  in the *in vitro* colony-forming activity of their 7 clinical AML samples, where the experiments employed echinomycin as a HIF1 $\alpha$  inhibitor (326). This was also demonstrated in another study using AML cell lines to study the effect of HIF1 $\alpha$  in AML (382). However,

since echinomycin blocks HIF1 $\alpha$  transcriptional activity by binding to DNA via bi-functional intercalation into the hypoxia response element, this would also compromise HIF2 $\alpha$  transcriptional activity (216). Vukovic et. al. revealed that HIF-1 $\alpha$  and HIF2 $\alpha$  are not required for leukaemia stem cell maintenance and AML propagation, but that they acted synergistically to suppress leukaemia development in mice. In their models, the knockout of HIF2 $\alpha$  or the pharmacological inhibition of the HIF pathway in human AML cells had no impact on their survival and proliferation under hypoxic conditions (253).

In my experiments, I showed that HIF2 $\alpha$  is detectable under normoxic conditions in AML patient samples and in the OCI-AML3 cell line. Interestingly, I observed that the HIF2 $\alpha$  protein, unlike HIF1 $\alpha$ , is not increased under hypoxic conditions, while I found that HIF1 $\alpha$  is only stabilised under hypoxic conditions. In AML cell lines (HL60 and THP-1), HIF1 $\alpha$  has been shown to be constitutively expressed under normoxic conditions (383). More recently, it has been shown that in primary and cell line CML cells HIF1 $\alpha$  is stabilised under normoxic conditions (384). The discrepancy in the status of HIF1 $\alpha$ , in primary and cell line AML models, indicate that they are intrinsically different from one another. Hence, observations in cell lines cannot always be generalised to the primary disease.

I demonstrated that specific KD of HIF1 $\alpha$  but not HIF2 $\alpha$  prevented MIF induction under hypoxic conditions. Taken together, these results suggest that HIF1 $\alpha$ , but not HIF2 $\alpha$ , is responsible for driving MIF expression in my AML samples. In my *in vivo* studies, HIF1 $\alpha$ -KD AML cells took longer to engraft, compared to the control-KD cells for which animal survival was longer. Therefore, this suggests that human AML benefits from the hypoxia present within the bone marrow microenvironment.

Previously published studies demonstrated that the overexpression of HIF2 $\alpha$  accelerate myeloid leukaemia in mice. Conversely, HIF2 $\alpha$ -KD in leukaemic cell lines prolonged the survival of transplanted mice (252). Rouault-Pierre and colleagues show that cells from primary AML samples were dependent on the level of HIF2 $\alpha$  for their survival, and were protected from apoptosis induced by



ER stress (251). This is in contrast to my results, where I found that the knockdown of HIF2 $\alpha$  in primary AML cells did not lower the survival of AML cells in culture, and it had a minimal effect on MIF secretion by the cells.

### **7.2.3. *In vivo* modelling of the role of MIF in AML BMM**

I found that knocking down MIF significantly reduces AML survival and colony forming ability. Moreover, animals transplanted with AML cells following MIF-KD had significantly improved survival compared to controls. This is in agreement with observations in MM, where MIF-KD in MM cells did not form tumours in bone of MM mouse models, whereas control KD cells caused tumours in the bone (385), thereby, suggesting a role for MIF in the microenvironment of AML and MM likewise. Moreover, I found that MIF-KD induced apoptosis in AML cells. Recently, the presence of MIF-KD in cervical adenocarcinoma cells was shown to induce apoptosis and to inhibit cell proliferation, via the upregulation of proapoptotic proteins and the downregulation of antiapoptotic proteins of the Bcl-2 family (386). MIF can also induce apoptosis by inhibiting wildtype p35 activity, as demonstrated in lung adenocarcinoma cells (154). The mechanism by which MIF induces apoptosis in AML cells remains to be investigated.

In the CI-AML3luc mouse models, MIF-KD mice had less tumour burden than the HIF1 $\alpha$ -KD mice. Moreover, survival was slightly more improved for the MIF-KD mice (section 5.9). This may be due to indirect protein interactions, by which MIF may regulate HIF1 $\alpha$  function, as deduced from a study in which the overexpression of MIF in selected cell lines enhanced HIF1 $\alpha$  activation under hypoxia, and was dependent on wildtype p53 (387). In my experiments, I did not investigate whether MIF regulates HIF1 $\alpha$  function in the AML cells. It would be interesting to determine the effect of exogenous MIF on HIF1 $\alpha$  activity in MIF-KD cells. Furthermore, in case this interaction is dependent on wildtype p53, this mechanism might be attenuated in p53 mutant AML. In conclusion, the functional interactions of MIF and HIF1 $\alpha$  in AML remain to be elucidated.

Finally, in the primary AML PDX used in my studies, MIF gene silencing with shRNA provided better survival differences than using the pharmacological

inhibitor, ISO-1, which only extended survival by less than 10 days. A possible explanation for this could be that the ISO-1 dosage was suboptimal. In fact, in a study using ISO-1 to inhibit MIF function in a model of sepsis, doses of up to 35 mg/kg/day were used (388), while the dose used in my studies was only 10mg/kg/day. I postulate that a higher dose could have improved survival and improved AML cell mobilisation to the PB.

In conclusion, my study presents a mechanism linking hypoxia to a chemokine factor, inducing a pro-tumoural signalling pathway in the AML microenvironment. In doing so I establish a potential strategy to target AML.

### **7.3. AML induces senescence in BMSC through upregulation of p16**

In chapter 6, I presented novel data that identified the BMM as a progressively senescent one which enhances the survival of AML within the BM. I also showed that the senescence of BMSCs in the environment is induced by AML cells and is brought about through the cyclin-dependant kinase inhibitor, p16. Finally, BMSCs from the p16-3MR mice were successfully cultured and p16 expression was determined in co-cultures with murine MN1 AML cells. Knockdown of p16 in BMSCs reduced AML survival in co-cultures; as a result, *in vivo* experiments with the p16-3MR animal model will be optimised for further senescence studies in AML.

#### **7.3.1. An ageing-induced malignant environment**

AML is a disease of the older population (27) and senescent cells have been shown to naturally accumulate with age (265). Moreover, it has been shown that, senescent fibroblasts stimulate the growth of neighbouring pre-neoplastic epithelial cells, in co-culture experiments of prostate cancer and in *in vivo* models of lung cancer (389, 390). These studies suggest that as aging cells accumulate, they create an environment which is favourable to cancer cell survival. Interestingly, it has also been shown that cancer cells can induce normal cells to become senescent. In *an vivo* model of p16 driven senescence, imaging revealed p16 expression in the emerging neoplasm and surrounding stromal cells (391). This is in line with my observation that AML cells induce

p16 expression in BMSCs. However, I did not study p16 expression in the malignant compartment.

### **7.3.2. Senescence in AML cells**

Müller-Tidow et. al. investigated the expression levels of cell cycle genes in primary AML patient cells and found that average expression levels of p16 (and tumour suppressor p14) were higher in AML samples, compared to control samples. However, the median age for the AML cohort in this study was 52 years and the control group included only six samples (392). In a more recent study, p16 mRNA was shown to be downregulated in AML cells with increasing age (393). Considering the differing outcomes of these studies, an interpretation of the significance of p16 expression in the AML compartment can only be accurate if the patient ages are comparable.

### **7.3.3. *In vitro* markers and inducers of senescence**

Since it was first described in 1995 by Professor Campisi's research group,  $\beta$ -galactosidase ( $\beta$ -gal) staining has been widely used for detecting senescence. Senescent cells are identified by their failure to synthesise DNA. Nonetheless, this is also characteristic of quiescent and differentiated cells. The  $\beta$ -gal staining assay has the following advantages: i) it is easy to detect, ii) it has been shown to be independent of DNA synthesis in senescent cells, and iii) it generally differentiates senescent cells from quiescent cells (394, 395). Hence, it was ideal for detecting AML-induced senescence in my co-culture model.

I found that BMSC from late passages become senescent in culture. This is not surprising as cultured primary BMSCs have been shown to undergo senescence (396, 397). Moreover, AML-derived BMSCs may be intrinsically different from normal BMSCs in terms of the rate at which they undergo senescence. Kim et. al. reported that AML derived BMSCs had lower proliferative activity than that of the controls due to increased senescence (343). Hence, in my study, the lack of normal BMSCs and the small sample size of AML-BMSCs may be a limiting factor in the interpretation of data. More

definite conclusions may be made from a bigger sample size, and including a comparison with normal BMSCs.

In my culture model, I used daunorubicin as a positive control to induce senescence in BMSCs. It is the immediate precursor of the more widely used doxorubicin (398). Doxorubicin and daunorubicin are both anthracyclins with the same mechanism of action (399), and they have been shown to induce a senescent-like phenotype *in vitro* and *in vivo* (282, 400). Additionally, daunorubicin is a critical component of standard induction chemotherapy in AML patients (401). It would be interesting to investigate whether the effect of daunorubicin and AML are synergistic on BMSC senescence, and how it can be eliminated.

Although SASP factors have been shown to develop slowly over time, not all of them are secreted at the same time (261). I have reported that AML cells induced SASP-related factors in 24-hour co-cultures. I then performed  $\beta$ -gal staining in BMSCs after 6 days of co-culture, however, I did not check for SASP factors at 6 days. It is possible that AML-derived BMSCs may be pre-conditioned to developing an SASP at an earlier time point once they are cultured *in vitro*. Ideally, AML-BMSCs should be compared to healthy, age matched BMSCs to allow identification of intrinsic differences between malignant and healthy BSMCs.

#### **7.3.4. *In vivo* modelling of the senescent BMM in AML**

In efforts to optimise the p16-3MR model to study AML BM senescence, I showed that murine AML cells, overexpressing the MN1 AML oncogene induced p16 protein expression in p16-3MR-derived murine BMSCs after 7 days of co-culture. Ideally, additional confirmatory experiments need to be performed to confirm this result and to optimise the AML p16-3MR mouse model. These include, determining luciferase activity of the senescent p16-3MR BMSCs in co-culture with MN1 cells, identifying if p16 expression developed at earlier time points while in culture, and assaying for SASP factors in co-cultures compared to monocultures of p16-3MR BMSCs.

The p16-3MR transgenic mouse model is instrumental in studying AML induced senescence. It has previously been used to study the role of senescent cells in wound healing and in age-related diseases (262). This model permits the non-invasive clearing of senescent cells *in vivo* using gancyclovir (explained in section 6.7). A similar mouse model, referred to as the INK-ATTAC mouse (283, 402) is the only other model where p16 senescent cells can be depleted *in vivo*.

I have reported that AML cell co-cultures with p16-KD BMSCs significantly reduced survival *in vitro*. This observation can be validated *in vivo* with the p16-3MR model. Using gancyclovir, the elimination of senescent cells from p16-3MR mice that have developed AML, would be expected to increase their survival compared to controls (no gancyclovir). Pharmacologically, senolytic agents have been shown to effectively and selectively ablate senescent cells. An example of this is ABT-263, which inhibits the anti-apoptotic proteins Bcl-2 and Bcl-xL in senescent cells, leading to their apoptosis. Interestingly, Chang et. al. used the p16-3MR mouse model in conjunction with ABT-263 to rejuvenate aging HSCs in the BM of mice (403). Importantly, ABT-263 has been shown to target AML cells too (404). As it is not known how this compound will perform in an AML and BMSC co-culture, its effects will need to be evaluated *in vitro* and *in vivo*.

In conclusion, senescence has been shown to be both, tumour-suppressing and tumour promoting, depending on the biological contexts of the disease being studied. In AML, senescence may be induced by both, the treatment and the malignancy. This creates a novel therapeutic angle which seeks to manipulate the tumour favouring environment to act against the tumour, and may be an important and interesting strategy in identifying the state and prognosis of AML patients.

#### **7.4. Conclusions and future directions**

Despite the progress made in understanding the biology of AML cells, relatively little has been achieved with regards to the treatment of AML in patients >70 years. With accumulating evidence supporting a key role for the

BMM in the pathogenesis of AML, it is imperative to believe that unless AML cells and critical components of the BM microenvironment are targeted concomitantly, progress in AML treatment may not be realised.

New insights into the cross-talk between AML cells and BMSCs were presented in this thesis, where I have identified MIF as a key AML-derived cytokine that alters the pro-tumoural BMM. Accordingly, MIF presents itself as a potential therapeutic target in AML, and pre-clinical studies of MIF would be instrumental in realising this. Moreover, as chemotherapy is indispensable for the treatment of AML, it is predicted that MIF inhibitors may improve tolerability and treatment outcomes for AML patients treated with chemotherapy.

Currently, chemotherapy treatment aims to eradicate leukaemic cells. However, treatment leaves behind an altered microenvironment that is highly permissive to disease recurrence. Tumour and therapy induced senescence is a novel aspect of the AML BMM. Future investigation should aim to re-establish a BMM that is conducive to normal haematopoiesis rather than leukaemogenesis.

## References

1. Ogawa M, Porter PN, Nakahata T. Renewal and commitment to differentiation of hemopoietic stem cells (an interpretive review). *Blood*. 1983;61(5):823.
2. McCulloch EA, Till JE. The radiation sensitivity of normal mouse bone marrow cells, determined by quantitative marrow transplantation into irradiated mice. *Radiat Res*. 1960;13:115-25.
3. Becker AJ, Mc CE, Till JE. Cytological demonstration of the clonal nature of spleen colonies derived from transplanted mouse marrow cells. *Nature*. 1963;197:452-4.
4. Rice KL, Hormaeche I, Licht JD. Epigenetic regulation of normal and malignant hematopoiesis. *Oncogene*. 2007;26(47):6697-714.
5. Martinez-Climent JA, Fontan L, Gascoyne RD, Siebert R, Prosper F. Lymphoma stem cells: enough evidence to support their existence? *Haematologica*. 2010;95(2):293.
6. Dingli D, Pacheco JM. Modeling the architecture and dynamics of hematopoiesis. *Wiley Interdisciplinary Reviews: Systems Biology and Medicine*. 2010;2(2):235-44.
7. Eaves CJ. Hematopoietic stem cells: concepts, definitions, and the new reality. *Blood*. 2015;125(17):2605.
8. Ceredig R, Rolink AG, Brown G. Models of haematopoiesis: seeing the wood for the trees. *Nat Rev Immunol*. 2009;9(4):293-300.
9. Velten L, Haas SF, Raffel S, Blaszkiewicz S, Islam S, Hennig BP, et al. Human haematopoietic stem cell lineage commitment is a continuous process. *Nat Cell Biol*. 2017;19(4):271-81.
10. McCulloch EA. The 1993 lewis schiffer memorial lecture to the cell kinetics society. *Cell Proliferation*. 1993;26(5):399-425.
11. Orkin SH, Zon LI. Hematopoiesis: An Evolving Paradigm for Stem Cell Biology. *Cell*. 2008;132(4):631-44.
12. Oksanen K, Elonen E. Impact of leucocyte-depleted blood components on the haematological recovery and prognosis of patients with acute myeloid leukaemia. *British Journal of Haematology*. 1993;84(4):639-47.
13. Arber DA, Orazi A, Hasserjian R, Thiele J, Borowitz MJ, Le Beau MM, et al. The 2016 revision to the World Health Organization classification of myeloid neoplasms and acute leukemia. *Blood*. 2016;127(20):2391.
14. Renneville A, Roumier C, Biggio V, Nibourel O, Boissel N, Fenaux P, et al. Cooperating gene mutations in acute myeloid leukemia: a review of the literature. *Leukemia*. 2008;22(5):915-31.
15. Shih AH, Abdel-Wahab O, Patel JP, Levine RL. The role of mutations in epigenetic regulators in myeloid malignancies. *Nat Rev Cancer*. 2012;12(9):599-612.
16. Dombret H. Gene mutation and AML pathogenesis. *Blood*. 2011;118(20):5366.
17. Martens JH, Stunnenberg HG. The molecular signature of oncofusion proteins in acute myeloid leukemia. *FEBS Lett*. 2010;584(12):2662-9.
18. Grimwade D, Ivey A, Huntly BJP. Molecular landscape of acute myeloid leukemia in younger adults and its clinical relevance. *Blood*. 2016;127(1):29.
19. Kumar CC. Genetic abnormalities and challenges in the treatment of acute myeloid leukemia. *Genes & cancer*. 2011;2(2):95-107.
20. Grimwade D, Walker H, Oliver F, Wheatley K, Harrison C, Harrison G, et al. The Importance of Diagnostic Cytogenetics on Outcome in AML: Analysis of 1,612 Patients Entered Into the MRC AML 10 Trial. *Blood*. 1998;92(7):2322-33.
21. McKerrell T, Moreno T, Ponstingl H, Bolli N, Dias JML, Tischler G, et al. Development and validation of a comprehensive genomic diagnostic tool for myeloid malignancies. *Blood*. 2016;128 (1):e1-e9.

22. Döhner H, Estey E, Grimwade D, Amadori S, Appelbaum FR, Büchner T, et al. Diagnosis and management of AML in adults: 2017 ELN recommendations from an international expert panel. *Blood*. 2017;129(4):424-47.
23. Degos L. John Hughes Bennett, Rudolph Virchow... and Alfred Donne: the first description of leukemia. *The hematology journal : the official journal of the European Haematology Association*. 2001;2(1):1.
24. Bennett JM, Catovsky D, Daniel MT, Flandrin G, Galton DA, Gralnick HR, et al. Proposals for the classification of the acute leukaemias. French-American-British (FAB) co-operative group. *British journal of haematology*. 1976;33(4):451-8.
25. Walter RB, Othus M, Burnett AK, Löwenberg B, Kantarjian HM, Ossenkoppele GJ, et al. Significance of FAB subclassification of "acute myeloid leukemia, NOS" in the 2008 WHO classification: analysis of 5848 newly diagnosed patients. *Blood*. 2013;121(13):2424-31.
26. Papaemmanuil E, Gerstung M, Bullinger L, Gaidzik VI, Paschka P, Roberts ND, et al. Genomic Classification and Prognosis in Acute Myeloid Leukemia. *New England Journal of Medicine*. 2016;374(23):2209-21.
27. Juliusson G, Antunovic P, Derolf A, Lehmann S, Mollgard L, Stockelberg D, et al. Age and acute myeloid leukemia: real world data on decision to treat and outcomes from the Swedish Acute Leukemia Registry. *Blood*. 2009;113(18):4179-87.
28. Burnett AK. Treatment of acute myeloid leukemia: are we making progress? *ASH Education Program Book*. 2012;2012(1):1-6.
29. Rowe JM. Optimal induction and post-remission therapy for AML in first remission. *ASH Education Program Book*. 2009;2009(1):396-405.
30. Shah A, Andersson TM, Rached B, Bjorkholm M, Lambert PC. Survival and cure of acute myeloid leukaemia in England, 1971-2006: a population-based study. *British journal of haematology*. 2013;162(4):509-16.
31. Meyers J, Yu Y, Kaye JA, Davis KL. Medicare Fee-for-Service Enrollees with Primary Acute Myeloid Leukemia: An Analysis of Treatment Patterns, Survival, and Healthcare Resource Utilization and Costs. *Applied Health Economics and Health Policy*. 2013;11(3):275-86.
32. Krug U, Büchner T, Berdel WE, Müller-Tidow C. The Treatment of Elderly Patients With Acute Myeloid Leukemia. *Deutsches Ärzteblatt International*. 2011;108(51-52):863-70.
33. Anthony B, Link DC. Regulation of Hematopoietic Stem Cells by Bone Marrow Stromal Cells. *Trends in immunology*. 2014;35(1):32-7.
34. Krause DS, Scadden DT. A hostel for the hostile: the bone marrow niche in hematologic neoplasms. *Haematologica*. 2015;100(11):1376.
35. Krause DS, Scadden DT, Preffer FI. The hematopoietic stem cell niche--home for friend and foe? *Cytometry Part B, Clinical cytometry*. 2013;84(1):7-20.
36. Adams GB, Scadden DT. The hematopoietic stem cell in its place. *Nat Immunol*. 2006;7(4):333-7.
37. Cordeiro-Spinetti E, Taichman RS, Balduino A. The bone marrow endosteal niche: how far from the surface? *Journal of cellular biochemistry*. 2015;116(1):6-11.
38. Morrison SJ, Scadden DT. The bone marrow niche for haematopoietic stem cells. *Nature*. 2014;505(7483):327-34.
39. Shiozawa Y, Havens AM, Pienta KJ, Taichman RS. The bone marrow niche: habitat to hematopoietic and mesenchymal stem cells, and unwitting host to molecular parasites. *Leukemia*. 2008;22(5):941-50.
40. Boulais PE, Frenette PS. Making sense of hematopoietic stem cell niches. *Blood*. 2015;125(17):2621-9.
41. Schofield R. The relationship between the spleen colony-forming cell and the haemopoietic stem cell. *Blood cells*. 1978;4(1-2):7-25.
42. Mendelson A, Frenette PS. Hematopoietic stem cell niche maintenance during homeostasis and regeneration. *Nature medicine*. 2014;20(8):833-46.



43. Schepers K, Campbell Timothy B, Passegué E. Normal and Leukemic Stem Cell Niches: Insights and Therapeutic Opportunities. *Cell Stem Cell*. 16(3):254-67.
44. Pittenger MF, Mackay AM, Beck SC, Jaiswal RK, Douglas R, Mosca JD, et al. Multilineage Potential of Adult Human Mesenchymal Stem Cells. *Science*. 1999;284(5411):143-7.
45. Bianco P, Robey PG, Simmons PJ. Mesenchymal Stem Cells: Revisiting History, Concepts, and Assays. *Cell Stem Cell*. 2008;2(4):313-9.
46. Shafat MS, Gnaneswaran B, Bowles KM, Rushworth SA. The bone marrow microenvironment – Home of the leukemic blasts. *Blood Reviews*. 2017 Sep;31(5):277-286.
47. Bianco P, Robey PG. Skeletal stem cells. *Development*. 2015;142(6):1023.
48. Bianco P. Bone and the hematopoietic niche: a tale of two stem cells. *Blood*. 2011;117(20):5281.
49. Sacchetti B, Funari A, Remoli C, Giannicola G, Kogler G, Liedtke S, et al. No Identical “Mesenchymal Stem Cells” at Different Times and Sites: Human Committed Progenitors of Distinct Origin and Differentiation Potential Are Incorporated as Adventitial Cells in Microvessels. *Stem Cell Reports*. 2016;6(6):897-913.
50. Dominici M, Le Blanc K, Mueller I, Slaper-Cortenbach I, Marini F, Krause D, et al. Minimal criteria for defining multipotent mesenchymal stromal cells. The International Society for Cellular Therapy position statement. *Cytotherapy*. 2006;8(4):315-7.
51. Lymperi S, Ferraro F, Scadden DT. The HSC niche concept has turned 31 Has our knowledge matured? *Annals of the New York Academy of Sciences*. 2010;1192:12-8.
52. Mendez-Ferrer S, Michurina TV, Ferraro F, Mazloom AR, MacArthur BD, Lira SA, et al. Mesenchymal and haematopoietic stem cells form a unique bone marrow niche. *Nature*. 2010;466(7308):829-34.
53. Aiuti A, Webb IJ, Bleul C, Springer T, Gutierrez-Ramos JC. The Chemokine SDF-1 Is a Chemoattractant for Human CD34+ Hematopoietic Progenitor Cells and Provides a New Mechanism to Explain the Mobilization of CD34+ Progenitors to Peripheral Blood. *The Journal of Experimental Medicine*. 1997;185(1):111.
54. Jung Y, Wang J, Schneider A, Sun YX, Koh-Paige AJ, Osman NI, et al. Regulation of SDF-1 (CXCL12) production by osteoblasts; a possible mechanism for stem cell homing. *Bone*. 2006;38(4):497-508.
55. Schajnovitz A, Itkin T, D'Uva G, Kalinkovich A, Golan K, Ludin A, et al. CXCL12 secretion by bone marrow stromal cells is dependent on cell contact and mediated by connexin-43 and connexin-45 gap junctions. *Nat Immunol*. 2011;12(5):391-8.
56. Sugiyama T, Kohara H, Noda M, Nagasawa T. Maintenance of the Hematopoietic Stem Cell Pool by CXCL12-CXCR4 Chemokine Signaling in Bone Marrow Stromal Cell Niches. *Immunity*. 2006;25(6):977-88.
57. Motabi IH, DiPersio JF. Advances in stem cell mobilization. *Blood Reviews*. 2012;26(6):267-78.
58. Broxmeyer HE, Orschell CM, Clapp DW, Hangoc G, Cooper S, Plett PA, et al. Rapid mobilization of murine and human hematopoietic stem and progenitor cells with AMD3100, a CXCR4 antagonist. *The Journal of Experimental Medicine*. 2005;201(8):1307-18.
59. Lapidot T, Dar A, Kollet O. How do stem cells find their way home? *Blood*. 2005;106(6):1901.
60. Shin JY, Hu W, Naramura M, Park CY. High c-Kit expression identifies hematopoietic stem cells with impaired self-renewal and megakaryocytic bias. *The Journal of Experimental Medicine*. 2014;211(2):217.
61. Ding L, Saunders TL, Enikolopov G, Morrison SJ. Endothelial and perivascular cells maintain haematopoietic stem cells. *Nature*. 2012;481(7382):457-62.

62. Heissig B, Hattori K, Dias S, Friedrich M, Ferris B, Hackett NR, et al. Recruitment of Stem and Progenitor Cells from the Bone Marrow Niche Requires MMP-9 Mediated Release of Kit-Ligand. *Cell*. 2002;109(5):625-37.
63. Li T, Wu Y. Paracrine Molecules of Mesenchymal Stem Cells for Hematopoietic Stem Cell Niche. *Bone Marrow Research*. 2011;2011:8.
64. Zhu GR, Zhou XY, Lu H, Zhou JW, Li AP, Xu W, et al. [Human bone marrow mesenchymal stem cells express multiple hematopoietic growth factors]. *Zhongguo shi yan xue ye xue za zhi*. 2003;11(2):115-9.
65. Huntly BJP, Gilliland DG. Leukaemia stem cells and the evolution of cancer-stem-cell research. *Nat Rev Cancer*. 2005;5(4):311-21.
66. Garrido SM, Appelbaum FR, Willman CL, Banker DE. Acute myeloid leukemia cells are protected from spontaneous and drug-induced apoptosis by direct contact with a human bone marrow stromal cell line (HS-5). *Experimental hematology*. 2001;29(4):448-57.
67. Matsunaga T, Takemoto N, Sato T, Takimoto R, Tanaka I, Fujimi A, et al. Interaction between leukemic-cell VLA-4 and stromal fibronectin is a decisive factor for minimal residual disease of acute myelogenous leukemia. *Nat Med*. 2003;9(9):1158-65.
68. Reikvam H, Brenner AK, Hagen KM, Liseth K, Skrede S, Hatfield KJ, et al. The cytokine-mediated crosstalk between primary human acute myeloid cells and mesenchymal stem cells alters the local cytokine network and the global gene expression profile of the mesenchymal cells. *Stem Cell Research*. 2015;15(3):530-41.
69. Yang X, Sexauer A, Levis M. Bone marrow stroma-mediated resistance to FLT3 inhibitors in FLT3-ITD AML is mediated by persistent activation of extracellular regulated kinase. *British Journal of Haematology*. 2014;164(1):61-72.
70. Chen P, Huang H, Wu J, Lu R, Wu Y, Jiang X, et al. Bone marrow stromal cells protect acute myeloid leukemia cells from anti-CD44 therapy partly through regulating PI3K/Akt-p27(Kip1) axis. *Mol Carcinog*. 2015;54(12):1678-85.
71. Sansonetti A, Bourcier S, Durand L, Chomienne C, Smadja-Joffe F, Robert-Lézénès J. CD44 activation enhances acute monoblastic leukemia cell survival via Mcl-1 upregulation. *Leukemia Research*. 2012;36(3):358-62.
72. Becker PS. Dependence of Acute Myeloid Leukemia on Adhesion within the Bone Marrow Microenvironment. *The Scientific World Journal*. 2012;2012:4.
73. Krause DS, Spitzer TR, Stowell CP. The concentration of CD44 is increased in hematopoietic stem cell grafts of patients with acute myeloid leukemia, plasma cell myeloma, and non-Hodgkin lymphoma. *Arch Pathol Lab Med*. 2010;134(7):1033-8.
74. Takam Kanga P, Bassi G, Cassaro A, Midolo M, Di Trapani M, Gatti A, et al. Notch signalling drives bone marrow stromal cell-mediated chemoresistance in acute myeloid leukemia. *Oncotarget*. 2016;7(16):21713-27.
75. Goh SL, Levesque J-P, Pettitt AR, Barbier V, Winkler IG. Therapeutic Blockade of Macrophage Colony Stimulating Factor (CSF-1) Delays AML Progression in Mice In Vivo. *Blood*. 2016;128(22):2835.
76. Jacamo R, Chen Y, Wang Z, Ma W, Zhang M, Spaeth EL, et al. Reciprocal leukemia-stroma VCAM-1/VLA-4-dependent activation of NF- $\kappa$ B mediates chemoresistance. *Blood*. 2014;123(17):2691.
77. Cho BS, Kim HJ, Konopleva M. Targeting the CXCL12/CXCR4 axis in acute myeloid leukemia: from bench to bedside. *The Korean journal of internal medicine*. 2017;32(2):248-57.
78. Zeng Z, Shi YX, Samudio IJ, Wang RY, Ling X, Frolova O, et al. Targeting the leukemia microenvironment by CXCR4 inhibition overcomes resistance to kinase inhibitors and chemotherapy in AML. *Blood*. 2009;113(24):6215-24.

79. Zaitseva L, Murray MY, Shafat MS, Lawes MJ, MacEwan DJ, Bowles KM, et al. Ibrutinib inhibits SDF1/CXCR4 mediated migration in AML. *Oncotarget*. 2014;5(30):9930-7.
80. Kim JA, Shim JS, Lee GY, Yim HW, Kim TM, Kim M, et al. Microenvironmental remodeling as a parameter and prognostic factor of heterogeneous leukemogenesis in acute myelogenous leukemia. *Cancer Res*. 2015;75(11):2222-31.
81. Agarwal P, Li H, Paterson AJ, He J, Nagasawa T, Bhatia R. Role of CXCL12-Expressing Bone Marrow Populations in Leukemic Stem Cell Regulation. *Blood*. 2016;128(22):26.
82. Flores-Figueroa E, Grattinger D. Beyond the Niche: Myelodysplastic Syndrome Topobiology in the Laboratory and in the Clinic. *Int J Mol Sci*. 2016;17(4):553.
83. Arranz L, Sanchez-Aguilera A, Martin-Perez D, Isern J, Langa X, Tzankov A, et al. Neuropathy of haematopoietic stem cell niche is essential for myeloproliferative neoplasms. *Nature*. 2014;512(7512):78-81.
84. Valadi H, Ekstrom K, Bossios A, Sjostrand M, Lee JJ, Lotvall JO. Exosome-mediated transfer of mRNAs and microRNAs is a novel mechanism of genetic exchange between cells. *Nat Cell Biol*. 2007;9(6):654-9.
85. Roccaro AM, Sacco A, Maiso P, Azab AK, Tai Y-T, Reagan M, et al. BM mesenchymal stromal cell-derived exosomes facilitate multiple myeloma progression. *The Journal of Clinical Investigation*. 2013;123(4):1542-55.
86. Muntion S, Ramos TL, Diez-Campelo M, Roson B, Sanchez-Abarca LI, Misiewicz-Krzeminska I, et al. Microvesicles from Mesenchymal Stromal Cells Are Involved in HPC-Microenvironment Crosstalk in Myelodysplastic Patients. *PLoS One*. 2016;11(2):e0146722.
87. Viola S, Traer E, Huan J, Hornick NI, Tyner JW, Agarwal A, et al. Alterations in acute myeloid leukaemia bone marrow stromal cell exosome content coincide with gains in tyrosine kinase inhibitor resistance. *British Journal of Haematology*. 2016;172(6):983-6.
88. Duan CW, Shi J, Chen J, Wang B, Yu YH, Qin X, et al. Leukemia propagating cells rebuild an evolving niche in response to therapy. *Cancer Cell*. 2014;25(6):778-93.
89. Colmone A, Amorim M, Pontier AL, Wang S, Jablonski E, Sipkins DA. Leukemic cells create bone marrow niches that disrupt the behavior of normal hematopoietic progenitor cells. *Science*. 2008;322(5909):1861-5.
90. Meads MB, Gatenby RA, Dalton WS. Environment-mediated drug resistance: a major contributor to minimal residual disease. *Nat Rev Cancer*. 2009;9(9):665-74.
91. Sallmyr A, Fan J, Datta K, Kim KT, Grosu D, Shapiro P, et al. Internal tandem duplication of FLT3 (FLT3/ITD) induces increased ROS production, DNA damage, and misrepair: implications for poor prognosis in AML. *Blood*. 2008;111(6):3173-82.
92. Hole PS, Pearn L, Tonks AJ, James PE, Burnett AK, Darley RL, et al. Ras-induced reactive oxygen species promote growth factor-independent proliferation in human CD34+ hematopoietic progenitor cells. *Blood*. 2010;115(6):1238-46.
93. Cogle CR, Bosse RC, Brewer T, Migdady Y, Shirzad R, Kampen KR, et al. Acute myeloid leukemia in the vascular niche. *Cancer Letters*. 2016;380(2):552-60.
94. Ghannadan M, Wimazal F, Simonitsch I, Sperr WR, Mayerhofer M, Sillaber C, et al. Immunohistochemical detection of VEGF in the bone marrow of patients with acute myeloid leukemia. Correlation between VEGF expression and the FAB category. *American journal of clinical pathology*. 2003;119(5):663-71.
95. Passaro D, Di Tullio A, Abarrategi A, Rouault-Pierre K, Foster K, Ariza-McNaughton L, et al. Increased Vascular Permeability in the Bone Marrow Microenvironment Contributes to Disease Progression and Drug Response in Acute Myeloid Leukemia. *Cancer Cell*. 2017;32(3):324-41.e6.

96. Schepers K, Pietras EM, Reynaud D, Flach J, Binnewies M, Garg T, et al. Myeloproliferative neoplasia remodels the endosteal bone marrow niche into a self-reinforcing leukemic niche. *Cell Stem Cell*. 2013;13(3):285-99.
97. Medyouf H, Mossner M, Jann JC, Nolte F, Raffel S, Herrmann C, et al. Myelodysplastic cells in patients reprogram mesenchymal stromal cells to establish a transplantable stem cell niche disease unit. *Cell Stem Cell*. 2014;14(6):824-37.
98. Groarke EM, Maung SW, Ewins K, Jeffers M, McHugh J, Desmond R, et al. The Role of Marrow Fibrosis in the Prognosis and Treatment of Myelodysplastic Syndromes: a Single Center Retrospective Study. *Blood*. 2016;128(22):5524.
99. Corrado C, Raimondo S, Saieva L, Flugy AM, De Leo G, Alessandro R. Exosome-mediated crosstalk between chronic myelogenous leukemia cells and human bone marrow stromal cells triggers an interleukin 8-dependent survival of leukemia cells. *Cancer letters*. 2014;348(1-2):71-6.
100. Huan J, Hornick NI, Shurtleff MJ, Skinner AM, Goloviznina NA, Roberts CT, Jr., et al. RNA trafficking by acute myelogenous leukemia exosomes. *Cancer Res*. 2013;73(2):918-29.
101. Kumar B, Garcia M, Weng L, Jung X, Murakami JL, Hu X, et al. Acute myeloid leukemia transforms the bone marrow niche into a leukemia-permissive microenvironment through exosome secretion. *Leukemia*. 2017.
102. Jacamo R, Davis RE, Ling X, Sonnylal S, Ma W, Zhang M, et al. Tumor Trp53 status and genotype affect the bone marrow microenvironment in acute myeloid leukemia. *Oncotarget*. 2017;8(48):83354-83369.
103. Raaijmakers MHGP, Mukherjee S, Guo S, Zhang S, Kobayashi T, Schoonmaker JA, et al. Bone progenitor dysfunction induces myelodysplasia and secondary leukaemia. *Nature*. 2010;464(7290):852-7.
104. Kode A, Manavalan JS, Mosialou I, Bhagat G, Rathinam CV, Luo N, et al. Leukaemogenesis induced by an activating beta-catenin mutation in osteoblasts. *Nature*. 2014;506(7487):240-4.
105. Santamaria C, Muntion S, Roson B, Blanco B, Lopez-Villar O, Carrancio S, et al. Impaired expression of DICER, DROSHA, SBDS and some microRNAs in mesenchymal stromal cells from myelodysplastic syndrome patients. *Haematologica*. 2012;97(8):1218-24.
106. Geyh S, Oz S, Cadeddu RP, Frobel J, Bruckner B, Kundgen A, et al. Insufficient stromal support in MDS results from molecular and functional deficits of mesenchymal stromal cells. *Leukemia*. 2013;27(9):1841-51.
107. Zhao Y, Wu D, Fei C, Guo J, Gu S, Zhu Y, et al. Down-regulation of Dicer1 promotes cellular senescence and decreases the differentiation and stem cell-supporting capacities of mesenchymal stromal cells in patients with myelodysplastic syndrome. *Haematologica*. 2015;100(2):194-204.
108. Geyh S, Rodriguez-Paredes M, Jager P, Khandanpour C, Cadeddu RP, Gutekunst J, et al. Functional inhibition of mesenchymal stromal cells in acute myeloid leukemia. *Leukemia*. 2016;30(3):683-91.
109. Kim YW, Koo BK, Jeong HW, Yoon MJ, Song R, Shin J, et al. Defective Notch activation in microenvironment leads to myeloproliferative disease. *Blood*. 2008;112(12):4628-38.
110. Kouvidi E, Stratigi A, Batsali A, Mavroudi I, Mastrodemou S, Ximeri M, et al. Cytogenetic evaluation of mesenchymal stem/stromal cells from patients with myelodysplastic syndromes at different time-points during ex vivo expansion. *Leukemia research*. 2016;43:24-32.
111. Blau O, Hofmann WK, Baldus CD, Thiel G, Serbent V, Schumann E, et al. Chromosomal aberrations in bone marrow mesenchymal stroma cells from patients with myelodysplastic syndrome and acute myeloblastic leukemia. *Exp Hematol*. 2007;35(2):221-9.

112. Schroeder T, Geyh S, Germing U, Haas R. Mesenchymal stromal cells in myeloid malignancies. *Blood research*. 2016;51(4):225-32.
113. Narendran A, Hawkins LM, Ganjavi H, Vanek W, Gee MF, Barlow JW, et al. Characterization of bone marrow stromal abnormalities in a patient with constitutional trisomy 8 mosaicism and myelodysplastic syndrome. *Pediatric hematology and oncology*. 2004;21(3):209-21.
114. von der Heide EK, Neumann M, Vosberg S, James AR, Schroeder MP, Ortiz-Tanchez J, et al. Molecular alterations in bone marrow mesenchymal stromal cells derived from acute myeloid leukemia patients. *Leukemia*. 2017;31(5):1069-78.
115. Kim Y, Jekarl DW, Kim J, Kwon A, Choi H, Lee S, et al. Genetic and epigenetic alterations of bone marrow stromal cells in myelodysplastic syndrome and acute myeloid leukemia patients. *Stem cell research*. 2015;14(2):177-84.
116. Soenen-Cornu V, Tourino C, Bonnet ML, Guillier M, Flamant S, Kotb R, et al. Mesenchymal cells generated from patients with myelodysplastic syndromes are devoid of chromosomal clonal markers and support short- and long-term hematopoiesis in vitro. *Oncogene*. 2005;24(15):2441-8.
117. Sorokina T, Shipounova I, Bigildeev A, Petinati N, Drize N, Turkina A, et al. The ability of multipotent mesenchymal stromal cells from the bone marrow of patients with leukemia to maintain normal hematopoietic progenitor cells. *European journal of haematology*. 2016;97(3):245-52.
118. Reikvam H, Fredly H, Kittang AO, Bruserud O. The possible diagnostic and prognostic use of systemic chemokine profiles in clinical medicine-the experience in acute myeloid leukemia from disease development and diagnosis via conventional chemotherapy to allogeneic stem cell transplantation. *Toxins*. 2013;5(2):336-62.
119. Kupsa T, Horacek JM, Jebavy L. The role of cytokines in acute myeloid leukemia: a systematic review. *Biomed Pap Med Fac Univ Palacky Olomouc Czech Repub*. 2012;156(4):291-301.
120. Van Etten RA. Aberrant cytokine signaling in leukemia. *Oncogene*. 0000;26(47):6738-49.
121. Kornblau SM, McCue D, Singh N, Chen W, Estrov Z, Coombes KR. Recurrent expression signatures of cytokines and chemokines are present and are independently prognostic in acute myelogenous leukemia and myelodysplasia. *Blood*. 2010;116(20):4251-61.
122. Gwang Kim J, Kyun Sohn S, Hwan Kim D, Ho Baek J, Young Lee N, Soo Suh J, et al. Clinical implications of angiogenic factors in patients with acute or chronic leukemia: Hepatocyte growth factor levels have prognostic impact, especially in patients with acute myeloid leukemia. *Leukemia & Lymphoma*. 2005;46(6):885-91.
123. Tsimberidou AM, Estey E, Wen S, Pierce S, Kantarjian H, Albitar M, et al. The prognostic significance of cytokine levels in newly diagnosed acute myeloid leukemia and high-risk myelodysplastic syndromes. *Cancer*. 2008;113(7):1605-13.
124. Aguayo A, Kantarjian HM, Estey EH, Giles FJ, Verstovsek S, Manshoury T, et al. Plasma vascular endothelial growth factor levels have prognostic significance in patients with acute myeloid leukemia but not in patients with myelodysplastic syndromes. *Cancer*. 2002;95(9):1923-30.
125. Lopes MR, Pereira JKN, de Melo Campos P, Machado-Neto JA, Traina F, Saad STO, et al. De novo AML exhibits greater microenvironment dysregulation compared to AML with myelodysplasia-related changes. *Scientific Reports*. 2017;7:40707.
126. Kittang AO, Hatfield K, Sand K, Reikvam H, Bruserud Ø. The Chemokine Network in Acute Myelogenous Leukemia: Molecular Mechanisms Involved in Leukemogenesis and Therapeutic Implications. In: Bruserud O, editor. *The Chemokine System in Experimental and Clinical Hematology*. Berlin, Heidelberg: Springer Berlin Heidelberg; 2010. p. 149-72.

127. Bruserud Ø, Rynningen A, Olsnes AM, Stordrange L, Øyan AM, Kalland KH, et al. Subclassification of patients with acute myelogenous leukemia based on chemokine responsiveness and constitutive chemokine release by their leukemic cells. *Haematologica*. 2007;92(3):332.
128. Hammond ME, Lapointe GR, Feucht PH, Hilt S, Gallegos CA, Gordon CA, et al. IL-8 induces neutrophil chemotaxis predominantly via type I IL-8 receptors. *The Journal of Immunology*. 1995;155(3):1428-33.
129. Lippert U, Artuc M, Grützkau A, Möller A, Kenderessy-Szabo A, Schadendorf D, et al. Expression and Functional Activity of the IL-8 Receptor Type CXCR1 and CXCR2 on Human Mast Cells. *The Journal of Immunology*. 1998;161(5):2600-8.
130. Waugh DJJ, Wilson C. The Interleukin-8 Pathway in Cancer. *Clinical Cancer Research*. 2008;14(21):6735-41.
131. Rynningen A, Wergeland L, Glenjen N, Gjertsen BT, Bruserud O. In vitro crosstalk between fibroblasts and native human acute myelogenous leukemia (AML) blasts via local cytokine networks results in increased proliferation and decreased apoptosis of AML cells as well as increased levels of proangiogenic Interleukin 8. *Leukemia research*. 2005;29(2):185-96.
132. Sharma B, Nawandar DM, Nannuru KC, Varney ML, Singh RK. Targeting CXCR2 enhances chemotherapeutic response, inhibits mammary tumor growth, angiogenesis, and lung metastasis. *Mol Cancer Ther*. 2013;12(5):799-808.
133. Lee YS, Choi I, Ning Y, Kim NY, Khatchadourian V, Yang D, et al. Interleukin-8 and its receptor CXCR2 in the tumour microenvironment promote colon cancer growth, progression and metastasis. *Br J Cancer*. 2012;106(11):1833-41.
134. Singh JK, Simoes BM, Howell SJ, Farnie G, Clarke RB. Recent advances reveal IL-8 signaling as a potential key to targeting breast cancer stem cells. *Breast Cancer Res*. 2013;15(4):210.
135. Vinante F, Rigo A, Vincenzi C, Ricetti MM, Marrocchella R, Chilosi M, et al. IL-8 mRNA expression and IL-8 production by acute myeloid leukemia cells. *Leukemia*. 1993;7(10):1552-6.
136. Tobler A, Moser B, Dewald B, Geiser T, Studer H, Baggiolini M, et al. Constitutive expression of interleukin-8 and its receptor in human myeloid and lymphoid leukemia. *Blood*. 1993;82(8):2517-25.
137. Denizot Y, Fixe P, Liozon E, Praloran V. Serum interleukin-8 (IL-8) and IL-6 concentrations in patients with hematologic malignancies. *Blood*. 1996;87(9):4016-7.
138. Broxmeyer HE, Cooper S, Cacalano G, Hague NL, Bailish E, Moore MW. Involvement of Interleukin (IL) 8 receptor in negative regulation of myeloid progenitor cells in vivo: evidence from mice lacking the murine IL-8 receptor homologue. *J Exp Med*. 1996;184(5):1825-32.
139. Broxmeyer HE, Sherry B, Cooper S, Lu L, Maze R, Beckmann MP, et al. Comparative analysis of the human macrophage inflammatory protein family of cytokines (chemokines) on proliferation of human myeloid progenitor cells. Interacting effects involving suppression, synergistic suppression, and blocking of suppression. *Journal of immunology (Baltimore, Md : 1950)*. 1993;150(8 Pt 1):3448-58.
140. Schinke C, Gircz O, Li W, Shastri A, Gordon S, Barreryo L, et al. IL8-CXCR2 pathway inhibition as a therapeutic strategy against MDS and AML stem cells. *Blood*. 2015;125(20):3144-52.
141. Kishimoto T. Interleukin-6: from basic science to medicine--40 years in immunology. *Annu Rev Immunol*. 2005;23:1-21.
142. Reynaud D, Pietras E, Barry-Holson K, Mir A, Binnewies M, Jeanne M, et al. IL-6 Controls Leukemic Multipotent Progenitor Cell Fate and Contributes to Chronic Myelogenous Leukemia Development. *Cancer Cell*. 2011;20(5):661-73.
143. Ferrario A, Merli M, Basilico C, Maffioli M, Passamonti F. Siltuximab and hematologic malignancies. A focus in non Hodgkin lymphoma. *Expert Opin Investig Drugs*. 2017;26(3):367-73.

144. Sugiyama H, Inoue K, Ogawa H, Yamagami T, Soma T, Miyake S, et al. The expression of IL-6 and its related genes in acute leukemia. *Leuk Lymphoma*. 1996;21(1-2):49-52.
145. Saily M, Koistinen P, Savolainen ER. The soluble form of interleukin-6 receptor modulates cell proliferation by acute myeloblastic leukemia blast cells. *Annals of hematology*. 1999;78(4):173-9.
146. Calandra T, Roger T. Macrophage migration inhibitory factor: a regulator of innate immunity. *Nat Rev Immunol*. 2003;3(10):791-800.
147. Bloom BR, Bennett B. Mechanism of a Reaction in Vitro Associated with Delayed-Type Hypersensitivity. *Science*. 1966;153(3731):80-2.
148. Bernhagen J, Calandra T, Mitchell RA, Martin SB, Tracey KJ, Voelker W, et al. MIF is a pituitary-derived cytokine that potentiates lethal endotoxaemia. *Nature*. 1993;365(6448):756-9.
149. Calandra T, Bernhagen J, Mitchell RA, Bucala R. The macrophage is an important and previously unrecognized source of macrophage migration inhibitory factor. *The Journal of Experimental Medicine*. 1994;179(6):1895-902.
150. Costa-Silva B, Aiello NM, Ocean AJ, Singh S, Zhang H, Thakur BK, et al. Pancreatic cancer exosomes initiate pre-metastatic niche formation in the liver. *Nat Cell Biol*. 2015;17(6):816-26.
151. Flieger O, Engling A, Bucala R, Lue H, Nickel W, Bernhagen J. Regulated secretion of macrophage migration inhibitory factor is mediated by a non-classical pathway involving an ABC transporter. *FEBS Letters*. 2003;551(1-3):78-86.
152. Flaster H, Bernhagen J, Calandra T, Bucala R. The macrophage migration inhibitory factor-glucocorticoid dyad: regulation of inflammation and immunity. *Mol Endocrinol*. 2007;21(6):1267-80.
153. Calandra T, Bernhagen J, Metz CN, Spiegel LA, Bacher M, Donnelly T, et al. MIF as a glucocorticoid-induced modulator of cytokine production. *Nature*. 1995;377(6544):68-71.
154. Brock SE, Rendon BE, Xin D, Yaddanapudi K, Mitchell RA. MIF Family Members Cooperatively Inhibit p53 Expression and Activity. *PLoS ONE*. 2014;9(6):e99795.
155. Lourenco S, Teixeira VH, Kalber T, Jose RJ, Floto RA, Janes SM. Macrophage Migration Inhibitory Factor–CXCR4 Is the Dominant Chemotactic Axis in Human Mesenchymal Stem Cell Recruitment to Tumors. *The Journal of Immunology*. 2015;194(7):3463.
156. Chatterjee M, Borst O, Walker B, Fotinos A, Vogel S, Seizer P, et al. Macrophage Migration Inhibitory Factor Limits Activation-Induced Apoptosis of Platelets via CXCR7-Dependent Akt Signaling. *Circulation Research*. 2014;115(11):939-49.
157. Shi X, Leng L, Wang T, Wang W, Du X, Li J, et al. CD44 Is the Signaling Component of the Macrophage Migration Inhibitory Factor-CD74 Receptor Complex. *Immunity*. 2007;25(4):595-606.
158. Leng L, Metz CN, Fang Y, Xu J, Donnelly S, Baugh J, et al. MIF signal transduction initiated by binding to CD74. *J Exp Med*. 2003;197(11):1467-76.
159. Bernhagen J, Krohn R, Lue H, Gregory JL, Zerneck A, Koenen RR, et al. MIF is a noncognate ligand of CXC chemokine receptors in inflammatory and atherogenic cell recruitment. *Nature medicine*. 2007;13(5):587-96.
160. Schwartz V, Lue H, Kraemer S, Korbil J, Krohn R, Ohl K, et al. A functional heteromeric MIF receptor formed by CD74 and CXCR4. *FEBS Letters*. 2009;583(17):2749-57.
161. Alampour-Rajabi S, El Bounkari O, Rot A, Müller-Newen G, Bachelier F, Gawaz M, et al. MIF interacts with CXCR7 to promote receptor internalization, ERK1/2 and ZAP-70 signaling, and lymphocyte chemotaxis. *The FASEB Journal*. 2015;29(11):4497-511.

162. He XX, Chen K, Yang J, Li XY, Gan HY, Liu CY, et al. Macrophage migration inhibitory factor promotes colorectal cancer. *Mol Med*. 2009;15(1-2):1-10.
163. Chen YC, Zhang XW, Niu XH, Xin DQ, Zhao WP, Na YQ, et al. Macrophage migration inhibitory factor is a direct target of HBP1-mediated transcriptional repression that is overexpressed in prostate cancer. *Oncogene*. 2010;29(21):3067-78.
164. Xu X, Wang B, Ye C, Yao C, Lin Y, Huang X, et al. Overexpression of macrophage migration inhibitory factor induces angiogenesis in human breast cancer. *Cancer Letters*. 2008;261(2):147-57.
165. Winner M, Meier J, Zierow S, Rendon BE, Crichlow GV, Riggs R, et al. A Novel, Macrophage Migration Inhibitory Factor Suicide Substrate Inhibits Motility and Growth of Lung Cancer Cells. *Cancer Research*. 2008;68(18):7253.
166. Reinart N, Nguyen PH, Boucas J, Rosen N, Kvasnicka HM, Heukamp L, et al. Delayed development of chronic lymphocytic leukemia in the absence of macrophage migration inhibitory factor. *Blood*. 2013;121(5):812-21.
167. Zheng Y, Wang Q, Li T, Qian J, Lu Y, Li Y, et al. Role of Myeloma-Derived MIF in Myeloma Cell Adhesion to Bone Marrow and Chemotherapy Response. *J Natl Cancer Inst*. 2016;108(11).
168. Kim MJ, Kim WS, Kim DO, Byun J-E, Huy H, Lee SY, et al. Macrophage migration inhibitory factor interacts with thioredoxin-interacting protein and induces NF- $\kappa$ B activity. *Cellular Signalling*. 2017;34:110-20.
169. Talos F, Mena P, Fingerle-Rowson G, Moll U, Petrenko O. MIF loss impairs Myc-induced lymphomagenesis. *Cell Death Differ*. 2005;12(10):1319-28.
170. Binsky I, Haran M, Starlets D, Gore Y, Lantner F, Harpaz N, et al. IL-8 secreted in a macrophage migration-inhibitory factor- and CD74-dependent manner regulates B cell chronic lymphocytic leukemia survival. *Proceedings of the National Academy of Sciences*. 2007;104(33):13408-13.
171. Konopleva MY, Jordan CT. Leukemia Stem Cells and Microenvironment: Biology and Therapeutic Targeting. *Journal of Clinical Oncology*. 2011;29(5):591-9.
172. Kornblau SM, Womble M, Qiu YH, Jackson CE, Chen W, Konopleva M, et al. Simultaneous activation of multiple signal transduction pathways confers poor prognosis in acute myelogenous leukemia. *Blood*. 2006;108(7):2358-65.
173. Morgensztern D, McLeod HL. PI3K/Akt/mTOR pathway as a target for cancer therapy. *Anticancer Drugs*. 2005;16(8):797-803.
174. Altomare DA, Testa JR. Perturbations of the AKT signaling pathway in human cancer. *Oncogene*. 2005;24(50):7455-64.
175. Pillinger G, Loughran NV, Pidcock RE, Shafat MS, Zaitseva L, Abdul-Aziz A, et al. Targeting PI3K $\delta$  and PI3K $\gamma$  signalling disrupts human AML survival and bone marrow stromal cell mediated protection. *Oncotarget*. 2016;7(26):39784-95.
176. Brenner AK, Andersson Tvedt TH, Bruserud O. The Complexity of Targeting PI3K-Akt-mTOR Signalling in Human Acute Myeloid Leukaemia: The Importance of Leukemic Cell Heterogeneity, Neighbouring Mesenchymal Stem Cells and Immunocompetent Cells. *Molecules*. 2016;21(11).
177. Xiang X, Zhao J, Xu G, Li Y, Zhang W. mTOR and the differentiation of mesenchymal stem cells. *Acta Biochim Biophys Sin (Shanghai)*. 2011;43(7):501-10.
178. Lee HJ, Ryu JM, Jung YH, Oh SY, Lee SJ, Han HJ. Novel Pathway for Hypoxia-Induced Proliferation and Migration in Human Mesenchymal Stem Cells: Involvement of HIF-1 $\alpha$ , FASN, and mTORC1. *Stem Cells*. 2015;33(7):2182-95.
179. Zhang Z, Yang M, Wang Y, Wang L, Jin Z, Ding L, et al. Autophagy regulates the apoptosis of bone marrow-derived mesenchymal stem cells under hypoxic condition via AMP-activated protein kinase/mammalian target of rapamycin pathway. *Cell Biol Int*. 2016;40(6):671-85.
180. Reikvam H, Nepstad I, Bruserud Ø, Hatfield KJ. Pharmacological targeting of the PI3K/mTOR pathway alters the release of angioregulatory mediators both from



- primary human acute myeloid leukemia cells and their neighboring stromal cells. *Oncotarget*. 2013;4(6):830-43.
181. Geest CR, Coffey PJ. MAPK signaling pathways in the regulation of hematopoiesis. *J Leukoc Biol*. 2009;86(2):237-50.
182. Towatari M, Iida H, Tanimoto M, Iwata H, Hamaguchi M, Saito H. Constitutive activation of mitogen-activated protein kinase pathway in acute leukemia cells. *Leukemia*. 1997;11(4):479-84.
183. Kim SC, Hahn JS, Min YH, Yoo NC, Ko YW, Lee WJ. Constitutive activation of extracellular signal-regulated kinase in human acute leukemias: combined role of activation of MEK, hyperexpression of extracellular signal-regulated kinase, and downregulation of a phosphatase, PAC1. *Blood*. 1999;93(11):3893-9.
184. Milella M, Kornblau SM, Estrov Z, Carter BZ, Lapillonne H, Harris D, et al. Therapeutic targeting of the MEK/MAPK signal transduction module in acute myeloid leukemia. *J Clin Invest*. 2001;108(6):851-9.
185. Siendones E, Barbarroja N, Torres LA, Buendia P, Velasco F, Dorado G, et al. Inhibition of Flt3-activating mutations does not prevent constitutive activation of ERK/Akt/STAT pathways in some AML cells: a possible cause for the limited effectiveness of monotherapy with small-molecule inhibitors. *Hematol Oncol*. 2007;25(1):30-7.
186. Yang XP, Li Y, Wang Y, Wang Y, Wang P. beta-Tryptase up-regulates vascular endothelial growth factor expression via proteinase-activated receptor-2 and mitogen-activated protein kinase pathways in bone marrow stromal cells in acute myeloid leukemia. *Leuk Lymphoma*. 2010;51(8):1550-8.
187. da Costa SV, Roela RA, Junqueira MS, Arantes C, Brentani MM. The role of p38 mitogen-activated protein kinase in serum-induced leukemia inhibitory factor secretion by bone marrow stromal cells from pediatric myelodysplastic syndromes. *Leukemia research*. 2010;34(4):507-12.
188. Steinberg SF. Structural Basis of Protein Kinase C Isoform Function. *Physiological Reviews*. 2008;88(4):1341-78.
189. Toker A. Protein Kinases as Mediators of Phosphoinositide 3-Kinase Signaling. *Molecular Pharmacology*. 2000;57(4):652-8.
190. Newton AC. Protein Kinase C: Structural and Spatial Regulation by Phosphorylation, Cofactors, and Macromolecular Interactions. *Chemical Reviews*. 2001;101(8):2353-64.
191. Rosse C, Linch M, Kermorgant S, Cameron AJM, Boeckeler K, Parker PJ. PKC and the control of localized signal dynamics. *Nat Rev Mol Cell Biol*. 2010;11(2):103-12.
192. Tan S-L, Parker PJ. Emerging and diverse roles of protein kinase C in immune cell signalling. *Biochemical Journal*. 2003;376(3):545-52.
193. Griner EM, Kazanietz MG. Protein kinase C and other diacylglycerol effectors in cancer. *Nat Rev Cancer*. 2007;7(4):281-94.
194. Hubmann R, Döchler M, Schnabl S, Hilgarth M, Demirtas D, Mitteregger D, et al. NOTCH2 links protein kinase C delta to the expression of CD23 in chronic lymphocytic leukaemia (CLL) cells. *British Journal of Haematology*. 2010;148(6):868-78.
195. Redig AJ, Plataniias LC. Protein kinase C signalling in leukemia. *Leuk Lymphoma*. 2008;49(7):1255-62.
196. Zheng Y, Wang L-S, Xia L, Han Y-H, Liao S-H, Wang X-L, et al. NDRG1 is down-regulated in the early apoptotic event induced by camptothecin analogs: The potential role in proteolytic activation of PKC $\delta$  and apoptosis. *PROTEOMICS*. 2009;9(8):2064-75.
197. Dupasquier S, Abdel-Samad R, Glazer RI, Bastide P, Jay P, Joubert D, et al. A new mechanism of SOX9 action to regulate PKC $\alpha$  expression in the intestine epithelium. *Journal of Cell Science*. 2009;122(13):2191-6.

198. Deng X, Kornblau SM, Ruvolo PP, May WS, Jr. Regulation of Bcl2 phosphorylation and potential significance for leukemic cell chemoresistance. *J Natl Cancer Inst Monogr.* 2001(28):30-7.
199. Hampson P, Chahal H, Khanim F, Hayden R, Mulder A, Assi LK, et al. PEP005, a selective small-molecule activator of protein kinase C, has potent antileukemic activity mediated via the delta isoform of PKC. *Blood.* 2005;106(4):1362-8.
200. Ersvaer E, Hampson P, Hatfield K, Ulvestad E, Wendelbo O, Lord JM, et al. T cells remaining after intensive chemotherapy for acute myelogenous leukemia show a broad cytokine release profile including high levels of interferon-gamma that can be further increased by a novel protein kinase C agonist PEP005. *Cancer Immunol Immunother.* 2007;56(6):913-25.
201. Lutzny G, Kocher T, Schmidt-Supprian M, Rudelius M, Klein-Hitpass L, Finch AJ, et al. Protein kinase c-beta-dependent activation of NF-kappaB in stromal cells is indispensable for the survival of chronic lymphocytic leukemia B cells in vivo. *Cancer Cell.* 2013;23(1):77-92.
202. Krock BL, Skuli N, Simon MC. Hypoxia-induced angiogenesis: good and evil. *Genes & cancer.* 2011;2(12):1117-33.
203. Muz B, de la Puente P, Azab F, Luderer M, Azab AK. The Role of Hypoxia and Exploitation of the Hypoxic Environment in Hematologic Malignancies. *Molecular Cancer Research.* 2014;12(10):1347-54.
204. Thomlinson RH, Gray LH. The Histological Structure of Some Human Lung Cancers and the Possible Implications for Radiotherapy. *British Journal of Cancer.* 1955;9(4):539-49.
205. Walsh JC, Lebedev A, Aten E, Madsen K, Marciano L, Kolb HC. The Clinical Importance of Assessing Tumor Hypoxia: Relationship of Tumor Hypoxia to Prognosis and Therapeutic Opportunities. *Antioxidants & Redox Signaling.* 2014;21(10):1516-54.
206. Semenza GL. Hypoxia-inducible factors: mediators of cancer progression and targets for cancer therapy. *Trends Pharmacol Sci.* 2012;33(4):207-14.
207. Irigoyen M, García-Ruiz JC, Berra E. The hypoxia signalling pathway in haematological malignancies. *Oncotarget.* 2017;8(22):36832-44.
208. Parmar K, Mauch P, Vergilio J-A, Sackstein R, Down JD. Distribution of hematopoietic stem cells in the bone marrow according to regional hypoxia. *Proceedings of the National Academy of Sciences of the United States of America.* 2007;104(13):5431-6.
209. Takubo K, Goda N, Yamada W, Iriuchishima H, Ikeda E, Kubota Y, et al. Regulation of the HIF-1 $\alpha$  Level Is Essential for Hematopoietic Stem Cells. *Cell Stem Cell.* 2010;7(3):391-402.
210. Koh MY, Powis G. Passing the baton: the HIF switch. *Trends Biochem Sci.* 2012;37(9):364-72.
211. Majmundar AJ, Wong WJ, Simon MC. Hypoxia-Inducible Factors and the Response to Hypoxic Stress. *Molecular Cell.* 2010;40(2):294-309.
212. Dengler VL, Galbraith MD, Espinosa JM. Transcriptional regulation by hypoxia inducible factors. *Critical reviews in biochemistry and molecular biology.* 2014;49(1):1-15.
213. Walmsley SR, Chilvers ER, Whyte MKB. Hypoxia. Hypoxia, hypoxia inducible factor and myeloid cell function. *Arthritis Research & Therapy.* 2009;11(2):219.
214. Bracken CP, Fedele AO, Linke S, Balrak W, Lisy K, Whitelaw ML, et al. Cell-specific regulation of hypoxia-inducible factor (HIF)-1 $\alpha$  and HIF-2 $\alpha$  stabilization and transactivation in a graded oxygen environment. *J Biol Chem.* 2006;281(32):22575-85.
215. Rechsteiner MP, von Teichman A, Nowicka A, Sulser T, Schraml P, Moch H. VHL gene mutations and their effects on hypoxia inducible factor HIF $\alpha$ :

- identification of potential driver and passenger mutations. *Cancer Res.* 2011;71(16):5500-11.
216. Rouault-Pierre K, Hamilton A, Bonnet D. Effect of hypoxia-inducible factors in normal and leukemic stem cell regulation and their potential therapeutic impact. *Expert Opin Biol Ther.* 2016;16(4):463-76.
217. Haeberle HA, Durrstein C, Rosenberger P, Hosakote YM, Kuhlicke J, Kempf VA, et al. Oxygen-independent stabilization of hypoxia inducible factor (HIF)-1 during RSV infection. *PLoS One.* 2008;3(10):e3352.
218. Zhang J, Sattler M, Tonon G, Grabher C, Lababidi S, Zimmerhackl A, et al. Targeting angiogenesis via a c-Myc/hypoxia-inducible factor-1alpha-dependent pathway in multiple myeloma. *Cancer Res.* 2009;69(12):5082-90.
219. Masoud GN, Li W. HIF-1 $\alpha$  pathway: role, regulation and intervention for cancer therapy. *Acta Pharmaceutica Sinica B.* 2015;5(5):378-89.
220. Mack FA, Rathmell WK, Arsham AM, Gnarra J, Keith B, Simon MC. Loss of pVHL is sufficient to cause HIF dysregulation in primary cells but does not promote tumor growth. *Cancer cell.* 2003;3(1):75-88.
221. Spencer JA, Ferraro F, Roussakis E, Klein A, Wu J, Runnels JM, et al. Direct measurement of local oxygen concentration in the bone marrow of live animals. *Nature.* 2014;508(7495):269-73.
222. Jensen PO, Mortensen BT, Hodgkiss RJ, Iversen PO, Christensen IJ, Helledie N, et al. Increased cellular hypoxia and reduced proliferation of both normal and leukaemic cells during progression of acute myeloid leukaemia in rats. *Cell Prolif.* 2000;33(6):381-95.
223. Konopleva M, Thall PF, Yi CA, Borthakur G, Coveler A, Bueso-Ramos C, et al. Phase I/II study of the hypoxia-activated prodrug PR104 in refractory/relapsed acute myeloid leukemia and acute lymphoblastic leukemia. *Haematologica.* 2015;100(7):927-34.
224. Grant WC, Root WS. The relation of oxygen tension in bone marrow blood to the erythropoiesis following hemorrhage. *Federation proceedings.* 1947;6(1 Pt 2):114.
225. Cipolleschi MG, Dello Sbarba P, Olivetto M. The role of hypoxia in the maintenance of hematopoietic stem cells. *Blood.* 1993;82(7):2031-7.
226. Chow DC, Wenning LA, Miller WM, Papoutsakis ET. Modeling pO<sub>2</sub> distributions in the bone marrow hematopoietic compartment. II. Modified Kroghian models. *Biophysical journal.* 2001;81(2):685-96.
227. Eliasson P, Jonsson JI. The hematopoietic stem cell niche: low in oxygen but a nice place to be. *J Cell Physiol.* 2010;222(1):17-22.
228. Miharada K, Karlsson G, Rehn M, Rorby E, Siva K, Cammenga J, et al. Hematopoietic stem cells are regulated by Cripto, as an intermediary of HIF-1alpha in the hypoxic bone marrow niche. *Ann N Y Acad Sci.* 2012;1266:55-62.
229. Piya S, Andreeff M, Borthakur G. Targeting autophagy to overcome chemoresistance in acute myelogenous leukemia. *Autophagy.* 2017;13(1):214-5.
230. Simsek T, Kocabas F, Zheng J, Deberardinis RJ, Mahmoud AI, Olson EN, et al. The distinct metabolic profile of hematopoietic stem cells reflects their location in a hypoxic niche. *Cell Stem Cell.* 2010;7(3):380-90.
231. Holyoake TL, Helgason GV. Do we need more drugs for chronic myeloid leukemia? *Immunological Reviews.* 2015;263(1):106-23.
232. Nombela-Arrieta C, Pivarnik G, Winkel B, Canty KJ, Harley B, Mahoney JE, et al. Quantitative imaging of haematopoietic stem and progenitor cell localization and hypoxic status in the bone marrow microenvironment. *Nat Cell Biol.* 2013;15(5):533-43.
233. Schioppa T, Uranchimeg B, Sacconi A, Biswas SK, Doni A, Rapisarda A, et al. Regulation of the chemokine receptor CXCR4 by hypoxia. *J Exp Med.* 2003;198(9):1391-402.

234. Ceradini DJ, Kulkarni AR, Callaghan MJ, Tepper OM, Bastidas N, Kleinman ME, et al. Progenitor cell trafficking is regulated by hypoxic gradients through HIF-1 induction of SDF-1. *Nature medicine*. 2004;10(8):858-64.
235. Schioppa T, Uranchimeg B, Sacconi A, Biswas SK, Doni A, Rapisarda A, et al. Regulation of the Chemokine Receptor CXCR4 by Hypoxia. *The Journal of Experimental Medicine*. 2003;198(9):1391.
236. Forristal CE, Nowlan B, Jacobsen RN, Barbier V, Walkinshaw G, Walkley CR, et al. HIF-1alpha is required for hematopoietic stem cell mobilization and 4-prolyl hydroxylase inhibitors enhance mobilization by stabilizing HIF-1alpha. *Leukemia*. 2015;29(6):1366-78.
237. Frolova O, Samudio I, Benito JM, Jacamo R, Kornblau SM, Markovic A, et al. Regulation of HIF-1alpha signaling and chemoresistance in acute lymphocytic leukemia under hypoxic conditions of the bone marrow microenvironment. *Cancer biology & therapy*. 2012;13(10):858-70.
238. Azab AK, Weisberg E, Sahin I, Liu F, Awwad R, Azab F, et al. The influence of hypoxia on CML trafficking through modulation of CXCR4 and E-cadherin expression. *Leukemia*. 2013;27(4):961-4.
239. Valsecchi R, Coltella N, Belloni D, Ponente M, Ten Hacken E, Scielzo C, et al. HIF-1alpha regulates the interaction of chronic lymphocytic leukemia cells with the tumor microenvironment. *Blood*. 2016;127(16):1987-97.
240. Fiegl M, Samudio I, Clise-Dwyer K, Burks JK, Mnjoyan Z, Andreeff M. CXCR4 expression and biologic activity in acute myeloid leukemia are dependent on oxygen partial pressure. *Blood*. 2009;113(7):1504-12.
241. Griessinger E, Anjos-Afonso F, Pizzitola I, Rouault-Pierre K, Vargaftig J, Taussig D, et al. A niche-like culture system allowing the maintenance of primary human acute myeloid leukemia-initiating cells: a new tool to decipher their chemoresistance and self-renewal mechanisms. *Stem Cells Transl Med*. 2014;3(4):520-9.
242. Wang Y, Liu Y, Tang F, Bernot KM, Schore R, Marcucci G, et al. Echinomycin protects mice against relapsed acute myeloid leukemia without adverse effect on hematopoietic stem cells. *Blood*. 2014;124(7):1127.
243. Vukovic M, Sepulveda C, Subramani C, Guitart AV, Mohr J, Allen L, et al. Adult hematopoietic stem cells lacking Hif-1alpha self-renew normally. *Blood*. 2016;127(23):2841-6.
244. Deeb G, Vaughan MM, McInnis I, Ford LA, Sait SN, Starostik P, et al. Hypoxia-inducible factor-1alpha protein expression is associated with poor survival in normal karyotype adult acute myeloid leukemia. *Leukemia research*. 2011;35(5):579-84.
245. Portwood S, Lal D, Hsu YC, Vargas R, Johnson MK, Wetzler M, et al. Activity of the hypoxia-activated prodrug, TH-302, in preclinical human acute myeloid leukemia models. *Clinical cancer research : an official journal of the American Association for Cancer Research*. 2013;19(23):6506-19.
246. Benito J, Ramirez MS, Millward NZ, Velez J, Harutyunyan KG, Lu H, et al. Hypoxia-Activated Prodrug TH-302 Targets Hypoxic Bone Marrow Niches in Preclinical Leukemia Models. *Clinical cancer research : an official journal of the American Association for Cancer Research*. 2016;22(7):1687-98.
247. Baran N, Konopleva M. Molecular Pathways: Hypoxia-activated prodrugs in cancer therapy. *Clinical Cancer Research*. 2017.
248. Velasco-Hernandez T, Hyrenius-Wittsten A, Rehn M, Bryder D, Cammenga J. HIF-1alpha can act as a tumor suppressor gene in murine acute myeloid leukemia. *Blood*. 2014;124(24):3597-607.
249. Schito L, Rey S, Konopleva M. Integration of hypoxic HIF-alpha signaling in blood cancers. *Oncogene*. 2017;36(38):5331-40.

250. Wang Y, Liu Y, Malek Sami N, Zheng P, Liu Y. Targeting HIF1 $\alpha$  Eliminates Cancer Stem Cells in Hematological Malignancies. *Cell Stem Cell*. 2011;8(4):399-411.
251. Rouault-Pierre K, Lopez-Onieva L, Foster K, Anjos-Afonso F, Lamrissi-Garcia I, Serrano-Sanchez M, et al. HIF-2 $\alpha$  protects human hematopoietic stem/progenitors and acute myeloid leukemic cells from apoptosis induced by endoplasmic reticulum stress. *Cell Stem Cell*. 2013;13(5):549-63.
252. Forristal CE, Brown AL, Helwani FM, Winkler IG, Nowlan B, Barbier V, et al. Hypoxia inducible factor (HIF)-2 $\alpha$  accelerates disease progression in mouse models of leukemia and lymphoma but is not a poor prognosis factor in human AML. *Leukemia*. 2015;29(10):2075-85.
253. Vukovic M, Guitart AV, Sepulveda C, Villacreces A, O'Duibhir E, Panagopoulou TI, et al. Hif-1 $\alpha$  and Hif-2 $\alpha$  synergize to suppress AML development but are dispensable for disease maintenance. *The Journal of Experimental Medicine*. 2015;212(13):2223-34.
254. Matsunaga T, Imataki O, Torii E, Kameda T, Shide K, Shimoda H, et al. Elevated HIF-1 $\alpha$  expression of acute myelogenous leukemia stem cells in the endosteal hypoxic zone may be a cause of minimal residual disease in bone marrow after chemotherapy. *Leukemia Research*. 2012;36(6):e122-e4.
255. Hayflick L. The cell biology of human aging. *N Engl J Med*. 1976;295(23):1302-8.
256. d'Adda di Fagagna F. Living on a break: cellular senescence as a DNA-damage response. *Nat Rev Cancer*. 2008;8(7):512-22.
257. Allsopp RC, Chang E, Kashefi-Azham M, Rogaev EI, Piatyszek MA, Shay JW, et al. Telomere shortening is associated with cell division in vitro and in vivo. *Exp Cell Res*. 1995;220(1):194-200.
258. Perez-Mancera PA, Young ARJ, Narita M. Inside and out: the activities of senescence in cancer. *Nat Rev Cancer*. 2014;14(8):547-58.
259. Rodier F, Coppe JP, Patil CK, Hoeijmakers WA, Munoz DP, Raza SR, et al. Persistent DNA damage signalling triggers senescence-associated inflammatory cytokine secretion. *Nat Cell Biol*. 2009;11(8):973-9.
260. Bartkova J, Rezaei N, Liontos M, Karakaidos P, Kletsas D, Issaeva N, et al. Oncogene-induced senescence is part of the tumorigenesis barrier imposed by DNA damage checkpoints. *Nature*. 2006;444(7119):633-7.
261. Coppe JP, Patil CK, Rodier F, Sun Y, Munoz DP, Goldstein J, et al. Senescence-associated secretory phenotypes reveal cell-nonautonomous functions of oncogenic RAS and the p53 tumor suppressor. *PLoS Biol*. 2008;6(12):2853-68.
262. Demaria M, Ohtani N, Youssef SA, Rodier F, Toussaint W, Mitchell JR, et al. An Essential Role for Senescent Cells in Optimal Wound Healing through Secretion of PDGF-AA. *Developmental cell*. 2014;31(6):722-33.
263. Ruhland MK, Coussens LM, Stewart SA. Senescence and cancer: An evolving inflammatory paradox. *Biochimica et Biophysica Acta (BBA) - Reviews on Cancer*. 2016;1865(1):14-22.
264. Chicas A, Wang X, Zhang C, McCurrach M, Zhao Z, Mert O, et al. Dissecting the unique role of the retinoblastoma tumor suppressor during cellular senescence. *Cancer Cell*. 2010;17(4):376-87.
265. Childs BG, Durik M, Baker DJ, van Deursen JM. Cellular senescence in aging and age-related disease: from mechanisms to therapy. *Nature medicine*. 2015;21(12):1424-35.
266. Terzi MY, Izmirli M, Gogebakan B. The cell fate: senescence or quiescence. *Mol Biol Rep*. 2016;43(11):1213-20.
267. Dulic V. Be quiet and you'll keep young: does mTOR underlie p53 action in protecting against senescence by favoring quiescence? *Aging (Albany NY)*. 2011;3(1):3-4.

268. Itahana K, Itahana Y, Dimri GP. Colorimetric Detection of Senescence-Associated  $\beta$  Galactosidase. *Methods in molecular biology* (Clifton, NJ). 2013;965:143-56.
269. He S, Sharpless NE. Senescence in Health and Disease. *Cell*.169(6):1000-11.
270. Menicacci B, Laurenzana A, Chilla A, Margheri F, Peppicelli S, Tanganelli E, et al. Chronic Resveratrol Treatment Inhibits MRC5 Fibroblast SASP-Related Protumoral Effects on Melanoma Cells. *J Gerontol A Biol Sci Med Sci*. 2017.
271. Shay JW, Tomlinson G, Piatyszek MA, Gollahon LS. Spontaneous in vitro immortalization of breast epithelial cells from a patient with Li-Fraumeni syndrome. *Molecular and Cellular Biology*. 1995;15(1):425-32.
272. Iwakuma T, Lozano G, Flores ER. Li-Fraumeni syndrome: a p53 family affair. *Cell Cycle*. 2005;4(7):865-7.
273. Campisi J, d'Adda di Fagagna F. Cellular senescence: when bad things happen to good cells. *Nat Rev Mol Cell Biol*. 2007;8(9):729-40.
274. Davalos AR, Coppe J-P, Campisi J, Desprez P-Y. Senescent cells as a source of inflammatory factors for tumor progression. *Cancer Metastasis Reviews*. 2010;29(2):273-83.
275. Kim YH, Choi YW, Lee J, Soh EY, Kim J-H, Park TJ. Senescent tumor cells lead the collective invasion in thyroid cancer. *Nature Communications*. 2017;8:15208.
276. Luo X, Fu Y, Loza Andrew J, Murali B, Leahy Kathleen M, Ruhland Megan K, et al. Stromal-Initiated Changes in the Bone Promote Metastatic Niche Development. *Cell Reports*. 2016;14(1):82-92.
277. Ruhland MK, Loza AJ, Capietto AH, Luo X, Knolhoff BL, Flanagan KC, et al. Stromal senescence establishes an immunosuppressive microenvironment that drives tumorigenesis. *Nat Commun*. 2016;7:11762.
278. Ewald JA, Desotelle JA, Wilding G, Jarrard DF. Therapy-Induced Senescence in Cancer. *JNCI Journal of the National Cancer Institute*. 2010;102(20):1536-46.
279. Gordon RR, Nelson PS. Cellular Senescence and Cancer Chemotherapy Resistance. *Drug Resistance Updates*. 2012;15(1-2):123-31.
280. Achuthan S, Santhoshkumar TR, Prabhakar J, Nair SA, Pillai MR. Drug-induced Senescence Generates Chemoresistant Stemlike Cells with Low Reactive Oxygen Species. *The Journal of Biological Chemistry*. 2011;286(43):37813-29.
281. Sanoff HK, Deal AM, Krishnamurthy J, Torrice C, Dillon P, Sorrentino J, et al. Effect of cytotoxic chemotherapy on markers of molecular age in patients with breast cancer. *J Natl Cancer Inst*. 2014;106(4):dju057.
282. Demaria M, Leary MN, Chang J, Shao L, Liu S, Alimirah F, et al. Cellular Senescence Promotes Adverse Effects of Chemotherapy and Cancer Relapse. *Cancer Discovery*. 2016.
283. Baker DJ, Childs BG, Durik M, Wijers ME, Sieben CJ, Zhong J, et al. Naturally occurring p16(Ink4a)-positive cells shorten healthy lifespan. *Nature*. 2016;530(7589):184-9.
284. Shafat MS, Oellerich T, Mohr S, Robinson SD, Edwards DR, Marlein CR, et al. Leukemic blasts program bone marrow adipocytes to generate a pro-tumoral microenvironment. *Blood*. 2017.
285. Roecklein BA, Torok-Storb B. Functionally distinct human marrow stromal cell lines immortalized by transduction with the human papilloma virus E6/E7 genes. *Blood*. 1995;85(4):997.
286. Schutte B, Nuydens R, Geerts H, Ramaekers F. Annexin V binding assay as a tool to measure apoptosis in differentiated neuronal cells. *Journal of Neuroscience Methods*. 1998;86(1):63-9.
287. Sarma NJ, Takeda A, Yaseen NR. Colony Forming Cell (CFC) Assay for Human Hematopoietic Cells. *Journal of Visualized Experiments : JoVE*. 2010(46):2195.

288. Maharshak N, Cohen S, Lantner F, Hart G, Leng L, Bucala R, et al. CD74 is a survival receptor on colon epithelial cells. *World Journal of Gastroenterology* : WJG. 2010;16(26):3258-66.
289. Shultz LD, Lyons BL, Burzenski LM, Gott B, Chen X, Chaleff S, et al. Human Lymphoid and Myeloid Cell Development in NOD/LtSz-scid IL2R gamma null mice Mice Engrafted with Mobilized Human Hemopoietic Stem Cells. *The Journal of Immunology*. 2005;174(10):6477-89.
290. Noto FK, Yeshi T. Humanized Mouse and Rat PDX Cancer Models. In: Wang Y, Lin D, Gout PW, editors. *Patient-Derived Xenograft Models of Human Cancer*. Cham: Springer International Publishing; 2017. p. 43-57.
291. Vick B, Rothenberg M, Sandhöfer N, Carlet M, Finkenzeller C, Krupka C, et al. An Advanced Preclinical Mouse Model for Acute Myeloid Leukemia Using Patients' Cells of Various Genetic Subgroups and In Vivo Bioluminescence Imaging. *PLoS ONE*. 2015;10(3):e0120925.
292. Cook MJ. *The anatomy of the laboratory mouse*: Academic Press; 1965.
293. Wierenga ATJ, Vellenga E, Schuringa JJ. Convergence of Hypoxia and TGF $\beta$  Pathways on Cell Cycle Regulation in Human Hematopoietic Stem/Progenitor Cells. *PLOS ONE*. 2014;9(3):e93494.
294. Bernardo ME, Zaffaroni N, Novara F, Cometa AM, Avanzini MA, Moretta A, et al. Human Bone Marrow-Derived Mesenchymal Stem Cells Do Not Undergo Transformation after Long-term in vitro Culture and Do Not Exhibit Telomere Maintenance Mechanisms. *Cancer Research*. 2007;67(19):9142.
295. Huang JC, Basu SK, Zhao X, Chien S, Fang M, Oehler VG, et al. Mesenchymal stromal cells derived from acute myeloid leukemia bone marrow exhibit aberrant cytogenetics and cytokine elaboration. *Blood Cancer Journal*. 2015;5:e302.
296. Rushworth SA, Pillinger G, Abdul-Aziz A, Piddock R, Shafat MS, Murray MY, et al. Activity of Bruton's tyrosine-kinase inhibitor ibrutinib in patients with CD117-positive acute myeloid leukaemia: a mechanistic study using patient-derived blast cells. *The Lancet Haematology*. 2015;2(5):e204-e11.
297. Rushworth SA, Murray MY, Zaitseva L, Bowles KM, MacEwan DJ. Identification of Bruton's tyrosine kinase as a therapeutic target in acute myeloid leukemia. *Blood*. 2014;123(8):1229-38.
298. Nervi B, Ramirez P, Rettig MP, Uy GL, Holt MS, Ritchey JK, et al. Chemosensitization of acute myeloid leukemia (AML) following mobilization by the CXCR4 antagonist AMD3100. *Blood*. 2009;113(24):6206-14.
299. Konopleva M, Konoplev S, Hu W, Zaritskey AY, Afanasiev BV, Andreeff M. Stromal cells prevent apoptosis of AML cells by up-regulation of anti-apoptotic proteins. *Leukemia*. 2002;16(9):1713-24.
300. Falantes JF, Trujillo P, Piruat JI, Calderon C, Marquez-Malaver FJ, Martin-Antonio B, et al. Overexpression of GYS1, MIF, and MYC is associated with adverse outcome and poor response to azacitidine in myelodysplastic syndromes and acute myeloid leukemia. *Clin Lymphoma Myeloma Leuk*. 2015;15(4):236-44.
301. Dokter WH, Tuyt L, Sierdsema SJ, Esselink MT, Vellenga E. The spontaneous expression of interleukin-1 beta and interleukin-6 is associated with spontaneous expression of AP-1 and NF-kappa B transcription factor in acute myeloblastic leukemia cells. *Leukemia*. 1995;9(3):425-32.
302. Sanchez-Correa B, Bergua JM, Campos C, Gayoso I, Arcos MJ, Bañas H, et al. Cytokine profiles in acute myeloid leukemia patients at diagnosis: Survival is inversely correlated with IL-6 and directly correlated with IL-10 levels. *Cytokine*. 2013;61(3):885-91.
303. Hoang T, Haman A, Goncalves O, Wong GG, Clark SC. Interleukin-6 enhances growth factor-dependent proliferation of the blast cells of acute myeloblastic leukemia. *Blood*. 1988;72(2):823-6.

304. Stojanovic I, Cvjeticanin T, Lazaroski S, Stosic-Grujicic S, Miljkovic D. Macrophage migration inhibitory factor stimulates interleukin-17 expression and production in lymph node cells. *Immunology*. 2009;126(1):74-83.
305. Chuang CC, Chuang YC, Chang WT, Chen CC, Hor LI, Huang AM, et al. Macrophage migration inhibitory factor regulates interleukin-6 production by facilitating nuclear factor-kappa B activation during *Vibrio vulnificus* infection. *BMC immunology*. 2010;11:50.
306. Xiong C, Huang B, Cun Y, Aghdasi BG, Zhou Y. Migration inhibitory factor enhances inflammation via CD74 in cartilage end plates with Modic type 1 changes on MRI. *Clinical orthopaedics and related research*. 2014;472(6):1943-54.
307. de Jong YP, Abadia-Molina AC, Satoskar AR, Clarke K, Rietdijk ST, Faubion WA, et al. Development of chronic colitis is dependent on the cytokine MIF. *Nat Immunol*. 2001;2(11):1061-6.
308. Straussman R, Morikawa T, Shee K, Barzily-Rokni M, Qian ZR, Du J, et al. Tumour micro-environment elicits innate resistance to RAF inhibitors through HGF secretion. *Nature*. 2012;487(7408):500-4.
309. Wilson JM, Coletta PL, Cuthbert RJ, Scott N, MacLennan K, Hawcroft G, et al. Macrophage Migration Inhibitory Factor Promotes Intestinal Tumorigenesis. *Gastroenterology*. 2005;129(5):1485-503.
310. Tarnowski M, Grymula K, Liu R, Tarnowska J, Drukala J, Ratajczak J, et al. Macrophage Migration Inhibitory Factor Is Secreted by Rhabdomyosarcoma Cells, Modulates Tumor Metastasis by Binding to CXCR4 and CXCR7 Receptors and Inhibits Recruitment of Cancer-Associated Fibroblasts. *Molecular Cancer Research*. 2010.
311. Mochmann LH, Neumann M, von der Heide EK, Nowak V, Kühl AA, Ortiz-Tanchez J, et al. ERG induces a mesenchymal-like state associated with chemoresistance in leukemia cells. *Oncotarget*. 2014;5(2):351-62.
312. Dios A, Mitchell RA, Aljabari B, Lubetsky J, O'Connor K, Liao H, et al. Inhibition of MIF bioactivity by rational design of pharmacological inhibitors of MIF tautomerase activity. *J Med Chem*. 2002;45(12):2410-6.
313. Lue H, Dewor M, Leng L, Bucala R, Bernhagen J. Activation of the JNK signalling pathway by macrophage migration inhibitory factor (MIF) and dependence on CXCR4 and CD74. *Cell Signal*. 2011;23(1):135-44.
314. Schwartz V, Lue H, Kraemer S, Korbiel J, Krohn R, Ohl K, et al. A functional heteromeric MIF receptor formed by CD74 and CXCR4. *FEBS Lett*. 2009;583(17):2749-57.
315. Park MS, Kim YH, Jung Y, Kim SH, Park JC, Yoon DS, et al. In Situ Recruitment of Human Bone Marrow-Derived Mesenchymal Stem Cells Using Chemokines for Articular Cartilage Regeneration. *Cell Transplant*. 2015;24(6):1067-83.
316. Liu N, Patzak A, Zhang J. CXCR4-overexpressing bone marrow-derived mesenchymal stem cells improve repair of acute kidney injury. *Am J Physiol Renal Physiol*. 2013;305(7):F1064-73.
317. Barrilleaux BL, Fischer-Valuck BW, Gilliam JK, Phinney DG, O'Connor KC. Activation of CD74 inhibits migration of human mesenchymal stem cells. *In Vitro Cell Dev Biol Anim*. 2010;46(6):566-72.
318. Sidahmed AME, León AJ, Bosinger SE, Banner D, Danesh A, Cameron MJ, et al. CXCL10 contributes to p38-mediated apoptosis in primary T lymphocytes in vitro. *Cytokine*. 2012;59(2):433-41.
319. Starlets D, Gore Y, Binsky I, Haran M, Harpaz N, Shvidel L, et al. Cell-surface CD74 initiates a signaling cascade leading to cell proliferation and survival. *Blood*. 2006;107(12):4807-16.



320. Gao Y, Guan Z, Chen J, Xie H, Yang Z, Fan J, et al. CXCL5/CXCR2 axis promotes bladder cancer cell migration and invasion by activating PI3K/AKT-induced upregulation of MMP2/MMP9. *Int J Oncol.* 2015;47(2):690-700.
321. Fu H, Luo F, Yang L, Wu W, Liu X. Hypoxia stimulates the expression of macrophage migration inhibitory factor in human vascular smooth muscle cells via HIF-1 $\alpha$  dependent pathway. *BMC Cell Biol.* 2010;11:66.
322. Gaber T, Schellmann S, Erekul KB, Fangradt M, Tykwinska K, Hahne M, et al. Macrophage migration inhibitory factor counterregulates dexamethasone-mediated suppression of hypoxia-inducible factor-1  $\alpha$  function and differentially influences human CD4<sup>+</sup> T cell proliferation under hypoxia. *J Immunol.* 2011;186(2):764-74.
323. Baugh JA, Gantier M, Li L, Byrne A, Buckley A, Donnelly SC. Dual regulation of macrophage migration inhibitory factor (MIF) expression in hypoxia by CREB and HIF-1. *Biochem Biophys Res Commun.* 2006;347(4):895-903.
324. Ortiz-Barahona A, Villar D, Pescador N, Amigo J, del Peso L. Genome-wide identification of hypoxia-inducible factor binding sites and target genes by a probabilistic model integrating transcription-profiling data and in silico binding site prediction. *Nucleic Acids Res.* 2010;38(7):2332-45.
325. Macrae T, Sargeant T, Lemieux S, Hebert J, Deneault E, Sauvageau G. RNA-Seq reveals spliceosome and proteasome genes as most consistent transcripts in human cancer cells. *PLoS One.* 2013;8(9):e72884.
326. Wang Y, Liu Y, Malek SN, Zheng P, Liu Y. Targeting HIF1 $\alpha$  eliminates cancer stem cells in hematological malignancies. *Cell Stem Cell.* 2011;8(4):399-411.
327. Zhang T, Niu X, Liao L, Cho E-A, Yang H. The Contributions of HIF-Target Genes to Tumor Growth in RCC. *PLoS ONE.* 2013;8(11):e80544.
328. Simons D, Grieb G, Hristov M, Pallua N, Weber C, Bernhagen J, et al. Hypoxia-induced endothelial secretion of macrophage migration inhibitory factor and role in endothelial progenitor cell recruitment. *J Cell Mol Med.* 2011;15(3):668-78.
329. Kong X, Alvarez-Castelao B, Lin Z, Castaño JG, Caro J. Constitutive/Hypoxic Degradation of HIF- $\alpha$  Proteins by the Proteasome Is Independent of von Hippel Lindau Protein Ubiquitylation and the Transactivation Activity of the Protein. *Journal of Biological Chemistry.* 2007;282(21):15498-505.
330. Tausendschön M, Rehli M, Dehne N, Schmidl C, Döring C, Hansmann M-L, et al. Genome-wide identification of hypoxia-inducible factor-1 and -2 binding sites in hypoxic human macrophages alternatively activated by IL-10. *Biochimica et Biophysica Acta (BBA) - Gene Regulatory Mechanisms.* 2015;1849(1):10-22.
331. Mathieu J, Zhou W, Xing Y, Sperber H, Ferreccio A, Agoston Z, et al. Hypoxia-Inducible Factors Have Distinct and Stage-Specific Roles during Reprogramming of Human Cells to Pluripotency. *Cell Stem Cell.* 2014;14(5):592-605.
332. Terwijn M, Zeijlemaker W, Kelder A, Rutten AP, Snel AN, Scholten WJ, et al. Leukemic Stem Cell Frequency: A Strong Biomarker for Clinical Outcome in Acute Myeloid Leukemia. *PLoS ONE.* 2014;9(9):e107587.
333. Manjunath N, Haoquan W, Sandesh S, Premlata S. Lentiviral delivery of short hairpin RNAs. *Advanced drug delivery reviews.* 2009;61(9):732-45.
334. Rajasekaran D, Gröning S, Schmitz C, Zierow S, Drucker N, Bakou M, et al. Macrophage Migration Inhibitory Factor-CXCR4 Receptor Interactions: Evidence for Partial Allosteric Agonism in Comparison to CXCL12. *Journal of Biological Chemistry.* 2016.
335. Meyer-Siegler KL, Iczkowski KA, Leng L, Bucala R, Vera PL. Inhibition of Macrophage Migration Inhibitory Factor or Its Receptor (CD74) Attenuates Growth and Invasion of DU-145 Prostate Cancer Cells. *The Journal of Immunology.* 2006;177(12):8730.
336. Cashen AF, Nervi B, DiPersio J. AMD3100: CXCR4 antagonist and rapid stem cell-mobilizing agent. *Future Oncol.* 2007;3(1):19-27.

337. Lopes MR, Machado-Neto JA, Traina F, Campos PdM, Saad STO, Favaro P. Differential profile of CDKN1A and TP53 expressions in bone marrow mesenchymal stromal cells from myeloid neoplasms. *Revista Brasileira de Hematologia e Hemoterapia*. 2016;38(4):368-70.
338. van Deursen JM. The role of senescent cells in ageing. *Nature*. 2014;509(7501):439-46.
339. Stab BR, Martinez L, Grismaldo A, Lerma A, Gutiérrez ML, Barrera LA, et al. Mitochondrial Functional Changes Characterization in Young and Senescent Human Adipose Derived MSCs. *Frontiers in Aging Neuroscience*. 2016;8:299.
340. Madeira A, da Silva CL, dos Santos F, Camafeita E, Cabral JMS, Sá-Correia I. Human Mesenchymal Stem Cell Expression Program upon Extended Ex-Vivo Cultivation, as Revealed by 2-DE-Based Quantitative Proteomics. *PLoS ONE*. 2012;7(8):e43523.
341. Kurpinski K, Jang DJ, Bhattacharya S, Rydberg B, Chu J, So J, et al. Differential effects of x-rays and high-energy <sup>56</sup>Fe ions on human mesenchymal stem cells. *Int J Radiat Oncol Biol Phys*. 2009;73(3):869-77.
342. Ito S, Barrett AJ, Dutra A, Pak E, Miner S, Keyvanfar K, et al. Long term maintenance of myeloid leukemic stem cells cultured with unrelated human mesenchymal stromal cells. *Stem Cell Research*. 2015;14(1):95-104.
343. Kim Y, Jekarl DW, Kim J, Kwon A, Choi H, Lee S, et al. Genetic and epigenetic alterations of bone marrow stromal cells in myelodysplastic syndrome and acute myeloid leukemia patients. *Stem Cell Research*. 2015;14(2):177-84.
344. Civini S, Jin P, Ren J, Sabatino M, Castiello L, Jin J, et al. Leukemia cells induce changes in human bone marrow stromal cells. *Journal of Translational Medicine*. 2013;11(1):298.
345. Itonaga H, Imanishi D, Wong YF, Sato S, Ando K, Sawayama Y, et al. Expression of myeloperoxidase in acute myeloid leukemia blasts mirrors the distinct DNA methylation pattern involving the downregulation of DNA methyltransferase DNMT3B. *Leukemia*. 2014;28(7):1459-66.
346. Reikvam H, Hatfield KJ, Oyan AM, Kalland KH, Kittang AO, Bruserud O. Primary human acute myelogenous leukemia cells release matrix metalloproteases and their inhibitors: release profile and pharmacological modulation. *European journal of haematology*. 2010;84(3):239-51.
347. Chen YB, Ren SM, Li SD, Du Z. Prognostic significance of osteopontin in acute myeloid leukemia: A meta-analysis. *Mol Clin Oncol*. 2017;7(2):275-80.
348. Hatfield KJ, Reikvam H, Bruserud O. The crosstalk between the matrix metalloprotease system and the chemokine network in acute myeloid leukemia. *Curr Med Chem*. 2010;17(36):4448-61.
349. Honnemyr M, Bruserud O, Brenner AK. The constitutive protease release by primary human acute myeloid leukemia cells. *J Cancer Res Clin Oncol*. 2017;143(10):1985-1998.
350. Burton JD, Stein R, Chandra A, Chen S, Mishra N, Shah T, et al. Expression of CD74 by AML blasts and cell lines, and enhanced in vitro cytotoxicity of anti-CD74 antibody after interferon-gamma (IFN- $\gamma$ ) treatment. *Journal of Clinical Oncology*. 2010;28:6576.
351. Attar EC, Maharry K, Mrózek K, Radmacher MD, Whitman SP, Paschka P, et al. Increased Expression of Macrophage Migration Inhibitory Factor (MIF) Receptor CD74 Is Associated with Inferior Outcome in Younger Patients (Pts) with Cytogenetically Normal Acute Myeloid Leukemia (CN-AML): a Cancer and Leukemia Group B (CALGB) Study. *Blood*. 2015;114(22):1616.
352. Simpson KD, Templeton DJ, Cross JV. Macrophage Migration Inhibitory Factor Promotes Tumor Growth and Metastasis by Inducing Myeloid-Derived Suppressor Cells in the Tumor Microenvironment. *The Journal of Immunology*. 2012;189(12):5533-40.

353. Balogh KN, Cross JV. Abstract A03: A role for Macrophage Migration Inhibitory Factor (MIF) in breast cancer growth and metastasis. *Cancer Immunology Research*. 2017;5(3 Supplement):A03.
354. Sugimoto H, Taniguchi M, Nakagawa A, Tanaka I, Suzuki M, Nishihira J. Crystal structure of human D-dopachrome tautomerase, a homologue of macrophage migration inhibitory factor, at 1.54 Å resolution. *Biochemistry*. 1999;38(11):3268-79.
355. Esumi N, Budarf M, Ciccarelli L, Sellinger B, Kozak CA, Wistow G. Conserved gene structure and genomic linkage for D-dopachrome tautomerase (DDT) and MIF. *Mammalian genome : official journal of the International Mammalian Genome Society*. 1998;9(9):753-7.
356. Merk M, Mitchell RA, Endres S, Bucala R. D-dopachrome tautomerase (D-DT or MIF-2): Doubling the MIF cytokine family. *Cytokine*. 2012;59(1):10-7.
357. Pasupuleti V, Du W, Gupta Y, Yeh I-J, Montano M, Magi-Galuzzi C, et al. Dysregulated D-dopachrome Tautomerase, a Hypoxia-inducible Factor-dependent Gene, Cooperates with Macrophage Migration Inhibitory Factor in Renal Tumorigenesis. *Journal of Biological Chemistry*. 2014;289(6):3713-23.
358. Coleman AM, Rendon BE, Zhao M, Qian MW, Bucala R, Xin D, et al. Cooperative regulation of non-small cell lung carcinoma angiogenic potential by macrophage migration inhibitory factor and its homolog, D-dopachrome tautomerase. *Journal of immunology (Baltimore, Md : 1950)*. 2008;181(4):2330-7.
359. Thiele M, Kerschbaumer RJ, Tam FWK, Völkel D, Douillard P, Schinagl A, et al. Selective Targeting of a Disease-Related Conformational Isoform of Macrophage Migration Inhibitory Factor Ameliorates Inflammatory Conditions. *The Journal of Immunology*. 2015;195(5):2343-52.
360. Schinagl A, Thiele M, Douillard P, Volkel D, Kenner L, Kazemi Z, et al. Oxidized macrophage migration inhibitory factor is a potential new tissue marker and drug target in cancer. *Oncotarget*. 2016;7(45):73486-96.
361. Liu X, Adib DR, Barak H, Goldberg RM, Yazji S. Development of a phase Ib/IIa proof-of-concept study of imalumab (BAX69), a first-in-class anti-macrophage migration inhibitory factor (MIF) antibody, as the 3rd or 4th line treatment in metastatic colorectal cancer (mCRC). *Journal of Clinical Oncology*. 2015;33(15\_suppl):TPS3633-TPS.
362. Mahalingam D, Patel MR, Sachdev JC, Hart LL, Halama N, Ramanathan RK, et al. Abstract CT046: First-in-human phase 1 study assessing imalumab (BAX69), an anti-oxidized macrophage migration inhibitory factor (oxMIF) antibody in advanced solid tumors. *Cancer Research*. 2016;76(14 Supplement):CT046.
363. Garg R, Benedetti LG, Abera MB, Wang H, Abba M, Kazanietz MG. Protein kinase C and cancer: what we know and what we do not. *Oncogene*. 2014;33(45):5225-37.
364. Baumann P, Armann J, Mandl-Weber S, Grün G, Oduncu F, Schmidmaier R. Inhibitors of protein kinase C sensitise multiple myeloma cells to common genotoxic drugs. *European journal of haematology*. 2008;80(1):37-45.
365. Abrams ST, Lakum T, Lin K, Jones GM, Treweeke AT, Farahani M, et al. B-cell receptor signaling in chronic lymphocytic leukemia cells is regulated by overexpressed active protein kinase C $\beta$ II. *Blood*. 2007;109(3):1193-201.
366. El-Gamal D, Williams K, LaFollette TD, Cannon M, Blachly JS, Zhong Y, et al. PKC- $\beta$  as a therapeutic target in CLL: PKC inhibitor AEB071 demonstrates preclinical activity in CLL. *Blood*. 2014;124(9):1481-91.
367. Banker DE, Mayer SJ, Li HY, Willman CL, Appelbaum FR, Zager RA. Cholesterol synthesis and import contribute to protective cholesterol increments in acute myeloid leukemia cells. *Blood*. 2004;104(6):1816-24.
368. Kornblau SM, Banker DE, Stirewalt D, Shen D, Lemker E, Verstovsek S, et al. Blockade of adaptive defensive changes in cholesterol uptake and synthesis in AML

by the addition of pravastatin to idarubicin + high-dose Ara-C: a phase 1 study. *Blood*. 2007;109(7):2999-3006.

369. Bhuiyan H, Masquelier M, Tatidis L, Gruber A, Paul C, Vitols S. Acute Myelogenous Leukemia Cells Secrete Factors that Stimulate Cellular LDL Uptake via Autocrine and Paracrine Mechanisms. *Lipids*. 2017;52(6):523-34.

370. Singer M, Sansonetti PJ. IL-8 Is a Key Chemokine Regulating Neutrophil Recruitment in a New Mouse Model of *Shigella*-Induced Colitis. *The Journal of Immunology*. 2004;173(6):4197-206.

371. Wang J, Mukaida N, Zhang Y, Ito T, Nakao S, Matsushima K. Enhanced mobilization of hematopoietic progenitor cells by mouse MIP-2 and granulocyte colony-stimulating factor in mice. *J Leukoc Biol*. 1997;62(4):503-9.

372. Gilkes DM, Semenza GL. Role of hypoxia-inducible factors in breast cancer metastasis. *Future Oncol*. 2013;9(11):1623-36.

373. Ammirante M, Shalapour S, Kang Y, Jamieson CA, Karin M. Tissue injury and hypoxia promote malignant progression of prostate cancer by inducing CXCL13 expression in tumor myofibroblasts. *Proc Natl Acad Sci U S A*. 2014;111(41):14776-81.

374. Selvendiran K, Bratasz A, Kuppusamy ML, Tazi MF, Rivera BK, Kuppusamy P. Hypoxia induces chemoresistance in ovarian cancer cells by activation of signal transducer and activator of transcription 3. *Int J Cancer*. 2009;125(9):2198-204.

375. Rapin N, Bagger FO, Jendholm J, Mora-Jensen H, Krogh A, Kohlmann A, et al. Comparing cancer vs normal gene expression profiles identifies new disease entities and common transcriptional programs in AML patients. *Blood*. 2014;123(6):894-904.

376. Cheung AMS, Chow HCH, Liang R, Leung AYH. A comparative study of bone marrow and peripheral blood CD34+ myeloblasts in acute myeloid leukaemia. *British Journal of Haematology*. 2009;144(4):484-91.

377. Bhattacharyya A, Chattopadhyay R, Hall EH, Mebrahtu ST, Ernst PB, Crowe SE. Mechanism of hypoxia-inducible factor 1 $\alpha$ -mediated Mcl1 regulation in *Helicobacter pylori*-infected human gastric epithelium. *American Journal of Physiology - Gastrointestinal and Liver Physiology*. 2010;299(5):G1177-G86.

378. Kučera J, Netušilová J, Sladeček S, Lánová M, Vašíček O, Štefková K, et al. Hypoxia Downregulates MAPK/ERK but Not STAT3 Signaling in ROS-Dependent and HIF-1-Independent Manners in Mouse Embryonic Stem Cells. *Oxidative Medicine and Cellular Longevity*. 2017;2017:4386947.

379. Ghosh AK, Shanafelt TD, Cimmino A, Taccioli C, Volinia S, Liu CG, et al. Aberrant regulation of pVHL levels by microRNA promotes the HIF/VEGF axis in CLL B cells. *Blood*. 2009;113(22):5568-74.

380. Shachar I, Cohen S, Marom A, Becker-Herman S. Regulation of CLL survival by hypoxia-inducible factor and its target genes. *FEBS Letters*. 2012;586(18):2906-10.

381. Velasco-Hernandez T, Tornero D, Cammenga J. Loss of HIF-1 $\alpha$  accelerates murine FLT-3(ITD)-induced myeloproliferative neoplasia. *Leukemia*. 2015;29(12):2366-74.

382. Yonekura S, Itoh M, Okuhashi Y, Takahashi Y, Ono A, Nara N, et al. Effects of the HIF1 inhibitor, echinomycin, on growth and NOTCH signalling in leukaemia cells. *Anticancer research*. 2013;33(8):3099-103.

383. Zhong H, Mabjeesh N, Willard M, Simons J. Nuclear expression of hypoxia-inducible factor 1 $\alpha$  protein is heterogeneous in human malignant cells under normoxic conditions. *Cancer letters*. 2002;181(2):233-8.

384. Cheloni G, Tanturli M, Tusa I, DeSouza NH, Shan Y, Gozzini A, et al. Targeting chronic myeloid leukemia stem cells with the hypoxia-inducible factor inhibitor acriflavine. *Blood*. 2017;130(5):655-665.

385. Zheng Y, Wang Q, Qian J, Li Y, Lu Y, Bi E, et al. Macrophage Migration Inhibitory Factor Regulates Multiple Myeloma Bone Marrow Homing. *Blood*. 2014;124(21):2015.
386. Guo P, Wang J, Liu J, Xia M, Li W, He M. Macrophage immigration inhibitory factor promotes cell proliferation and inhibits apoptosis of cervical adenocarcinoma. *Tumor Biology*. 2015;36(7):5095-102.
387. Oda S, Oda T, Nishi K, Takabuchi S, Wakamatsu T, Tanaka T, et al. Macrophage migration inhibitory factor activates hypoxia-inducible factor in a p53-dependent manner. *PLoS One*. 2008;3(5):e2215.
388. Al-Abed Y, Dabideen D, Aljabari B, Valster A, Messmer D, Ochani M, et al. ISO-1 Binding to the Tautomerase Active Site of MIF Inhibits Its Pro-inflammatory Activity and Increases Survival in Severe Sepsis. *Journal of Biological Chemistry*. 2005;280(44):36541-4.
389. Bavik C, Coleman I, Dean JP, Knudsen B, Plymate S, Nelson PS. The gene expression program of prostate fibroblast senescence modulates neoplastic epithelial cell proliferation through paracrine mechanisms. *Cancer Res*. 2006;66(2):794-802.
390. Krtolica A, Parrinello S, Lockett S, Desprez P-Y, Campisi J. Senescent fibroblasts promote epithelial cell growth and tumorigenesis: A link between cancer and aging. *Proceedings of the National Academy of Sciences*. 2001;98(21):12072-7.
391. Burd Christin E, Sorrentino Jessica A, Clark Kelly S, Darr David B, Krishnamurthy J, Deal Allison M, et al. Monitoring Tumorigenesis and Senescence In Vivo with a p16INK4a-Luciferase Model. *Cell*. 2013;152(1-2):340-51.
392. Muller-Tidow C, Metzelder SK, Buerger H, Packeisen J, Ganser A, Heil G, et al. Expression of the p14ARF tumor suppressor predicts survival in acute myeloid leukemia. *Leukemia*. 2004;18(4):720-6.
393. de Jonge HJM, Woolthuis CM, de Bont ESJM, Huls G. Paradoxical down-regulation of p16(INK4a) mRNA with advancing age in Acute Myeloid Leukemia. *Aging (Albany NY)*. 2009;1(11):949-53.
394. Dimri GP, Lee X, Basile G, Acosta M, Scott G, Roskelley C, et al. A biomarker that identifies senescent human cells in culture and in aging skin in vivo. *Proc Natl Acad Sci U S A*. 1995;92(20):9363-7.
395. Itahana K, Campisi J, Dimri GP. Methods to detect biomarkers of cellular senescence: the senescence-associated beta-galactosidase assay. *Methods Mol Biol*. 2007;371:21-31.
396. Digirolamo CM, Stokes D, Colter D, Phinney DG, Class R, Prockop DJ. Propagation and senescence of human marrow stromal cells in culture: a simple colony-forming assay identifies samples with the greatest potential to propagate and differentiate. *British journal of haematology*. 1999;107(2):275-81.
397. Wagner W, Bork S, Lepperdinger G, Jousen S, Ma N, Strunk D, et al. How to track cellular aging of mesenchymal stromal cells? *Aging (Albany NY)*. 2010;2(4):224-30.
398. Malla S, Prasad Niraula N, Singh B, Liou K, Kyung Sohng J. Limitations in doxorubicin production from *Streptomyces peucetius*. *Microbiological Research*. 2010;165(5):427-35.
399. Gewirtz D. A critical evaluation of the mechanisms of action proposed for the antitumor effects of the anthracycline antibiotics adriamycin and daunorubicin. *Biochemical Pharmacology*. 1999;57(7):727-41.
400. Mansilla S, PiÑA B, Portugal J. Daunorubicin-induced variations in gene transcription: commitment to proliferation arrest, senescence and apoptosis. *Biochemical Journal*. 2003;372(3):703-11.
401. Stein EM, Tallman MS. Emerging therapeutic drugs for AML. *Blood*. 2016;127(1):71.

402. Baker DJ, Wijshake T, Tchkonia T, LeBrasseur NK, Childs BG, van de Sluis B, et al. Clearance of p16(Ink4a)-positive senescent cells delays ageing-associated disorders. *Nature*. 2011;479(7372):232-6.
403. Chang J, Wang Y, Shao L, Laberge R-M, Demaria M, Campisi J, et al. Clearance of senescent cells by ABT263 rejuvenates aged hematopoietic stem cells in mice. *Nature medicine*. 2016;22(1):78-83.
404. Airiau K, Prouzet-Mauleon V, Rousseau B, Pigneux A, Jeanneteau M, Giraudon M, et al. Synergistic cooperation between ABT-263 and MEK1/2 inhibitor: effect on apoptosis and proliferation of acute myeloid leukemia cells. *Oncotarget*. 2016;7(1):845-59.

## Appendix

**Table 1: Cytogenetic profiles of primary BMSCs**

<b>BMSC</b>	<b>Sex</b>	<b>BMSC cytogenetics</b>	<b>AML cytogenetics</b>
<b>BMSC#1</b>	M	N/A	Normal
<b>BMSC#2</b>	F	N/A	t(5;12)(q13;q24)
<b>BMSC#3</b>	M	Normal	Normal
<b>BMSC#4</b>	F	Normal	t(8;21)(q22;q22),del(9)(q13q22)
<b>BMSC#5</b>	M	Normal	Normal
<b>BMSC#6</b>	M	N/A	add(5)(q35),add(6)(q22)

AML cytogenetics refers to the cytogenetics of the AML sample from which the BMSC were derived.

Karyotype reports provided by the Norwich Cytogenetics Service, where the karyotyping/cytogenetic analysis was performed, are included below. Karyotype results for samples 1 and 2 were communicated by e-mail to Dr Stuart Rushworth.

**NORWICH CYTOGENETICS SERVICE**

Telephone 01603 286038  
Fax 01603 286839  
Email [sandra.edwards@nnuh.nhs.uk](mailto:sandra.edwards@nnuh.nhs.uk)

Cytogenetics Department  
Norfolk and Norwich University Hospital  
Colney Lane  
NORWICH  
NR4 7UY

Dr K Bowles  
Consultant Haematologist  
Norfolk & Norwich University Hospital  
Colney Lane  
NORWICH  
NR4 7UY

**CHROMOSOME ANALYSIS - CULTURED CELLS**

PATIENT DETAILS		SAMPLE DETAILS	
Surname	BMMSC	Lab. No.	P16-0928
Other Name	1048	Date of Receipt	04/07/2016
Date of Birth	04/07/2016	Date of Report	29/07/2016
Hospital No.	NYK		

REASON FOR REFERRAL PRIVATE KARYOTYPE  
Research sample.

**REPORT**

KARYOTYPE 46,XY

Apparently normal male karyotype in the 10 cells examined.

Please note that the quality of the preparations obtained was unsuitable for the detection of subtle chromosomal abnormalities.

*[Faint, illegible text, possibly a stamp or signature]*

Authorised By *Seel*

Copies to



**NORWICH CYTOGENETICS SERVICE**

Telephone 01603 286038  
Fax 01603 286839  
Email [sandra.edwards@nnuh.nhs.uk](mailto:sandra.edwards@nnuh.nhs.uk)

Cytogenetics Department  
Norfolk and Norwich University Hospital  
Colney Lane  
NORWICH  
NR4 7UY

Dr K Bowles  
Consultant Haematologist  
Norfolk & Norwich University Hospital  
Colney Lane  
NORWICH  
NR4 7UY

**CHROMOSOME ANALYSIS - CULTURED CELLS**

PATIENT DETAILS		SAMPLE DETAILS	
Surname	BMMSC	Lab. No.	P16-0929
Other Name	836	Date of Receipt	04/07/2016
Date of Birth	04/07/2016	Date of Report	29/07/2016
Hospital No.	NYK		

REASON FOR REFERRAL PRIVATE KARYOTYPE  
Research sample.

**REPORT**

KARYOTYPE FAILED

Preparations from this culture sample failed to yield any analysable metaphases so chromosome analysis could not be done.

Authorised By 

Copies to

**CPA** Accredited Laboratory

**NORWICH CYTOGENETICS SERVICE**

Telephone 01603 286038  
Fax 01603 286839  
Email sandra.edwards@nnuh.nhs.uk

Cytogenetics Department  
Norfolk and Norwich University Hospital  
Colney Lane  
NORWICH  
NR4 7UY

Dr K Bowles  
Consultant Haematologist  
Norfolk & Norwich University Hospital  
Colney Lane  
NORWICH  
NR4 7UY

**CHROMOSOME ANALYSIS - CULTURED CELLS**

PATIENT DETAILS		SAMPLE DETAILS	
Surname	BMMSC	Lab. No.	P16-0931
Other Name	734	Date of Receipt	04/07/2016
Date of Birth	04/07/2016	Date of Report	29/07/2016
Hospital No.	NYK		

REASON FOR REFERRAL PRIVATE KARYOTYPE  
Research sample.

**REPORT**

KARYOTYPE 46,XX

Apparently normal female karyotype in the 10 cells examined.

Please note that the quality of the preparations obtained was suitable for the detection of aneuploidy and major structural abnormalities only.

Authorised By *SES*

Copies to



**NORWICH CYTOGENETICS SERVICE**

Telephone 01603 286038  
Fax 01603 286839  
Email sandra.edwards@nnuh.nhs.uk

Cytogenetics Department  
Norfolk and Norwich University Hospital  
Colney Lane  
NORWICH  
NR4 7UY

Dr K Bowles  
Consultant Haematologist  
Norfolk & Norwich University Hospital  
Colney Lane  
NORWICH  
NR4 7UY

**CHROMOSOME ANALYSIS - CULTURED CELLS**

PATIENT DETAILS		SAMPLE DETAILS	
Surname	BMMSC	Lab. No.	P16-0930
Other Name	1040	Date of Receipt	04/07/2016
Date of Birth	04/07/2016	Date of Report	29/07/2016
Hospital No.	NYK		


REASON FOR REFERRAL PRIVATE KARYOTYPE  
Research sample.

**REPORT**

KARYOTYPE 46,XY

Apparently normal male karyotype in the 10 cells examined.

Please note that the quality of the preparations obtained was unsuitable for the detection of subtle chromosomal abnormalities.

Authorised By 

Copies to

**Table 2: AML, BMSC and AML/BMSC cytokine array data sets**

Cytokine array blots were analysed for mean optical densities using HImage++ software. Outputs are presented in the tables below. AML only refers to AML cell culture control, BMSC only refers to BMSC cell culture control.







## **Copies of publications arising from this thesis**

Attached are the following publications:

**A. Abdul-Aziz**, M. Shafat, T. Mehta, F. Di Palma, M. Lawes, S. Rushworth, K.M. Bowles, MIF-Induced Stromal PKC $\beta$ /IL8 Is Essential in Human Acute Myeloid Leukaemia, *Cancer Research* (2017). DOI: 10.1158/0008-5472.CAN-16-1095.

**A. Abdul-Aziz**, D.J. MacEwan, K.M. Bowles, S.A. Rushworth, Oxidative Stress Responses and NRF2 in Human Leukaemia, *Oxidative Medicine and Cellular Longevity* (2015). DOI: 10.1155/2015/454659.



## Review Article

# Oxidative Stress Responses and NRF2 in Human Leukaemia

Amina Abdul-Aziz,<sup>1</sup> David J. MacEwan,<sup>2</sup> Kristian M. Bowles,<sup>1,3</sup> and Stuart A. Rushworth<sup>1</sup>

<sup>1</sup>Norwich Medical School, University of East Anglia, Norwich Research Park, Norwich NR4 7UQ, UK

<sup>2</sup>Department of Molecular & Clinical Pharmacology, Institute of Translational Medicine, University of Liverpool, Liverpool L69 3GE, UK

<sup>3</sup>Department of Haematology, Norfolk and Norwich University Hospitals National Health Service Trust, Norwich NR4 7UY, UK

Correspondence should be addressed to Stuart A. Rushworth; [s.rushworth@uea.ac.uk](mailto:s.rushworth@uea.ac.uk)

Received 11 December 2014; Revised 15 March 2015; Accepted 20 March 2015

Academic Editor: Victor M. Victor

Copyright © 2015 Amina Abdul-Aziz et al. This is an open access article distributed under the Creative Commons Attribution License, which permits unrestricted use, distribution, and reproduction in any medium, provided the original work is properly cited.

Oxidative stress as a result of elevated levels of reactive oxygen species (ROS) has been observed in almost all cancers, including leukaemia, where they contribute to disease development and progression. However, cancer cells also express increased levels of antioxidant proteins which detoxify ROS. This includes glutathione, the major antioxidant in human cells, which has recently been identified to have dysregulated metabolism in human leukaemia. This suggests that critical balance of intracellular ROS levels is required for cancer cell function, growth, and survival. Nuclear factor (erythroid-derived 2)-like 2 (NRF2) transcription factor plays a dual role in cancer. Primarily, NRF2 is a transcription factor functioning to protect nonmalignant cells from malignant transformation and oxidative stress through transcriptional activation of detoxifying and antioxidant enzymes. However, once malignant transformation has occurred within a cell, NRF2 functions to protect the tumour from oxidative stress and chemotherapy-induced cytotoxicity. Moreover, inhibition of the NRF2 oxidative stress pathway in leukaemia cells renders them more sensitive to cytotoxic chemotherapy. Our improved understanding of NRF2 biology in human leukaemia may permit mechanisms by which we could potentially improve future cancer therapies. This review highlights the mechanisms by which leukaemic cells exploit the NRF2/ROS response to promote their growth and survival.

## 1. Introduction

Acute myeloid leukaemia (AML) is primarily a disease of the elderly with 75% of cases being diagnosed in patients over 60 years of age [1]. AML comprises a biologically heterogeneous group of disorders that occur as a consequence of a wide variety of genetic abnormalities in haematopoietic progenitors that are derived from the bone marrow. In fitter, generally younger patients complete remission can be achieved only in a minority with current chemotherapeutic regimens. Patients who are not fit for intensive chemotherapy are generally managed with a palliative approach without a chance of cure. Furthermore, even in patients who do achieve remission following intensive chemotherapy many relapse from the persistence of a small clone of minimal residual disease [2, 3] and, despite considerable efforts over the last 30 years to develop and improve therapy, presently two-thirds of younger adults and 90% of older adults still die of their

disease [4]. It is envisaged that improved outcomes for all patients will now only come from novel treatment strategies (beyond increasing doses of conventional cytotoxic drugs) derived from an improved understanding of the biology of the disease.

## 2. Oxidative Stress

Oxidative stress is described as a change in the balance between reactive oxygen species and antioxidant defence mechanisms, where the balance is disturbed for the support of the oxidants [5]. Together, oxidants and antioxidants are essential for normal cellular function including metabolism and signal transduction which allow for the maintenance of cellular homeostasis [6, 7]. However, oxidative stress, if unconstrained, results in the damage of important cellular components which may result in DNA mutations or cell death.

Reactive oxygen species (ROS) are oxygen-containing chemical species with reactive properties, including free radicals such as superoxide and nonradical molecules such as hydrogen peroxide [8]. These reactive species result from both endogenous and exogenous cellular sources. Endogenous sources of cellular ROS include oxidative phosphorylation within mitochondria, which results in the formation of dioxygen, which is normally reduced to water but in some instances is partially reduced to form superoxide. Further reduction reactions can subsequently give rise to hydrogen peroxide [9, 10], which has long been thought of as a harmful molecule; however, recently, new evidence has emerged which suggests that at low concentrations hydrogen peroxide acts as an intracellular signaling molecule involved in survival and proliferation mechanism. In contrast, exogenous ROS is produced by many environmental mediators which have demonstrated involvement in a number of pathological states including cardiovascular disease [11], chronic inflammation [12], and neurodegenerative diseases [13] as well as cancer [14].

### 3. Reactive Oxygen Species

There is a complex interaction between ROS generation, signaling, and toxicity that results in the initiation, growth, and survival of cancer. Cancer may be induced through oxidative damage to cellular macromolecules as a result of overproduction of ROS, which subsequently affects antioxidant and/or DNA repair mechanisms [15]. In addition, ROS can stimulate signal transduction pathways leading to activation of key protumoural transcription factors [16]. Once the malignant state has been established, the same cellular survival mechanisms that the cell had employed to protect against tumorigenesis are subsequently subverted to support a protumoural state and protect the cancer cells from chemotherapy. ROS have a physiological cellular response to trigger cellular inflammation and damage that may lead to cell death. This protective effect is lost in cancer cells and thus endogenous and exogenous efforts to induce cytotoxicity may also be lost in cancer. Specifically in human leukaemia the NRF2 pathway appears central to the control of the redox state functioning at least in part through its regulation of glutathione synthesis and regeneration. It is envisaged that the identification of tumour-specific dependence within this pathway may ultimately be exploited to develop much needed new treatments.

### 4. Acute Myeloid Leukaemia

AML develops from a common myeloid progenitor, a cell which would physiologically differentiate to form monocytes, granulocytes, platelets, and erythrocytes in the bone marrow [17, 18]. AML is the most common acute leukaemia affecting adults, and its incidence increases with age [19]. However, AML is a heterogeneous disease driven by a wide variety of genetic lesions [20]. In patients fit enough for conventional intensive cytotoxic chemotherapy, the treatment destroys actively cycling leukaemic cells and initial remission rates

are high. However, in these patients following remission induction and despite in many cases the disease becoming undetectable by current testing technologies, a subpopulation of cells with leukaemic stem cell properties frequently survives chemotherapy and it is this subpopulation (minimal residual disease) that is responsible for the relapse commonly encountered in this disease [21]. In patients not fit for such cytotoxic chemotherapy, management is presently based around palliation and symptom control.

The discovery of specific mutant genes in AML has provided increased biologic understanding, new potential targets for drug development [22], and new diagnostic methods for detection of minimal residual disease [23, 24]. For instance, mutations of the FMS-like tyrosine kinase-3 (FLT3) receptor (internal tandem duplication (ITD)) are found in approximately 25% of new cases of AML [25, 26]. FLT3-ITD has been found to cause increased levels of ROS within murine Ba/F3 or 32D cells expressing FLT3-ITD as well as MOLM-14 and MV-4-11 human AML cell lines which carry FLT3-ITD mutations [27], suggesting that ROS are important in regulating FLT3 mutated AML.

### 5. Manipulation of the Redox Status by Leukaemia Oncogenes

A number of oncogenes such as KRAS, cMYC, BCR/ABL, NRF2, and NF- $\kappa$ B (NF- $\kappa$ B) are able to alter the redox balance of human cancer cells including leukaemic cells [26, 28–32]. The oncogenic BCR/ABL fusion gene found mainly in chronic myeloid leukaemia (CML) is capable of inducing ROS levels in both human and murine cell lines [33, 34]. Moreover, BCR/ABL-induced ROS can also result in signaling changes including the upregulation of the nonreceptor tyrosine kinase FYN [35, 36]. FYN deficiency in the presence of BCR/ABL expression is a mediator of chronic myeloid leukaemia (CML) proliferation and CML resistance to the drug of choice for CML, the BCR/ABL inhibitor, imatinib. Together, these findings illustrate how a cancer associated tyrosine kinase can induce ROS resulting in leukaemia proliferation and drug resistance.

It has also been described that leukaemic oncogenes may also affect the transcription, stability, or activity of antioxidant proteins within leukaemic cells. For example, BCR/ABL and NF- $\kappa$ B can increase the transcription of NRF2 and by association its regulated genes, which have been shown to have cytoprotective properties. Furthermore, activation of NRF2 requires a phosphorylation process which results in the stabilisation of NRF2 and its release from its negative regulator allowing transcription of the antioxidant genes [37]. The transcription factor NRF2 is activated by increased oxidative stress inducing protection of normal cells against electrophilic and oxidative stress [38]. This provides an example of transcriptional pathways by which leukaemic oncogenes can influence the redox environment of leukaemia cells and represent possible targets for therapeutic intervention.

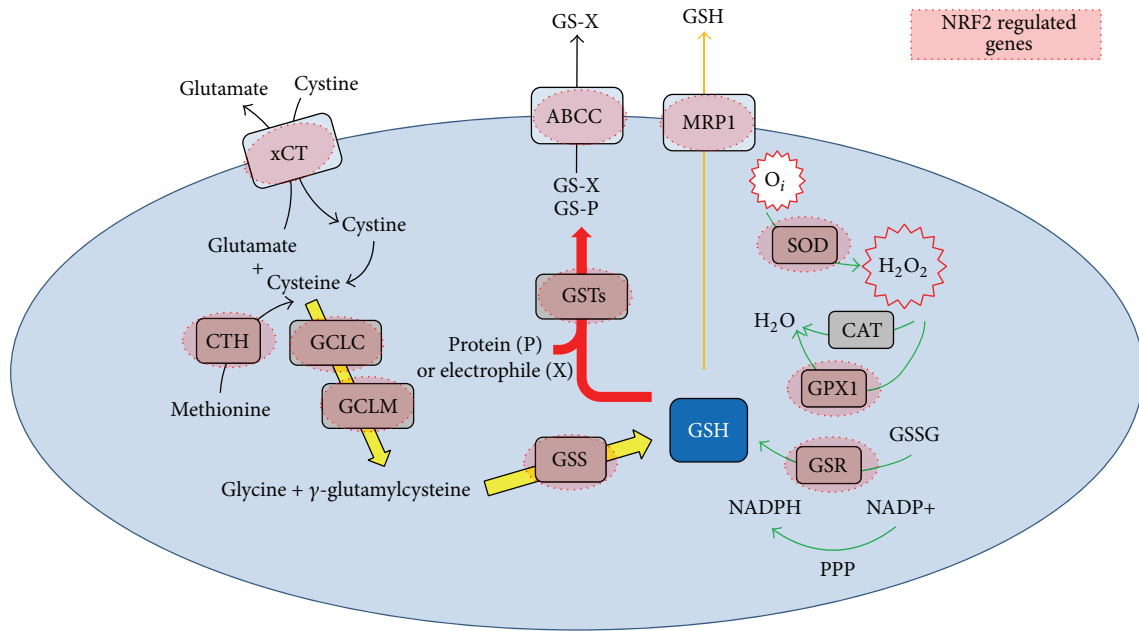


FIGURE 1: Glutathione synthesis as seen through NRF2. GSH is a two-step synthesis reaction catalysed by glutamate-cysteine ligase (GCL) and GSH synthetase. GSH is consumed in many ways, such as by oxidation or conjugation. In addition, cells may lose GSH due to export of its reduced, oxidized, or conjugated forms and intracellular GSH is regenerated via reduction at the expense of one NADPH molecule. Highlighted in red are the genes regulated by NRF2 activity.

## 6. NRF2 Regulated Cellular Antioxidants in Leukaemia

Our research has previously shown that current standard AML chemotherapy (cytarabine and daunorubicin) induces an increase in ROS in AML cells as part of their mechanism of cytotoxic action [39]. Furthermore, we also recently reported that malignant blasts from AML patients have inappropriate constitutive NRF2 activation, resulting in increased cell survival and chemotherapy resistance [40, 41]. The NRF2 signaling pathway is a major cellular pathway that under normal conditions protects nonmalignant cells against electrophilic and oxidative stress [38]; however, in AML as well as many other malignancies, including chronic lymphocytic leukaemia (CLL), NRF2 is constitutively activated [42]. In AML, constitutive activation of NRF2 occurs not through somatic mutation of NRF2 or its inhibitor KEAP1 but as a result of upstream constitutive activation of NF- $\kappa$ B.

NRF2 regulates the expression of over 200 genes including many antioxidant genes and phase II enzymes such as heme oxygenase-1 (HO-1) and NAD(P)H: quinone oxidoreductase 1 (NQO1) [43, 44] and genes involved in glutathione metabolism and regeneration [45–48]. No single gene induced by NRF2 can be identified as the most important for cell protection, as cell protection is a result of the coordinated induction of NRF2 target genes. As well as the work on AML, NRF2 genes have also been dysregulated in other human blood cancers including CLL and multiple myeloma (MM). In CLL, experiments show the presence of NRF2 signaling and suggest that altered NRF2 responses may contribute to the observed selective cytotoxicity of electrophilic

compounds in this disease [49]. In MM, HO-1 is increased in bortezomib-resistant MM cells, suggesting a possible role for HO-1 and NRF2 in chemotherapy resistance [50]. Together these results highlight the importance of NRF2 in human blood cancer.

**6.1. Glutathione Metabolism, Regeneration, and Control of ROS.** GSH has emerged as an important regulator of chemotherapy resistance in human cancer. GSH is present in all mammalian tissues at 1–10 millimolar concentrations and protects against oxidative stress [51]. In the cell GSH exists in the thiol-reduced GSH and disulfide-oxidized (GSSG) forms [52] and its major reservoir is the cytosol (80–85%) [53–55]. GSH synthesis occurs via a two-step ATP-requiring enzymatic process and exerts a negative feedback inhibition on key rate limiting enzymes including glutathione cysteine ligase (GCL) [56, 57] either by phosphorylation or by protein expression [58]. The regulation of GSH synthesis is under tight control involving key enzymes including GCL, GSH synthetase, and GSH reductase. More importantly these enzymes are all regulated, at least in part, by NRF2 through its activation of the ARE [59]. This highlights the importance of addressing the link between NRF2 and GSH in disease, especially leukaemia. Figure 1 shows the link between NRF2 and GSH synthesis and regeneration.

It is becoming apparent that NRF2 is the main transcription factor that controls the regulation of many aspects of GSH synthesis and regeneration [60, 61]. Importantly the regulation of GCL at the transcriptional level is essential for the maintenance of GSH homeostasis in response to oxidative stress. In addition, levels of GCLC and GCLM are

decreased in NRF2 knockout mice; the resulting lack of GSH synthesis is lethal during embryogenesis [62]. Moreover, GSH synthetase which catalyses the second step of GSH generation is also regulated by NRF2 and overexpression of either NRF1 or NRF2 induced the GSS promoter activity by 130 and 168%, respectively. Other genes involved in GSH metabolism, regeneration, and function are also regulated by NRF2 activation, which include GSH S-transferases (GSTs), GSH reductase (GR), and GSH peroxidase (GPX) [48, 63, 64]. Together, this information suggests that NRF2 controls the effectiveness of GSH to combat the excess of ROS.

Hydrogen peroxide is one of the main activators of the NRF2-KEAP1 pathway. It is metabolised by GPX in the cytosol resulting in GSH being oxidized to GSSG in the mitochondria. GSSG can be reduced back to GSH by GR at the expense of NADPH, thereby forming a redox cycle, where organic peroxides can be reduced by either GPX or GSH S-transferase (GST) [65]. GSTs are a family of phase II conjugation enzymes under the regulation of the NRF2/ARE pathway [66]. The main role of GST is to catalyse the detoxification of various harmful compounds [67]. This detoxification process is under the tight control of NRF2 as GST mRNA and protein expression are decreased in NRF2-null mice, and NRF2 is required for GST induction [68]. Moreover, the mRNA expression of GST is markedly increased in KEAP1-null mice [69]. This provides evidence that not only GSTs but also many other enzymes that are involved in GSH synthesis and regeneration are coordinately regulated by NRF2 and justifies the necessity to address the NRF2 GSH axis in human cancers, especially leukaemia.

**6.2. NRF2, GSH, and Leukaemic Cell Survival.** Although NRF2 is protective against tumorigenesis by reducing the amount of ROS and DNA damage in cells, tumour cells were found to be capable of harnessing the protective function of NRF2 for their own protection and survival [42, 70]. Indeed, NRF2 activity itself is elevated in some leukaemia types where it contributes to leukaemogenesis [71]. Elevated nuclear localization of NRF2 and the subsequent genetic changes result in reduced sensitivity to proteasome inhibitors in AML cell lines [41], suggesting that NRF2 may also regulate sensitivity to ROS-producing therapeutic agents. Moreover, molecular analyses have revealed that treatment with stress inducers (e.g., tumour necrosis factor) results in increased NRF2 activity in THP-1, HL-60, and AML 193 cell lines, which in turn increases the transcription of antioxidants [72].

Primitive hematopoietic stem and progenitor cells reside within the bone marrow and express the CD34 surface antigen [73, 74]. Moreover, primitive AML cells also generally express CD34 and are more resistant to chemotherapy [74, 75]. A recent study by Pei et al. evaluates the characteristics of primary CD34+ cells derived from patients with AML in comparison to normal CD34+ controls [76]. This is consistent with the finding that CLL cells have elevated levels of reactive oxygen species (ROS) compared to normal controls [77]. Taken together, this suggests that altered GSH content might be a common property of primary hematopoietic malignant tissues.

The prognostic value of GST deletions in adult AML, including individuals with GSTM1 or GSTT1 deletions (or deletions of both), is found to have enhanced resistance to chemotherapy, lower complete remission, and a shorter survival [78]; this further supports the suggestion of a disturbed glutathione metabolism in AML cells. AML cells have elevated expression of multiple GSH metabolising enzymes including GCL and GST compared to control CD34+ cells and knockdown of GCLC or GPX1 impaired the growth of leukaemic cells in vitro [76]. Moreover, a significantly decreased GSH to GSSG ratio further indicates aberrant glutathione homeostasis in AML cells; this is consistent with findings of increased basal levels of nuclear NRF2 in primary AMLs [41]. This highly suggests that increased NRF2 activity in AML cells is responsible for the elevated expression of these genes as a mechanism by which AML cells compensate for increased oxidative stress in leukaemic cells. The aberrant glutathione metabolism presents a unique and potentially useful asset for targeting of primitive leukaemic cells.

## 7. Conclusion

ROS play an important functional role in human leukaemia. NRF2 and its control of GSH regulate ROS. Recent data suggests that GSH is fundamental to NRF2 function in AML suggesting that this pathway may yield future therapeutic targets for leukaemia cells in which GSH is dysregulated.

## Abbreviations

ABCC/MRP1:	Multidrug resistance proteins
AML:	Acute myeloid leukaemia
GSR:	GSH reductase
GPX1:	GSH peroxidase
GST:	GSH S-transferase
NADPH:	Nicotinamide adenine dinucleotide phosphate
ATP:	Adenosine triphosphate
ADP:	Adenosine diphosphate
H <sub>2</sub> O <sub>2</sub> :	Hydrogen peroxide
GCL:	Glutamate-cysteine ligase
ROS:	Reactive oxygen species
NRF2:	Nuclear factor (erythroid-derived 2)-like 2
FR:	Free radicals
RNS:	Reactive nitrogen species
CML:	Chronic myeloid leukaemia.

## Conflict of Interests

The authors declare that there is no conflict of interests regarding the publication of this paper.

## Acknowledgments

The authors wish to thank Worldwide Cancer Research, National Institutes for Health Research (Flexibility and Sustainability Funding), and The Big C. Amina Abdul-Aziz is funded by a Ph.D. studentship from the Department of

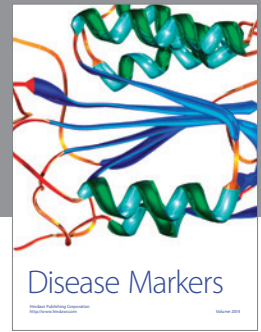
Higher Education and Scientific Research of the Libyan government.

## References

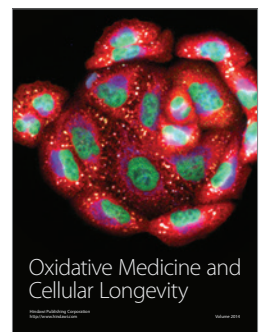
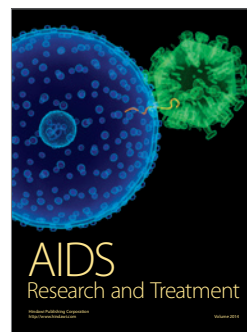
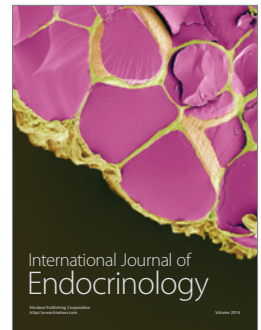
- [1] G. Juliusson, P. Antunovic, Å. Derolf et al., "Age and acute myeloid leukemia: Real world data on decision to treat and outcomes from the Swedish Acute Leukemia Registry," *Blood*, vol. 113, no. 18, pp. 4179–4187, 2009.
- [2] F. Buccisano, L. Maurillo, M. I. del Principe et al., "Prognostic and therapeutic implications of minimal residual disease detection in acute myeloid leukemia," *Blood*, vol. 119, no. 2, pp. 332–341, 2012.
- [3] K. J. Hope, L. Jin, and J. E. Dick, "Acute myeloid leukemia originates from a hierarchy of leukemic stem cell classes that differ in self-renewal capacity," *Nature Immunology*, vol. 5, no. 7, pp. 738–743, 2004.
- [4] J. M. Rowe and M. S. Tallman, "How I treat acute myeloid leukemia," *Blood*, vol. 116, no. 17, pp. 3147–3156, 2010.
- [5] H. Sies, "Oxidative stress: from basic research to clinical application," *The American Journal of Medicine*, vol. 91, no. 3, supplement 3, pp. S31–S38, 1991.
- [6] B. Halliwell, "How to characterize a biological antioxidant," *Free Radical Research Communications*, vol. 9, no. 1, pp. 1–32, 1990.
- [7] B. Halliwell, "Free radicals, proteins and DNA: oxidative damage versus redox regulation," *Biochemical Society Transactions*, vol. 24, no. 4, pp. 1023–1027, 1996.
- [8] A. M. Shah and K. M. Channon, "Free radicals and redox signalling in cardiovascular disease," *Heart*, vol. 90, no. 5, pp. 486–487, 2004.
- [9] M. Saraste, "Oxidative phosphorylation at the fin de siècle," *Science*, vol. 283, no. 5407, pp. 1488–1493, 1999.
- [10] K. J. Davies, "Oxidative stress: the paradox of aerobic life," *Biochemical Society Symposium*, vol. 61, pp. 1–31, 1995.
- [11] D. J. Reuland, J. M. McCord, and K. L. Hamilton, "The role of Nrf2 in the attenuation of cardiovascular disease," *Exercise and Sport Sciences Reviews*, vol. 41, no. 3, pp. 162–168, 2013.
- [12] S. Singh, S. Vrishni, B. K. Singh, I. Rahman, and P. Kakkar, "Nrf2-ARE stress response mechanism: a control point in oxidative stress-mediated dysfunctions and chronic inflammatory diseases," *Free Radical Research*, vol. 44, no. 11, pp. 1267–1288, 2010.
- [13] C. P. Ramsey, C. A. Glass, M. B. Montgomery et al., "Expression of Nrf2 in neurodegenerative diseases," *Journal of Neuropathology & Experimental Neurology*, vol. 66, no. 1, pp. 75–85, 2007.
- [14] J. E. Klaunig, Y. Xu, J. S. Isenberg et al., "The role of oxidative stress in chemical carcinogenesis," *Environmental Health Perspectives*, vol. 106, supplement 1, pp. 289–295, 1998.
- [15] D. Ziech, R. Franco, A. Pappa, and M. I. Panayiotidis, "Reactive Oxygen Species (ROS)—induced genetic and epigenetic alterations in human carcinogenesis," *Mutation Research/Fundamental and Molecular Mechanisms of Mutagenesis*, vol. 711, no. 1-2, pp. 167–173, 2011.
- [16] A. K. Jaiswal, "Nrf2 signaling in coordinated activation of antioxidant gene expression," *Free Radical Biology and Medicine*, vol. 36, no. 10, pp. 1199–1207, 2004.
- [17] K. Akashi, D. Traver, T. Miyamoto, and I. L. Weissman, "A clonogenic common myeloid progenitor that gives rise to all myeloid lineages," *Nature*, vol. 404, no. 6774, pp. 193–197, 2000.
- [18] D. G. Tenen, R. Hromas, J. D. Licht, and D.-E. Zhang, "Transcription factors, normal myeloid development, and leukemia," *Blood*, vol. 90, no. 2, pp. 489–519, 1997.
- [19] B. Löwenberg, J. R. Downing, and A. Burnett, "Acute myeloid leukemia," *The New England Journal of Medicine*, vol. 341, no. 14, pp. 1051–1062, 1999.
- [20] J. Radich, "The molecular biology of acute myeloid leukemia," in *Advances in Malignant Hematology*, pp. 86–102, Wiley-Blackwell, 2011.
- [21] F. Ishikawa, S. Yoshida, Y. Saito et al., "Chemotherapy-resistant human AML stem cells home to and engraft within the bone-marrow endosteal region," *Nature Biotechnology*, vol. 25, no. 11, pp. 1315–1321, 2007.
- [22] M. S. Tallman, D. G. Gilliland, and J. M. Rowe, "Drug therapy for acute myeloid leukemia," *Blood*, vol. 106, no. 4, pp. 1154–1163, 2005.
- [23] S. Schnittger, C. Schoch, M. Dugas et al., "Analysis of FLT3 length mutations in 1003 patients with acute myeloid leukemia: correlation to cytogenetics, FAB subtype, and prognosis in the AMLCG study and usefulness as a marker for the detection of minimal residual disease," in *Proceedings of the 42nd Annual Meeting of the American Society of Hematology*, vol. 100, pp. 59–66, San Francisco, Calif, USA, December 2002, abstract 3569.
- [24] P. Gorello, G. Cazzaniga, F. Alberti et al., "Quantitative assessment of minimal residual disease in acute myeloid leukemia carrying *nucleophosmin* (NPM1) gene mutations," *Leukemia*, vol. 20, no. 6, pp. 1103–1108, 2006.
- [25] P. D. Kottaridis, R. E. Gale, M. E. Frew et al., "The presence of a FLT3 internal tandem duplication in patients with acute myeloid leukemia (AML) adds important prognostic information to cytogenetic risk group and response to the first cycle of chemotherapy: analysis of 854 patients from the United Kingdom Medical Research Council AML 10 and 12 trials," *Blood*, vol. 98, no. 6, pp. 1752–1759, 2001.
- [26] T. Kindler, D. B. Lipka, and T. Fischer, "FLT3 as a therapeutic target in AML: still challenging after all these years," *Blood*, vol. 116, no. 24, pp. 5089–5102, 2010.
- [27] A. Sallmyr, J. Fan, K. Datta et al., "Internal tandem duplication of FLT3 (FLT3/ITD) induces increased ROS production, DNA damage, and misrepair: implications for poor prognosis in AML," *Blood*, vol. 111, no. 6, pp. 3173–3182, 2008.
- [28] J. L. Bos, "*ras* Oncogenes in human cancer: a review," *Cancer Research*, vol. 49, no. 17, pp. 4682–4689, 1989.
- [29] X. Dolcet, D. Llobet, J. Pallares, and X. Matias-Guiu, "NF- $\kappa$ B in development and progression of human cancer," *Virchows Archiv*, vol. 446, no. 5, pp. 475–482, 2005.
- [30] A. B. Raitano, J. R. Halpern, T. M. Hambuch, and C. L. Sawyers, "The Bcr-Abl leukemia oncogene activates Jun kinase and requires Jun for transformation," *Proceedings of the National Academy of Sciences of the United States of America*, vol. 92, no. 25, pp. 11746–11750, 1995.
- [31] H. Kiyoi, T. Naoe, Y. Nakano et al., "Prognostic implication of FLT3 and N-RAS gene mutations in acute myeloid leukemia," *Blood*, vol. 93, no. 9, pp. 3074–3080, 1999.
- [32] J. E. Roderick, J. Tesell, L. D. Shultz et al., "c-Myc inhibition prevents leukemia initiation in mice and impairs the growth of relapsed and induction failure pediatric T-ALL cells," *Blood*, vol. 123, no. 7, pp. 1040–1050, 2014.
- [33] M. Sattler, S. Verma, G. Shrikhande et al., "The BCR/ABL tyrosine kinase induces production of reactive oxygen species in hematopoietic cells," *The Journal of Biological Chemistry*, vol. 275, no. 32, pp. 24273–24278, 2000.

- [34] J. H. Kim, S. C. Chu, J. L. Gramlich et al., "Activation of the PI3K/mTOR pathway by BCR-ABL contributes to increased production of reactive oxygen species," *Blood*, vol. 105, no. 4, pp. 1717–1723, 2005.
- [35] K. Ban, Y. Gao, H. M. Amin et al., "BCR-ABL1 mediates up-regulation of Fyn in chronic myelogenous leukemia," *Blood*, vol. 111, no. 5, pp. 2904–2908, 2008.
- [36] Y. Gao, A. Howard, K. Ban, and J. Chandra, "Oxidative stress promotes transcriptional up-regulation of Fyn in BCR-ABL1-expressing cells," *The Journal of Biological Chemistry*, vol. 284, no. 11, pp. 7114–7125, 2009.
- [37] M. McMahan, K. Itoh, M. Yamamoto, and J. D. Hayes, "Keap1-dependent proteasomal degradation of transcription factor Nrf2 contributes to the negative regulation of antioxidant response element-driven gene expression," *The Journal of Biological Chemistry*, vol. 278, no. 24, pp. 21592–21600, 2003.
- [38] E. Kansanen, S. M. Kuosmanen, H. Leinonen, and A.-L. Levonen, "The Keap1-Nrf2 pathway: mechanisms of activation and dysregulation in cancer," *Redox Biology*, vol. 1, no. 1, pp. 45–49, 2013.
- [39] S. A. Heasman, L. Zaitseva, K. M. Bowles, S. A. Rushworth, and D. J. MacEwan, "Protection of acute myeloid leukaemia cells from apoptosis induced by front-line chemotherapeutics is mediated by haem oxygenase-1," *Oncotarget*, vol. 2, no. 9, pp. 658–668, 2011.
- [40] S. A. Rushworth, L. Zaitseva, M. Y. Murray, N. M. Shah, K. M. Bowles, and D. J. MacEwan, "The high Nrf2 expression in human acute myeloid leukemia is driven by NF- $\kappa$ B and underlies its chemo-resistance," *Blood*, vol. 120, no. 26, pp. 5188–5198, 2012.
- [41] S. A. Rushworth, K. M. Bowles, and D. J. MacEwan, "High basal nuclear levels of Nrf2 in acute myeloid leukemia reduces sensitivity to proteasome inhibitors," *Cancer Research*, vol. 71, no. 5, pp. 1999–2009, 2011.
- [42] J. D. Hayes and M. McMahan, "NRF2 and KEAP1 mutations: permanent activation of an adaptive response in cancer," *Trends in Biochemical Sciences*, vol. 34, no. 4, pp. 176–188, 2009.
- [43] B. N. Chorley, M. R. Campbell, X. Wang et al., "Identification of novel NRF2-regulated genes by ChIP-Seq: influence on retinoid X receptor alpha," *Nucleic Acids Research*, vol. 40, no. 15, pp. 7416–7429, 2012.
- [44] Y.-S. Keum, Y.-H. Han, C. Liew et al., "Induction of heme oxygenase-1 (HO-1) and NAD[P]H: quinone oxidoreductase 1 (NQO1) by a phenolic antioxidant, butylated hydroxyanisole (BHA) and its metabolite, tert-butylhydroquinone (tBHQ) in primary-cultured human and rat hepatocytes," *Pharmaceutical Research*, vol. 23, no. 11, pp. 2586–2594, 2006.
- [45] A. C. Wild, J. J. Gipp, and R. T. Mulcahy, "Overlapping antioxidant response element and PMA response element sequences mediate basal and  $\beta$ -naphthoflavone-induced expression of the human  $\gamma$ -glutamylcysteine synthetase catalytic subunit gene," *Biochemical Journal*, vol. 332, part 2, pp. 373–381, 1998.
- [46] A. C. Wild, H. R. Moinova, and R. T. Mulcahy, "Regulation of  $\gamma$ -glutamylcysteine synthetase subunit gene expression by the transcription factor Nrf2," *The Journal of Biological Chemistry*, vol. 274, no. 47, pp. 33627–33636, 1999.
- [47] H. Sasaki, H. Sato, K. Kuriyama-Matsumura et al., "Electrophile response element-mediated induction of the cystine/glutamate exchange transporter gene expression," *The Journal of Biological Chemistry*, vol. 277, no. 47, pp. 44765–44771, 2002.
- [48] C. J. Harvey, R. K. Thimmulappa, A. Singh et al., "Nrf2-regulated glutathione recycling independent of biosynthesis is critical for cell survival during oxidative stress," *Free Radical Biology and Medicine*, vol. 46, no. 4, pp. 443–453, 2009.
- [49] R. P. Wu, T. Hayashi, H. B. Cottam et al., "Nrf2 responses and the therapeutic selectivity of electrophilic compounds in chronic lymphocytic leukemia," *Proceedings of the National Academy of Sciences of the United States of America*, vol. 107, no. 16, pp. 7479–7484, 2010.
- [50] L. N. Barrera, S. A. Rushworth, K. M. Bowles, and D. J. MacEwan, "Bortezomib induces heme oxygenase-1 expression in multiple myeloma," *Cell Cycle*, vol. 11, no. 12, pp. 2248–2252, 2012.
- [51] P. J. Ansell, S.-C. Lo, L. G. Newton et al., "Repression of cancer protective genes by 17 $\beta$ -estradiol: ligand-dependent interaction between human Nrf2 and estrogen receptor alpha," *Molecular and Cellular Endocrinology*, vol. 243, no. 1-2, pp. 27–34, 2005.
- [52] N. Kaplowitz, T. Y. Aw, and M. Ookhtens, "The regulation of hepatic glutathione," *Annual Review of Pharmacology and Toxicology*, vol. 25, pp. 715–744, 1985.
- [53] M. J. Meredith and D. J. Reed, "Status of the mitochondrial pool of glutathione in the isolated hepatocyte," *The Journal of Biological Chemistry*, vol. 257, no. 7, pp. 3747–3753, 1982.
- [54] C. Hwang, A. J. Sinskey, and H. F. Lodish, "Oxidized redox state of glutathione in the endoplasmic reticulum," *Science*, vol. 257, no. 5076, pp. 1496–1502, 1992.
- [55] L. Yuan and N. Kaplowitz, "Glutathione in liver diseases and hepatotoxicity," *Molecular Aspects of Medicine*, vol. 30, no. 1-2, pp. 29–41, 2009.
- [56] S. C. Lu, "Regulation of hepatic glutathione synthesis: current concepts and controversies," *The FASEB Journal*, vol. 13, no. 10, pp. 1169–1183, 1999.
- [57] C. C. Franklin, D. S. Backos, I. Mohar, C. C. White, H. J. Forman, and T. J. Kavanagh, "Structure, function, and post-translational regulation of the catalytic and modifier subunits of glutamate cysteine ligase," *Molecular Aspects of Medicine*, vol. 30, no. 1-2, pp. 86–98, 2009.
- [58] W.-M. Sun, Z.-Z. Huang, and S. C. Lu, "Regulation of  $\gamma$ -glutamylcysteine synthetase by protein phosphorylation," *Biochemical Journal*, vol. 320, no. 1, pp. 321–328, 1996.
- [59] P. Xue, Y. Hou, Y. Chen et al., "Adipose deficiency of Nrf2 in ob/ob mice results in severe metabolic syndrome," *Diabetes*, vol. 62, no. 3, pp. 845–854, 2013.
- [60] Y. Chen, H. G. Shertzer, S. N. Schneider, D. W. Nebert, and T. P. Dalton, "Glutamate cysteine ligase catalysis: dependence on ATP and modifier subunit for regulation of tissue glutathione levels," *The Journal of Biological Chemistry*, vol. 280, no. 40, pp. 33766–33774, 2005.
- [61] Y. Yang, M. Z. Dieter, Y. Chen, H. G. Shertzer, D. W. Nebert, and T. P. Dalton, "Initial characterization of the glutamate-cysteine ligase modifier subunit Gclm(-/-) knockout mouse. Novel model system for a severely compromised oxidative stress response," *The Journal of Biological Chemistry*, vol. 277, no. 51, pp. 49446–49452, 2002.
- [62] J. Y. Chan and M. Kwong, "Impaired expression of glutathione synthetic enzyme genes in mice with targeted deletion of the Nrf2 basic-leucine zipper protein," *Biochimica et Biophysica Acta—Gene Structure and Expression*, vol. 1517, no. 1, pp. 19–26, 2000.
- [63] A. Singh, T. Rangasamy, R. K. Thimmulappa et al., "Glutathione peroxidase 2, the major cigarette smoke-inducible isoform of GPX in lungs, is regulated by Nrf2," *The American Journal of*

- Respiratory Cell and Molecular Biology*, vol. 35, no. 6, pp. 639–650, 2006.
- [64] R. K. Thimmulappa, K. H. Mai, S. Srisuma, T. W. Kensler, M. Yamamoto, and S. Biswal, “Identification of Nrf2-regulated genes induced by the chemopreventive agent sulforaphane by oligonucleotide microarray,” *Cancer Research*, vol. 62, no. 18, pp. 5196–5203, 2002.
- [65] J. Nordberg and E. S. J. Arnér, “Reactive oxygen species, antioxidants, and the mammalian thioredoxin system,” *Free Radical Biology and Medicine*, vol. 31, no. 11, pp. 1287–1312, 2001.
- [66] K. Itoh, T. Chiba, S. Takahashi et al., “An Nrf2/small Maf heterodimer mediates the induction of phase II detoxifying enzyme genes through antioxidant response elements,” *Biochemical and Biophysical Research Communications*, vol. 236, no. 2, pp. 313–322, 1997.
- [67] R. N. Armstrong, “Glutathione S-transferases: reaction mechanism, structure, and function,” *Chemical Research in Toxicology*, vol. 4, no. 2, pp. 131–140, 1991.
- [68] L. E. Huang, Z. Arany, D. M. Livingston, and H. F. Bunn, “Activation of hypoxia-inducible transcription factor depends primarily upon redox-sensitive stabilization of its  $\alpha$  subunit,” *Journal of Biological Chemistry*, vol. 271, no. 50, pp. 32253–32259, 1996.
- [69] S. A. Reisman, I. I. Csanaky, L. M. Aleksunes, and C. D. Klaassen, “Altered disposition of acetaminophen in Nrf2-null and keap1-knockdown mice,” *Toxicological Sciences*, vol. 109, no. 1, pp. 31–40, 2009.
- [70] X.-J. Wang, Z. Sun, N. F. Villeneuve et al., “Nrf2 enhances resistance of cancer cells to chemotherapeutic drugs, the dark side of Nrf2,” *Carcinogenesis*, vol. 29, no. 6, pp. 1235–1243, 2008.
- [71] S. A. Rushworth, D. J. MacEwan, and M. A. O’Connell, “Lipopolysaccharide-induced expression of NAD(P)H:quinone oxidoreductase 1 and heme oxygenase-1 protects against excessive inflammatory responses in human monocytes,” *The Journal of Immunology*, vol. 181, no. 10, pp. 6730–6737, 2008.
- [72] S. A. Rushworth and D. J. MacEwan, “HO-1 underlies resistance of AML cells to TNF-induced apoptosis,” *Blood*, vol. 111, no. 7, pp. 3793–3801, 2008.
- [73] D. S. Krause, M. J. Fackler, C. I. Civin, and W. S. May, “CD34: structure, biology, and clinical utility,” *Blood*, vol. 87, no. 1, pp. 1–13, 1996.
- [74] A. Blair, D. E. Hogge, and H. J. Sutherland, “Most acute myeloid leukemia progenitor cells with long-term proliferative ability *in vitro* and *in vivo* have the phenotype CD34<sup>+</sup>/CD71<sup>-</sup>/HLA-DR<sup>-</sup>,” *Blood*, vol. 92, no. 11, pp. 4325–4335, 1998.
- [75] R. T. Costello, F. Mallet, B. Gaugler et al., “Human acute myeloid leukemia CD34<sup>+</sup>/CD38<sup>-</sup> progenitor cells have decreased sensitivity to chemotherapy and Fas-induced apoptosis, reduced immunogenicity, and impaired dendritic cell transformation capacities,” *Cancer Research*, vol. 60, no. 16, pp. 4403–4411, 2000.
- [76] S. Pei, M. Minhajuddin, K. P. Callahan et al., “Targeting aberrant glutathione metabolism to eradicate human acute myelogenous leukemia cells,” *The Journal of Biological Chemistry*, vol. 288, no. 47, pp. 33542–33558, 2013.
- [77] D. Trachootham, H. Zhang, W. Zhang et al., “Effective elimination of fludarabine-resistant CLL cells by PEITC through a redox-mediated mechanism,” *Blood*, vol. 112, no. 5, pp. 1912–1922, 2008.
- [78] M. T. Voso, F. D’Alo, R. Putzulu et al., “Negative prognostic value of glutathione S-transferase (GSTM1 and GSTT1) deletions in adult acute myeloid leukemia,” *Blood*, vol. 100, no. 8, pp. 2703–2707, 2002.



**Hindawi**  
Submit your manuscripts at  
<http://www.hindawi.com>





## MIF-Induced Stromal PKC $\beta$ /IL8 Is Essential in Human Acute Myeloid Leukemia

Amina M. Abdul-Aziz<sup>1</sup>, Manar S. Shafat<sup>1</sup>, Tarang K. Mehta<sup>2</sup>, Federica Di Palma<sup>2</sup>, Matthew J. Lawes<sup>3</sup>, Stuart A. Rushworth<sup>1</sup>, and Kristian M. Bowles<sup>1,3</sup>

### Abstract

Acute myeloid leukemia (AML) cells exhibit a high level of spontaneous apoptosis when cultured *in vitro* but have a prolonged survival time *in vivo*, indicating that tissue microenvironment plays a critical role in promoting AML cell survival. *In vitro* studies have shown that bone marrow mesenchymal stromal cells (BM-MSCs) protect AML blasts from spontaneous and chemotherapy-induced apoptosis. Here, we report a novel interaction between AML blasts and BM-MSCs, which benefits AML proliferation and survival. We initially examined the cytokine profile in cultured human AML compared with AML cultured with BM-MSCs and found that macrophage migration inhibitory factor (MIF) was highly expressed by

primary AML, and that IL8 was increased in AML/BM-MSCs cocultures. Recombinant MIF increased IL8 expression in BM-MSCs via its receptor CD74. Moreover, the MIF inhibitor ISO-1 inhibited AML-induced IL8 expression by BM-MSCs as well as BM-MSCs-induced AML survival. Protein kinase C  $\beta$  (PKC $\beta$ ) regulated MIF-induced IL8 in BM-MSCs. Finally, targeted IL8 shRNA inhibited BM-MSCs-induced AML survival. These results describe a novel, bidirectional, prosurvival mechanism between AML blasts and BM-MSCs. Furthermore, they provide biologic rationale for therapeutic strategies in AML targeting the microenvironment, specifically MIF and IL8. *Cancer Res*; 77(2); 303–11. ©2016 AACR.

### Introduction

Survival of patients with acute myeloid leukemia (AML) is presently poor; two thirds of young adults and 90% of older adults die of their disease (1). Even in patients who achieve remission with chemotherapy, relapse is common and occurs from minimal residual disease sequestered in protective niches in the bone marrow microenvironment (2). Accordingly, it is envisaged that improved outcomes will come from novel treatment strategies derived from an improved understanding of the biology of AML within the bone marrow microenvironment.

AML cells exhibit a high level of spontaneous apoptosis when cultured *in vitro* but have a prolonged survival time *in vivo*, indicating that the tissue microenvironment plays a critical role in promoting AML cell survival (3–6). Knowledge of the complexity of the bone marrow microenvironment is increasing, especially with respect to the bone marrow mesenchymal stromal

cells (BM-MSCs), which are considered a major protective cell type (7). BM-MSCs generate various factors whose primary functions are to influence tumor cell survival and homing (4, 8, 9). The apoptotic defect in AML is not cell autonomous but highly dependent on extrinsic signals derived from their microenvironment. The complex cell–cell interactions between the AML tumor cells and their microenvironment are therefore essential for tumor growth and survival and thus present an attractive target for novel drug therapies.

Macrophage migration inhibitory factor (MIF) is a pleiotropic cytokine, which under normal conditions regulates cell-mediated immunity and inflammation (10). In cancer, MIF is overexpressed in a number of solid tumors, including breast, prostate, and colon cancers (11–13). MIF has also been shown to be overexpressed in various blood cancers, including chronic lymphocytic leukemia (CLL; ref. 14). In CLL, MIF is expressed by the malignant cells and induces protective IL8 release in an autocrine-dependent manner. Blocking either MIF or IL8 reduces survival of CLL. The increased secretion of IL8 from tumor cells is thought to have wider significance to the tumor microenvironment. Serum IL8 is known to be higher in patients with AML, myelodysplasia (MDS), and non-Hodgkin lymphoma than in normal controls, and levels of IL8 in these patients are similar to those found in patients with multiple organ failure of nonseptic origin (15, 16). Furthermore, leukemic blasts from the majority of patients with AML constitutively express IL8 (17). In addition, inhibition of the IL8 receptor, CXCR2, selectively inhibits proliferation of MDS/AML cell lines and patient samples (18). Together, these studies suggest that MIF and IL8 are functionally important in regulating the survival and proliferation of multiple tumors, including AML.

In the current study, we investigate how AML cells program BM-MSCs via MIF to produce the survival cytokine IL8 and

<sup>1</sup>Department of Molecular Haematology, Norwich Medical School, University of East Anglia, Norwich, United Kingdom. <sup>2</sup>The Genome Analysis Centre (TGAC), Colney, Norwich, United Kingdom. <sup>3</sup>Department of Haematology, Norfolk and Norwich University Hospitals NHS Trust, Norwich, United Kingdom.

**Note:** Supplementary data for this article are available at Cancer Research Online (<http://cancerres.aacrjournals.org/>).

S.A. Rushworth and K.M. Bowles are co-senior authors of this article.

**Corresponding Authors:** S.A. Rushworth, University of East Anglia, Norwich Research Park, Norwich, Norfolk NR4 7TJ, United Kingdom. Phone: 075-4725-4801; Fax: 016-0359-3752; E-mail: s.rushworth@uea.ac.uk; and Kristian M. Bowles, k.bowles@uea.ac.uk.

**doi:** 10.1158/0008-5472.CAN-16-1095

©2016 American Association for Cancer Research.

Abdul-Aziz et al.

characterize the signaling pathways underlying this interdependent cell–cell communication.

## Materials and Methods

### Materials

Anti-PKC, MAPK, and AKT antibodies were purchased from Cell Signaling Technology. Anti-CD74, anti-CXCR2, and anti-CXCR4 antibodies were purchased from Miltenyi Biotec. All inhibitors were purchased from Tocris. The CD74 blocking antibody was purchased from BD Biosciences. Proteome Profiler Human XL array and recombinant human MIF were purchased from R&D Systems. MIF ELISA was purchased from BioLegend. IL8 ELISA was purchased from eBioscience. All other reagents were obtained from Sigma-Aldrich.

### Cell culture

For primary cell isolation, heparinized blood was collected from volunteers, and human peripheral blood mononuclear cells were isolated by Histopaque (Sigma-Aldrich) density gradient centrifugation. AML samples that comprised less than 80% blasts were purified using the CD34 Positive Selection Kit. Cell type was confirmed by microscopy and flow cytometry. BM-MSCs were isolated by bone marrow aspirates from AML patients. Mononuclear cells were collected by gradient centrifugation and plated in growth medium containing DMEM and 20% FBS and 1% L-glutamine. The nonadherent cells were removed after 2 days. When 60% to 80% confluent, adherent cells were trypsinized and expanded for 3 to 5 weeks. BM-MSCs were checked for positive expression of CD105, CD73, and CD90 (BM-MSC markers) and the lack of expression of CD45 and CD34 by flow cytometry. All patient information, including genotype and WHO classification for AML and genotype and phenotype of AML BM-MSCs, are included in Supplementary Tables S1 and S2.

### RNA extraction and real-time PCR

Total RNA was extracted from  $5 \times 10^5$  cells using the Nucleic Acid PrepStation from Applied Biosystems, according to the manufacturer's instructions. Reverse transcription was performed using the RNA PCR Core Kit (Applied Biosystems). Relative qRT-PCR used SYBR Green technology (Roche) on cDNA generated from the reverse transcription of purified RNA. After preamplification (95°C for 2 minutes), the PCRs were amplified for 45 cycles (95°C for 15 seconds and 60°C for 10 seconds and 72°C for 10 seconds) on a 384-well LightCycler 480 (Roche). Each mRNA expression was normalized against GAPDH mRNA expression using the standard curve method.

### Western immunoblotting and ELISAs

SDS-PAGE and Western blot analyses were performed. Briefly, whole-cell lysates were extracted and SDS-PAGE separation was performed. Protein was transferred to nitrocellulose membrane and Western blot analysis performed with the indicated antisera according to their manufacturer's guidelines. To examine MIF and IL8 secretion into media, we used LEGEND MAX Human Active MIF ELISA Kit (BioLegend) and Human IL-8 ELISA Ready-SET-Go (eBioscience).

### shRNA silencing of CD74, PKC $\beta$ , and IL8

Five Mission shRNA targeted lentivirus particles (Sigma-Aldrich) for each target were obtained. BM-MSCs ( $2 \times 10^4$  cells) were infected with each lentivirus. For all gene expression experi-

ments, the cells were incubated for 72 hours posttransfection before RNA extraction.

### Flow cytometry

Flow cytometry for measuring AML cell number was performed on the Cube 6 (Sysmex Partec). For the AML/BM-MSC cocultures, AML cell viability was measured using flow cytometry. After exclusion of BM-MSCs by electronic gating using forward scatter, AML cells were counted using CD34 gating.

### Cytokine array expression analysis

Primary AML blasts  $0.25 \times 10^6$  were cultured alone or cocultured on confluent primary BM-MSCs. Conditioned medium was then collected from these cultures as well as from BM-MSC culture and analyzed using the Proteome Profiler Human XL Cytokine Array following the manufacturer's instructions. Quantification of cytokine optical densities was obtained with the HLIimage++ software (WesternVision).

### Statistical analyses

The Mann–Whitney *U* test was used to compare test groups where stated. Results where  $P < 0.05$  were considered statistically significant. Results represent the mean  $\pm$  SD of four or more independent experiments. We generated statistics with GraphPad Prism 5 software (GraphPad). For Western blotting, data are representative images of three independent experiments.

### Study approval

AML cells and BM-MSCs were obtained from AML patient bone marrow or blood following informed consent and under approval from the UK National Research Ethics Service (LRECref07/H0310/146).

## Results

### BM-MSCs support AML survival

The microenvironment supports AML survival and proliferation (4, 5, 19). To study the cell–cell communication between BM-MSCs and AML cells, we established a coculture system using primary AML cells and BM-MSCs derived from treatment-naïve AML patients. Here, we show a significant difference in primary AML survival when cultured on BM-MSCs for 6 and 14 days compared with AML blast survival when cultured in basal media alone (Fig. 1A; Supplementary Fig. S1). Supplementary Figure S2 shows the different combinations of AML and BM-MSCs in all experiments.

To determine what factors are responsible for improved primary AML blast survival on BM-MSCs, we analyzed the profile of cytokines and chemokines present in primary AML cultures, BM-MSC cultures, and primary AML blasts cultured in combination with BM-MSCs. Cytokine array profiles of the three culture conditions (Fig. 1B) show a consistent upregulation of IL8 in the coculture sample media (Fig. 1C). Moreover, we also observed high levels of MIF in all AML supernatants, low levels of MIF in all BM-MSC supernatants, and high levels of MIF in the AML/BM-MSC cocultures (Fig. 1B and D). To verify these observations, we carried out IL8- and MIF-specific ELISAs. IL8 concentrations peak at 8 and 24 hours in the AML/BM-MSC coculture supernatants (Fig. 1E), whereas MIF concentrations were high and at similar levels in AML culture supernatants and AML/BM-MSC coculture supernatants (Fig. 1F).

**Figure 1.**

BM-MSCs support AML survival.

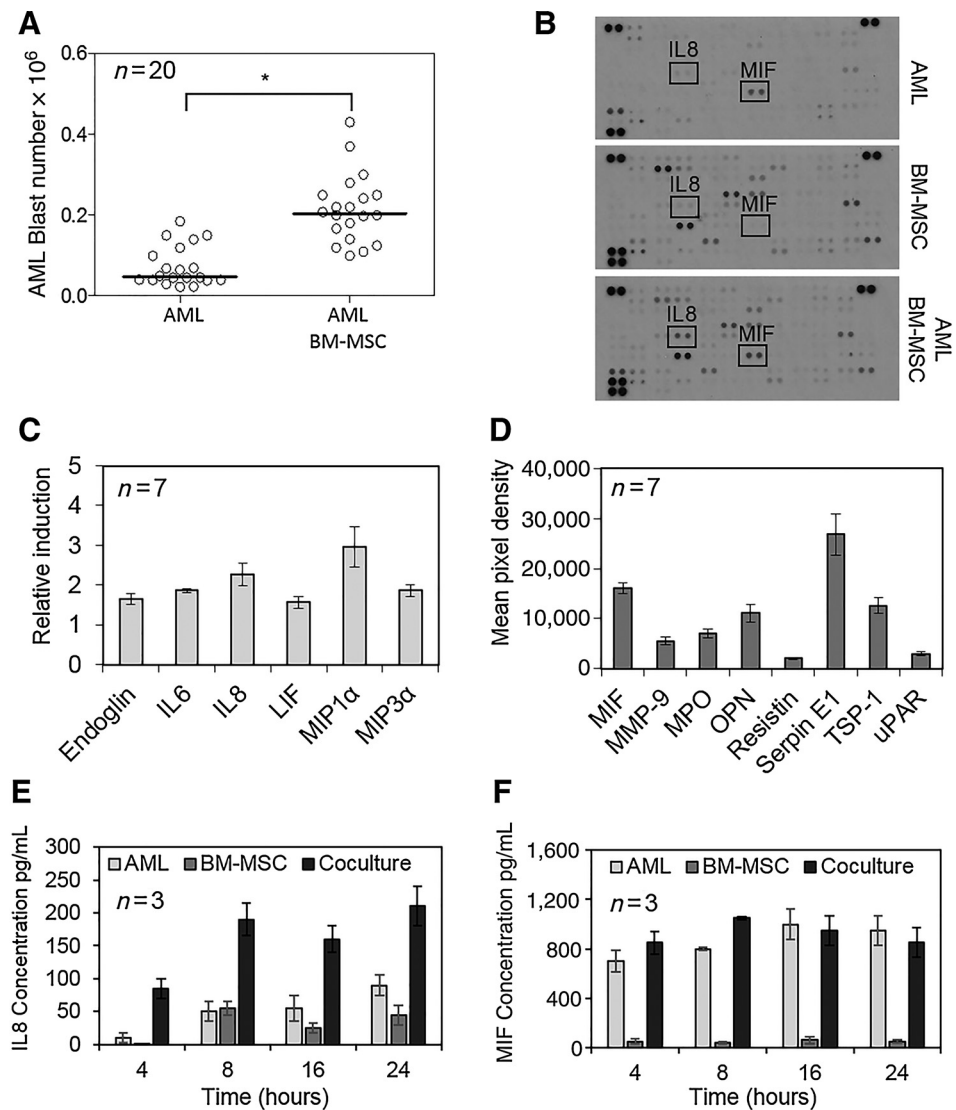
**A**, AML blasts ( $0.25 \times 10^6$ ) were cocultured with primary BM-MSCs on a 12-well plate for 6 days ( $n = 20$ ); AML blast number was assessed using Trypan blue exclusion hemocytometer-based counts and CD34<sup>+</sup> staining using flow cytometry.

**B**, Cell-free supernatants from 7 individual AML patient blasts ( $0.25 \times 10^6$ ) were cocultured with primary BM-MSCs for 24 hours and a representative cytokine antibody array of each of the cell culture conditioned media using the Human Cytokine Proteome Profiler Array.

**C**, Fold induction of cytokines between BM-MSCs and AML cultured on BM-MSCs. Results from 7 different primary AML on four different BM-MSCs. Bars, mean and SEM. Significantly upregulated cytokines are included in the graph.

**D**, Quantification of cytokine optical density of AML only arrays (7 individual AML samples). Graph shows the top 8 cytokines expressed by AML. Bars, mean and SEM.

**E**, IL8 ELISA of each of the cell culture conditioned media from various time points (three individual AML samples). **F**, MIF ELISA of each of the cell culture conditioned media from various time points (three individual AML samples). The Mann-Whitney *U* test was used to compare between treatment groups (\*,  $P < 0.05$ ).



#### AML-derived MIF induces IL8 expression in BM-MSCs

Next, we looked to determine whether BM-MSCs needed direct contact with AML to increase IL8 expression. RT-PCR showed that IL8 mRNA from BM-MSCs incubated with AML increased by 57-fold when in direct contact and by 50-fold when in indirect contact with AML blasts (Fig. 2A). This confirms that direct tumor cell to stromal cell contact is not necessary for AML to induce increased IL8 expression by BM-MSCs.

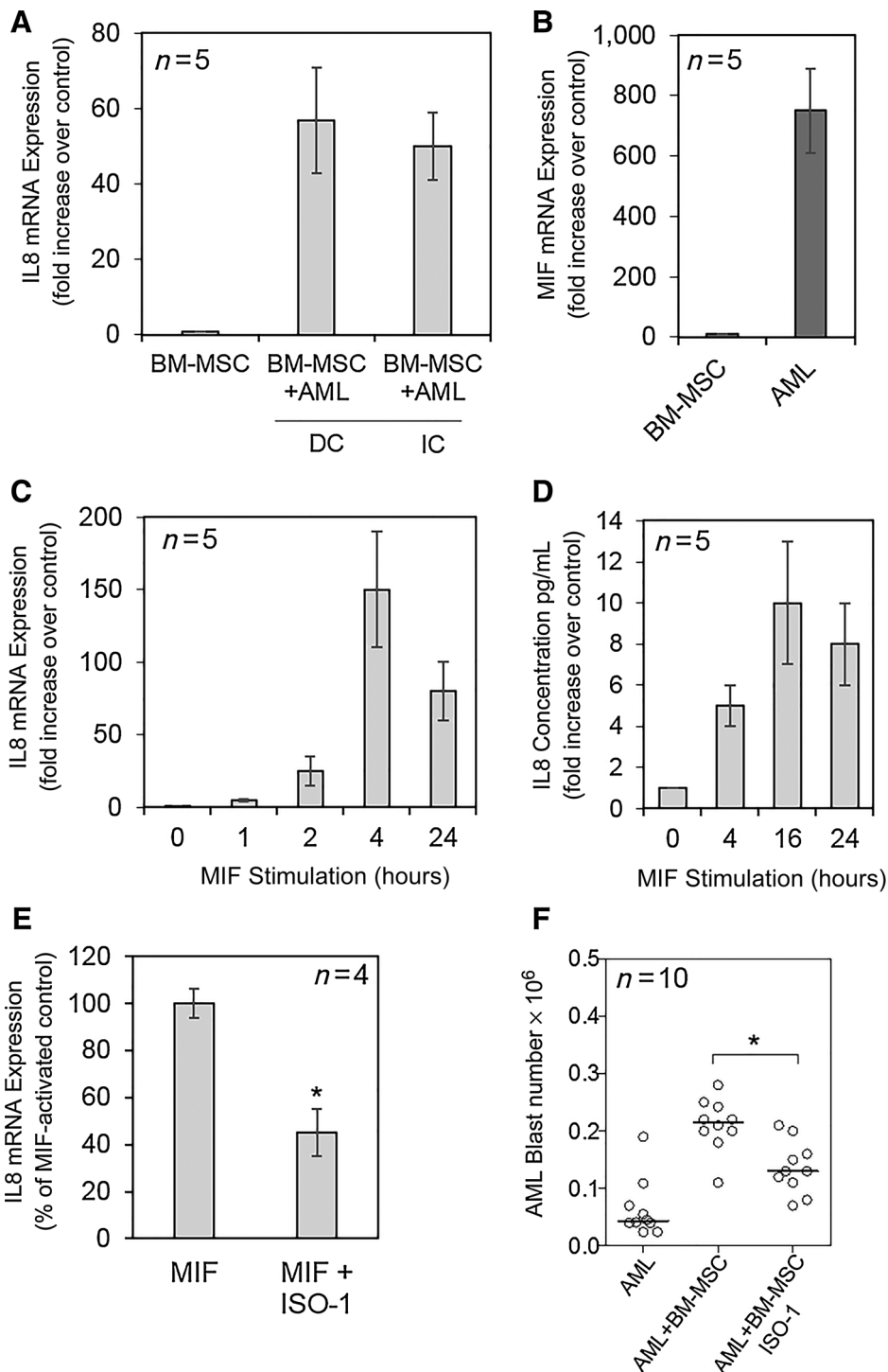
Next, we examined the mRNA expression levels of MIF in primary AML ( $n = 5$ ) and BM-MSC ( $n = 5$ ) cultures. RT-PCR showed that primary AML cultures, but not BM-MSC cultures, express high levels of MIF mRNA under normal basal conditions (Fig. 2B). As MIF expression has been shown to be increased in AML patients compared with normal patients (20) and the ability of MIF to induce IL8 production by primary CLL (14), we hypothesized that MIF from AML was responsible for the increased IL8 expression in BM-MSCs. To test this hypothesis, we stimulated BM-MSCs with 100ng/mL recombinant human MIF and assayed for IL8 mRNA and protein expression over a

period of 24 hours. We show that IL8 mRNA and protein increased (Fig. 2C and D) in response to MIF. To confirm that MIF secreted from AML cells regulates IL8 expression, we used ISO-1, a nontoxic inhibitor of MIF, which functions by binding to bioactive MIF at its N-terminal tautomerase site (21). MIF-stimulated BM-MSCs pretreated with ISO-1 showed a decrease in IL8 mRNA levels compared with untreated BM-MSCs (Fig. 2E). Moreover, AML survival was inhibited when cultured with BM-MSCs in the presence of ISO-1 compared with control AML-BM-MSC cultures (Fig. 2F). Together, these data confirm that MIF secreted by AML cells induces IL8 expression in BM-MSCs.

#### MIF-induced IL8 upregulation is mediated through CD74

Depending on the cellular context and the disease involved, MIF signaling is mediated by its receptors CXCR2 (IL8 receptor, ILR8) and/or CXCR4 (stromal-derived factor 1 receptor), and/or CD74 (22, 23). BM-MSCs have been reported to express all three receptors (24–26). Using CD105 as a BM-MSC marker to confirm mesenchymal cell phenotype, we show that CD74 and CXCR4 are expressed but CXCR2 is not expressed on

Abdul-Aziz et al.

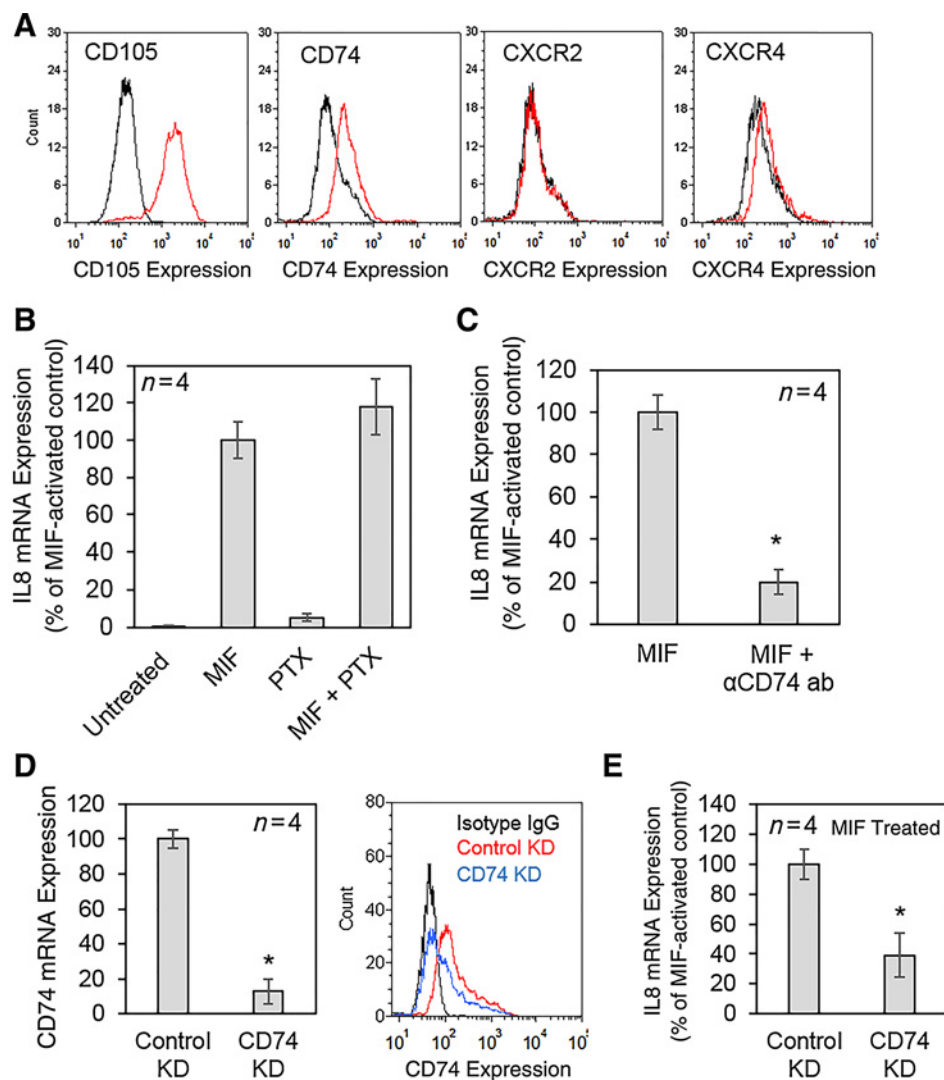
**Figure 2.**

AML-derived MIF induces IL8 expression in BM-MSCs. **A**, AML blasts from 5 patients ( $0.25 \times 10^6$ ) were cocultured with primary BM-MSCs either in direct contact (DC) or indirect contact (IC, transwell insert) for 24 hours. IL8 mRNA in BM-MSCs was then assessed by real-time PCR. mRNA expression was normalized to GAPDH mRNA levels ( $n = 5$ ). **B**, BM-MSCs and primary AML from 5 patients were cultured alone and measured for MIF mRNA levels ( $n = 5$ ). mRNA expression was normalized to GAPDH mRNA levels ( $n = 5$ ). **C**, BM-MSCs from 5 patients were treated with rhMIF (100 ng/mL) for indicated times, and then extracted RNA was assessed for IL8 mRNA by real-time PCR. mRNA expression was normalized to GAPDH mRNA levels ( $n = 5$ ). **D**, BM-MSCs from 5 patients were treated with rhMIF (100 ng/mL) for indicated times, and then, media were assessed for IL8 protein expression by ELISA. ( $n = 5$ ). **E**, BM-MSCs from four patients were pretreated with ISO-1 (10  $\mu\text{mol/L}$ ) for 5 minutes before treatment with rhMIF (100 ng/mL) for 4 hours and then assessed for IL8 mRNA expression ( $n = 4$ ). **F**, BM-MSCs were pretreated with ISO-1 (10  $\mu\text{mol/L}$ ) for 5 minutes before the addition of primary AML blasts from 10 patient samples for 48 hours. AML blast number was assessed using Trypan blue exclusion hemocytometer-based counts ( $n = 10$ ). The Mann-Whitney  $U$  test was used to compare between treatment groups (\*,  $P < 0.05$ ).

all primary BM-MSCs isolated from AML patients (Fig. 3A). BM-MSCs were further characterized using CD73 and CD90, and lack of CD45 expression.

We used specific inhibitors of CXCR2, CXCR4, and CD74 to determine which receptor/s were responsible for MIF-induced IL8 upregulation. Inhibition of CXCR2 and CXCR4 using pertussis toxin (a GPCR inhibitor) had no effect on MIF-induced IL8 mRNA expression (Fig. 3B). However, the anti-

CD74 blocking antibody inhibited MIF-induced IL8 expression in BM-MSCs (Fig. 3C). These results suggest that CD74 is the dominant receptor in regulating MIF-induced IL8 expression in AML patient-derived BM-MSCs. To further characterize this interaction, we used lentiviral-mediated knockdown (KD) of CD74 in AML patient-derived BM-MSCs, confirming reduced mRNA and protein expression of CD74 after transduction with control KD or CD74 KD lentivirus (Fig. 3D). Furthermore, we

**Figure 3.**

MIF-induced IL8 upregulation is mediated through CD74. **A**, BM-MSCs were assessed for CD105, CD74, CXCR2, and CXCR4 using flow cytometry. **B** and **C**, BM-MSCs from four patient samples were pretreated with the GPCR inhibitor pertussis toxin (PTX; 100 ng/mL) or for CD74 (αCD74 ab; 10 μg/mL) for 30 minutes before being stimulated with MIF for 4 hours. RNA was extracted and assessed for IL8 mRNA by real-time PCR. mRNA expression was normalized to GAPDH mRNA levels ( $n = 4$ ). **D**, BM-MSCs from four patient samples were infected with control shRNA or CD74 shRNA for 72 hours and analyzed for CD74 mRNA expression by RT-PCR and protein expression by flow cytometry. **E**, BM-MSCs from four patient samples were infected with control shRNA or CD74 shRNA for 72 hours and then treated with recombinant MIF and analyzed for IL8 mRNA expression by RT-PCR. The Mann-Whitney  $U$  test was used to compare between treatment groups (\*,  $P < 0.05$ ).

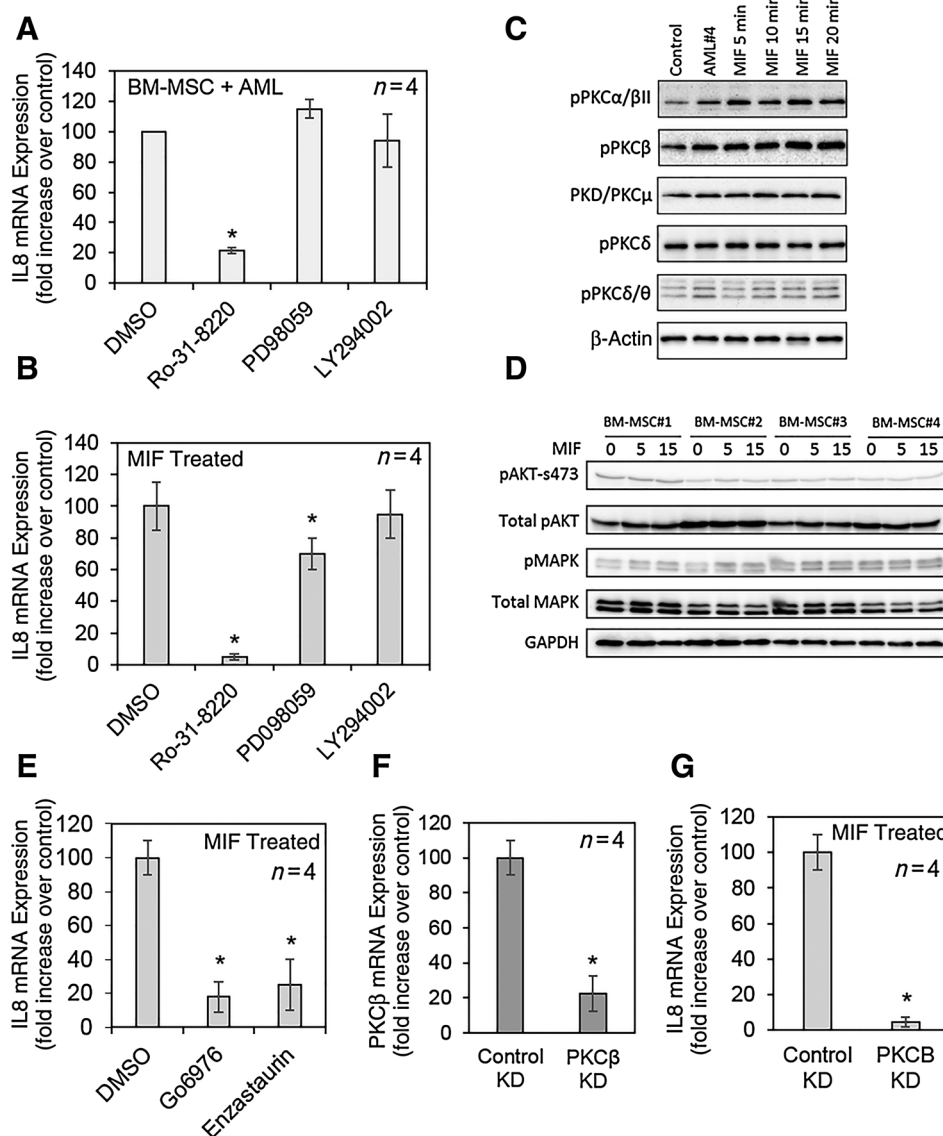
demonstrate that CD74 knockdown inhibits MIF-induced IL8 mRNA expression in AML patient-derived BM-MSCs (Fig. 3E).

#### Pharmacologic inhibition of PKC $\beta$ inhibits MIF-induced IL8 induction in BM-MSCs

We next investigated the signaling cascade in AML patient-derived BM-MSCs downstream of MIF-induced CD74 activation. It has been shown that MIF binding to CD74 activates downstream signaling through the PI3K/protein kinase B (AKT) and MAPK signaling pathways and promotes cell proliferation and survival (27). In addition, Lutzny and colleagues recently described the activation of a PKC pathway in murine stromal cells cocultured with chronic lymphocytic leukemia (28). We treated AML-stimulated BM-MSCs with LY294002 (a PI3K/Akt inhibitor), PD098059 [a MAPK kinase (MEK) 1 inhibitor], or Ro-31-8220 (a PKC pan inhibitor) to determine which pathway/s regulate AML-induced BM-MSC IL8 mRNA induction. We show that Ro-31-8220, the PKC inhibitor, was able to significantly inhibit IL8 expression by approximately 80%, whereas LY294002 and PD098059 had little or no effect (Fig. 4A). Similarly, we found that Ro-31-8220 was able to

inhibit IL8 expression by circa 90% in experiments where BM-MSCs were directly activated using recombinant human MIF (rhMIF; rather than AML cells; Fig. 4B). However, in addition, we observed that PD98059 was able to moderately inhibit rhMIF-induced IL8 mRNA induction in BM-MSCs by approximately 30% (Fig. 4B).

To clarify whether PKC, MAPK, or both are activated in response to MIF, we performed Western blot analysis on BM-MSCs for specific phosphorylation of PKC isoforms, MAPK, or AKT in response to MIF activation. BM-MSCs were activated by AML for 15 minutes or MIF treatment (100 ng/mL) for various times. We initially show that MIF and AML both induce phosphorylation of PKC  $\alpha/\beta$  and PKC  $\beta$  in BM-MSCs (Fig. 4C). BM-MSCs from 4 patient samples treated with MIF had no increase in phosphorylation of AKT and MAPK (Fig. 4D). Next, the PKC isoform-specific inhibitors, Go6976 (PKC $\alpha/\beta$ ) and enzastaurin (PKC $\beta$ ), were used to block MIF-induced IL8 expression in BM-MSCs. Both inhibitors showed inhibition of MIF-induced IL8 upregulation (Fig. 4E). Finally, we used lentiviral-mediated KD for PKC $\beta$ , confirming reduced mRNA expression of PKC $\beta$  after transduction of BM-MSCs with control KD or PKC $\beta$  KD virus (Fig. 4F). We then

**Figure 4.**

Inhibition of PKC $\beta$  regulates AML-derived MIF-induced IL8 mRNA induction in BM-MSCs. **A**, BM-MSCs from four patients samples were pretreated with Ro-31-8220 (1  $\mu$ mol/L), PD98059 (10  $\mu$ mol/L), and LY294002 (10  $\mu$ mol/L) and then incubated with primary AML blast for 4 hours. RNA was extracted and assessed for IL8 mRNA by real-time PCR. mRNA expression was normalized to GAPDH mRNA levels ( $n = 4$ ). **B**, BM-MSCs from four different samples were pretreated with Ro-31-8220 (250 nmol/L), PD98059 (10  $\mu$ mol/L), and LY294002 (10  $\mu$ mol/L) and then incubated with MIF for 4 hours. RNA was extracted and assessed for IL8 mRNA by real-time PCR. mRNA expression was normalized to GAPDH mRNA levels ( $n = 4$ ). **C**, BM-MSCs were cultured with AML for 15 minutes or recombinant MIF (100 ng/mL) for various times. Protein was extracted and Western blotting performed. Blots were probed for pPKC $\alpha/\beta$ II, pPKC $\beta$ , PKD/PKC $\mu$ , PKC $\delta$ , and PKC $\delta/\theta$ . Blots were then reprobated for  $\beta$ -actin to show equal sample loading. **D**, Four different BM-MSCs with recombinant MIF (100 ng/mL) at various times. Protein was extracted and Western blotting performed. Blots were probed for pAKT and pMAPK as well as total AKT and total MAPK. Blots were then reprobated for  $\beta$ -actin to show equal sample loading. **E**, Four different BM-MSCs were pretreated with Go 6976 (1  $\mu$ mol/L) and enzastaurin (1  $\mu$ mol/L) and then incubated with MIF for 4 hours. RNA was extracted and assessed for IL8 mRNA by real-time PCR. mRNA expression was normalized to GAPDH mRNA levels ( $n = 4$ ). **F**, Four different BM-MSCs were infected with control shRNA or PKC $\beta$  shRNA for 72 hours and analyzed for PKC $\beta$  mRNA expression by RT-PCR. **G**, Four different BM-MSCs were infected with control shRNA or PKC $\beta$  shRNA for 72 hours, then treated with recombinant MIF and analyzed for IL8 mRNA expression by RT-PCR. The Mann-Whitney  $U$  test was used to compare between treatment groups (\*,  $P < 0.05$ ).

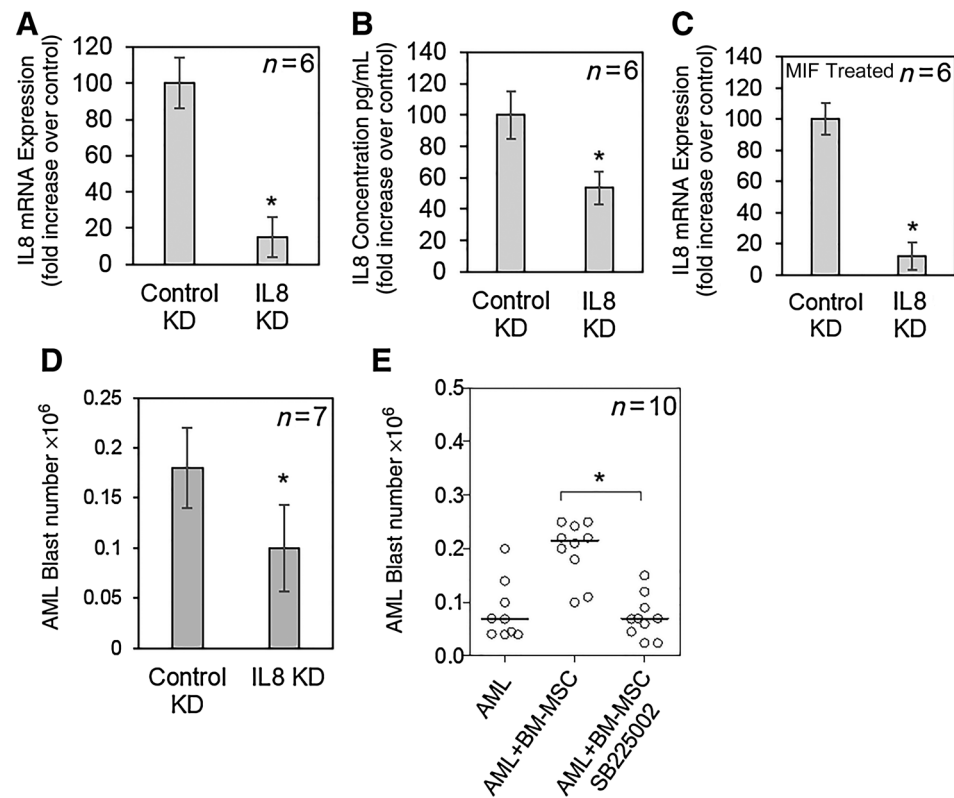
demonstrate that knockdown of PKC $\beta$  inhibits MIF-induced IL8 mRNA expression (Fig. 4G). Together, these results confirm that MIF-induced IL8 expression in AML patient-derived BM-MSCs requires PKC $\beta$ .

#### Targeting the MIF-PKC $\beta$ -IL8 axis disrupts BM-MSC-induced protection of primary human AML blasts

Finally, to examine the effect of blocking IL8 on BM-MSC protection and survival of primary AML blasts, we cocultured

**Figure 5.**

Targeting MIF-PKC-IL8 axis in AML disrupts BM-MSc-derived protection. **A** and **B**, BM-MSCs from six samples were infected with control shRNA or IL8 shRNA for 72 hours and analyzed for IL8 mRNA expression by RT-PCR and protein expression by ELISA. **C**, BM-MSCs from six samples were infected with control shRNA or IL8 shRNA for 72 hours and then treated with recombinant MIF and analyzed for IL8 mRNA expression by RT-PCR. **D**, BM-MSCs were infected with control shRNA or IL8 shRNA for 72 hours and cocultured with AML blasts from seven samples for 48 hours. AML blast number was assessed using Trypan blue exclusion hemocytometer-based counts ( $n = 7$ ). **E**, BM-MSCs were pretreated with SB225002 (100 nmol/L) for 30 minutes before the addition of primary AML blasts from 10 samples for 48 hours. AML blast number was assessed using Trypan blue exclusion hemocytometer-based counts. The Mann-Whitney  $U$  test was used to compare between treatment groups (\*,  $P < 0.05$ ).



primary AML blasts derived from treatment-naïve AML patients with BM-MSCs (either control KD or IL8 KD). First, we used lentiviral-mediated KD for IL8. Figure 5A and B shows the mRNA expression and protein expression of IL8 after transduction of BM-MSCs with control KD or IL8 KD virus. Figure 5C demonstrates that knockdown of IL8 inhibits MIF-induced IL8 mRNA expression. Next, we show that KD of IL8 in BM-MSCs significantly inhibits AML survival when in coculture compared with control KD BM-MSCs (Fig. 5D). Finally, blocking the IL8R using SB225002 inhibited AML survival when cultured with BM-MSCs (Fig. 5E). Taken together, these results identify a novel protumoral regulatory pathway in the AML microenvironment.

## Discussion

AML is primarily a disease of the elderly with a median age at diagnosis in the Swedish Acute Leukemia Registry of 72 years (29). Outcomes for the 75% of patients who get AML over the age of 60 remain generally poor, largely because the intensity and side effects of existing curative therapeutic strategies (which are commonly used to treat younger fitter patients), coupled with patient comorbidities, frequently limit their use in this older less fit population (30). Accordingly, there is an urgent need to identify pharmacologic strategies to tackle AML, which are not only effective but can also be tolerated by both older and less well patients. It is envisaged that treatments that target the tumor microenvironment may well help realize this goal.

Here, we report a novel survival pathway within the human AML microenvironment, which functions as a feedback/autocrine loop involving the constitutive expression of the chemokine MIF by the AML blasts, which in turn induces IL8 expression in BM-

MSCs. Interestingly, another group showed that the repertoire of constitutive *in vitro* chemokine release from AML shows variation between different AML patient samples (31). We find that although baseline expression of MIF by AML varies between patient samples tested, all samples analyzed expressed MIF. Moreover in coculture experiments, AML patient-derived BM-MSCs were found to be ubiquitously responsive to AML-derived MIF, which resulted in an increase in IL8 expression by the BM-MSCs. This is in keeping with similar reports on other cytokine pathways, which have shown that BM-MSCs can constitutively express various chemokines (32), and AML cells are able to respond to these chemokines (32, 33). In this study, we also examined the genotype of six BM-MSCs used for the experiments and found three of six to be normal and in other three, the genotyping failed (Supplementary Table S2). This is apparently in contrast to Huang and colleagues, who found that three of four BM-MSCs from AML patients tested had cytogenetic abnormalities within the stromal cells (34). Presently therefore, the incidence and functional consequences of cytogenetic mutations within stromal cells remain undefined. Nevertheless, taken together, despite the established heterogeneity in AML, we find the MIF/IL8 autocrine loop a constant finding across the samples we tested, which makes this an attractive druggable target.

IL8 is a proinflammatory chemokine whose primary function is to activate two cell surface G protein-coupled receptors, CXCR1 and CXCR2, which promote neutrophil migration and degranulation (35–37). Elevated IL8 secretion in tumor biology is well characterized, with a number of studies showing the importance of this chemokine in AML. In 1993, Tobler and colleagues described the constitutive expression of IL8 and its receptor in human myeloid leukemia, and more recently, Schinke and

colleagues have reported that inhibition of the IL8 receptor CXCR2 selectively inhibits immature hematopoietic stem cells from MDS/AML samples (17, 18). In other malignancies, IL8 has been characterized in endothelial cells and tumor-associated macrophages, suggesting that IL8 has a function in the liver and prostate tumor microenvironments (38, 39). As rodents lack a direct homologue of IL8, we purified BM-MSCs extracted from patient bone marrow aspirates at the time of diagnosis of AML. Our study describes for the first time how AML stimulates the production of IL8 from BM-MSCs and inhibiting this process prevents AML survival.

Extensive studies of MIF function have revealed its central role in innate and adaptive immunity (10). More recently, the ability of this cytokine to support tumor progression has been highlighted, revealing MIF as a potential target for anticancer therapies in melanoma and colon cancer (40). MIF occurs in immunologically distinct conformational isoforms, reduced MIF and oxidized MIF (oxMIF), with the latter predominantly expressed in patients with inflammatory diseases (41) and is highly expressed by various cancer cell lines (42). This has led to the evaluation of an oxMIF = blocking antibody (imalumab) in early-phase clinical studies of selected solid tumors (<https://clinicaltrials.gov/ct2/show/NCT01765790>). Our findings provide a biological rationale for the clinical assessment of imalumab or other MIF inhibitors in AML patients.

Activation of PKC signaling pathway has been characterized in cancer cells. In hematologic malignancies, different PKC isoforms have been identified as key players in the leukemia microenvironment. In multiple myeloma, pharmacologic inhibition of activated PKC $\beta$ II using enzastaurin inhibited growth factors and cytokines secreted by multiple myeloma-derived bone marrow stromal cells (28). In CLL, PKC $\beta$  is immediately downstream of the B-cell receptor and has been shown to be important to CLL cell autocrine survival and proliferation *in vivo* (43). PKC $\beta$  is also essential for the development of CLL in the TCL1 transgenic mouse model, making it a valid therapeutic target in this malignancy (44). Furthermore, induction of PKC $\beta$ II in stromal cells is required for the survival of leukemic B cells, and stromal PKC $\beta$ II is upregulated in samples from CLL, ALL, and MCL patients (28). Our results demonstrate that in primary samples from AML patients at diagnosis, PKC $\beta$  is phosphorylated in the BM-MSCs

in response to MIF stimulation. This leads us to hypothesize that this pathway may commonly be activated in other hematologic malignancies, and moreover, the cancer cell is inducing this activation. In summary, this study links secretion of MIF from primary AML to a specific BM-MSC pathway, utilizing PKC $\beta$  to feedback survival signals, including IL8 secretion to AML. In doing so, we have identified *in vitro* the potential efficacy of targeting any one of these molecules to disrupt AML/BM-MSC pro-survival interactions.

### Disclosure of Potential Conflicts of Interest

No potential conflicts of interest were disclosed.

### Authors' Contributions

**Conception and design:** A.M. Abdul-Aziz, S.A. Rushworth, K.M. Bowles

**Development of methodology:** A.M. Abdul-Aziz, M.S. Shafat, S.A. Rushworth, K.M. Bowles

**Acquisition of data (provided animals, acquired and managed patients, provided facilities, etc.):** A.M. Abdul-Aziz, M.S. Shafat, M.J. Lawes, S.A. Rushworth, K.M. Bowles

**Analysis and interpretation of data (e.g., statistical analysis, biostatistics, computational analysis):** A.M. Abdul-Aziz, T.K. Mehta, F. Di Palma, S.A. Rushworth, K.M. Bowles

**Writing, review, and/or revision of the manuscript:** A.M. Abdul-Aziz, S.A. Rushworth, K.M. Bowles

**Administrative, technical, or material support (i.e., reporting or organizing data, constructing databases):** A.M. Abdul-Aziz, M.S. Shafat, S.A. Rushworth, K.M. Bowles

**Study supervision:** S.A. Rushworth, K.M. Bowles

### Acknowledgments

The authors wish to thank the Worldwide Cancer Research, The Big C, the National Institutes for Health Research (United Kingdom), and The Ministry of Higher Education and Scientific Research of the State of Libya for funding. We thank Professor Richard Ball and Iain Sheriffs, Norfolk and Norwich tissue bank (United Kingdom) for help with sample collection and storage.

The costs of publication of this article were defrayed in part by the payment of page charges. This article must therefore be hereby marked *advertisement* in accordance with 18 U.S.C. Section 1734 solely to indicate this fact.

Received April 28, 2016; revised September 22, 2016; accepted October 21, 2016; published OnlineFirst November 21, 2016.

### References

- Rowe JM, Tallman MS. How I treat acute myeloid leukemia. *Blood* 2010; 116:3147–56.
- Zeng Z, Shi YX, Samudio IJ, Wang RY, Ling X, Frolova O, et al. Targeting the leukemia microenvironment by CXCR4 inhibition overcomes resistance to kinase inhibitors and chemotherapy in AML. *Blood* 2009;113: 6215–24.
- Matsunaga T, Takemoto N, Sato T, Takimoto R, Tanaka I, Fujimi A, et al. Interaction between leukemic-cell VLA-4 and stromal fibronectin is a decisive factor for minimal residual disease of acute myelogenous leukemia. *Nat Med* 2003;9:1158–65.
- Nervi B, Ramirez P, Rettig MP, Uy GL, Holt MS, Ritchey JK, et al. Chemo-sensitization of acute myeloid leukemia (AML) following mobilization by the CXCR4 antagonist AMD3100. *Blood* 2009;113:6206–14.
- Rushworth SA, Murray MY, Zaitseva L, Bowles KM, MacEwan DJ. Identification of Bruton's tyrosine kinase as a therapeutic target in acute myeloid leukemia. *Blood* 2014;123:1229–38.
- Lane SW, Scadden DT, Gilliland DG. The leukemic stem cell niche: current concepts and therapeutic opportunities. *Blood* 2009;114:1150–7.
- Linenberger ML, Jacobson FW, Bennett LG, Broudy VC, Martin FH, Abkowitz JL. Stem cell factor production by human marrow stromal fibroblasts. *Exp Hematol* 1995;23:1104–14.
- Reuss-Borst MA, Klein G, Waller HD, Muller CA. Differential expression of adhesion molecules in acute leukemia. *Leukemia* 1995;9:869–74.
- Zaitseva L, Murray MY, Shafat MS, Lawes MJ, MacEwan DJ, Bowles KM, et al. Ibrutinib inhibits SDF1/CXCR4 mediated migration in AML. *Oncotarget* 2014;5:9931–9938.
- Nishihira J. Macrophage migration inhibitory factor (MIF): its essential role in the immune system and cell growth. *J Interferon Cytokine Res* 2000; 20:751–62.
- Chen YC, Zhang XW, Niu XH, Xin DQ, Zhao WP, Na YQ, et al. Macrophage migration inhibitory factor is a direct target of HBP1-mediated transcriptional repression that is overexpressed in prostate cancer. *Oncogene* 2010;29:3067–78.
- Verjans E, Noetzel E, Bektas N, Schütz AK, Lue H, Lennartz B, et al. Dual role of macrophage migration inhibitory factor (MIF) in human breast cancer. *BMC Cancer* 2009;9:1–18.



13. Wilson JM, Coletta PL, Cuthbert RJ, Scott N, MacLennan K, Hawcroft G, et al. Macrophage migration inhibitory factor promotes intestinal tumorigenesis. *Gastroenterology* 2005;129:1485–503.
14. Reinart N, Nguyen P-H, Boucas J, Rosen N, Kvasnicka H-M, Heukamp L, et al. Delayed development of chronic lymphocytic leukemia in the absence of macrophage migration inhibitory factor. *Blood* 2013;121:812–21.
15. Reikvam H, Fredly H, Kittang AO, Bruserud O. The possible diagnostic and prognostic use of systemic chemokine profiles in clinical medicine—the experience in acute myeloid leukemia from disease development and diagnosis via conventional chemotherapy to allogeneic stem cell transplantation. *Toxins* 2013;5:336–62.
16. Denizot Y, Fixe P, Liozon E, Praloran V. Serum interleukin-8 (IL-8) and IL-6 concentrations in patients with hematologic malignancies. *Blood* 1996;87:4016–7.
17. Tobler A, Moser B, Dewald B, Geiser T, Studer H, Baggolini M, et al. Constitutive expression of interleukin-8 and its receptor in human myeloid and lymphoid leukemia. *Blood* 1993;82:2517–25.
18. Schinke C, Giricz O, Li W, Shastri A, Gordon S, Barreyro L, et al. IL8-CXCR2 pathway inhibition as a therapeutic strategy against MDS and AML stem cells. *Blood* 2015;125:3144–52.
19. Rushworth SA, Pillinger G, Abdul-Aziz A, Piddock R, Shafat MS, Murray MY, et al. Activity of Bruton's tyrosine-kinase inhibitor ibrutinib in patients with CD117-positive acute myeloid leukaemia: a mechanistic study using patient-derived blast cells. *Lancet Haematol* 2015;2:e204–e11.
20. Falantes JF, Trujillo P, Piruat JL, Calderón C, Márquez-Malaver FJ, Martín-Antonio B, et al. Overexpression of GYS1, MIF, and MYC is associated with adverse outcome and poor response to azacitidine in myelodysplastic syndromes and acute myeloid leukemia. *Clin Lymphoma Myeloma Leuk* 2015;15:236–44.
21. Dios A, Mitchell RA, Aljabari B, Lubetsky J, O'Connor K, Liao H, et al. Inhibition of MIF bioactivity by rational design of pharmacological inhibitors of MIF tautomerase activity. *J Med Chem* 2002;45:2410–6.
22. Leng L, Metz CN, Fang Y, Xu J, Donnelly S, Baugh J, et al. MIF signal transduction initiated by binding to CD74. *J Exp Med* 2003;197:1467–76.
23. Bernhagen J, Krohn R, Lue H, Gregory JL, Zernecke A, Koenen RR, et al. MIF is a noncognate ligand of CXC chemokine receptors in inflammatory and atherogenic cell recruitment. *Nat Med* 2007;13:587–96.
24. Park MS, Kim YH, Jung Y, Kim SH, Park JC, Yoon DS, et al. *In situ* recruitment of human bone marrow-derived mesenchymal stem cells using chemokines for articular cartilage regeneration. *Cell Transplant* 2015;24:1067–83.
25. Liu N, Patzak A, Zhang J. CXCR4-overexpressing bone marrow-derived mesenchymal stem cells improve repair of acute kidney injury. *Am J Physiol Renal Physiol* 2013;305:F1064–73.
26. Barrilleaux BL, Fischer-Valuck BW, Gilliam JK, Phinney DG, O'Connor KC. Activation of CD74 inhibits migration of human mesenchymal stem cells. *In Vitro Cell Dev Biol Anim* 2010;46:566–72.
27. Starlets D, Gore Y, Binsky I, Haran M, Harpaz N, Shvidel L, et al. Cell-surface CD74 initiates a signaling cascade leading to cell proliferation and survival. *Blood* 2006;107:4807–16.
28. Lutzny G, Kocher T, Schmidt-Supprian M, Rudelius M, Klein-Hitpass L, Finch AJ, et al. Protein kinase c-beta-dependent activation of NF-kappaB in stromal cells is indispensable for the survival of chronic lymphocytic leukemia B cells in vivo. *Cancer Cell* 2013;23:77–92.
29. Juliusson G, Antunovic P, Derolf A, Lehmann S, Mollgard L, Stockelberg D, et al. Age and acute myeloid leukemia: real world data on decision to treat and outcomes from the Swedish acute leukemia registry. *Blood* 2009;113:4179–87.
30. Burnett A. Ham-Wasserman Lecture. Treatment of acute myeloid leukemia: are we making progress? *Hematology* 2012;2012:1–6.
31. Bruserud Ø, Rynning A, Olsnes AM, Stordrange L, Øyan AM, Kalland KH, et al. Subclassification of patients with acute myelogenous leukemia based on chemokine responsiveness and constitutive chemokine release by their leukemic cells. *Haematologica* 2007;92:332–41.
32. Reikvam H, Brenner AK, Hagen KM, Liseth K, Skrede S, Hatfield KJ, et al. The cytokine-mediated crosstalk between primary human acute myeloid cells and mesenchymal stem cells alters the local cytokine network and the global gene expression profile of the mesenchymal cells. *Stem Cell Res* 2015;15:530–41.
33. Brenner AK, Reikvam H, Bruserud Ø. A subset of patients with acute myeloid leukemia has leukemia cells characterized by chemokine responsiveness and altered expression of transcriptional as well as angiogenic regulators. *Front Immunol* 2016;7:205.
34. Huang JC, Basu SK, Zhao X, Chien S, Fang M, Oehler VG. Mesenchymal stromal cells derived from acute myeloid leukemia bone marrow exhibit aberrant cytogenetics and cytokine elaboration. *Blood Cancer J* 2015;5:e302.
35. Hartl D, Latzin P, Hordijk P, Marcos V, Rudolph C, Woischnik M, et al. Cleavage of CXCR1 on neutrophils disables bacterial killing in cystic fibrosis lung disease. *Nat Med* 2007;13:1423–30.
36. Gao Y, Guan Z, Chen J, Xie H, Yang Z, Fan J, et al. CXCL5/CXCR2 axis promotes bladder cancer cell migration and invasion by activating PI3K/AKT-induced upregulation of MMP2/MMP9. *Int J Oncol* 2015;47:690–700.
37. Nomellini V, Brubaker AL, Mahub S, Palmer JL, Gomez CR, Kovacs EJ. Dysregulation of neutrophil CXCR2 and pulmonary endothelial ICAM-1 promotes age-related pulmonary inflammation. *Aging Dis* 2012;3:234–47.
38. Inoue K, Slaton JW, Eve BY, Kim SJ, Perrotte P, Balbay MD, et al. Interleukin 8 expression regulates tumorigenicity and metastases in androgen-independent prostate cancer. *Clin Cancer Res* 2000;6:2104–19.
39. Fu XT, Dai Z, Song K, Zhang ZJ, Zhou ZJ, Zhou SL, et al. Macrophage-secreted IL-8 induces epithelial-mesenchymal transition in hepatocellular carcinoma cells by activating the JAK2/STAT3/Snail pathway. *Int J Oncol* 2015;46:587–96.
40. Ioannou K, Cheng KF, Crichlow GV, Birmipilis AI, Lolis EJ, Tsitsilonis OE, et al. ISO-66, a novel inhibitor of macrophage migration, shows efficacy in melanoma and colon cancer models. *Int J Oncol* 2014;45:1457–68.
41. Thiele M, Kerschbaumer RJ, Tam FW, Volkel D, Douillard P, Schinagl A, et al. Selective targeting of a disease-related conformational isoform of macrophage migration inhibitory factor ameliorates inflammatory conditions. *J Immunol* 2015;195:2343–52.
42. Schinagl A, Hagemann T, Douillard P, Thiele M, Voelkel D, Freissmuth M, et al. Abstract 4841: Oxidized macrophage migration inhibitory factor (oxMIF) expressed by tumor stroma and tumor cells, contributes to tumor growth. In: *Proceedings of the 105th Annual Meeting of the American Association for Cancer Research*; 2014 Apr 5–9; San Diego, CA. Philadelphia, PA: AACR. Abstract nr 4841.
43. El-Gamal D, Williams K, LaFollette TD, Cannon M, Blachly JS, Zhong Y, et al. PKC-beta as a therapeutic target in CLL: PKC inhibitor AEB071 demonstrates preclinical activity in CLL. *Blood* 2014;124:1481–91.
44. Holler C, Pinon JD, Denk U, Heyder C, Hofbauer S, Greil R, et al. PKCbeta is essential for the development of chronic lymphocytic leukemia in the TCL1 transgenic mouse model: validation of PKCbeta as a therapeutic target in chronic lymphocytic leukemia. *Blood* 2009;113:2791–4.

# Cancer Research

The Journal of Cancer Research (1916–1930) | The American Journal of Cancer (1931–1940)

## MIF-Induced Stromal PKC $\beta$ /IL8 Is Essential in Human Acute Myeloid Leukemia

Amina M. Abdul-Aziz, Manar S. Shafat, Tarang K. Mehta, et al.

*Cancer Res* 2017;77:303-311. Published OnlineFirst November 21, 2016.

<b>Updated version</b>	Access the most recent version of this article at: doi: <a href="https://doi.org/10.1158/0008-5472.CAN-16-1095">10.1158/0008-5472.CAN-16-1095</a>
<b>Supplementary Material</b>	Access the most recent supplemental material at: <a href="http://cancerres.aacrjournals.org/content/suppl/2016/11/19/0008-5472.CAN-16-1095.DC1">http://cancerres.aacrjournals.org/content/suppl/2016/11/19/0008-5472.CAN-16-1095.DC1</a>

<b>Cited articles</b>	This article cites 43 articles, 19 of which you can access for free at: <a href="http://cancerres.aacrjournals.org/content/77/2/303.full#ref-list-1">http://cancerres.aacrjournals.org/content/77/2/303.full#ref-list-1</a>
<b>Citing articles</b>	This article has been cited by 1 HighWire-hosted articles. Access the articles at: <a href="http://cancerres.aacrjournals.org/content/77/2/303.full#related-urls">http://cancerres.aacrjournals.org/content/77/2/303.full#related-urls</a>

<b>E-mail alerts</b>	<a href="#">Sign up to receive free email-alerts</a> related to this article or journal.
<b>Reprints and Subscriptions</b>	To order reprints of this article or to subscribe to the journal, contact the AACR Publications Department at <a href="mailto:pubs@aacr.org">pubs@aacr.org</a> .
<b>Permissions</b>	To request permission to re-use all or part of this article, contact the AACR Publications Department at <a href="mailto:permissions@aacr.org">permissions@aacr.org</a> .